U.PORTO

DOUTORAMENTO

BIOLOGIA MOLECULAR E CELULAR

SRCR proteins as pattern recognition receptors: expanding the search for interactions with pathogens

Marcos S. Cardoso

D

2022

U.PORTO

Marcos S. Cardoso. SRCR proteins as pattern recognition receptors: expanding the search for interactions with pathogens

D.ICBAS **2022**

SRCR proteins as pattern recognition receptors: expanding the search for interactions with pathogens

Marcos Levi dos Santos Cardoso

SEDE ADMINISTRATIVA

INSTITUTO DE CIÊNCIAS BIOMÉDICAS ABEL SALAZAR

FACULDADE DE CIÊNCIAS

MARCOS LEVI DOS SANTOS CARDOSO

SRCR PROTEINS AS PATTERN RECOGNITION RECEPTORS: EXPANDING THE SEARCH FOR INTERACTIONS WITH PATHOGENS

Tese de Candidatura ao grau de Doutor em Biologia Molecular e Celular

Programa Doutoral da Universidade do Porto (Instituto de Ciências Biomédicas de Abel Salazar e Faculdade de Ciências)

Orientador – Doutor Alexandre Valentim Xavier Mourão do Carmo

Categoria – Investigador Principal

Afiliação – Instituto de Investigação e Inovação em Saúde da Universidade do Porto e Instituto de Biologia Molecular e Celular

O trabalho desenvolvido nesta tese foi efetuado no Instituto de Investigação e Inovação em Saúde da Universidade do Porto – Instituto de Biologia Molecular e Celular. Este trabalho foi financiado pela Fundação para a Ciência e Tecnologia (FCT) através da bolsa de doutoramento SFRH/BD/116791/2016 e pelos projetos SRecognite Infect-ERA/0003/2015 e UIDB/04293/2020.

Publications

De acordo com o disposto no ponto n.º 2 do Art.º 31º do Decreto-Lei n.º 74/2006, de 24 de Março, aditado pelo Decreto-Lei n.º 230/2009, de 14 de Setembro, o autor declara que na elaboração desta tese foram incluídos dados das publicações abaixo indicadas. O autor participou ativamente na conceção e execução dos trabalhos que estiveram na origem dos mesmos, assim como na sua interpretação, discussão e redação.

Cardoso MS, Santos RF, Almeida S, Sá M, Pérez-Cabezas B, Oliveira L, Tavares J, Carmo AM (2021) Physical interactions with bacteria and protozoan parasites establish the scavenger receptor SSC4D as a broad-spectrum pattern recognition receptor. Front. Immunol. https://doi.org/10.3389/fimmu.2021.760770

Acknowledgments

“As you set out for Ithaka
hope your road is a long one,
full of adventure, full of discovery (…).” C. P. Cavafy

Esta jornada de mil e oitocentos dias cheios de aventuras e descobertas só foi possível graças a um grupo valioso de pessoas que durante este período de tempo revelaram-se imprescindíveis para o sucesso desta jornada. A todos estes agradeço do fundo do meu coração.

Em primeiro lugar, quero agradecer profundamente ao meu orientador Alexandre do Carmo. Durante a nossa jornada para Ithaka, passamos pelo “*Laistrygonians, Cyclops, angry Poseidon*” e tal como o poema diz: “*don’t be afraid of them: as long as you keep your thoughts raised high*”. Sempre com a sua calma característica foi capaz de dirigir o rumo desta jornada mesmo quando as vicissitudes da viagem ameaçaram a chegada a um bom porto. Obrigado pela confiança que depositou em mim e acima de tudo por acreditar sempre no sucesso deste projeto. Obrigado pela dedicação e por todos os momentos construtivos de aprendizagem quer dentro ou fora do laboratório. Não tenho palavras suficientes para agradecer a oportunidade que me deu e por ajudar a realizar o sonho de uma criança que um dia sonhou ser cientista. Será sempre uma parte imprescindível desta estória e será sempre relembrado como o Capitão desta incrível aventura.

Apesar de no papel não ter co-orientadores, sinto que fui um felizardo por ao longo desta jornada ter conhecido a Joana Tavares e a Liliana Oliveira. Vocês foram verdadeiras orientadoras!

Joana, apareceste talvez no período mais crítico desta viagem. Quando tudo não resultava lá apareceu a ideia de usar os parasitas. E é aí que nasce este trabalho. Obrigado pela ajuda incansável e por todas as discussões científicas! O sucesso desta viagem em grande parte deve-se ao teu entusiasmo, profissionalismo, altruísmo e dedicação! Muito obrigado!

Lili a post doc! O teu título devia de ser mudado para Chefe Lili. Foste parte indispensável durante todos estes anos. Soubeste ser crítica e reticente quando foi preciso, mas também foste mão amiga, conselheira e tudo fizeste para levar este barco a bom porto. Foste a pessoa com quem mais discuti ciência durante estes anos. Além disso, foste companheira de viagem na China, companheira em largas centenas de almoços e muitos jantares. Muito obrigado pela tua amizade! Será certamente das melhores coisas que levo

desta aventura. Admiro a tua organização, forma de trabalho e excelência em tudo o que fazes! Espero que por osmose leve também um bocado dessas tuas virtudes.

Aos elementos do CAGE, passados e presentes. O sucesso de uma viagem de navio está sempre intimamente ligado ao profissionalismo, interajuda, e boa disposição entre todos os tripulantes. Obrigado por todas as discussões científicas, pela ajuda nos maus momentos e pelas celebrações ao longo desta viagem. Obrigado, Sónia, Carine, Diana, Emma, Fátima e tantos outros que ao longo dos últimos anos passaram pelo CAGE. Um agradecimento especial a todos os membros dos Didiers e dos FIV pelo bom ambiente, amizade, e interajuda ao longo destes anos.

Durante todos estes anos de aprendizagem nunca conheci ninguém que ensinasse com tanta paixão como a Fátima. Este bichinho pela ciência, pela investigação e pela imunologia é em grande parte “culpa” tua. Obrigado porque a primeira vez que pisei o IBMC foi graças a ti.

Apesar de não ter feito parte desta viagem específica, quero agradecer ao Rui Appelberg. Foste uma das fontes de inspirações que trouxe comigo nesta viagem e que certamente continuarei a levar em viagens futuras.

Considero-me uma pessoa sortuda. Ao longo desta jornada conheci várias pessoas incríveis que ao longo do tempo se tornaram em amigos. Mariana! Muito do que sou no laboratório devo-o a ti! Obrigado. Meireles, Rosas, Elva, Cassilda, Johnny, Begonã obrigado por todos os momentos dentro e fora do laboratório.

Às minhas preferidas, Sandrinha e Curinha. Finalmente! Está feito! Obrigado porque mesmo à distância souberam sempre estar presentes.

À OD team ou ONGEST. Era dentro da quadra que a sanidade mental era recarregada. Obrigado por cada treino, por cada jogo e por cada vitória (e foram muitas!). Obrigado ao Cevadas24, Muke6, Guga13, Levi20, Marcelinho8, Basler9, Vítor10, Manchas5 e Panu17.

Aos três seres de quatro patas que alegram a minha vida. Foram quase sempre a única receção que tive ao chegar a casa após as longas noites de experiências e isso mostra bem a vossa lealdade. Além disso foram sempre a melhor terapia para a frustração de uma experiência falhada. Obrigado pelas nossas longas conversas!

À minha família. Que aquilo que temos nunca mude. Há alguma coisa mais incrível, mas ao mesmo tempo mais simples, que os nossos almoços de família? Somos muitos, falamos alto, mas somos unidos. À minha segunda mãe e irmãs emprestadas obrigado por

todos os almoços de sábado. Todos vocês foram tantas vezes um escape à vida absorvente do laboratório. Obrigado!

Quando em criança dizia que queria ser cientista. Muitos se riram, outros, acreditaram que havia algum potencial. Obrigado, prima Alice e Tia Fernanda Amélia, porque acreditaram no potencial e por trocarem as minhas prendas de brinquedos para microscópios, livros de banda desenhada sobre Pasteur e Marie Curie e tantas outras coisas que ainda hoje guardo com tanta estima.

À minha segunda família. Aquela que adquiri por opção própria! Obrigado por me receberem tão bem e por todo o apoio e carinho que recebi.

TITA(nium)! Propriedades do titânio: Resistente à corrosão; usado para aumentar a resistência de várias ligas metálicas; usado amplamente na indústria aerospacial. Foste aquela que garantiu a resistência do meu navio à corrosão das chuvas e da água salgada e ao mesmo tempo aquela que tornou a embarcação forte, estável e dirigível para sobreviver às tempestades. Durante esta viagem sempre foste o meu refúgio nas desilusões e as águas mansas e calmas nas incertezas. Obrigado porque todos os dias me incentivas a ser melhor pessoa e melhor cientista. Obrigado por tornares esta viagem única. Obrigado por todas as viagens ao asteroide B-612 que ainda faltam fazer. "(…) *Hope your road is a long one. May there be many summer mornings when, with what pleasure, what joy, you enter harbors you're seeing for the first time; may you stop at Phoenician trading stations to buy fine things, mother of pearl and coral, amber and ebony, sensual perfume of every kind — as many sensual perfumes as you can; and may you visit many Egyptian cities to learn and go on learning from their scholars (…).*

Lau e Marta! Quando nasceram tornaram-se o centro das atenções de toda a gente. Além disso estragaram os meus carros de coleção. Não têm desculpa possível! Mas a verdade é que são a alegria da nossa casa e a minha também! São parte de mim e eu parte de vocês. Obrigado por todos os momentos ao longo desta jornada e que mais 1800 dias de novas aventuras vezes 70 estejam pela frente. "(…) *Keep Ithaka always in your mind. Arriving there is what you're destined for. But don't hurry the journey at all. Better if it lasts for years, so you're old by the time you reach the island, wealthy with all you've gained on the way, not expecting Ithaka to make you rich (…)."*

Aos meus Pais. Vocês são a minha inspiração e exemplo. Acredito que durante a construção do meu carácter herdei a paciência e calma da Mãe e a teimosia e perseverança do Pai. Acredito firmemente que essas características contribuíram decisivamente para o sucesso desta viagem. Obrigado por apostarem e investirem na minha formação. Não tenho palavras suficientes para agradecer tudo aquilo que fizeram,

fazem e irão continuar a fazer por mim. É um sentimento inexplicável e intraduzível. Dedico-vos esta tese e esta jornada como símbolo do meu reconhecimento, admiração, respeito e amor.

"(…) Ithaka gave you the marvelous journey.
Without her you wouldn't have set out.
She has nothing left to give you now.

And if you find her poor, Ithaka won't have fooled you.
Wise as you will have become, so full of experience,
you'll have understood by then what these Ithakas mean."
"Ithaka" by C. P. Cavafy

Table of contents

Summary

The scavenger receptor cysteine-rich (SRCR) superfamily is emerging as a novel class of pattern recognition receptors (PRR) that bind bacteria, fungi, and viruses. Thus, the host's array of SRCR receptors is putatively well suited for targeting a broad range of highly conserved pathogen-associated molecular patterns (PAMPs) solely expressed on microbes. However, the microbe-recognizing spectrum of each SRCR member remains to be investigated. In addition, over the last decade, many different observations have uncovered distinct roles for the SRCR proteins, ranging from the well-established function as anti-apoptotic protein to inhibitory signaling hubs, modulators of T cell activation or regulators of lipid metabolism, and among others. This multifunctionality impacts directly on the regulation of several key immunological events, namely in infection, metabolic disorders, cancer, autoimmune disease, and consequently during an inflammatory response.

We here address a pioneer study by describing the first functional characterization of SSC4D. Using conventional protein-cell binding assays we uncovered its capacity to physically bind to different species of bacteria and protozoan parasites. In addition, SSC4D also shows the capacity to recognize specific bacterial surface structures, such as lipopolysaccharide (LPS) and lipoteichoic acid (LTA).

Furthermore, we also revealed new insights related to the microbe-recognizing spectrum of the well-established PRR for bacteria and fungi – CD5 antigen-like (CD5L). Similar to SSC4D, we found for the first time that CD5L also has the capacity to recognize protozoan parasites, including *Trypanosoma brucei*, *Plasmodium berghei*, *Neospora caninum*, and *Leishmania* infantum.

Having established CD5L as a parasite-binding protein we further addressed its role in parasitic infections and, surprisingly, we observed a significant increase in the circulating CD5L levels upon *T. brucei* infection, which led us to hypothesize a putative role for CD5L in Trypanosomatid infections. To further dissect this hypothesis, we infected mice, in which the *cd5l* gene was abrogated, with luciferase-expressing *T. brucei* GVR35 bloodstream forms. Interestingly, we found no differences neither in parasitemia nor in the whole-body bioluminescence signal analysis between the WT and the CD5L KO mice. Strikingly, the CD5L KO mice show greatly enhanced susceptibility to *T. brucei* infection. Twenty-eight days upon infection, we witnessed an exacerbated pro-inflammatory response in *T. brucei*-infected CD5L KO mice characterized by an increase in T_H1 CD4+ T cells. In addition, we

also observed augmented recruitment of macrophages and inflammatory monocytes to the spleen, followed by an increased secretion of the pro-inflammatory cytokines IFN-γ and TNF-α, corroborating the hypothesis that CD5L in addition to the PRR function is an important anti-inflammatory mediator, and its absence leads to an imbalanced immune response.

Collectively, we identified and proceeded to the functional characterization of SSC4D as a new PRR family member. Additionally, our studies also provided new valuable insights into the puzzling role of CD5L during the inflammatory response.

Resumo

A superfamília de recetores scavenger ricos em cisteínas (SRCR) tem vindo a ser identificada como uma nova classe de recetores de reconhecimento de padrões (PRR) capaz de se ligar a bactérias, fungos e vírus. Dessa forma, a matriz de recetores SRCR do hospedeiro deverá ser adequada para permitir o reconhecimento de uma ampla gama de padrões moleculares associados a patogénios (PAMPs) altamente conservados expressos exclusivamente em microrganismos. No entanto, o espectro de patogénios reconhecidos por cada membro da superfamília SRCR continua por esclarecer. Adicionalmente, ao longo da última década, diferentes observações sugeriram papéis distintos para as proteínas SRCR, desde a função bem estabelecida como proteínas anti-apoptóticas até à modulação da ativação de células T ou à regulação do metabolismo lipídico, entre outras. Esta multifuncionalidade tem impacto direto na regulação de vários eventos imunológicos, nomeadamente na infeção, distúrbios metabólicos, cancro, doença autoimune e, consequentemente, durante uma resposta inflamatória.

Abordamos, neste trabalho, um estudo pioneiro ao descrever a primeira caracterização funcional da proteína solúvel SSC4D, para isso, recorremos a metodologias convencionais de ligação proteína-célula, onde descrevemos a capacidade do SSC4D se ligar fisicamente a diferentes espécies de bactérias e parasitas protozoários. Além disso, SSC4D também reconhece estruturas específicas da superfície bacteriana, como lipopolissacarídeo (LPS) e ácido lipoteicóico (LTA).

Adicionalmente, revelamos novos detalhes acerca do espectro de reconhecimento de patogénios do CD5L, previamente identificado como PRR para bactérias e fungos. Semelhantemente ao observado para o SSC4D, os nossos resultados descrevem pela primeira vez que o CD5L também tem a capacidade de reconhecer parasitas protozoários, incluindo *Trypanosoma brucei*, *Plasmodium berghei*, *Neospora caninum* e *Leishmania infantum*.

Tendo estabelecido o CD5L como uma proteína capaz de se ligar a parasitas, decidimos explorar o seu papel *in vivo* durante uma infeção parasitária e, surpreendentemente, observamos um aumento significativo na concentração de CD5L em circulação após infeção por *T. brucei*, sugerindo uma possível função para o CD5L em infeções por Tripanossomatídeos. Com o objetivo de explorar esta hipótese, infetamos murganhos geneticamente modificados para excluir o gene *cd5l* com formas sanguíneas de *T. brucei* GVR35 que expressam luciferase. Curiosamente, não encontramos diferenças nem na parasitemia nem na análise do sinal de bioluminescência no corpo inteiro dos

ratinhos WT em comparação com ratinhos CD5L KO. No entanto, os ratinhos CD5L KO mostram uma maior suscetibilidade à infeção por *T. brucei*. Vinte e oito dias após infeção por *T. brucei*, observamos uma resposta pró-inflamatória exacerbada em ratinhos CD5L KO, caracterizada por um aumento de células T $CD4^+$ T_H1. Complementarmente, também reportamos um aumento do recrutamento de macrófagos e monócitos inflamatórios para o baço, seguido por um aumento da secreção de citocinas pró-inflamatórias, IFN-γ e TNF-α, corroborando a hipótese de que o CD5L além da função como PRR é, também, um importante mediador anti-inflamatório e sua ausência leva a uma resposta imune desequilibrada.

Coletivamente, identificamos e procedemos à caracterização funcional do SSC4D como novo membro da família dos PRR. Além disso, os nossos estudos também forneceram novas visões valiosos sobre o papel intrigante do CD5L durante a resposta inflamatória.

List of Abbreviations

aa: Amino acid

AAT: Animal African trypanosomiasis

AKI: Acute kidney injury

APC: Antigen-presenting cell

BBB: Blood-brain barrier

BCR: B cell receptor

BMDM: Bone marrow-derived macrophages

CD5L: CD5 molecule like

CLP: Cecal ligation and puncture

CLR: C-type lectin receptors

CM: Cerebral malaria

CNS: Central nervous system

CUB: C1r/C1s Uegf Bmp1

DAMP: Damage-associated molecular pattern

DC: Dendritic cell

DMBT1: Deleted in malignant brain tumor 1

DP: Double positive

dsRNA: Double-stranded RNA

EAE: Experimental autoimmune encephalomyelitis

Foxp3: Forkhead box P3

GM-CSF: Granulocyte-macrophage colony-stimulating factor

GPI: Glycophosphatidylinositol

HAT: Human African trypanosomiasis

IFN: Interferon

Ig: Immunoglobulin

IgAN: IgA nephropathy

IL: Interleukin

ILC: Innate lymphoid cell

iNOS: Inducible nitric oxide synthase

iRBC: Infected red blood cell

IRF: Interferon regulatory transcription factor

KO: Knockout

LPS: Lipopolysaccharide

LRR: Leucine-rich repeats

LTA: Lipoteichoic acid

LXR/RXR: nuclear receptor liver X receptor/retinoid X receptor

M-CSF: Macrophage colony stimulating factor

MAL: MyD88 adaptor-like

MAPK: Mitogen-activated protein kinase

MHC: Major histocompatibility complex

MyD88: Myeloid differentiation factor 88

NF-κB: Nuclear factor-κB

NK: Natural killer

NLR: NOD-like receptors

NO: Nitric oxide

NOD: Nucleotide oligomerization domain

oxLDL: Oxidized low-density lipoprotein

PAMP: Pathogen-associated molecular pattern

PRR: Pattern recognition receptor

RIG: Retinoic acid-inducible

RLR: RIG I-like receptors

ROS: Reactive oxygen species

sPRR: Soluble pattern recognition receptor

SRCR-SF: Scavenger receptor cysteine-rich superfamily

ssRNA: Single-stranded RNA

STAT: Signal transducer and activator of transcription

sVSG: Soluble variant surface glycoprotein

TCR: T cell receptor

Tfh: Follicular helper T cell

TGF: Transforming growth factor

T_H: T helper

TIP-DC: TNF/inducible NO synthase-producing dendritic cells

TLR: Toll-like receptor

TNF: Tumor necrosis factor

TRAM: TRIF-related adaptor molecule

Treg: Regulatory T cell

TRIF: TIR domain-containing adaptor-inducing IFN-β

VL: Visceral leishmaniasis

VSG: Variant surface glycoprotein

WHO: World health organization

WT: Wild type

ZP: Zona pellucida

Chapter I

Introduction

Human beings have been living in a world that is heavily populated by both pathogenic and non-pathogenic microbes that constantly exert enormous pressure on hosts and threaten their normal homeostasis. This state of equilibrium depends on a complex array of protective mechanisms that grants the ability of our body to defend and resist microbes. The efficiency and success of this protective framework, called the immune system, rely on its capacity to develop an immune response, which depending on the specificity and the timing of activation can be subdivided into two branches. A rapid and broad response (innate immune response) that is always immediately available upon invasion of a wide range of pathogens, and a specific and adaptative response (adaptive immune response) that relies on the antigen-specific reactions and confers lifelong protective immunity against a specific pathogen. Although the division of the immune system into two different compartments is generally accepted, this does not mean a strict separation of both innate and adaptive immune responses. Instead, for effective host protection against pathogenic microbes, both responses must cooperate closely and work tightly synchronized.

One of the most crucial functions of the immune system is its ability to intercept, recognize, respond and destroy foreign antigens while avoiding responses that produce excessive damage to the host's own components. For this purpose, both innate and adaptive immune systems employ a complex network of different molecules regulated by several mechanisms that grant their ability to discriminate between "self" *versus* "non-self". While the innate immune system can recognize microorganisms *via* a limited number of germline-encoded pattern-recognition receptors (PRRs), the adaptive immune system displays a vast repertoire of different antigen receptors generated somatically during the development of T and B cells.

Innate Immunity

Historically, innate immunity was first recognized in the light of the work of the Russian immunologist Elie Metchnikoff, who described that many microorganisms could be engulfed by phagocytic cells, which he called "macrophages". When Metchnikoff studied phagocytosis in 1883, he also linked this mechanism to the first line of defense against pathogens (1).

In the last century, these phagocytic cells and their functions including the engulfment of either microorganisms or dead cells were crucial to the understanding of the basic principles of the innate immune response and host defense. However, it is now

accepted that an innate immune response has several additional key players and features. The initial defenses against microbes encompass all physical and chemical barriers, such as the skin, the mucosal surfaces of the respiratory and gastrointestinal tracts, and also enzymes and mucus, which either is antimicrobial or inhibits the attachment of the microbe. Since neither the skin nor the mucosal cavities are ideal habitats for most organisms, microbes must breach the ectoderm. If these barriers are overcome or evaded, other components of the innate immune system come into play.

Accordingly, the innate immune response relies on two main defense strategies that work closely orchestrated – cellular and molecular. From the cellular point of view, innate responses use phagocytic cells, namely macrophages, neutrophils, dendritic cells (DCs), and monocytes; cells that release inflammatory mediators, namely basophils, mast cells, and eosinophils; natural killer cells (NK cells) and innate lymphoid cells (ILC). On the other hand, the molecular mechanisms include soluble proteins that are either constitutively expressed (such as complement, defensins, and ficolins) or that are secreted from cells (including cytokines, chemokines, reactive free radical species, among others). Lastly, as proposed by Charles Janeway, the innate immune system also includes a repertoire of membrane-bound and soluble germline-encoded pattern recognition receptors (PRRs) that identify highly conserved microbial structures termed pathogen-associated molecular patterns (PAMPs) (2). These invariant molecular structures constitute the molecular immunogenic signatures of pathogens, and they are solely expressed on microbes and are not amenable to mutation without involving loss of viability and/or pathogenicity (2).

Bacterial PAMPs are diverse and include different molecules such as lipopolysaccharide (LPS), lipoteichoic acids (LTA), peptidoglycan and flagellin, to unique types of nucleic acids such as cyclic dinucleotides (CDNs) (3). By contrast, viruses are mainly recognized through surface viral glycoproteins and through unique nucleic acids such as double-stranded RNA (dsRNA), uncapped single-stranded RNA (ssRNA) and viral DNA (4). While most fungi are recognized through fungal cell wall components such as β-glucans, mannans, mannoproteins and chitin, as well as fungal-derived RNA and unmethylated DNA (5), the parasites, including protozoan parasites, are mainly recognized through a glycolipid present at their surface termed glycophosphatidylinositol (GPI) (6). The recognition of invasive pathogens by the innate immune system is discussed in more detailed in the next topic. Additionally, the sensing of pathogens by PRRs expressed on antigen-presenting cells (APCs), particularly DCs, leads to the activation of the adaptive system. Furthermore, the role of different PRRs in the sensing of pathogens determines the

type of infection encountered, provides information about pathogen presence, and instructs lymphocytes to induce the appropriate adaptive immune response (7).

Adaptive immunity

Although the innate immune system recognizes an enormous variability and heterogeneity of PAMPs, the range of pathogenic molecular patterns it can recognize is limited. The overwhelming diversity of antigenic structures as well as the ability of pathogens to mutate to avoid host detection has created an enormous selective pressure to the emergence of a more advanced mechanism of protection – called adaptive immunity (8, 9). In contrast to the PRRs of the innate immune system, which are all germline-encoded, the adaptive immune response depends on antigen-specific receptors that are custom-tailored and selected through a process of somatic rearrangement of different variable (V), diversity (D), and joining (J) immunoglobulin (Ig)-type gene segments (10). V(D)J rearrangement allows the formation of an almost unlimited repertoire of different T cell receptors (TCRs) and B cell receptors (BCRs), each with unique specificities. Thus, each lymphocyte expresses only one receptor that is specific to an antigen. Importantly, these individual antigen-specific lymphocytes will, upon antigen recognition, become activated and triggered to proliferate and expand the individual cell clone. This phenomenon, called clone expansion, serves to amplify the number of antigen-specific lymphocytes in order to mount a robust protective response against a given antigen (pathogen) (11). Moreover, these clones can persist in the host for life, providing immunologic memory and the capacity for a rapid response in the event of re-exposure to that antigen (12).

The adaptive immune response is mediated by two major types of chain reactions – the antibody response and the cell-mediated immune response, which are mainly controlled by conventional B (also known as B2 cells) and T cells (mostly $\alpha\beta$ T cells), respectively. There are two types of conventional $\alpha\beta$ T cells: T-helper (T_H) cells, which express the co-receptor CD4 on the cell surface and recognize antigenic peptides bound to major histocompatibility complex (MHC) class II, and cytotoxic T cells, which express the co-receptor CD8 on the cell surface and recognize antigenic peptides bound to MHC class I.

The recognition of an invasive pathogen by a PRR-expressing APC leads to its activation and consequent induction of cytokine production and expression of cell-surface receptors, followed by migration to the lymph nodes through the lymphatic vessels. When those APCs reach the lymph nodes they present the processed antigen to naïve T cells via

MHC-TCR interactions (13, 14). This results in T cell activation and, in the case of T_H cells, differentiation into one of several types of effector T_H cells (*e.g.*, T_H1, T_H2, T_H17 cells).

Briefly, T_H1 cells are polarized in response to intracellular pathogens and IL-12 produced by DCs (15). T_H1 cells secrete interferon (IFN)-γ, a signature cytokine that specifically enhances the anti-microbial capacity of macrophages (16). Additionally, T_H1 also produces IL-12 and tumor necrosis factor (TNF)-α, which creates a positive loop to amplify the type 1 response while inhibiting T_H2 and T_H17 responses (17). More often, T_H1 cells are involved in the induction and maintenance of the chronic inflammatory process (18-20). T_H2 cells are involved in type 2 immune responses, which are crucial for the elimination of parasitic helminths. In contrast to T_H1 and T_H17 cell priming, in which DCs produce T cell-polarizing cytokines in response to microbial stimuli, in T_H2 polarization the polarizing cytokine (IL-4) is mainly produced by basophils (21, 22). Additionally, allergens can also trigger the polarization of naïve $CD4^+$ T cells into T_H2 cells. Upon activation, T_H2 cells produce IL-4, IL-5 and IL-13, which are important for Ig class-switching to IgE, macrophage polarization to an M2-like phenotype, and stimulate the bone marrow to produce eosinophils (23, 24). Naïve $CD4^+$ T cells polarize into T_H17 cells in the presence of IL-1β, IL-6, IL-23 and transforming growth factor (TGF)-β. Classically, upon activation T_H17 cells produce IL-17 that assures a pro-inflammatory environment, which is critical for the defense against extracellular microbial and fungi infections (25). IL-17, the signature cytokine of T_H17 cells, appears to be crucial for the recruitment of innate immune cells, such as neutrophils (23, 26). Although historically, T_H17 cells are described as inducers of the inflammatory response, recently it was found that T_H17 cells are a heterogeneous and high plastic subset of cells that switch between a pathogenic and non-pathogenic status. On one hand, IL-17-producing T_H17 cells are considered pathogenic T_H17 cells, since they promote a pro-inflammatory environment; however, on the other hand IL-10-producing T_H17 cells are considered as non-pathogenic T_H17 cells, given that IL-10 promotes tissue regeneration and acts as an anti-inflammatory cytokine (27-29).

Several sophisticated regulatory mechanisms are used to control $CD4^+$ T cell differentiation, maintaining immune homeostasis, preventing autoimmunity, and moderating inflammation induced by pathogens. Thus, regulatory T (Treg) cells are a unique subset of helper T-cells which regulate and refrain immune responses and establish peripheral tolerance (30). Although Tregs are characterized by the expression of the master transcription factor forkhead box P3 (Foxp3), other transcriptional factors may mediate Treg cell development (31, 32). Genetically modified mice that lack Foxp3 develop a profound autoimmune-like lymphoproliferative disease that emphasizes the crucial role of Tregs in

the maintenance of peripheral tolerance (33). Tregs can be further subdivided into two major subsets – nature-derived Tregs (nTregs) and peripheral-induced Tregs (iTregs) (34). While nTregs are selected during thymic T cell maturation, iTregs arise from naïve CD4+ T cell differentiation under an appropriate selective environment, normally rich in TGF-β and IL-2. IL-10, the signature cytokine of Tregs, is a suppressive cytokine and is essential in limiting immune responses to numerous pathogens and subsequent immune pathologies (35, 36). For example, IL-10 KO mice mount an overexuberant immune response when infected with *Plasmodium chabaudi* (37).

New $CD4^+$ T cell subsets such as T_H9, T_H22, and follicular helper T (Tfh) cells were recently described. Naïve $CD4^+$ T cells polarize into T_H9 cells in the presence of TGF-β and IL-4 (38, 39). Moreover, it has been shown that activation of T_H9 cell transcription factors, such as PU.1 and interferon regulatory transcription factor (IRF) 4, triggers the differentiation of T_H9 cells, which regulate the expression of IL-9 (38, 40-42). This particular T cell subset has been found to play important roles in inflammatory diseases, autoimmune diseases, tumors, and other related clinical diseases (43-45). T_H22 cells are abundant in human skin, play a key role in epidermal wound healing, and exhibit anti-inflammatory, antibacterial, and antiviral proprieties (46, 47). The activation of the transcription factor aryl hydrocarbon receptor (AhR) enhances the differentiation of naïve $CD4^+$ T cells into T_H22 cells and leads to the secretion of the signature cytokine IL-22, but also IL-13, IL-26, TNF-α and granzyme B (47, 48). Tfh cells have a key role in protective immunity helping B cells to produce antibodies against foreign antigens. To perform their function, Tfh cells are located in the B cell zones of the secondary lymphoid organs (spleen, lymph nodes, and tonsils) in close contact with B cells (49, 50). Tfh cells are differentiated by the expression of the transcription factor Bcl6, and by the induction of IL-6 and IL-21 (51, 52).

The different pathways and types of recognition by the innate immune system are critical for the choice of the appropriate effector immune response. Although a considerable amount of information has been accumulated over the past years, the exact mechanism by which the adaptive immune system interprets the innate immune signals is not fully understood. Recent evidence has suggested that different DC subsets, which express a specific array of PRRs, and consequently specific signals and cytokines are critically involved in the choice of the effector response (7, 53). For example, *Irf8*$^+$Batf3-dependent $CD103^+$ DCs seem to be required for effective T_H1 responses, whereas *Irf4*$^+$Klf4-dependent DCs appear to be required for T_H2 responses (54, 55).

Pattern-recognition receptors (PRRs)

PRRs are strategically found extracellularly, in secreted forms present in the bloodstream and interstitial fluids, as well as expressed in different subcellular compartments such as the plasma membrane, vacuolar membranes, and cytosol. Accordingly, host cells such as epithelial and effector innate cells express a spectrum of PRRs in order to sense and detect threats that have different anatomical and subcellular locations during infection. Consequently, upon pathogen invasion PRRs trigger several defense mechanisms that impact directly on the enhancement of phagocytosis, production of pro-inflammatory cytokines, cell recruitment and stimulation of cell differentiation, culminating in the production of different anti-microbial products like the induction of reactive oxygen species (56-59).

Our understanding of the nature of PRRs has progressed enormously since the elegant theory of Janeway in 1989 (2). This is mainly due to the research work of Hoffmann, which demonstrated that mutant *Drosophila melanogaster* carrying mutations in a receptor called 'Toll' decreased the production of antimicrobial peptides and led to a higher susceptibility of the fly to fungal infections (60). Subsequently, homologs of Toll, now known as Toll-like receptors (TLRs), were found in other animals, including mammals (61). TLRs were the first PRRs to be identified and they are also the better characterized; however, it has become apparent that non-TLR PRRs are also involved in pathogen recognition (12). These include membrane-bound C-type lectin receptors (CLRs), cytosolic proteins such as NOD-like receptors (NLRs) and RIG-I-like receptors (RLRs), and scavenger receptors (SR) (13, 14). These observations suggest that many aspects of innate immunity are more sophisticated and complex than initially anticipated.

Toll-like receptors (TLRs)

TLRs are type I transmembrane proteins with an extracellular region composed of 18-25 copies of leucine-rich repeats (LRR) that mediate the recognition of PAMPs (62). They also have a transmembrane region and a cytosolic Toll-IL-1 receptor (TIR) domain in the cytoplasmic tail, which activate downstream signaling pathways (63, 64). To date, 10 TLRs have been identified in humans (13 in mice), with TLR-1 to TLR-9 being conserved in both species (65). These receptors are differentially expressed among immune cells, they can be expressed either on the cell surface or associated with intracellular vesicles, and their expression is modulated in response to various stimuli (66, 67). Moreover, these sensors have distinct functions in terms of PAMP recognition and immune responses. Each

TLR detects distinct PAMPs derived from viruses, bacteria, mycobacteria, fungi or parasites. These include lipoproteins (recognized by TLR1, TLR2, and TLR6), double-stranded RNA (TLR3), LPS (TLR4), flagellin (TLR5), single-stranded RNA (TLR7 and TLR8), and DNA (TLR9) (68, 69). This concept is, however, turning out to be more complex than a single TLR molecule per pathogen. At least some TLRs have been shown to form heterodimers with other TLRs. Additionally, an efficient immune response often requires the sequential detection of a pathogen by different PRRs in different subcellular compartments, which results in a complex interplay of downstream signaling pathways (69, 70).

After PAMP recognition, TLRs activate intracellular signaling pathways that lead to the production of inflammatory cytokines such as IL-1β, IL-6, IL-12 and TNF-α. Moreover, some TLRs also induce type I IFN production to elicit antiviral responses. Recognition of PAMPs by TLRs stimulates the recruitment of different adaptor molecules, including myeloid differentiation factor 88 (MyD88), MyD88 adaptor-like (MAL), TIR domain-containing adaptor-inducing IFN-β (TRIF), and TRIF-related adaptor molecule (TRAM) (71, 72). Following stimulation, all TLRs, except TLR3, recruit MyD88 via their TIR domains that consequently leads to the activation of nuclear factor-κB (NF-κB) and mitogen-activated protein kinases (MAPKs), to control the expression of inflammatory cytokine genes (71, 73, 74). Importantly, each TLR interacts with different combinations of adapters to activate different transcription factors, giving rise to appropriate and effective responses to pathogens. TLR-5, TLR-7 and TLR-9 interact only with MyD88. TLR-2 heterodimers (TLR-2/1 and TRL2/6) and TLR-4 use MyD88 paired with MAL for the activation of the MyD88-dependent pathway. TRIF is recruited alone to TLR-3 or paired with TRAM to TLR-4 and activates an alternative pathway (TRIF-dependent pathway) that leads to the activation of NF-κB, MAPKs, and the transcription factor IRF3. The activation of IRF3 is crucial for the induction of type I IFN (71, 74-76).

NOD-like receptors (NLRs)

Nucleotide oligomerization domain (NOD)-like receptors (NLRs) are a specialized group of more than 20 intracellular proteins that also play a critical role in host-pathogen interactions and in an inflammatory response (77, 78). Members of this PRR family are defined by a tripartite structure consisting of (a) a C-terminal LRR domain involved in pathogen detection; (b) a central NOD (or NACHT) domain required for self-oligomerization during activation; and (c) a variable N-terminal effector domain, in which four subfamilies of NLRs can de distinguished: NLRA contains an acid transactivation domain; NLRB possess

a baculovirus inhibitor of apoptosis protein repeat (BIR); NLRC has a caspase recruitment domain (CARD); NLRP contains a pyrin domain (PYD) (79).

The NLRA and NLRB subfamilies include only one member, CIITA and NAIP respectively. NOD1 and NOD2 are two well-studied members of the NLRC subfamily, which comprises 6 different proteins (77). NOD1 recognizes D-glutamyl-meso-diaminopimelic acid (iE-DAP), which is a peptidoglycan component of Gram-negative bacteria, while NOD2 recognizes muramyl dipeptide (MDP), which is present in the peptidoglycans of both Gram-positive and Gram-negative bacteria (80-82). NOD2 also seems to recognize mycobacteria cell wall components (83, 84) and viral ssRNA (85). Upon pathogen recognition, these receptors undergo oligomerization leading to the recruitment of mediators such as RIPK2, which interact with NOD1 and NOD2 via a CARD domain. This association results in the activation of NF-κB and MAPK signaling pathways, and consequently the induction of proinflammatory genes (78, 86). NRL members that have a pyrin domain at their amino termini constitute the NRLP subfamily. NALP3 is the best-characterized member and together with other NRLs have been shown to form inflammasomes upon activation (87). The inflammasome is a pro-inflammatory protein complex that activates caspases, resulting in the proteolytic activation of IL-1β and IL-18, as well as in apoptotic and pyroptotic cell death (87, 88). Additionally, inflammasomes are activated by 8 NLRs and their formation is triggered by either endogenous or exogenous, sterile or infectious stimuli. The NLRP3 inflammasome can be activated by the pore-forming activity of a wide range of Gram-positive and Gram-negative bacteria but also with endogenous damage-associated molecular patterns (DAMPs), such as ion efflux, mitochondrial dysfunction, and reactive oxygen species (ROS) (77, 78, 87, 89).

RIG-I-like receptors (RLRs)

Retinoic acid-inducible (RIG) I-like receptors (RLRs) are a family of cytoplasmic RNA helicases responsible for intracellular immune surveillance against viral infections (90-92). This family of sensors encompasses 3 members: retinoic acid-inducible gene I (RIG-I), melanoma differentiation-associated protein 5 (MDA5), and laboratory of genetics and physiology 2 (LGP2) (93). Moreover, this family is characterized by the presence of a central RNA helicase-like domain that recognizes and binds to viral RNAs, and a carboxy-terminal domain (CTD). RIG-I and MDA5 additionally have 2 N-terminal CARD domains that interact with adaptor proteins and activate downstream signaling pathways when viral RNAs are bound (91, 94). The interaction between RLRs and viral RNA activates IRF3 and IRF7 that induce the transcription of genes encoding type I interferons, and NF-κB that leads to the

expression of pro-inflammatory cytokines (95, 96). Interestingly, RLRs not only detect non-self RNA but also self RNAs that are unusual, mislocalized, or misprocessed. The presence of such forms of cellular RNA can be an indirect molecular signature of infection or occur in sterile inflammatory pathologies (96-98).

Scavenger receptor cysteine rich (SRCR)

SRCR receptors constitute a superfamily of extracellular membrane-bound or secreted glycoproteins that is characterized by the inclusion of one or several repeats of a highly conserved scavenger domain having approximately 90 to 110 amino acids (aa) and a high and well-defined cysteine content (99, 100). Based on the number of coding exons and intradomain cysteine residues, two types of SRCR members are described. Those with type A domains, each encoded by two or more exons and containing six cysteine residues forming three disulfide bonds, and those with type B domains, which are encoded by a single exon and have eight cysteine residues forming four disulfide bonds (99-102). Despite their name, scavenger receptors are involved in more than just scavenging. In the past few years, an impressively broad range of functions have been attributed to SRCR members including lipid transport, pattern recognition, mediating apoptosis, regulating T cell activation, and others (103-105). Although no unifying role for this superfamily has been described, all members seem to have some immune-related function. This heterogeneity in SRCR members arise from slight differences in the domain sequences that can impact on the overall structure of each protein, by the number of SRCR domains present in each protein, that are found singly or in tandem, and because some SRCR receptors are multidomain proteins containing other functional domains such as mucin-like, C1r/C1s Uegf Bmp1 (CUB), and zona pellucida (ZP) domains, among others (106-108).

SRCR proteins as pattern recognition receptors

Scavenger receptors were first identified by Golstein and Brown in late of 1970s and their activity was initially associated with the ability to bind and internalize oxidized low-density lipoprotein (oxLDL) (109, 110). It is now accepted that the range of ligands that they recognize is extremely diverse and includes microbial structures, such as LPS and LTA, but also viral, fungal, and parasitic structures (99, 111, 112). Indeed, given their ability to recognize such a large repertoire of ligands, over the last few years the SRCR-SF is emerging as an important class of PRRs. Additionally, other evidence has highlighted the distinctive PRR role of SRCR proteins. Firstly, unlike most members of other PRRs classes, where each receptor seems to have some specificity to a certain PAMP, SRCR proteins

typically bind multiple PAMPs (113-115). Secondly, the SRCR proteins are extracellular proteins expressed at the surface of cells, or secreted and therefore in circulation, which provides SRCR proteins an exceptional feature to intercept and recognize invasive pathogens (116-118). Thirdly, besides playing a role as PRR, SRCR proteins often share other important functions in the immune response such as in cell adhesion, endocytosis, phagocytosis, antigen presentation and cell signaling that ultimately lead to the modulation of the immune response (99).

The microbial binding capacity of the highly conserved SRCR domains was first addressed using different fragments of the group B protein deleted in malignant brain tumors 1 (DMBT1). Only the peptides that corresponded to the SRCR domains were found to bind to microbes, suggesting that it is the SRCR domain that mediates pathogen recognition (119). Moreover, further studies using the group B CD5 molecule like (CD5L) and the group A macrophage receptor with collagenous structure (MARCO) proteins also demonstrated the involvement of the SRCR domain in microbial binding (120, 121). However, in the macrophage scavenger receptor (MSR1), also known as scavenger receptor class A member 1 (SR-A), one of the natural isoforms that lacks the SRCR domains, SR-AII, could also bind bacteria, demonstrating that for the MSR1/SR-A receptor the SRCR domain is not required for microbial binding (122).

CD5L

CD5L was first identified in 1997 as a lymphoid tissue-secreted protein (Spα), although due to its anti-apoptotic functions it is also known as apoptosis inhibitor expressed by macrophages (AIM) and apoptosis inhibitor 6 (Api6) (105, 123). CD5L has the same extracellular domain organization as the ectodomain of the T lymphocyte antigen CD5, both possessing three SRCR domains, but unlike the latter which is membrane bound, CD5L is a secreted glycoprotein with 347 aa (123, 124). CD5L is mainly produced by tissue-resident macrophages in lymphoid tissues, including spleen, lymph nodes, thymus, bone marrow and fetal liver, via transcriptional activation of nuclear receptor liver X receptor/retinoid X receptor (LXR/RXR) heterodimers and/or the transcriptional factor MafB (105, 125, 126).

CD5L circulates in the blood at high concentrations (~5 μg/ml), with relatively higher levels in women (6.06 ± 2.09 μg/ml) than in men (4.99 ± 1.76 μg/ml), and it is higher in young men and women (aged 20s) (127). Importantly, CD5L in blood associates with pentameric immunoglobulin M (IgM) in the Fc region, which prevents CD5L from being excreted into the urine due to the large molecular size of the IgM-CD5L complex (128-132). Although the association between IgM and CD5L seems to be crucial for the maintenance

of high levels of circulating CD5L, the mechanism and how IgM controls CD5L levels remains unclear (128). Recent studies have shown that IgM-bound CD5L is functionally inactive and that CD5L dissociates from IgM to exert its functions (111, 133). Thus, IgM may control the activity of circulating CD5L and the amount of free CD5L molecules to defend the host against different diseases (133, 134).

As mentioned before, in normal conditions CD5L does not reach the renal tubular lumen since IgM-CD5L complexes cannot pass through the glomerulus. However, during acute kidney injury (AKI), dissociated CD5L was found in urine samples from individuals with active disease. It was also found that CD5L accumulates on the intratubular debris where it binds to kidney injury molecule 1 (KIM-1), which is expressed on injury tubular epithelial cells and enhances the phagocytic elimination of the cellular debris by epithelial cells, thus contributing to kidney tissue repair. Additionally, in mice subjected to ischemia-reperfusion-induced AKI, CD5L-deficient mice showed abrogated debris clearance, persistent renal inflammation, and consequently higher mortality than in wild-type (WT) mice. Moreover, treatment with recombinant CD5L protein leads to the removal of cell debris, decrease of inflammation, and a marked improvement of survival (133).

CD5L as anti-apoptotic factor

CD5L has also been reported as a factor that protects macrophages against different apoptosis-inducing stimuli, including oxidized low-density lipoprotein (oxLDL), cycloheximide, but also, caused by infection with *Bacillus anthracis*, *Escherichia coli*, *Listeria monocytogenes*, and *Salmonella typhimurium* (125, 135-137). In accordance, the development of the CD5L knockout (KO) mice has highlighted the role played by the mouse homolog of CD5L as an anti-apoptotic protein. In the CD5L KO mouse, CD4-CD8 double-positive (DP) thymocytes were more susceptible to apoptosis induced by dexamethasone and irradiation *in vivo*. Additionally, in *in vitro* experiments, recombinant mCD5L improved significantly cell viability of DP thymocytes and monocyte-derived cell line J774A.1 from different apoptotic stimuli (105). More recently in another study, it was reported that CD5L promotes survival of *Listeria monocytogenes*-infected macrophage-like ZBM2 cells by inhibiting the activation of caspase-1 (136). Although some data exist both in the human and mouse CD5L, further studies are needed to clarify the intracellular mechanisms underlying CD5L and apoptosis.

CD5L as pattern recognition receptor

Like other SRCR proteins, both human and mouse CD5L can also recognize and bind to different pathogens (99). It was first showed that human CD5L can act as a PRR for several Gram-negative and Gram-positive bacteria through the direct binding of LPS and LTA respectively. Curiously, using a truncated form of CD5L containing only the first SRCR domain, it was demonstrated that the isoform retained the bacterial binding properties of the full molecule. Additionally, it was also revealed that CD5L promotes bacterial aggregation, which additionally strongly suggests that CD5L has multiple binding sites in each of the three scavenger domains (121). *In vitro* experiments also showed that mouse CD5L can bind to both Gram-negative and Gram-positive bacteria and promotes bacterial aggregation. In addition, both human and mouse CD5L can also physically interact with fungi and can recognize fungal cell wall components, such as zymosan, β-D-glucan, and mannan (113).

Clearance of pathogens and their components are crucial to tissue homeostasis. Different studies have shown that soluble pattern recognition receptors (sPRRs) such as collectins, ficolins and pentraxins, in addition to their ability to bind to a wide range of pathogens can also contribute to pathogen clearance by promoting opsonization and subsequently increased phagocytosis by phagocytic cells (138-141). This feature is also extended to some SRCR proteins, including CD5L. *In vitro* experiments showed that CD5L enhances phagocytosis of latex beads, cellular debris, and apoptotic cells (133, 142, 143). More recently, it has also been shown that *Staphylococcus aureus* pretreated with CD5L improves the phagocytic capacity of both macrophages and neutrophils (144).

CD5L as inflammatory mediator

During the last years, there has been an increased interest in CD5L and its function in inflammation. It is noteworthy that the multifunctional role of CD5L makes an overall understanding of this receptor difficult. Additionally, some reports have been shown apparent contradictory results, which highlight not just the complexity of CD5L but also the importance of this protein in the immune system.

T_H17 cells are critical for the maintenance of mucosal immunity and in the host defense against fungal and extracellular bacteria (145-147). However, pathogenic T_H17 cells, can contribute to the pathogenesis of numerous autoimmune diseases (28, 148). Recently, it was found that CD5L is a key player that controls the switch between pathogenic and non-pathogenic T_H17 cells. CD5L is expressed in non-pathogenic but not in pathogenic T_H17 cells, and loss of CD5L converts non-pathogenic into pathogenic T_H17 cells that can

promote autoimmunity and inflammatory diseases (103, 149, 150). The functional role of CD5L in the plasticity of T_H17 cells was observed *in vivo* in experimental autoimmune encephalomyelitis (EAE), a murine model that mimics human multiple sclerosis. Wang *et al.* reported that CD5L KO mice exhibited more severe clinical EAE symptoms than the WT mice. This observation was consistent with increased levels of both T_H17 $CD4^+$ T cells and IL-17/IFN-γ double producer $CD4^+$ T cells in the central nervous system (CNS) of CD5L KO mice and an overall augment of a pro-inflammatory environment (103). Although Wang and colleagues showed increased susceptibility of CD5L KO mice to EAE, a recent study has reported the opposite. In this study, the authors showed that CD5L binds to the p19 subunit of IL-23, which activates STAT5 and enhances the differentiation into granulocyte-macrophage colony-stimulating factor (GM-CSF)-producing $CD4^+$ T cells. Furthermore, using CD5L KO mice there were observed significantly alleviated EAE symptoms with a reduction of GM-CSF $CD4^+$ T cells. Thus, this study suggested that the p19/CD5L heterodimer induces cell proliferation, augmentation of GM-CSF expression, resulting in exacerbation of the CNS inflammation in EAE (151).

CD5L as polarizing cytokine

The role of CD5L in the plasticity of macrophages was also addressed recently. Depending on the microenvironment, macrophages can be activated and polarized into diverse subsets that display a differential expression profile of cytokines and cell-surface markers. Based on their function, macrophages can be divided into two main categories: classical M1 and alternative M2 macrophages (152, 153). The M1 prototypic macrophages are driven by IFN-γ alone or together with microbial products, such as LPS, or cytokines, namely TNF. M1 macrophages are potent effector cells integrated into T_H1 responses and are characterized by a high capacity to present antigen, production of IL-12 and IL-23 and consequently activation of a pro-inflammatory response (type I response), and high production of nitric oxide (NO) and reactive oxygen species (ROS) (154-156). The M2 phenotype can be subdivided into M2a, M2b, M2c, and M2d subsets. The M2a phenotype can be polarized by T_H2 cytokines, namely IL-4 and IL-13, whereas immune complexes, IL-1 receptor (IL-1R) ligands, and LPS induce the M2b lineage, and M2c is driven by glucocorticoids, IL-10 and TGF-β. The fourth subtype, M2d macrophages, are induced by IL-6 and adenosine (155-157). Overall, M2 macrophages tune the inflammatory responses by scavenging cell debris (M2 macrophages show more phagocytic activity), promoting angiogenesis, tissue remodeling, and repair (155, 158, 159).

Interestingly, it was found that CD5L promotes the polarization of macrophages towards an M2 phenotype, similar to the M2c. Both peripheral blood monocytes and THP-1 cells (an acute monocytic leukemia cell line) cultured with CD5L induced the expression of CD136, MERTK, CD36, and VEGF, as IL-10 did. Moreover, it was also found that the CD5L-polarized macrophages in response to LPS secreted lower amounts of pro-inflammatory cytokines such as TNF-α, IL-1β and IL-6, and showed an increased phagocytic capacity to remove apoptotic cells. Accordingly, CD5L-polarized macrophages also showed, as IL-10 did, increased signal transducer and activator of transcription 3 (STAT3) phosphorylation, which is a master transcriptional factor of M2c macrophages (143). Notably, a recent report linked IL-10 and CD5L, whereby demonstrated that treatment of murine bone marrow-derived macrophages (BMDMs) with IL-10 augment CD5L expression through STAT3 activation. Stimulation with IL-10 promotes STAT3 phosphorylation and translocation to the nucleus where it binds directly to the promoter of the CD5L gene, leading to increases in the CD5L promoter activity and consequently the production of CD5L (160).

CD5L as modulator of autophagy and inflammasome formation

Autophagy is a crucial cellular homeostatic mechanism, whereby cells autodigest unnecessary or dysfunctional cytoplasmatic components by enclosing this material in a double-membrane vacuole called an autophagosome which, through fusion with lysosomes, delivers sequestered material for degradation (161). Nevertheless, this eukaryotic pathway also plays multiple functions in innate and adaptive immunity, such as elimination of intracellular microorganisms, contributes to antigen presentation, and affects T cell homeostasis (162-165). Moreover, autophagy is also a potent anti-inflammatory process that downregulates type I IFN responses and inhibits inflammasome activation (162, 166).

Accordingly, in a recent study it was shown that CD5L-expressing THP-1 cells infected with *M. tuberculosis* have an enhancement of mycobactericidal activity. Importantly, in this study CD5L did not enhance the phagocytic capacity of THP-1 cells against *M. tuberculosis*. Rather, two antimicrobial peptides, DEF4B and cathelicidin, involved in the vitamin D dependent antimicrobial pathway were enhanced in the *M. tuberculosis* infected CD5L-expressing THP-1 cells (167-169). This observation is relevant given that recent discoveries have revealed the importance of vitamin D-dependent pathway in the induction of autophagy and their contribution to intracellular killing (170). Additionally, CD5L increased cellular levels of autophagy markers such as LC3 II and LC3

puncta in CD5L-expressing THP-1 cells upon *M. tuberculosis* infection or CD5L-treated PB monocytes challenged with LPS or Pam3CSK4. Electron microscopy analyses also revealed the presence of autophagosome vesicles in CD5L-expressing THP-1 cells while no vesicles were observed in the control THP-1 cells. Moreover, silencing experiments implied that the role of CD5L in autophagy is dependent on CD36; however, the mechanisms underlying the CD5L-CD36 interaction and autophagy activation remain unclear (167, 171).

Saitoh *et al.* were the first to demonstrate the link between autophagy, inflammasome activation, and cytokine production (172). The inflammasome was first described in 2002 by Martinon *et al.* as a large multimeric protein complex required for caspase-1 processing and activation of IL-1β (88). As mentioned previously, the inflammasome can be assembled by a set of NLRs that include NLRP1b, NLRP3, and NLRC4, upon the recognition of PAMPs by TLRs to induce the priming signals (NF-κB and MAPK signaling pathways, and consequently the induction of proinflammatory genes) that are necessary for the upregulation of inflammasome components, followed by the recognition of cytoplasmic danger signals by NLRs (173-176). Recent studies have shown that CD5L can downregulate IL-1β secretion. CD5L-treated PB monocytes stimulated with Pam3CSK4 or LPS produced considerably lower amounts of IL-1β (171). Additionally, Kim *et al*. have shown that BMDMs from CD5L KO mice treated with IL-10 in response to LPS produce considerably higher levels of IL-1β than WT BMDMs treated with IL-10 in response to LPS (160). Importantly, IL-10 was recently described as a negative regulator of inflammasome activation and inducer of autophagy, and in both cases IL-10 signaling via STAT3 inhibits mammalian target of rapamycin (mTOR) activation (177, 178). Remarkably, the involvement of CD5L in the inhibition of the inflammasome seems to be IL-10 independent. It was demonstrated, using BMDMs from IL-10 KO mice stimulated with LPS/ATP, that the subsequent addition of exogenous CD5L still inhibits the production of IL-1β. Furthermore, the mechanisms underlying IL-10 and CD5L inflammasome inhibition seem to be different. Although CD5L reduced the levels of mature caspase-1 in the supernatants of BMDMs from both IL-10 KO and WT mice, exogenous CD5L did not affect the levels of NLRP3 and ASC expression, as IL-10 did. Additionally, it was found that CD5L inhibits the production of cellular and mitochondrial reactive oxygen species (ROS), which are triggers of inflammasome activation (160, 179). Taken together, these observations suggest that CD5L inhibits ROS production, that may lead to the downregulation of inflammasome activation and consequently downregulation of IL-1β. Nonetheless, whether

and how CD5L and IL-10 could affect each other's signaling pathways in the inflammasome regulation remains for further investigation.

CD5L in atherosclerosis

Atherosclerosis is the major contributor to cardiovascular diseases and has been one of the leading causes of morbidity and mortality worldwide (180). This disease is characterized by the accumulation of fatty and fibrous material in the innermost layer of the arterial wall, that leads to the formation of the typical atherosclerotic plaque. The retention of LDL particles, the major extracellular carrier of cholesterol, can induce biochemical modifications by proteases and lipases (181). These oxidative modifications lead to the formation of oxidized LDL (oxLDL), which can elicit an innate inflammatory response.

Atherosclerosis is indeed an inflammatory disease. In response to the accumulation of modified lipoproteins, endothelial cells produce GM-CSF and also macrophage colony stimulating factor (M-CSF), which elicit the recruitment of infiltrating monocytes that will differentiate into macrophages (180-182). Importantly, the continuous engulfment of oxLDL by monocyte-derived macrophages leads to the transformation of macrophages into foam cells, the hallmark of atherosclerosis (183). Additionally, this uptake of modified LDL particles by macrophages is mostly mediated by two scavenger receptors, SR-A and CD36 (184-186). Modified LDL is known to induce a persistent pro-inflammatory microenvironment and to promote apoptosis in a variety of different cells, including foam macrophages (187). In late disease stages, atherosclerotic lesions reveal large necrotic cores caused by apoptosis of foam macrophages and, eventually, plaque rupture and acute vascular events (180, 188).

As expected, macrophages from CD5L deficient mice are highly susceptible to oxLDL-induced apoptosis *in vitro* and undergo accelerated apoptosis *in vivo* in atherosclerotic lesions (189). Additionally, it was found that CD5L binds to oxLDL and enhances oxLDL endocytosis via CD36 (137). Surprisingly, the atherosclerosis lesions in CD5L KO mice are significantly reduced when compared to WT control mice (189). These observations are in accordance with other studies, whereby deficiency of pro-apoptotic factors, such as Bax and p53 leads to suppression of apoptosis in foam cells and accelerates atherosclerosis progression (190, 191). Additionally, deficiency in the transcription factor MafB that regulates the expression of CD5L leads to accelerated foam-cell apoptosis due to the reduction of CD5L expression, and subsequently reduced atherosclerotic lesions. Macrophage apoptosis prevents the formation of the atherosclerotic plaque and the development of atherosclerosis since foam cells are cleared by efferocytosis

in early lesions (126). Altogether, these observations imply that the anti-apoptotic role of CD5L promotes long-surviving of mature foam cells that accumulates within the artery wall leading to the expansion of the lesions, contributing to increased inflammation and disease progression.

CD5L in IgA nephropathy

IgA nephropathy (IgAN) is the most common primary glomerulonephritis that can progress to renal failure (192, 193). IgAN progression requires at least four different processes: (1) increased serum levels of aberrant *O*-galactosylated IgA1 (Gd-IgA1); (2) production of autoantibodies against Gd-IgA1; (3) formation of pathogenic IgA1 immune complexes (together with IgM, IgG, and complement 3 (C3)); and (4) glomerular mesangial deposition of IgA1 immune complexes, that leads to activation and proliferation of mesangial cells and consequently overproduction of cytokines, chemokines, and complement (194). These immune deposits result in chronic inflammation and glomerular damage, which are associated with the infiltration of macrophages and T cells in the glomerular mesangial region (192, 194, 195).

Since CD5L associates with IgM, the role of CD5L in IgAN has been addressed recently (130, 196). During IgAN, it was found that in humans and mice CD5L colocalized with IgA/IgM/IgG immune complexes in the glomerular region, while healthy controls did not exhibit CD5L deposition. Using the gddY mouse model, a model that spontaneously exhibits IgAN-like symptoms, together with CD5L KO gddY, it was observed that both exhibit glomerular accumulation of IgA at comparable levels. Interestingly, CD5L KO gddY mice were protected from glomerular lesion, since they did not exhibit accumulation of IgM/IgG/C3, leukocyte infiltration, neither upregulation of inflammatory genes. Moreover, recombinant CD5L administration restored the IgAN phenotype in the CD5L KO gddY mice (196).

CD5L in sepsis

According to the World Health Organization (WHO) global epidemiology and burden of sepsis report, in 2017 it was estimated that 49 million individuals worldwide were affected and approximately 11 million individuals died due to sepsis. This represents roughly 20% of the annual death toll – approximately 1 in 5 deaths worldwide. The concept and definition of “sepsis” have evolved over time as medical and scientific knowledge has increased and improved. The most recent definition of sepsis (Sepsis-3) defines sepsis as a “life-threatening organ dysfunction caused by a dysregulated host response to infection”.

Additionally, sepsis is the ultimate cause of death for severe infectious diseases, including not just bacterial infections, but also parasitic, viral, and systemic fungal infections (197).

Recently, the role of CD5L in sepsis was investigated using a cohort of 150 adult patients with sepsis. The serum levels of CD5L were dramatically increased in patients with sepsis in comparison with healthy control subjects. Additionally, the levels of CD5L were increased in patients with septic shock, in patients with bacterial-associated sepsis, and in non-surviving patients, in contrast with patients without septic shock, in patients with non-bacterial-associated sepsis, and in patients that outlived sepsis, respectively (198). Gao *et al.* also attributed a role for CD5L in sepsis, using the polymicrobial sepsis-induced murine model of cecal ligation and puncture (CLP) (199). Similarly to CD5L levels in human patients with sepsis, mice developing sepsis presented a substantial increase of CD5L in the peritoneal lavage fluid (PLF) and blood 6 hours after CLP (198, 199). Additionally, CLP-induced C57BL/6 mice treated intraperitoneally with a mouse anti-CD5L antibody had an increased survival percentage in a dose-dependent manner. The reduced mortality observed in the CD5L-blocked mice after CLP induction was associated with a general improvement in organ damage. Also, mice treated with anti-CD5L antibodies showed a significant reduction of TNF-α, IL-6, IL-10 and CCL2 levels in serum, and a reduction in macrophages, neutrophils, and T cells infiltration in the peritoneum. Furthermore, exogenously administration of CD5L immediately after CLP induction decreased the percentage of survival, which seems to be associated with increased inflammation and organ damage (199).

Apparently contradictory results were observed with the administration of growth differentiation factor 3 (GDF3) either before or after CLP surgery since GDF3 improved the percentage of survival. Notably, RNA-seq analysis revealed that CD5L was the most significantly upregulated gene in GDF3-treated macrophages. Mice treated with GDF3 showed a significant reduction of bacterial load, pro-inflammatory cytokines, and organ damage. The authors suggested that the mechanism underlying GDF3-induced phagocytosis could be due to the activation of LXRα, and consequently upregulation of CD5L, which promotes phagocytosis of bacteria and cell debris, contributing to the resolution of the inflammatory process (200).

In another study, Tomita *et al.* showed that CD5L KO mice were more susceptible than WT mice to zymosan-induced peritonitis, developed by daily intraperitoneal injection with zymosan for 5 days (201). The CD5L KO mouse showed at days 28 post-induction strong inflammatory cell infiltrates associated with necrotic areas while the WT mouse showed signs of resolution of the inflammation and tissue regeneration without necrosis.

Similarly, in other studies CD5L KO mice have at day 28 more inducible nitric oxide synthase (iNOS) positive macrophages (M1-like), whereas M2-like CD206 positive macrophages were predominant in the WT mouse. Additionally, the administration of CD5L ameliorates peritoneal inflammation associated with necrosis in the CD5L KO mouse, suggesting that CD5L appears to be involved in the repairment of zymosan-induced peritonitis by the enhancement of necrotic tissue clearance (201). Curiously, quantification of circulating CD5L in patients with chronic kidney disease on peritoneal dialysis indicated a higher risk of peritonitis in patients with low levels of CD5L, suggesting that CD5L could have some protective role against peritonitis (201). In contrast, Kimura *et al.* have shown that the resolution of inflammation was accelerated in CD5L KO mice when compared with WT mice in the LPS-induced acute lung injury model (202). Moreover, the exogenous administration of CD5L reversed the phenotype observed in the CD5L KO mouse. The observed phenotype was attributed to the presence of CD5L leading to the suppression of macrophage phagocytosis of apoptotic neutrophils, indicating a possible role of CD5L in the inhibition of efferocytosis (202).

SSC4D

Human SSC4D (also known as S4D-SRCRB) is a 575-aa-long soluble protein organized in four SRCR domains arranged in tandem. Each domain contains 101 aa spaced by small Pro-, Ser-, and Thr-rich regions (~30 aa), except the interdomain that separates domains 2 (SSC4D-d2) and 3 (SSC4D-d3), which is longer (~50 aa). The aa sequence contains an N-terminal signal peptide (10 aa) but no transmembrane-encoding region, and no potential *N*-linked glycosylation sites were found. In contrast, some putative *O*-glycosylation sites are annotated in the SSC4D aa sequence. This observation may bring to light some possible biologic functions of SSC4D since some recent studies reveal the relevance of glycosylation in pathogen recognition, modulation of the innate immune response, and inflammation. Thus far, no data has revealed either the function or the characterization of the SSC4D protein. Indeed, there is only one publication documenting SSC4D. Padilla *et al.* have shown by northern blot analysis that *SSC4D* might be broadly expressed in human tissues, particularly highly expressed in the kidney and placenta and moderately expressed in the liver, small intestine, spleen, and thymus. It was also shown that *SSC4D* is expressed in epithelial cells lines, namely HepG2 and CACO-2, which might suggest that SSC4D is mainly produced by epithelial cells across human tissues (203).

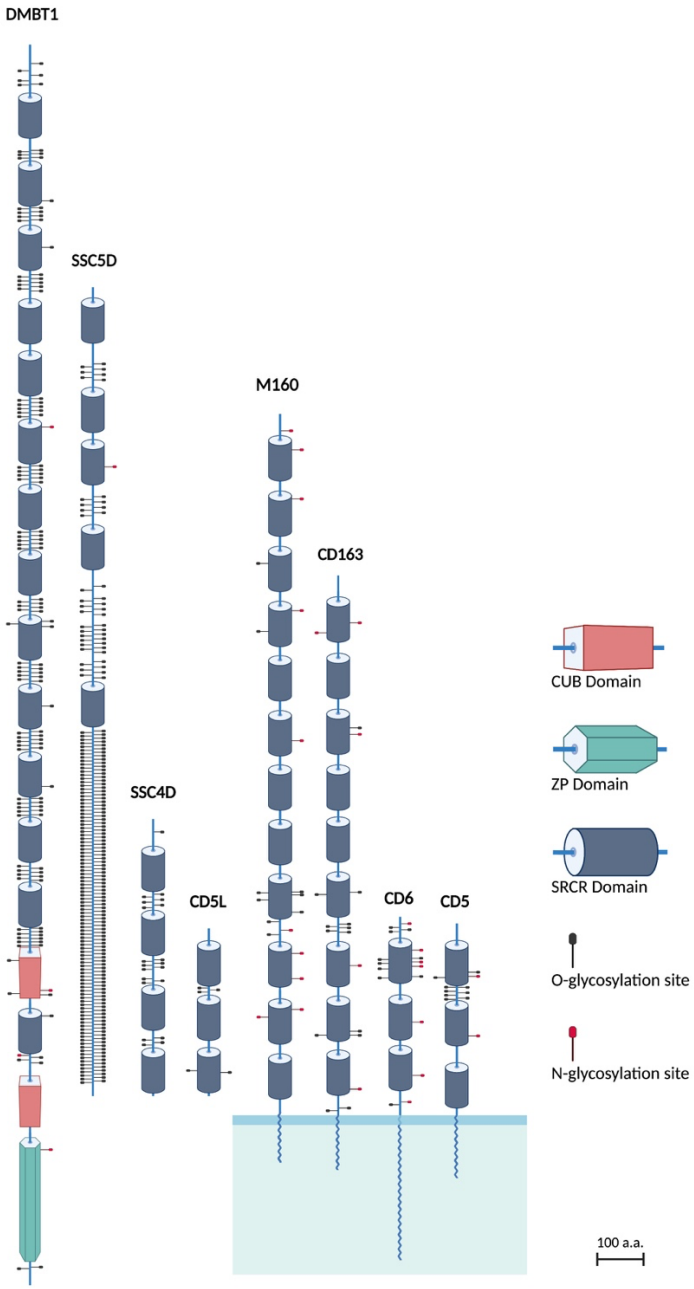

Figure 1 – Schematic representation of the human group B SRCR members. SRCR proteins were drawn to scale according to the amino acid (a.a.) sequence. SRCR domains are represented as dark cylinders. CUB domains are represented as reddish cube. ZP domain is represented as greenish hexagon. Putative *O*-linked glycosylation sites are represented as short lines with black circles and *N*-linked glycosylation sites as lines topped with red circles.

The inflammatory response

According to Medzhitov, the inflammatory response is a biological reaction to a disrupted tissue homeostasis triggered by noxious stimuli, such as infection or tissue injury (204). This response involves the coordination of a substantial range of mediators and inducers. Inducers, such as PAMPs and DAMPs, are signals that activate specific immune sensors, which elicit an inflammatory response. On other hand, mediators are produced in response to a particular combination of an inducer-sensor pathway. Upon invasion of a Gram-negative bacteria, the LPS (inducer) present at the surface of bacteria is recognized by the membrane-bound TLR4 (sensor) that elicits an inflammatory response and triggers cells to produce TNF-α (mediator). Many of these mediators can alter the functionality of tissues and organs by promoting a proper inflammatory environment that impacts on the vasculature, cell activation, and cell recruitment (67, 205). The ultimate goal is to eliminate the source of the disrupted homeostasis, restoring the tissue functionality and homeostasis. If the inducer persists in the host, then the early or acute inflammatory response shifts to a long-term or chronic inflammatory response. However, these inflammatory responses came at a price. In fact, a large number of human diseases are caused by uncontrolled inflammatory reactions that may induce permanent tissue destruction. Different effector cells, such as neutrophils or macrophages, released noxious soluble factors including highly reactive oxygen species (ROS) that are destructive to both pathogens and hosts (59, 204). For these reasons, the last phase of inflammation is its resolution; otherwise, the persistent pro-inflammatory environment might cause dysregulated inflammation, cytokine storm, septic shock, and ultimately death. The inflammatory response resolution is orchestrated by different mediators that through several events such as the influx of recruited cells, must be halted, cell debris must be removed, and inflammatory cells present at the site must be polarized to an anti-inflammatory phenotype, promoting tissue repairment (204, 205).

Considerable advances have been made in the last decade, mostly in the identification of new inflammatory components (inducers, sensors, effectors, and mediators). However, inflammation is an exceedingly complex process that is not fully understood. Thus, more data, about the interplay between the different inflammatory components and which signals regulate all the inflammatory processes will be necessary for further pursuit of this critically important and fascinating field.

One of the major aims of my PhD work is to understand the role of a particular molecule (CD5L), which can act as a sensor and mediator during the inflammatory

response, and how CD5L orchestrates the inflammatory response against *Trypanosoma*, *Leishmania*, and *Plasmodium* infections.

Trypanosoma

Human African trypanosomiasis (HAT), also known as sleeping sickness, is a neglected tropical disease that occurs mainly in sub-Saharan regions. Although HAT is classically transmitted by the bite of the blood-sucking tsetse flies (Diptera, genus *Glossina*), other routes of transmission have been sporadically described, including sexual, blood transfusion, and organ transplantation (206-208). There are two clinical variants of HAT, the slow-progressing form, caused by *Trypanosoma brucei gambiense* (*T. b. gambiense*), which is endemic in Western Africa, and, the faster-progressing form, caused by *Trypanosoma brucei rhodesiense* (*T. b. rhodesiense*), found in Eastern Africa (206, 209, 210). Although approximately 60 million people throughout 36 African countries are at risk from developing the disease, nowadays the disease frequency is rare, mostly due to large-scale coordinated efforts and efficient deployment of an albeit incomplete arsenal of control tools. In the absence of a vaccine, disease control relies on vector control, efficient case detection, and treatment. The current pharmacological therapy for HAT relies on suboptimal drugs that were developed many years ago and have some degree of toxicity; however, ongoing clinical trials promise safer and simpler treatments (211, 212).

In addition to *T. b. rhodesiense* and *T. b. gambiense*, *T. brucei* species also includes *Trypanosoma brucei brucei* (*T. b. brucei*), which causes animal African trypanosomiasis (AAT). AAT is also known as nagana, is not infectious to human beings and affects mostly cattle and horses. According to the Food and Agriculture Organization of the United Nations (FAO), ATT has profoundly affected the settlement and economic development of a major part of a continent. Although ATT still imposes devastating impacts on agriculture, current drugs and increased surveillance has been crucial for disease control (213, 214).

Trypanosoma life cycle

The parasite's journey through the mammalian host starts with the injection of metacyclic trypanosomes into the skin. During the first stage (hemolymphatic stage) of infection, the parasite multiplies by binary fission and spreads via the lymph and blood to different organs and tissues. The parasite then can cross the blood-brain barrier (BBB) into the central nervous system (CNS), a process that marks the second stage (encephalitic stage) of the disease (206). This stage is characterized by a marked CNS pathology with a

typical inflammatory infiltrate. In addition to CNS pathology, hemolytic anemia, hepatomegaly, and abnormal liver function, splenomegaly, cardiac involvement such as pericarditis and congestive cardiac failure are some of the most prevalent clinical manifestations associated with *T. brucei* infection in mammals (215, 216). All *T. brucei* subspecies are morphologically indistinguishable and all cells contain a nucleus, a mitochondrion that contains the kinetoplast, and a flagellum. During its lifecycle, which includes both mammalian and tsetse fly, *T. brucei* remains extracellular. The cycle is continued when the tsetse fly bites and ingest a "blood meal" from an infected individual or animal. Once ingested, trypanosomes undertake a complex journey through the fly tissues where they undergo a series of biochemical and structural changes until they reach the salivary glands and develop into the human infective metacyclic forms (217-219).

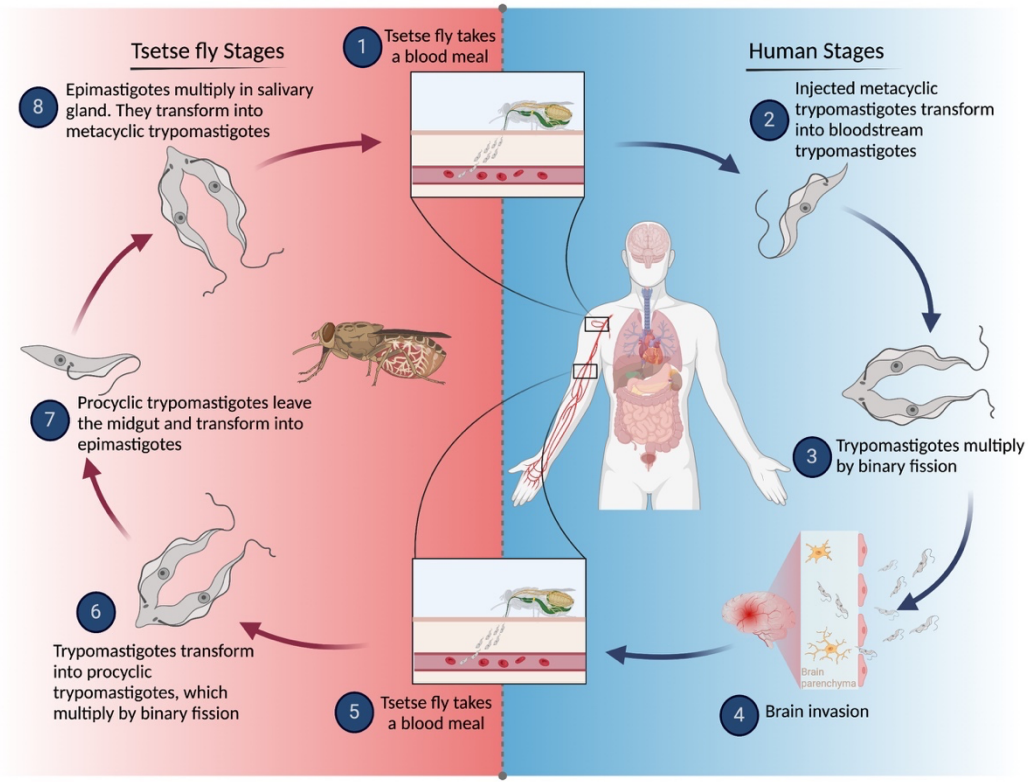

Figure 2 - The life cycle of Trypanosoma. During a blood meal, an infected tsetse fly injects metacyclic trypomastigotes into the mammalian host (1). Infective trypomastigotes migrate into the bloodstream and then transform into bloodstream trypomastigotes (2). The circulating parasites can initiate replicative cycles by binary fission (3). The trypomastigotes can invade different organs, including the brain (4). Naïve tsetse fly becomes infected by taking bloodstream trypomastigotes during a blood meal (5). Trypomastigotes transform into procyclic trypomastigotes in the fly midgut (6). Procyclic trypomastigotes leave the midgut and transform into epimastigotes (7). Epimastigotes migrate to the salivary glands and continue multiplication by binary fission and transform into metacyclic trypomastigotes (8). Adapted from the US Centers for Disease Control and Prevention.

Immune response against Trypanosoma

In the mammalian host, the *T. brucei* cell membrane is coated with a GPI-anchored antigen termed variant surface glycoprotein (VSG) that protects the parasite from innate immunological attacks (206, 220). These immunogenic glycoproteins induce a specific antibody response that triggers the destruction of all antibody-opsonized trypanosomes. To survive and escape to the antibody-mediated immune response, trypanosomes developed an antigenic variation strategy, whereby the glycoprotein coat is replaced by an antigenically different coat. This strategy generates consecutive waves of parasitemia, which enable the parasite to constantly evade the host's immune response that would otherwise have the ability to destroy the parasite (221, 222). Consequently, *T. brucei* infection usually induces a non-specific polyclonal B-cell activation and therefore high levels of circulating IgM and autoantibodies during the first peak of parasitemia (223). However, several studies have indicated that *T. brucei* leads to B-cell clonal exhaustion, destruction of the splenic B cell compartment, and impairment of B-cell lymphopoiesis, resulting in the hammering of the humoral immune response (224, 225).

In addition, upon cellular stress the activation of a GPI-specific phospholipase C (VSG lipase) elicits a massive release of soluble VSG and CpG DNA into circulation and subsequently PRR recognition triggers T_H1 cell activation. Although the precise macrophage activation mechanism by parasite-derived products remains unclear, different studies have suggested that *T. brucei* PAMP recognition is mainly mediated through TLR9 and SR-A (226-228). Initially, it was showed that mouse macrophages deficient for TLR9 are less responsive to *T. brucei* genomic DNA whereby in *in vivo* experiments TLR9 KO mice displayed an increase in parasite burdens. Importantly, despite the increased parasite numbers in the TLR9 KO mice, no survival differences were observed, which suggest that other PRRs may be involved in *T. brucei* recognition (228). In a later study, it was demonstrated that sVSG uptake by macrophages is mediated by SR-A (227, 229).

Additionally, activation of the innate immune system by sVSG and CpG DNA either triggered by TLR9 or SR-A recognition followed by type 1 immune response activation seems to be dependent on MyD88 (228, 229). In both clonal and nonclonal *T. brucei* infection models, the deficiency in MyD88 was correlated with increased parasitemia and decreased survival (228). PAMP recognition by extracellular SR-A followed by internalization of sVGS initiates a cascade of subcellular TLR-independent signaling events that activate the NF-κB and MAPK pathways (227, 229, 230). This sVGS-SR-A ligand/receptor interaction leads to subsequent TLR9 activation followed by the recruitment of MyD88 and activation of pro-inflammatory genes, such as TNF-α, IL-6, IL-12 and GM-

CSF (229, 231). It is known that different classes of PRR can interact functionally and synergistically with other classes of PRR, including TLRs, to generate a fully functional innate immune response. Although different studies showed that SR-A-TLR9 interaction is beneficial to an efficient immune response, the exact mechanism remains poorly understood.

The immune response is further amplified when myeloid cells are primed with IFN-γ. It was shown that different cell populations play a role on IFN-γ production, where NK and NKT cells are the earliest IFN-γ producers, followed by $CD4^+$ and $CD8^+$ T cells (232). The role of IFN-γ has been shown to be critical in host resistance against trypanosomatid parasitic infections (232-234). Deficiencies in IFN-γ have been associated with elevated levels of parasitemia and higher susceptibility (235). On the other hand, early IFN-γ production triggers an acute inflammatory reaction that leads to the development of acute anemia (236-238). Furthermore, it has been proposed that *T. brucei* parasites penetrate the blood-brain barrier (BBB) in an IFN-γ- and TNF-α-dependent manner, whereby TNF-α can induce the expression of adhesion molecules (such as ICAM-1 and VCAM-1) in brain endothelial cells, and IFN-γ can promote the infiltration of T cells and parasites into the brain (231, 239).

Efficient clearance of *T. brucei* by the host requires either IFN-γ, which is crucial for T_H1 and monocytic lineage cell activation, but also TNF-α (240, 241). It was shown that inflammatory monocytes, putatively derived from the bone marrow and IFN-γ primed, gradually accumulate in the spleen, liver, and lymph nodes. These inflammatory monocytes differentiate into inflammatory macrophages or DCs (a particular subset of DCs called TNF/inducible NO synthase-producing dendritic cells (TIP-DCs)), which during *T. brucei* infection were the major source of TNF-α (242). On one hand, it was shown that TNF-α contributes to the clearance of *T. brucei* through its trypanolytic activity. Moreover, results from TNF-α KO mice infected with *T. brucei* have confirmed the role of TNF-α in the control of parasitemia since the TNF-α deficient mice exhibited a significantly higher parasitemia during the consecutive peaks of infection (241). On the other hand, different studies have suggested that TNF-α can be detrimental to the host and may cause immunopathology. First, despite a clear difference in the parasitemia peaks, TNF-α KO mice infected with *T. brucei* are not more susceptible. Moreover, and specifically during the chronic stage of disease, infection-related signs of morbidity were much less pronounced in TNF-α KO mice when compared with WT animals (241). Second, higher levels of TNF-α are correlated with the severity of neuropathological symptoms in human sleeping sickness (243). Third,

dysregulated production of TNF-α by monocytes is associated with the severity of the disease, particularly with anemia in trypanosome-infected cattle (244). Fourth, the expression of TNF-α is augmented in the brain of *T. brucei* infected mice (245). Lastly, the severe reduction of TNF-α levels in the serum leads to increased mouse survival (235). Taken together, the accumulated knowledge about trypanosome-elicited production of both IFN-γ and TNF-α indicates that these cytokines exert dual effects during trypanosome infections, influencing both the parasite and the host.

In deep contrast with IFN-γ and TNF-α, which have been classified as highly pathogenic, IL-10 has been reported as an antipathogenic molecule in African trypanosome-infected hosts (234, 246, 247). $CD4^+Foxp3^+$ cells as well as M2 phenotype monocytic cells are the major sources of IL-10, which contributes to host protection against trypanosomatid parasitic infections (248, 249). The absence of IL-10 in *T. brucei* infected mice leads to extreme susceptibility that results in death within ~8 days post-infection, compared with ~36 days for WT mice. Importantly, the increased susceptibility in the IL-10 KO mice occurred without a further increase in parasitemia (234). However, this clear difference in survival was associated with an increased percentage of inflammatory cells, namely TIP-DCs. The enrichment of TIP-DCs in IL-10 KO mice is followed by an increase of inflammatory molecules, such as IFN-γ and TNF-α, and consequently associated with enhanced liver injury and early death of the host (234, 246). On the contrary, IL-10 treatment in infected mice resulted in a reduction of monocyte differentiation into TIP-DCs, reduction of pro-inflammatory molecules, lower anemia, protection from liver injury, and prolonged survival (246). Overall, these observations strongly suggest that IL-10 is a key regulator of the balance between protective and pathogenic cellular immune responses during *T. brucei* infection.

Leishmania

Leishmaniasis is one of the most significant neglected tropical diseases, with twelve million people worldwide being affected by one of the many forms of the disease. Moreover, leishmaniases are vector-borne parasitic diseases caused by one of several different species of intracellular protozoan parasites of the genus *Leishmania* and affect people and domestic and wild animals worldwide (250). Leishmaniasis is transmitted between mammalian hosts by sandflies and during their life cycle alternate between two different forms, a flagellated or motile form called promastigote that is found within the sandfly, and an aflagellate form called amastigote, which does not have an exteriorized flagellum and

lives as an intracellular parasite in the mammalian cells (251). Leishmaniases are caused by a total of about 21 leishmanial species, ranging in severity from mild cutaneous or mucocutaneous, to life-threatening visceral manifestations. Distinct species of *Leishmania* cause different clinical manifestations, such as *Leishmania major* and *Leishmania braziliensis* that cause cutaneous lesions, whereas *Leishmania donovani* and *Leishmania infantum* cause visceral leishmaniasis (VL) (250, 252).

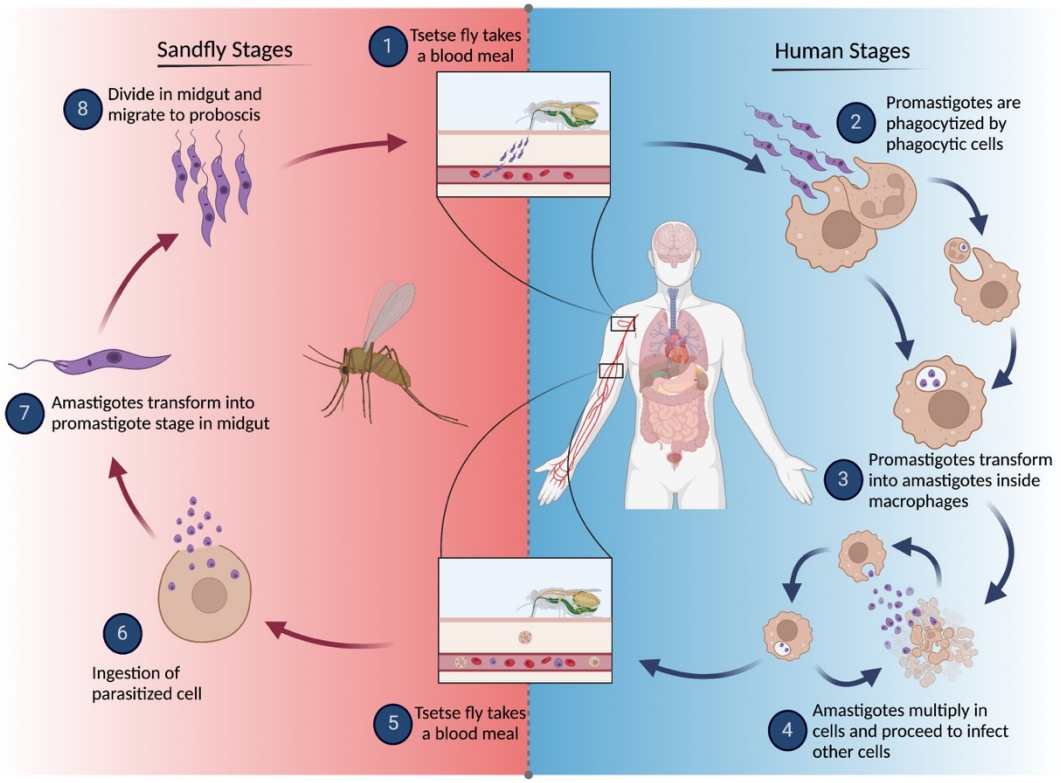

Figure 3 - The life cycle of Leishmania. During a blood meal, infected female phlebotomine sandflies inject metacyclic promastigotes (1). These promastigotes are phagocyted by mononuclear phagocytic cells at the bite site (2). Once inside the host cells, promastigotes transform into amastigotes, which can survive and replicate inside phagolysosomes (3). Amastigote replication may lead to host cells rupture allowing reinfection of other phagocytic cells (4). Sandflies become infected by ingesting infected cells during blood meals (5), which transform back into promastigotes in the sandfly gut (6). Then procyclic promastigotes differentiate into infective metacyclic promastigotes followed by the migration to proboscis (8). Adapted from the US Centers for Disease Control and Prevention.

Visceral leishmaniasis

Although the global incidence of VL decreased substantially in the past decade, more than 50,000 new cases were described worldwide in 2017. *Leishmania infantum* is one of the etiological agents of VL; however, in some cases it can also cause cutaneous lesions (250). The common symptoms of VL include fever, malaise, weight loss, diarrhea, hepatosplenomegaly, and anemia. Parasite visceralization results in impaired function of the liver, spleen and bone marrow with fatal consequences if left untreated.

The life cycle of *Leishmania* parasites starts when a sandfly ingests a blood meal from an infected host. In the vector, the amastigotes undergo a series of morphological changes culminating in the transformation into the metacyclic promastigote forms. This infectious form of the parasite is then inoculated into the host's skin during a blood meal, and the promastigotes are then phagocyted by resident macrophages or other types of mononuclear phagocytic cells. Importantly, in VL, the parasites migrate and replicate in lymphoid organs including the spleen, liver, and bone marrow, eventually leading to organ malfunction. After being established in the intracellular compartment, flagellated promastigotes transform into aflagellate amastigotes. These forms undergo replication inside the phagocytic cell, which ruptures allowing dissemination and reinfection of other cells. The cycle is completed when an infected host is bitten by another sandfly (251).

Host immunity against leishmaniasis

Upon inoculation of an infectious metacyclic promastigote form by sandflies, the parasite immediately starts its battle for survival against the host immune defenses. The sandfly bite attracts different innate immune cells, being neutrophils the fastest to arrive at the infection site and phagocytize the parasites. After residing within neutrophils for an as-yet-unknown period of time after infection, *Leishmania* spp. will colonize macrophages (253). This event is one of the most critical steps for parasite success even though the mechanism is still poorly understood. It has been suggested that *Leishmania* parasites are primarily phagocyted by neutrophils; however, promastigotes use neutrophils as 'Trojan Horses' to achieve their goal. *In vitro* studies have shown that *Leishmania* survives within neutrophil phagosomes, and the infected neutrophils undergo apoptosis and express "eat-me-signals" which are recognized and phagocyted by macrophages. Thus, the parasite evades the macrophage defense mechanisms and allows *Leishmania* promastigotes to be efficiently and safely shuttled into the macrophage phagosome. Importantly, once promastigotes are transformed into amastigotes, the parasite can resist to phagolysosome acidification, resulting in the replication and spreading of the parasite throughout the host's

reticuloendothelial system (251). The involvement of *Leishmania* in the reticuloendothelial system might result in some pathological lesions in the spleen, liver, and bone marrow. Additionally, the role of neutrophils during the early stages of leishmaniasis infection is well established; however, their role in the chronic phase of infection is much less understood probably due to the lack of suitable animal models (254, 255).

Although parasites can be found inside neutrophils, it is in macrophages that there are the best conditions for their replication and long-term survival. Upon infection, *Leishmania* migrates to the liver where is phagocyted by resident Kupffer cells; however, *Leishmania* is well adapted to survive to the hostile environment inside the macrophage phagosome (256). Moreover, recently it has been shown that *Leishmania infantum* can subvert the activation of macrophages into a dormancy state by decreasing the expression of PRRs and cytokine production, and at the same time extending macrophage viability, buying time to establish a visceral infection in the host (251, 257). Therefore, the control of infection relies mostly on successful macrophage activation. To achieve this, the host innate immune system recognizes the parasite through the MyD88-dependent TLR pathway, which triggers the production of T_H1 signature cytokines and consequently initiates type 1 immune response, ultimately leading to the activation of macrophages via IFN-γ (251, 258). It is widely accepted that a refined balance between the inflammatory and regulatory responses is crucial to achieve immune control against *Leishmania* infections. IFN-γ produced by NK and T_H1 cells enhances macrophage activation and promotes leishmanicidal activity mediated by nitric oxide (NO). In contrast, *Leishmania* survival is correlated with a predominantly immunosuppressive response mediated by $CD4^+$ T regulatory cells and regulatory B cells. These cells produce IL-10 and TGF-β (18), decreasing the proliferation of T_H1 cells and then resulting in a lack of M1 macrophage activation, and consequently parasite killing (258, 259).

Although different species of *Leishmania* express specific cell surface molecules, lipophosphoglycan (LPG) is the most abundant present in promastigote forms of different species of *Leishmania* spp., including *L. infantum* (260). The current knowledge concerning *Leishmania*-PAMP recognition is still limited; however, some evidence has shown that different PRRs, including TLRs, might be involved in the recognition of *Leishmania*-derived products (261, 262). It was shown that TRL2 expressed on DCs recognizes *L. infantum* LPG and induces the production of IL-12, which plays a critical role in the development of the protective T_H1 immune response. When compared with wild type mice, $TLR2^{-/-}$ mice infected with *L. infantum* expressed lower levels of IFN-γ and iNOS, while in contrast, $TLR2^{-/-}$ splenocytes produce higher levels of IL-10 after stimulation with parasite antigen

(263, 264). Additionally, it has been shown that TLR9 also plays an important role in the recognition of *L. infantum*. DCs are activated via TLR9 upon infection with *L. infantum* to produce IL-12 that subsequently triggers NK cell cytotoxicity and IFN-γ production (265). Furthermore, the abrogation of TLR9 impaired neutrophil recruitment to the liver and spleen, and consequently protection against parasites (266).

Plasmodium

Malaria is a vector-borne parasitic disease transmitted through the bite of an infected female *Anopheles* spp. mosquito and found in tropical and subtropical regions, causing an estimated 216 million cases across the world, including around 445,000 deaths. The vast majority of malaria incidence occurs in sub-Saharan Africa (approximately 190 million cases) where transmission remains intense in many locations (267). Malaria is caused by the protozoan parasite *Plasmodium*, a member of phylum Apicomplexa, which encompasses more than 120 *Plasmodium* species infecting mammals, birds, and reptiles; nevertheless, only six are known to infect human beings regularly. Among the *Plasmodium* species that can infect humans, *P. falciparum* causes the most severe form of malaria and with higher mortality rates (267, 268). Malaria is classically characterized by two distinct disease classifications: uncomplicated and severe. Symptoms of uncomplicated malaria are non-specific and can include fever, chills, body-aches, headache, cough, and diarrhea. In contrast, severe malaria is characterized by acute manifestations, which include cerebral malaria (CM), severe malaria anemia, acute lung injury that can progress to acute respiratory distress syndrome, acute kidney injury, typically presented as acute tubular necrosis, and acidosis (267).

Plasmodium life cycle

Infection with *Plasmodium* begins when female *Anopheles* mosquitoes inject a small number of motile forms of the parasite, which are called sporozoites, into the skin. Some parasites are rapidly eliminated by skin resident macrophages, whereas others travel through the bloodstream to the liver where they infect hepatocytes. Importantly, liver infection is the first step of *Plasmodium* infection and is characterized by an asymptomatic stage of the disease (269-271). Within hepatocytes, the sporozoites undergo successive cycles of asexual replication that produce thousands of merozoites, which are released into the bloodstream. Each merozoite can invade a red blood cell, marking the beginning of the erythrocytic stages of infection. During this stage, the exponential asexual replication also

results in the generation of sexual forms of the parasites, called female and male gametocytes. When a female *Anopheles* mosquito ingests a blood meal from an infected host, sexual gametocytes enter the midgut of the mosquito, which will fuse to form a motile zygote. Then, they develop into oocysts, in which hundreds of sporozoites are produced and migrate to the mosquito salivary glands, completing the *Plasmodium* lifecycle (267, 270-273).

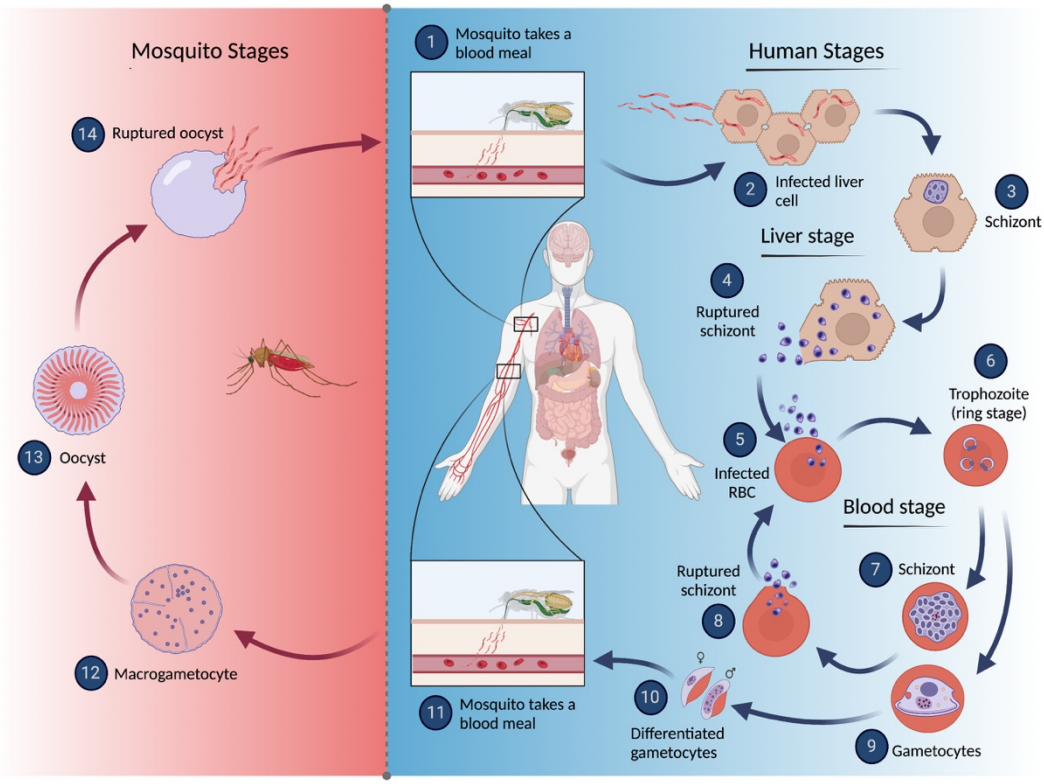

Figure 4 -The life cycle of Plasmodium. Two major well-defined stages can be distinguished according to whether the parasites are in the mosquito or the host. Subsequently, the human stage can be subdivided into two phases, the liver and blood stage. The human infection starts upon infected female anopheles mosquito blood meal and consequently injection of sporozoites (1). Sporozoites migrate from the infection site to the liver through the bloodstream, whereby infects liver cells (2). In the liver cells, sporozoites multiply and mature into schizonts (3). Schizonts rupture and release merozoites (4). Merozoites enter the bloodstream and infect red blood cells (RBCs) (5). Merozoites reproduce and develop into ring forms (trophozoites) (6). Trophozoites mature into schizonts (7). Schizonts rupture and release merozoites into the bloodstream (8). Sexual forms (gametocytes) are also produced (9-10). Gametocytes are taken up by a mosquito upon a blood meal (11). Gametocytes mature in the mosquito gut (12). Male and female gametes fuse by sexual reproduction and form an oocyst (13). Oocyst develop new sporozoites that migrate to the mosquito salivary glands (14).

Plasmodium immune response

Malaria is characterized by systemic inflammation during the blood-stage infection. The rupture of an infected red blood cell (iRBC) and consequent release into circulation of new merozoites and other parasitic components, including nucleic acid–derived factors, urate crystals, histidine-rich proteins, among others, stimulates a strong inflammatory response from phagocytic cells (274-276). As in many other diseases, the activation of innate immunity and inflammatory responses should be strong enough to control parasite replication while at the same time avoiding a response that damages the host. In severe malaria, different innate immune effectors, including monocytes and neutrophils, have been implicated in the pathogenesis of severe malaria through the production of damaging pro-inflammatory cytokines and chemokines. The myriad of parasitic stimulatory products in circulation triggers the activation of different PRRs either cell-related or soluble molecules, leading to downstream responses, including the massive production of pro-inflammatory cytokines by different innate cells (277, 278). Many PRRs have been described in the recognition of *Plasmodium* structures (279). *Plasmodium* GPI is one of the major constituents of the plasma membrane and induces the production of pro-inflammatory cytokines by monocytes through recognition mainly by TLR2-TLR1 heterodimers and to a lesser extent by TLR4 (280, 281). It was also shown that TLR9 sense unmethylated CpG motifs found in parasitic DNA leading to the activation of MyD88-NF-κB signaling pathways, whereas TLR7 recognizes parasitic RNA within DC phagolysosomes, inducing type I IFN production (282, 283). In addition, other PRRs have been described to be involved in the recognition of parasitic PAMPs and DAMPs, namely CD36, which has been involved in the recognition and parasitemia control by up-regulating IFN-γ production by NK cells. Moreover, hemozoin (Hz), a *Plasmodium* product released into circulating, activates the NLRP3 inflammasome and consequently leads to the production of IL-1β (284, 285).

During the liver stage, infected hepatocytes produce type I IFNs in response to the activation of TLR7 by parasitic RNA, which in early time points contribute to parasite-infected hepatocyte elimination by NKT cells (283, 286). Importantly, since the parasite burden during the liver stage is low, the innate immune response is also limited. Thus, antigen-presenting cells do not potentiate the immune response during the liver stage. In contrast, during the blood stage of infection parasites grow exponentially which induces an efficient and vigorous immune response against the parasite (274). The stimulation of PRRs expressed by DCs and monocytes leads to the activation of different signaling pathways that impact on the expression of pro-inflammatory cytokines, namely TNF-α, IL-12, and IL-1β. The production of IL-12 by DCs is fundamental to induce the production of IFN-γ by NK

and T_H1 cells. Although the production of IFN-γ contributes to the efficient control of parasitemia, it is also known that IFN-γ influences CM and other severe malaria clinical conditions (287-289). Either neutralization of IFN-γ, or using IFN-γ KO and IFN-γ receptor KO mice, resulted in a greater resistance to CM (290, 291). Although the nature and molecular mechanisms of CM remain poorly understood, different observations suggest that CM is dependent on the sequestration of iRBCs to the brain parenchyma (292). During the blood stage, iRBCs express ligands on the cell surface that enhance their capacity to adhere to host endothelial receptors. Additionally, different studies propose that increased circulating levels of either pro-inflammatory cytokines (TNF, IL-1β, and IFN-γ) or parasitic products might activate endothelial cells leading to an over-expression of endothelial adhesion molecules such as ICAM-1 and V-CAM (293, 294). This up-regulation improves the interaction between iRBCs and the endothelium, which promotes iRBC sequestration to the micro-vasculature, namely cerebral micro-vasculature, and consequently contributes to blood flow obstruction in micro-vessels causing hypoxia, nutrient deprivation, metabolic disturbances, and ultimately invasion of infected parasites into the brain parenchyma (295). Thus, parasite sequestration contributes to fatal pathologic conditions such as CM, but also to multiorgan pathologic conditions, including renal, liver, and lung dysfunction and failure (294).

Project Presentation

One of the most central functions of the immune system is its ability to recognize and destroy invasive pathogens while avoiding deleterious responses to the host's own components. Different players work in a synchronized way allowing innate immune cells to recognize microorganisms *via* a limited number of germline encoded PRRs, while T and B lymphocytes, from the so called adaptive immunity, display a vast repertoire of different antigen receptors generated somatically during the development.

SRCR receptors belong to a superfamily of extracellular membrane-bound or secreted glycoproteins that is characterized by the inclusion of one or several repeats of a highly conserved scavenger domain and a high and well-defined cysteine content. So far, no unifying function as been attributed to the SRCR superfamily. Actually, an impressively broad range of functions have been attributed to SRCR members including lipid transport, pattern recognition, mediating apoptosis, regulating T cell activation, among others.

Historically, our lab has been interested in study some SRCR-proteins, having recently characterized the ability of SSC5D and CD5L in binding bacteria. The current thesis popped-up as following work where our main goals are:

- characterize novel interactions between SRCR proteins and microbes, pursuing the hypothesis that SRCR members bind preferentially to high pathogenic microorganisms:
  - address the microbial specificity of SSC4D **(Chapter II)**;
  - extend the knowledge of CD5L as a PRR **(Chapter III)**;
- test the susceptibility of CD5L deficient mice to infection with the previous identified pathogens.

To address these questions, we took advantage of classical approaches for protein-bacteria or protein-cell interaction previously established in the lab, together with an in-house developed mouse model where the *cd5l* gene was abrogated by CRISPR/Cas9-mediated engineering. CD5L KO mice will allow to study the role of this protein in different experimental infectious diseases.

Altogether, uncover the immune function of two secreted SRCR proteins (SSc4D and CD5L) will also contribute to the path of understanding the overall role of the SRCR-SF, and possibly provide insights in a putative use of these proteins for future therapeutic approaches in the course of an identified infection.

Chapter II

Physical Interactions With Bacteria and Protozoan Parasites Establish the Scavenger Receptor SSC4D as a Broad-Spectrum Pattern Recognition Receptor

Front. Immunol., 24 December 2021

doi.org/10.3389/fimmu.2021.760770

Physical Interactions With Bacteria and Protozoan Parasites Establish the Scavenger Receptor SSC4D as a Broad-Spectrum Pattern Recognition Receptor

Marcos S. Cardoso[1,2,3], Rita F. Santos[1,2,3], Sarah Almeida[1,2,4], Mónica Sá[1,2,5], Begoña Pérez-Cabezas[1,2], Liliana Oliveira[1,2], Joana Tavares[1,2], Alexandre M. Carmo[1,2]

[1]Instituto de Investigação e Inovação em Saúde, Universidade do Porto, Porto, Portugal

[2]IBMC–Instituto de Biologia Molecular e Celular, Porto, Portugal

[3]Programa Doutoral em Biologia Molecular e Celular (MCbiology), Instituto de Ciências Biomédicas Abel Salazar, Universidade do Porto, Porto, Portugal

[4]Departamento de Biologia, Universidade de Aveiro, Aveiro, Portugal

[5]Doutoramento em Ciências Farmacêuticas (especialidade Microbiologia), Faculdade de Farmácia, Universidade do Porto, Porto, Portugal

Abstract

Since the pioneering discoveries, by the Nobel laureates Jules Hoffmann and Bruce Beutler, that Toll and Toll-like receptors can sense pathogenic microorganisms and initiate, in vertebrates and invertebrates, innate immune responses against microbial infections, many other families of pattern recognition receptors (PRRs) have been described. One of such receptor clusters is composed by, if not all, at least several members of the scavenger receptor cysteine-rich (SRCR) superfamily. Many SRCR proteins are plasma membrane receptors of immune cells; however, a small subset consists of secreted receptors that are therefore in circulation. We here describe the first characterization of biological and functional roles of the circulating human protein SSC4D, one of the least scrutinized members of the family. Within leukocyte populations, SSC4D was found to be expressed by monocytes/macrophages, neutrophils, and B cells, but its production was particularly evident in epithelial cells of several organs and tissues, namely, in the kidney, thyroid, lung, placenta, intestinal tract, and liver. Similar to other SRCR proteins, SSC4D shows the capacity of physically binding to different species of bacteria, and this opsonization can increase the phagocytic capacity of monocytes. Importantly, we have uncovered the capacity of SSC4D of binding to several protozoan parasites, a singular feature seldom described for PRRs in general and here demonstrated for the first time for an SRCR family member. Overall, our study is pioneer in assigning a PRR role to SSC4D.

Key words: scavenger receptor cysteine-rich; pattern recognition receptors; bacteria; parasites

Introduction

The initial sensing of an invasive pathogen is one of the most critical events during an infection and is mediated by germline-encoded pattern recognition receptors (PRRs), which identify and bind conserved pathogen-associated molecular patterns (PAMPs) of microbes. Many different families of PRRs displaying either target-specific or broad recognition of different types of microbes have been described. Membrane-bound Toll-like receptors (TLRs) or C-type lectin receptors bind or sense microbe-exposed PAMPs and initiate signaling cascades to trigger innate immune cell activation, whereas intracellular pathogens or their by-products are recognized by intracellular PRRs such as cytoplasmic

NOD-like receptors or by RIG-I-like receptors and endosomal TLRs that identify microbial genetic material (1–4).

Recent work has revealed that pattern recognition is a common feature of many scavenger receptor cysteine-rich (SRCR) proteins. The macrophage scavenger receptor type I (MSR1) and MARCO plasma membrane trimeric proteins have long been known to bind bacteria or bacterial endotoxins and to promote microbial phagocytosis (5, 6), but only more recently it was described that the cell surface receptors CD6 and CD163 of T cells and macrophages, respectively, can recognize Gram-positive and Gram-negative bacteria (7, 8). By contrast, CD5 has not been shown to bind bacteria, but its extracellular domain interacts with fungal cell wall components (9).

A small subset of SRCR consists of secreted receptors that are therefore in circulation and as such they have exceptional features to intercept, recognize, and neutralize invasive microbes and thus to contain infections. Galectin-3-binding protein (MAC2BP, LGALS3BP) is a small mosaic protein that contains, besides an SRCR domain, a BTB dimerization domain and a BACK domain (10). Although historically viewed as a malignant tumor-associated antigen, this protein has recently been identified as a possible biomarker for human sepsis (11). Better known for their infection-related immune functions, the circulating proteins CD5 antigen-like (CD5L), also known as apoptosis inhibitor expressed by macrophages (AIM) or secreted protein α (Spα) (12, 13), soluble scavenger protein with 5 SRCR domains (SSC5D) (14), and deleted in malignant brain tumors 1 (DMBT1) (15), containing respectively three, five, and 14 SRCR domains, display characteristic PRR features including a strong avidity to bind Gram-positive and Gram-negative bacteria (16–18).

Compared with the wealth of information gathered on the various roles of, for example, CD5L, spreading across a multitude of functions in numerous biological systems and phenomena (19), the attention on the very similar SSC4D protein has been almost inexistent. SSC4D is a 575-amino acid (aa)-long protein containing an N-terminal signal peptide, no transmembrane-encoding sequence, and four SRCR domains, all indicating that SSC4D is the last member of the subgroup of circulating SRCR proteins (20). In fact, SSC4D can be found in human blood plasma, albeit at a very low concentration (1 ng/ml) (21, 22). Although no extensive protein characterization, tissue distribution, or functional studies have been performed, northern blotting analyses imply that SSC4D is well expressed in the human kidney and placenta and moderately expressed in the liver, small intestine, spleen, and thymus (20).

Here, we describe the first comprehensive data on the roles and distribution of the SSC4D glycoprotein in a mammalian organism and how the evidence obtained clearly indicates that SSC4D functionally belongs to the PRR arm within the SRCR family.

Materials and Methods

Recombinant Scavenger Receptor Cysteine-Rich Proteins

Recombinant soluble proteins were produced in human embryonic kidney 293T cells and supplied in lyophilized form by INVIGATE GmbH. Specifically, recombinant forms of human CD5L and of the extracellular domain of human CD6 were produced from templates already described (17, 23) and modified to obtain chimeric proteins containing a signal peptide, the specific CD5L (Ser20 to Gly347) or CD6 (Asp25 to Glu398) sequences, HA and BirA recognition sequences, and 8—12-His tag sequences. Recombinant human SSC4D (UniProtKB accession no. Q8WTU2) was produced in a similar manner to include the specific protein sequence spanning domains 1–4 (Leu48-Ser575) of SSC4D. Recombinant human SSC4D-d1d2 (spanning SRCR domains 1 and 2) and SSC4D-d3d4 (domains 3 and 4) were produced to result in the SSC4D sequences Leu48-Gly318 and Ser324-Ser575 being fused to 8·His tag sequences.

For the expression in Caco-2 cells of full-length SSC4D fused to citrine and containing an HA tag, cDNA was amplified by PCR from Hep G2 cells using forward (5′-TAGACGCGTATGCACAAGGAAGCAGAGA-3′) and reverse (5′-CTAGGATCCCGAGCGTAGTCTGGGACGTCGTATGGGTATGAAGGCTGGCACAGGAC ACT-3′) primers. The resulting PCR product was cloned into the lentiviral expression vector pHR-mCitrine, using *Mlu*I and *Bam*HI restriction sites, to be under the control of the spleen focus-forming virus (SFFV) promoter and transduced into Caco-2 cells.

Analysis of SSC4D Protein Expression

Cell lysates were prepared using radioimmunoprecipitation assay (RIPA) lysis buffer containing a mixture of protease and phosphatase inhibitors (Sigma-Aldrich). Protein concentration was measured by Bradford assay (Bio-Rad), and 60 μg of each sample were denatured in Laemmli's sample buffer at 95°C for 10 min. Cell lysates and supernatants were separated by sodium dodecyl sulfate polyacrylamide gel electrophoresis (SDS-PAGE) and transferred to nitrocellulose membranes using Trans-Blot Turbo Transfer System (Bio-Rad). Membranes were blocked with 5% non-fat dried milk in Tris-buffered saline, 0.1%

Tween 20 (TBS-T) for 1 h and probed with rabbit anti-SSC4D polyclonal antibody (raised against polypeptides corresponding to sequences R346-C364 and E470-R485 of mouse SSC4D; BIOTEM), followed by a goat anti-rabbit horseradish peroxidase (HRP) secondary antibody (Sigma-Aldrich). Immunoblots were developed using enhanced chemiluminescence (ECL) detection reagent (GE Healthcare Life Sciences), and luminescence signals were detected using the Fujifilm FPM-100A film processor (Fujifilm).

To determine the molecular mass of the recombinant proteins, 5 μg of recombinant SSC4D, SSC4D-d1d2, and SSC4D-d3d4 were run on SDS-PAGE, and proteins were detected by Coomassie blue staining; also, 0.5 μg of each recombinant protein were detected by western blotting.

Cells and Cell Lines

Human peripheral blood mononuclear cells (PBMCs) were obtained from buffy coats of healthy adult volunteers at Banco de Sangue, Hospital São João, Porto, and were separated by Lymphoprep density gradient (STEMCELL Technologies). $CD14^+$ monocytes were then isolated by positive magnetic cell sorting using CD14 microbeads (Miltenyi Biotec).

Differentiation of *ex vivo* monocytes into macrophages was achieved using 30 ng/ml of macrophage colony-stimulating factor (M-CSF) for 6 days in culture. Macrophages were then polarized toward an M1-like phenotype with 100 ng/ml lipopolysaccharide (LPS; *Escherichia coli* O111:B4; Sigma) and 25 ng/ml interferon (IFN)-γ (PeproTech), an M2a-like phenotype using 20 ng/ml interleukin (IL)-4 (PeproTech), or an M2c-like phenotype using 25 ng/ml IL-10 (PeproTech), all for 24 h. Polarization of undifferentiated monocytes was done similarly but for 72 h. Cell surface labeling using CD80 APC (2D10), CD206 PE (15.2), and CD163 BV421 (6H1/61) mAbs (all from BioLegend) confirmed the polarization of monocytes and macrophages into the correct subtype. Treatments with CD5L (1 μg/ml) or SSC4D (1 μg/ml) were assayed to check whether either of these stimuli would polarize cells toward any given subtype. Data were acquired in FACSCanto II (BD Biosciences). Post-acquisition analysis was performed using FlowJo software v10 (Tree Star).

Cell lines used in this study were Hep G2 (24), K562 (25), Caco-2 (26), E6.1 (27), JEG-3 (28), HEK 293T (29), TCCSUP (30), Raji (31), HL-60 (32), THP-1 (33), and HeLa (34). All lines were maintained at 37°C in a 5% CO2 humidified incubator in RPMI 1640 supplemented with 10% fetal calf serum (FCS), 1 mM sodium pyruvate, 2 mM L-glutamine, 50 U/ml penicillin G, and 50 μg/ml streptomycin, except HEK 293T, HeLa, Hep G2, and Caco-2 that were grown in Dulbecco's modified Eagle's medium (DMEM)/high-glucose

medium containing 10% FCS, 1 mM sodium pyruvate, 4 mM L-glutamine, 50 U/ml penicillin, and 50 µg/ml streptomycin.

Flow Cytometry and Cell Sorting

Blood from buffy coats was added to red blood cell (RBC) lysis buffer (BioLegend), and after washing, 1×10^6 leukocytes were incubated with FcR blocking (Miltenyi Biotec) for 10 min at 4°C. Cells were stained with mAbs CD14 Pacific Blue (63D3), CD177 APC/Cy7 (MEM-166), CD19 PE/Cy7 (HIB19), CD4 Alexa Fluor 488 (OKT4), and CD8 APC (HIT8a) (all from BioLegend), fixed, and permeabilized with the eBioscience fixation/permeabilization kit (Thermo Fisher Scientific).

Intracellular staining was performed with rabbit anti-SSC4D polyclonal antibody, followed by anti-rabbit PE labeling (Life Technologies). Data were acquired in the FACSCanto II and post-acquisition analysis performed using FlowJo v10.

For cell sorting, blood from buffy coats was added to RBC lysis buffer, and 1×10^7 leukocytes were stained with mAbs CD14 APC (63D3), CD177 APC/Cy7 (MEM-166), CD19 PE/Cy7 (HIB19), and CD3 PerCP/Cy5 (OKT3). The labeled cells were sorted with FACSAria (BD Biosciences).

Immunostaining

SSC4D protein expression was detected in sections of human tissues kindly provided by the Unidade Local de Saúde de Matosinhos–Hospital Pedro Hispano. All ethical and legal issues were secured, along with the guarantee of confidentiality/no disclosure or violation of personal information or other data of the patients.

Four-micrometer sections of paraffin-embedded human blocks were deparaffinized and hydrated. Antigen retrieval was performed in 10 mM sodium citrate buffer for 30 min in a 96°C water bath.

Immunohistochemistry (IHC) was performed using UltraVision Quanto Detection System HRP DAB (Thermo Scientific). Endogenous peroxidase activity and nonspecific background staining were blocked using Hydrogen Peroxidase Block and Ultra V Block reagents, respectively. Tissues were immunostained with mouse anti-human SSC4D mAb 46-M or with a negative control normal mouse IgG sc-2025 (Santa Cruz Biotechnology) at 4°C overnight (ON), incubated with the primary antibody amplifier for 10 min followed by incubation with HRP Polymer Quanto and developed with 3, 3'-diaminobenzidine (DAB). The slides were counterstained with hematoxylin and visualized under light microscopy.

Colon, stomach, and liver sections were analyzed by immunofluorescence (IF). Non-specific staining was blocked with PBS containing 1% bovine serum albumin (BSA) for 1 h at room temperature (RT). Slides were then immunostained at 4°C ON with rabbit anti-SSC4D polyclonal followed by incubation with goat anti-rabbit Alexa Fluor 488-conjugated antibody (Life Technologies) for 1 h at RT. Nuclei were stained with "4′,6-diamidino-2-phenylindole (DAPI)" (Invitrogen), and cell preparations were mounted with Vectashield mounting media (Vector Laboratories). The slides were analyzed using confocal microcopy (Leica TCS SP5).

Fluorescence-activated cell sorting (FACS)-separated blood cells were adhered to poly-L-lysine (Sigma-Aldrich)-treated coverslips followed by blocking of non-specific staining with PBS containing 1% BSA for 1 h at RT. SSC4D was then detected with rabbit anti-SSC4D antibody ON at 4°C followed by incubation with goat anti-rabbit Alexa Fluor 488- conjugated antibody for 1 h at RT. Nuclei were stained with DAPI, and cell preparations were mounted with Vectashield. The slides were analyzed using confocal microcopy.

Bacteria and Parasites

E. coli strains [BL21(DE3), IHE3034, RS218, and CFT073] were kindly provided by Claire Poyart (Institut Cochin, Paris), *Listeria monocytogenes* strain EGD-e *and Salmonella enterica* serovar typhimurium were provided by Didier Cabanes (i3S, Porto), and *Streptococcus agalactiae* [group B streptococcus (GBS)] strain BM110 was provided by Patrick Trieu-Cuot (Institut Pasteur, Paris). *Klebsiella pneumoniae*, *Enterococcus faecalis*, and *Pseudomonas aeruginosa* were also used in this study. Bacteria were grown to mid-logarithmic phase (OD_{600} of 0.45) in brain heart infusion medium at 37°C. *Mycobacterium avium* strain 2447 was prepared as described previously (35).

Parasites were prepared as previously described: *Neospora caninum* tachyzoites (Nc-1, ATCC 50843) (36), *Plasmodium berghei* ANKA strain blood merozoites (clone 676cl1) (37), *Trypanosoma brucei brucei* Lister 427 bloodstream forms (38), *Leishmania major* strain LV39, and *Leishmania tarentolae* strain Parrot-TarII promastigotes (39). A green fluorescent protein (GFP)-expressing *T. brucei brucei* Lister 427 line was engineered by cloning an enhanced gfp into a modified pHD1034 vector where the puromycin resistance cassette was replaced by the hygromycin resistance from the pHD1145 vector. Transfected parasites were selected with 5 μg/ml hygromycin (38).

Scavenger Receptor Cysteine-Rich Protein–Microbial Cell Binding Assays

Binding of SRCR proteins to microbial cells was performed as described previously (17) using 2 μg of each protein interacting with 1×10^8 live bacteria or 1×10^7 live parasites in binding medium (TBS with 1% BSA, 5 mM Ca^{2+}) for 1 h in an orbital shaker at 4°C. Microbe-bound proteins were detected using mouse anti-Tetra HIS mAb (Qiagen) followed by incubation of anti-mouse HRP-conjugated antibody (BioLegend) for 1 h at RT. Immunoblots were developed using ECL. Sample loading was evaluated with a rabbit anti-*Leishmania infantum* cysteine synthase (at 1:2,000 dilution) for *Leishmania* parasites and a rabbit anti-*T. brucei* aldolase (1:5,000) for *T. brucei*.

For the visualization of SSC4D binding to *T. brucei* bloodstream forms by IF, a GFP-expressing *T. brucei* Lister 427 line was incubated with 2 μg of HA-tagged SSC4D-FL in the binding medium. The cell pellet was transferred onto poly-L-lysine-treated coverslips and fixed with PFA 4% for 15 min at RT, and the presence of SSC4D was detected using anti-HA mAb 16B12 (BioLegend) followed by incubation with anti-mouse Alexa Fluor 568-conjugated antibody (Invitrogen). Nuclei were stained with DAPI, and the preparations were mounted with Vectashield. The slides were analyzed using confocal microcopy.

Scavenger Receptor Cysteine-Rich Protein–Endotoxin Binding Assays

High-binding 96-well microtiter plates were coated ON with 10 μg/ml of purified LPS (E. coli O111:B4; Sigma) or 10 μg/ml lipoteichoic acid (LTA; Staphylococcus aureus; Sigma) in PBS at 4°C. The plates were blocked with PBS, 1% BSA, for 1 h at RT. Serial 2-fold dilutions of HIS-tagged SRCR proteins were added to the plates and incubated for 2 h at RT. Bound proteins were detected using mouse anti-HIS mAb for 1 h at RT, followed by goat anti-mouse HRP-conjugated antibody for 1 h at RT. Reactions were developed using SIGMAFAST o-Phenylenediamine dihydrochloride (OPD) for 30 min at RT and stopped with 1 M H_2SO_4. Absorbance was read at 490 nm using Synergy 2 (BioTek).

To calculate the calibration of the LPS- and LTA-binding assays, samples of serially diluted HIS-tagged SRCR proteins were directly coated on 96-well microtiter plates ON in PBS at 4°C. Plates were blocked with blocking solution for 1 h at RT, followed by detection of bound protein, as described above.

In between each step, plates were washed four times with PBS, 0.1% Tween-20.

Scavenger Receptor Cysteine-Rich Protein–Eukaryotic Cell Binding Assays

To detect binding of SSC4D to putative ligands in eukaryotic plasma membranes, 2 × 10^5 primary monocytes or Caco-2, Hep G2, Raji, K562, HL-60, THP-1, HeLa, or E6.1 cells were incubated with 3 µg of recombinant soluble extracellular CD6 (sCD6) or SSC4D-FL, or left untreated, in binding medium for 1 h at 4°C. Cells were then washed twice and incubated with fixable viability dye (Invitrogen) to exclude dead cells. The presence of SRCR proteins was detected with anti-HIS primary antibody followed by incubation with anti-mouse Alexa Fluor 647-conjugated antibody (Invitrogen) at 4°C. Data were acquired in FACSCanto II, and post-acquisition analysis was performed using FlowJo v10.

Phagocytosis Assays

Monocytes were plated at a density of 2 × 10^5 cells/well using imaging media (RPMI without phenol red, 10% FBS, 50 U/ml penicillin, and 50 µg/ml streptomycin) in 96-well plates (CellCarrier Ultra, PerkinElmer). After ON incubation, imaging media were removed without disturbing the monolayer and replaced with new media containing Hoechst for 45 min at 37°C. Then, 40 µg/ml of Invitrogen™ pHrodo™ Red *E. coli* BioParticles™ (Fisher Scientific) were added to the cells alone or with 5 µg/ml of recombinant SSC4D or CD5L. Immediately after, the 96-well plates were inserted in the IN Cell Analyzer (GE Healthcare Life Sciences), previously heated for 37°C, and nine images per well were collected 45 and 120 min after the addition of the BioParticles. Images were analyzed using FIJI software, and the percentage of cells containing *E. coli* BioParticles was determined.

SSC4D Secretion Upon Infection of Caco-2 Cells

Caco-2 cells expressing an SSC4D-citrine-HA fusion protein were plated at a density of 3.5 × 10^5 cells/well in 12-well plates. After cell attachment, cultures were infected for 1 h with live *E. coli* RS218 or *L. monocytogenes* EGD-e with a multiplicity of infection (MOI) of 1:50 or left uninfected. Cells were then washed with PBS and supplied with new media containing 20 µg/ml gentamicin. Supernatants were collected 2, 8, and 24 h after infection and resuspended in Laemmli's sample buffer for SDS-PAGE and western blotting. SSC4D from supernatants was detected using mouse anti-HA mAb followed by anti-mouse HRP-conjugated antibody and ECL detection.

Results

Human SSC4D Protein Structure and Expression

SSC4D belongs to the group B of SRCR domain-containing proteins characterized by having an extraordinary sequence similarity between all individual domains and a nearly perfect conservation of key residues, namely, eight regularly spaced cysteine residues that establish intra-domain disulfide bonds in very defined combinations, also sequences that are 100% conserved in all known domains, especially in the β1 and β2 strands and in the boundaries between the α1 helix and the β4 strand (14) (Figure 1A). One other characteristic feature of this family of extracellular proteins consists of its extended level of glycosylation, as assessed by the high number of putative *O*-GalNAc glycosylation sites, characteristic of mucins. In particular, the four SRCR domains of SSC4D are interspaced with sequences rich in *O*-linked sugars, as predicted by NetOGlyc 4.0 (41) (Figure 1B). However, a certain separation can be established between the SRCR group B members that are secreted from those that are membrane bound, such as CD5, CD6, CD163, and CD163 antigen-like 1 (M160), in that in this latter set, *N*-linked glycosylation seems to be more prevalent, despite that the whole level of sequence similarity between the different proteins would not predict that sort of cleavage (14, 42). In fact, neither SSC4D nor CD5L, which are here investigated, contain any *N*-linked sugars as predicted by NetNGlyc 1.0 (43), contrasting with the extracellular domain of CD6 that contains seven such modifications.

We assessed the expression of SSC4D in lysates of several human cell lines and detected by western blotting the expression of the SSC4D protein in Hep G2, Caco-2, K562, and HeLa cells, and the molecular mass of intracellular SSC4D was calculated to be 70.8 KDa (Figure 1C). Few smaller bands of lower intensity could be observed in the blots, and these could hypothetically represent alternative splicing-dependent isoforms. Indeed, a common property of most SRCR members is the generation of alternative splicing-dependent isoforms, many of them resulting in the absence of individual or multiple SRCR domains, as described for DMTB1, CD6, CD163, and M160 (44–46). Padilla *et al.* (20) had in fact detected by northern blotting different transcripts that could account for alternative SSC4D isoforms, and one SSC4D mRNA isoform described in a transcriptome-wide study does miss the sequences encoding domains 3 and 4 (44). However, it is unlikely that the smaller bands in the gel correspond to this isoform because the detecting antibody was raised against sequences within domains 3 and 4 of the protein; rather, they either are unspecific blot bands or may represent degradation products.

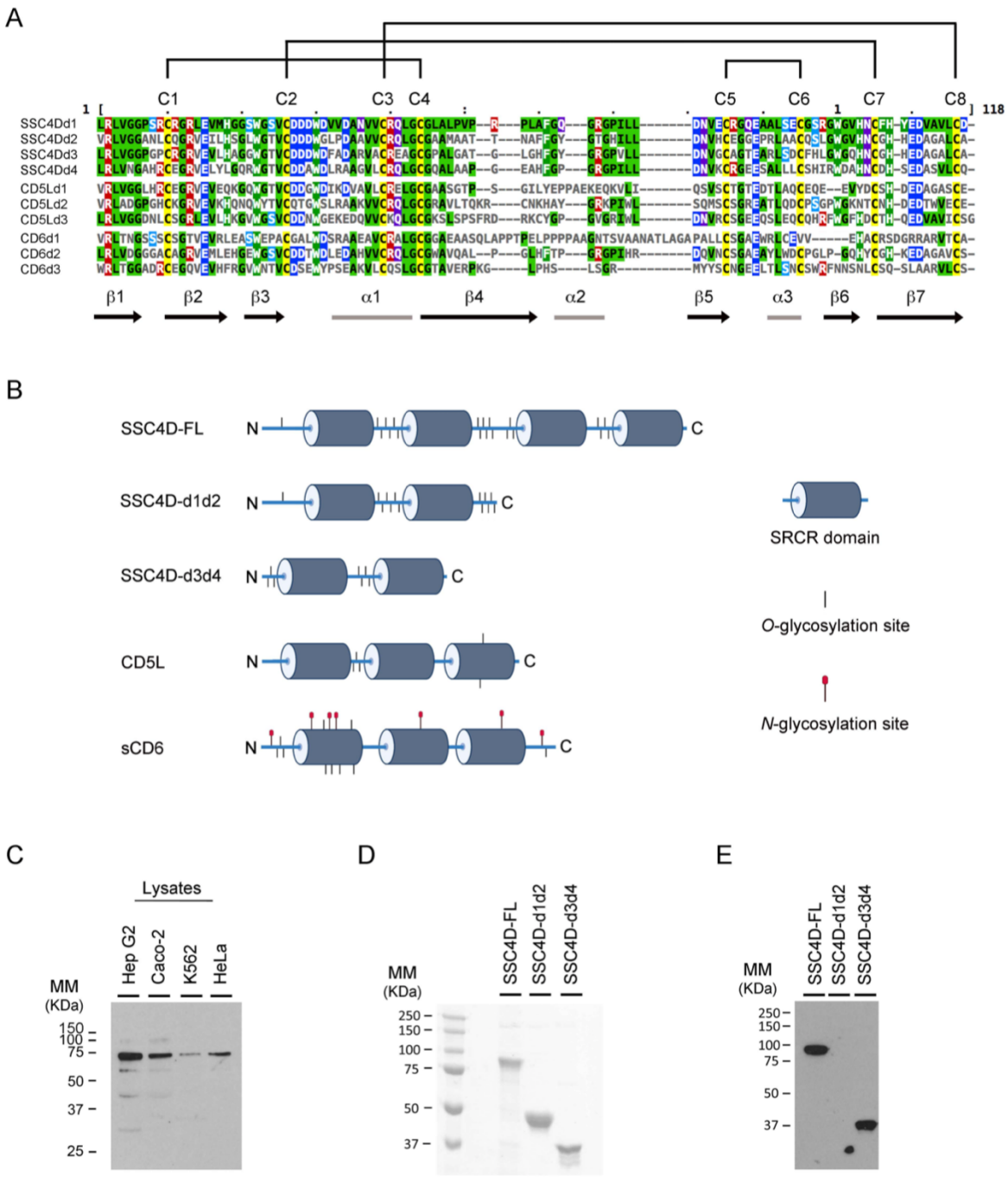

Figure 1 - Amino acid sequence and structure of group B scavenger receptor cysteine-rich (SRCR) domains of SSC4D, CD5L, and CD6. (A) SRCR domains are typically ~100–110 amino acids in length compacted into a heart-shaped fold, where a six/seven-stranded β sheet cradles a core α1-helix. Each line represents one SRCR domain of the indicated protein. Amino acid sequences were aligned using Clustal Omega and MView (40). Amino acid side chain color codes for conserved residues: Green/black, aliphatic; Green/white, aromatic; Blue, anionic; Red, cationic; Cyan, polar; Magenta, amide; Yellow, sulfur-containing. Intrachain disulfide bonds established between conserved cysteine residues are shown on the top by connecting lines. (B) Schematic representation of the protein structures of SSC4D-FL, SSC4D-d1d2, SSC4D-d3d4, CD5L, and extracellular domain of CD6 (sCD6). SRCR domains are represented as dark cylinders. (Continues on the next page)

Figure 1 (continuation) - Putative *O*-linked glycosylation sites are represented as short vertical lines and *N*-linked glycosylation sites as lines topped with red circles. N and C termini of the proteins are indicated by "N" and "C," respectively. Design was created using BioRender.com. (C) SSC4D protein expression detected by western blotting from cell lysates of Hep G2, Caco-2, K562, and HeLa cells. The molecular mass of intracellular SSC4D was calculated as 70.8 KDa. (D) Recombinant SSC4D, SSC4D-d1d2, and SSC4D-d3d4 were run on sodium dodecyl sulfate polyacrylamide gel electrophoresis (SDS-PAGE), and gels were stained with Coomassie blue. The size of recombinant extracellular full-length SSC4D was measured as 90.6 KDa, SSC4D-d1d2 as 45 KDa, and SSC4D-d3d4 as 36 KDa. (E) Recombinant SSC4D, SSC4D-d1d2, and SSC4D-d3d4 were run on SDS-PAGE, transferred to nitrocellulose membranes, and detected by immunoblotting. SSC4D and SSC4D-d3d4 were confirmed at the correct sizes, while SSC4D-d1d2 is not detected given that the polyclonal antibodies recognize sequences within domains 3 and 4.

Nevertheless, for the purpose of this study, we generated and expressed recombinant human full-length SSC4D and two recombinant hemi-SSC4D forms, each corresponding to one-half of the molecule and consisting of either the SRCR domains 1 and 2 (SSC4D-d1d2) or 3 and 4 (SSC4D-d3d4) (Figure 1B). The recombinant proteins were run on SDS and stained with Coomassie blue (Figure 1D) and detected by western blotting using an anti-SSC4D-d3d4 polyclonal antibody (Figure 1E). The molecular mass of the mature full-length extracellular protein was measured at 90.6 KDa, suggesting that the secreted protein undergoes posttranslational modifications, possibly *O*-linked glycosylation.

SSC4D Expression in Human Epithelia and Leukocytes

Based on the reported tissue distribution of the mRNA coding for human SSC4D (20), we screened by PCR different human cell lines for the presence of SSC4D mRNA. We found that SSC4D is mostly expressed in cell lines with epithelial morphology like Hep G2 (hepatocellular carcinoma), Caco-2 (colorectal adenocarcinoma), JEG-3 (placental choriocarcinoma), HEK 293T (adenovirus 5 DNA-transfected embryonic adrenal precursor cells), and HeLa (cervical adenocarcinoma), but not in TCCSUP (urinary bladder carcinoma) (Supplementary Figure S1). Also, SSC4D mRNA was detected in hematopoietic-derived cells such as K562 (myelogenous leukemia) and very faintly in E6.1 (acute T-cell leukemia), but not in Raji (Burkitt's lymphoma).

We then assessed the expression of the protein in human organs. Relevant expression was observed in the gastrointestinal tract, with SSC4D being detected in intestinal crypts, namely, in mucous goblet cells in the colon, while in the stomach, staining was visualized in the simple columnar epithelium of the gastric mucosa and showing a broad distribution in gastric glands, compatible with SSC4D being expressed by surface mucous cells, mucous neck cells, and chief cells (Figure 2A). SSC4D was also expressed in the

parenchyma of hepatic lobules in hepatocytes. Regarding the genitourinary tract, strong SSC4D expression was detected in the epithelial cells of the tubules (Figure 2B). SSC4D was also found in follicular and parafollicular cells of the thyroid and in pneumocytes of the alveolar ducts. Interestingly, strong and specific expression of SSC4D was found in chorionic villi in placenta, mostly in the outer layer corresponding to the syncytiotrophoblasts.

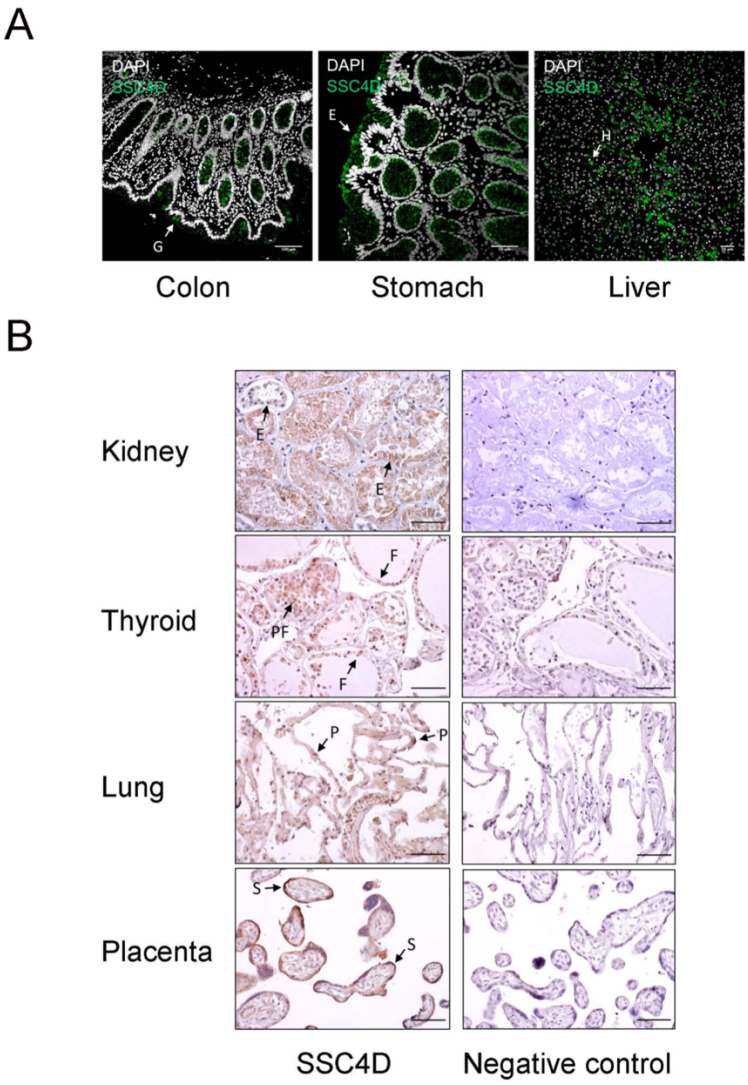

Figure 2 - SSC4D distribution in human organs. (A) Detection of SSC4D by immunofluorescence (IF) in sections of the colon, stomach, and liver from normal human subjects. SSC4D labeling in mucous goblet cells (G) in the colon, simple columnar epithelium cells (E) in the stomach, and hepatocytes (H) in hepatic lobules is shown by arrows. Cell nuclei were stained with 4′,6-diamidino-2-phenylindole (DAPI; white). No unspecific staining was seen following incubation with secondary antibody alone, confirming specificity of the primary antibody. Scale bar, 50 μm. (B) Immunohistochemical analysis of SSC4D expression in sections of the kidney, thyroid, lung, and placenta. On the left column, SSC4D labeling was visualized by horseradish peroxidase (HRP) and substrate chromogen 3, 3'-diaminobenzidine (DAB). Positive staining of tubular epithelial cells (E) in the kidney, follicular (F) and parafollicular cells (PF) in the thyroid, pneumocytes (P) of the alveolar ducts, and of syncytiotrophoblasts (S) in the placenta is indicated by arrows. (Continues on the next page)

Figure 2 (Continuation) - On the right column, images of sections labeled with unspecific mouse IgG mAb (negative control, sc-2025). Scale bar, 50 µm. Immunohistochemistry (IHC) and IF experiments were performed multiple times using samples from at least three different individuals.

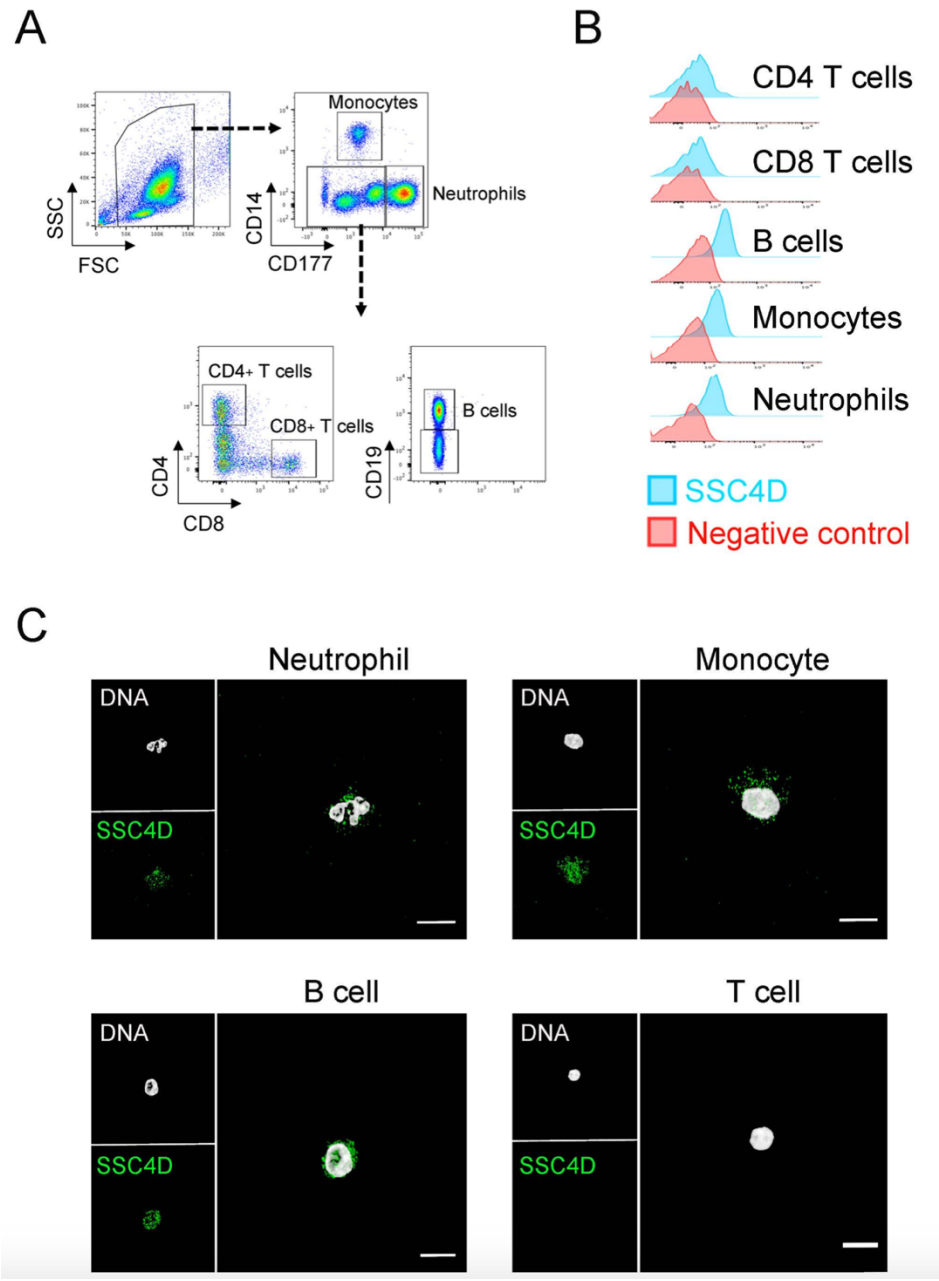

Figure 3 - SSC4D expression in human leukocytes. (A) Flow cytometry gating strategy for the identification of monocytes, neutrophils, B cells, and CD4$^+$ and CD8$^+$ T cells from human blood. (B) Intracellular labeling of SSC4D in different human cell populations, visualized by flow cytometry. In the control samples, the anti-SSC4D antibody was omitted. Representative results shown are from one of four independent experiments. (C) Representative single-cell images of FACS-sorted leukocytes, immunostained for SSC4D (green) and visualized by immunofluorescence (IF). White indicates DAPI staining. Representative results shown are from one of three independent experiments using different donors.

We additionally assessed the expression of SSC4D in leukocyte subpopulations by flow cytometry and IF of FACS-sorted cells and detected the presence of intracellular SSC4D in monocytes, neutrophils, and B cells, but not in $CD4^+$ or $CD8^+$ T lymphocytes (Figure 3). Being a secreted protein, we questioned whether SSC4D could bind and exert any effect in target cells. For that purpose, we tested the binding of recombinant SSC4D to a panel of cell lines; however, none of the cells used were bound by SSC4D, whereas recombinant soluble extracellular CD6 (sCD6), used as a positive control, displayed the characteristic pattern of binding to cells that express its ligand, CD166 (47) (Supplementary Figure S2). This raises the possibility that SSC4D does not have a binding receptor at the surface of human cells or that a hypothetical receptor is not widespread.

SSC4D Physically Binds to Gram-Positive and Gram-Negative Bacteria

The SSC4D-related proteins CD5L and SSC5D are able to identify a large spectrum of bacterial species and strains (16, 17); moreover, the ectodomain of CD6 was reported to bind and induce the aggregation of bacteria through the recognition of the bacterial endotoxins LTA and LPS (8). We investigated whether SSC4D could also detect different bacterial species and how the strength of interactions would compare with those of other SRCR family members.

Recombinant SSC4D, CD5L, and sCD6 were incubated with samples of live *E. coli* strains BL21(DE3), IHE3034, and RS218, with *L. monocytogenes* EGD-e, and with GBS BM110, followed by centrifugation and immunoblotting of the pelleted bacteria. As anticipated, we observed a strong interaction between CD5L and all tested bacteria, particularly in the presence of calcium given that many SRCR protein-mediated interactions are Ca^{2+}-dependent (Figure 4A). By contrast, the interactions between sCD6 and the different bacteria were not visually detectable. Importantly, SSC4D clearly bound all bacteria tested, demonstrating its ability to physically interact with conserved structures present at the surface of these microorganisms.

Consequently, we included in our bacteria binding assays the two recombinant hemi-SSC4D forms, SRCR-d1d2 and SRCR-d3d4. Performing the assays using the same bacterial samples, we observed in several cases that the two halves of the molecule had

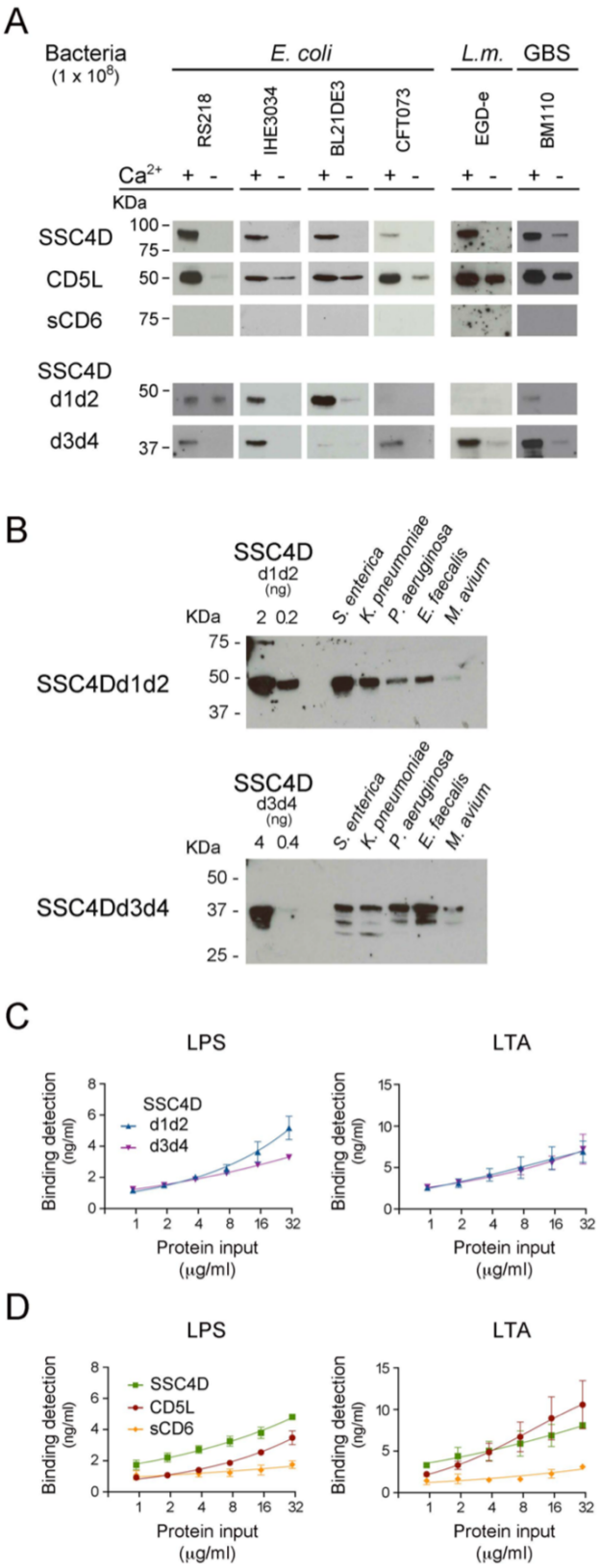

Figure 4 - SSC4D physically binds to bacteria and bacterial endotoxins. (A) Two micrograms of each recombinant protein SSC4D, CD5L, sCD6, SSC4D-d1d2, and SSC4D-d3d4 were incubated with suspensions of 1 × 10^8 CFU of live *Escherichia coli* strains BL21(DE3), RS218, IHE3034, or CFT073, *Listeria monocytogenes* strain EGD-e, or GBS strain BM110 in the presence or absence of Ca^{2+}. (Continues on the next page)

Figure 4 (Continuation) - Cell-bound proteins were detected by immunoblotting using anti-HIS mAb. Blots are representative of at least three independent experiments. (B) Recombinant SSC4D-d1d2 and SSC4D-d3d4 (2 µg each sample) were incubated with suspensions of 1 × 10^8 CFU of live *Salmonella enterica*, *Klebsiella pneumoniae*, *Enterococcus faecalis*, *Pseudomonas aeruginosa*, or *Mycobacterium avium* in the presence of Ca^{2+}. Bacteria-bound proteins were detected by immunoblotting using an anti-HIS mAb. The sensitivity of detection of this mAb for each of the recombinant hemi-forms of SSC4D can be evaluated by the detection, shown on the left side of the membranes, of 2 and 0.2 ng of purified SSC4D-d1d2 (upper blot) or 4 and 0.4 ng of purified SSC4D-d3d4 (lower blot). (C) Binding of SSC4D-d1d2 and SSC4D-d3d4 to plate-bound lipopolysaccharide (LPS) and lipoteichoic acid (LTA). Proteins were added at the indicated concentrations, and signals were detected by anti-HIS mAb followed by horseradish peroxidase (HRP)-conjugated antibody and o-Phenylenediamine dihydrochloride (OPD) substrate. Absorbance was read at 490 nm. Binding values shown were interpolated from standard curves of detection of plate-bound SSC4D-d1d2 and SSC4D-d3d4, shown in Supplementary Figure S3. Graphs show the mean ± SD of two independent experiments performed in duplicate. (D) Binding of SSC4D, CD5L, and sCD6 to plate-bound purified LPS and LTA. Detection and measurement of binding were as in panel (C).

differential binding profiles, such that SSC4D-d3d4 bound well to *Listeria* and GBS, whereas binding of SSC4D-d1d2 to these bacteria was much less evident (Figure 4A, lower panels). Conversely, although not as clear as the above, it seemed that the *E. coli* strains, with the exception of *E. coli* CFT073, were better recognized by SSC4D-d1d2. We hypothesized that each half of SSC4D might bind preferentially to different groups of bacteria and therefore increased the sampling of our assays by adding supplementary bacterial species. In each assay, recombinant SSC4D-d1d2 or SSC4D-d3d4 was incubated with live Gram-negative *S. enterica*, *K. pneumoniae*, and *P. aeruginosa* and with Gram-positive *E. faecalis* or *M. avium* (Figure 4B). Although there was not an absolute compartmentalization in the recognition profiles, in general, it appears that SSC4D-d1d2 displays a preference for binding Gram-negative bacteria. Although the converse correlation cannot be fully established for SSC4D-d3d4, as this half of the molecule is more homogeneous in the identification of both bacterial groups, it appears that SSC4D-d3d4 binds better to Gram-positive bacteria than does SSC4D-d1d2 (Figure 4B).

We thus evaluated whether each typical endotoxin of Gram-negative and Gram-positive bacteria would be a preferential target of one-half of the SSC4D molecule over the other using an ELISA to measure the affinity of each protein to LPS and LTA. We first assessed the sensitivity of the detecting antibody to plate-bound purified SRCR proteins (Supplementary Figure S3A), following which we measured the binding of serially diluted HIS-tagged SRCR proteins to microtiter plates coated with 10 µg/ml of purified LTA or LPS (Supplementary Figure S3B). The conversion of the obtained values to binding detection units showed that both SSC4D hemi-forms bound to LPS and LTA in a dose-dependent manner, but whereas in fact LPS was superiorly targeted by SSC4D-d1d2 than by SSC4D-

d3d4 at higher protein concentrations, the plots for binding to LTA were indistinguishable between the two subunits (Figure 4C).

Comparing the binding forces to LPS and LTA between CD5L, SSC4D, and sCD6, again binding of the proteins to the endotoxins is differentiated: SSC4D binds to LPS with higher avidity than CD5L, whereas binding to LTA is not significantly different between these two proteins (Figure 4D). In accordance with the previous experiments and our earlier work (17), binding of sCD6 to either live or fixed bacteria, or to bacterial endotoxins, although detectable, is inferior when compared with the microbe-binding capacity of the natural circulating SRCR proteins.

SSC4D Promotes Phagocytosis but Does Not Induce Macrophage Polarization

Because SSC4D is produced by phagocytes and binds to bacteria, we questioned whether this circulating molecule could have a direct impact on pathogen clearance. To measure protein-mediated phagocytosis, monocytes were incubated with pHrodo™ Red *E. coli* BioParticles™ in the presence of CD5L or SSC4D or in the absence of the recombinant proteins. These BioParticles become fluorescent in acidic pH, only identifying those bacteria that are inside phagosomes (48). Monocyte phagocytosis of the *E. coli* particles increased over time but was not different whether CD5L was present or not (Figures 5A, B). By contrast, the presence of SSC4D induced a significant increase in the phagocytic capacity. To test whether SSC4D could mediate the internalization of the bacteria through an interaction to a putative cellular receptor in the phagocyte, we checked for a direct interaction between recombinant SSC4D and monocytes. However, as can be seen in Figure 5C, no such interaction is obvious, whereas sCD6, used as a binding control, is able to interact slightly with monocytes, given that these cells express low levels of CD166. An alternative explanation is that the increase in phagocytosis could be due to increased activation of monocytes induced by SSC4D. Although conceivable, this possibility is unlikely, given that SSC4D was added to the cells at the same time as the *E. coli* particles and the duration of the experiment was perhaps too short to allow for a vigorous monocyte activation-mediated phagocytosis.

Also displaying opposite effects from CD5L, SSC4D did not induce the polarization of macrophages toward an M2 phenotype (Figure 5D). Differentiation of *ex vivo* monocytes with CD5L for 3 days had an equivalent result as utilizing IL-4 in the development of an M2a-like phenotype, as previously reported (49). However, in no other differentiation and polarization protocol did SSC4D, nor CD5L, induce monocyte/macrophage polarization, including no effect on an M1-type phenotype.

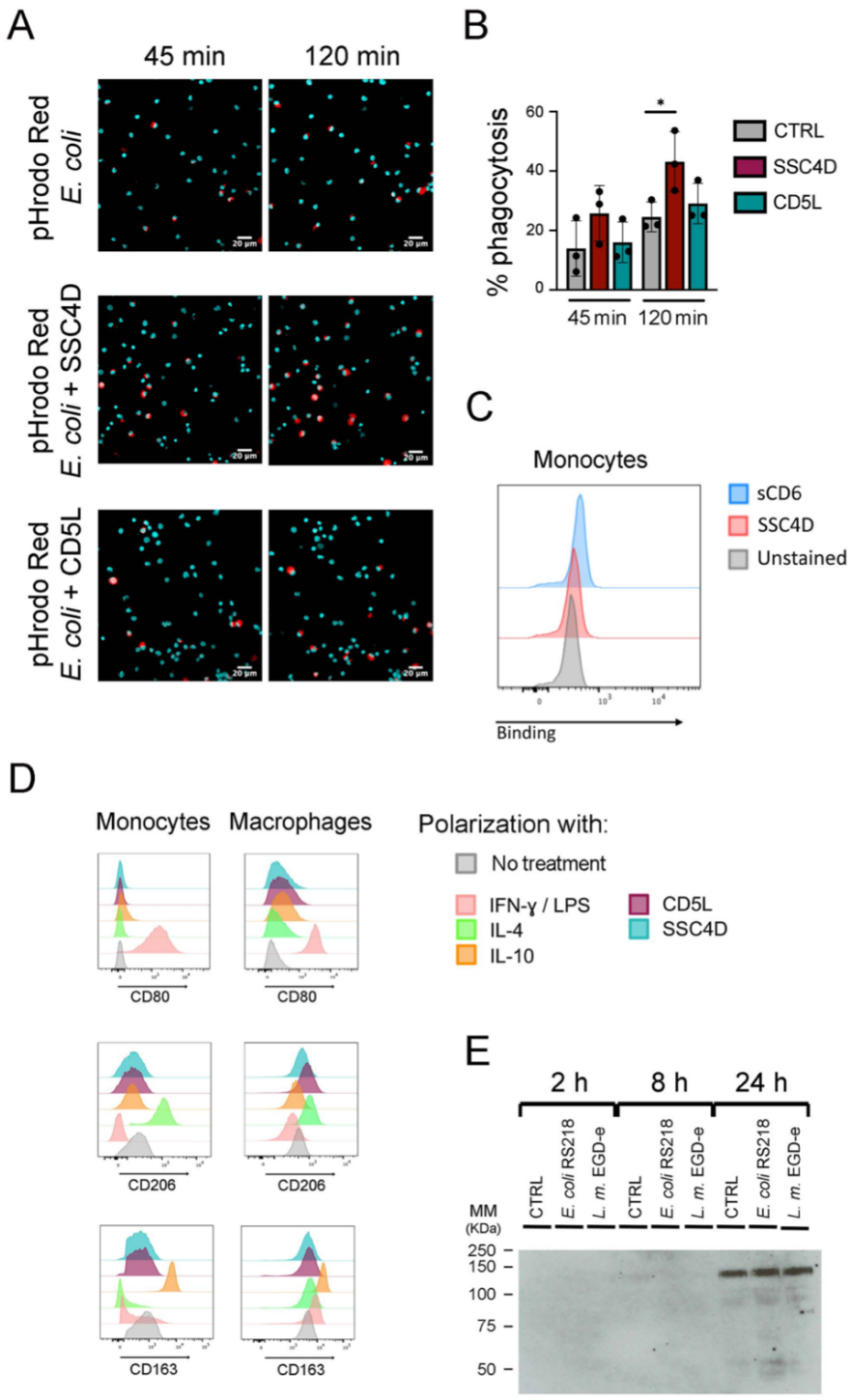

Figure 5 - SSC4D promotes phagocytosis without binding to a ligand on human monocytes and does not induce macrophage polarization. (A) *Escherichia coli* pHrodo BioParticles (40 µg/ml) were added to isolated human monocytes, together with 5 µg/ml of SSC4D (middle panels) or CD5L (bottom panels), or no protein (top panels). Images were acquired for each well at 45 and 120 min after the addition of *E. coli* BioParticles using an IN Cell Analyzer, followed by analysis using FIJI software. Blue indicates DAPI staining, and red indicates phagocyted *E. coli* BioParticles. (B) The percentage of monocytes containing *E. coli* BioParticles was quantified. Graph shows the mean ± SD of three independent experiments performed in duplicate. Statistical analysis was performed using Student's t test. * $p < 0.05$. (Continues on the next page)

Figure 5 (Continuation) - (C) *Ex vivo* monocytes were incubated with 3 µg of SSC4D or sCD6 or left unstained. Cell-bound proteins were detected with anti-HIS antibody followed with Alexa Fluor 647-conjugated anti-mouse antibody and analyzed by flow cytometry. Gray histograms represent control cells, not stained with scavenger receptor cysteine-rich (SRCR) protein but incubated with secondary antibody, red histograms represent labeling with SSC4D, and blue histograms represent labeling with sCD6. (D) Flow cytometry analysis of *ex vivo* monocytes (left column) and macrophage colony-stimulating factor (M-CSF)-differentiated macrophages (right column). Monocytes received for 72 h the appropriate stimuli to polarize toward M1 [interferon (IFN)-γ/lipopolysaccharide (LPS)], M2a [interleukin (IL)-4], or M2C (IL-10) subtypes. Macrophages received the same treatment, but for 24 h. CD80, CD206, and CD163 labeling confirms the polarization of monocytes and macrophages into the correct subtype. Stimulations with SSC4D or CD5L had no effect on cell polarization except for a slight effect of CD5L in polarizing macrophages into an M2a-like phenotype. Representative histograms are from one of three independent experiments. (E) SSC4D secretion upon culture infection with live bacteria. Caco-2 cells were engineered to express SSC4D fused to citrine and were cultured for 3 days at 3×10^5 cells/well in a 12-well plate. Live *E. coli* RS218 or *L. monocytogenes* EGD-e were added at 1:50 multiplicity of infection (MOI). Supernatants were collected at the indicated time points, and the presence of HA-tagged SSC4D-citrine was detected by western blotting. The blot shown is representative of two independent experiments.

SSC4D is normally detected in cell culture media at very low levels, so we questioned whether SSC4D secretion could escalate due to any type of immune response and what would be the external cues that could stimulate this secretion. Caco-2 cells that were engineered to produce a chimeric protein consisting of SSC4D fused to mCitrine and an HA-tag sequence (Supplementary Figure S4A) were incubated with live *E. coli* RS218 or *L. monocytogenes* EGD-e at a 1:50 MOI or left uninfected. Culture supernatants were collected at different time points, and the presence of SSC4D was assessed by western blotting. As seen in Figure 5E, secreted SSC4D was detected at 24 h post infection, but there were no differences between infected (with *E. coli* or *L. monocytogenes*) and non-infected cultures. It is possible that in this specific case, the detection of SSC4D in the media could result from cell death instead of induced, or passive, secretion; nonetheless, in all other tested conditions using different immune-inflammatory mediators or bacterial endotoxins to stimulate SSC4D secretion, there was no single specific stimulus that would further augment the rate of secretion (Supplementary Figures S4B, C). Instead, SSC4D was being continuously released into the medium at moderate levels, independently of any tested external cues.

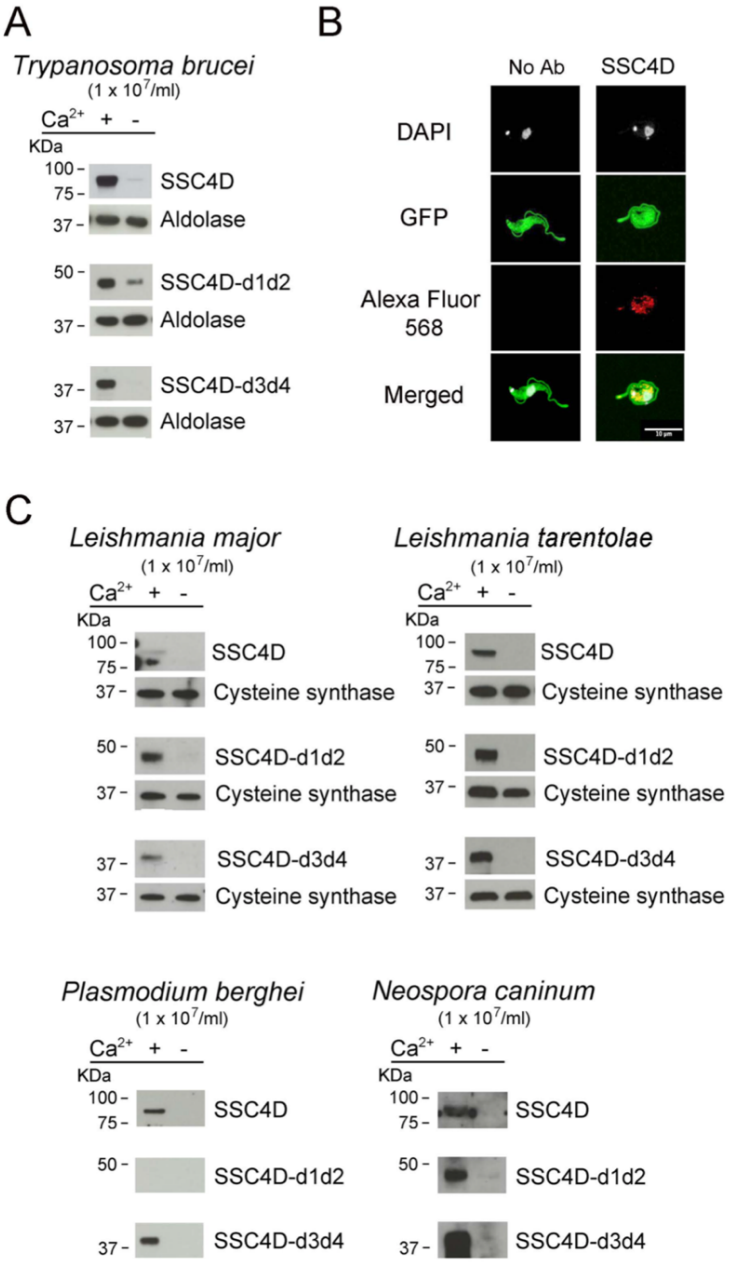

Figure 6 - SSC4D binds to protozoan parasites. (A) Two micrograms of recombinant SSC4D, or of the hemi-forms SSC4D-d1d2 and SSC4Dd3d4, were incubated with suspensions of 1 × 10^7 live *Trypanosoma brucei brucei* bloodstream forms in the presence or absence of Ca^{2+}. Parasite-bound proteins were detected by immunoblotting using anti-HIS mAb. Membranes were reprobed with an anti-aldolase immune serum for loading control. Results shown are of one of three independent experiments. (B) Representative images of SSC4D interacting with green fluorescent protein (GFP)-expressing *T. brucei*. In both panels, GFP^+ parasites (green) were allowed to interact with SSC4D (red), being the primary antibody omitted in the left panel, as control. DAPI (white) indicates DNA staining. The results shown are representative of four independent experiments. (C) Two micrograms of recombinant SSC4D, SSC4D-d1d2, and SSC4D-d3d4 were incubated with suspensions of 1 × 10^7 live *Leishmania major* and *Leishmania tarentolae* promastigotes, *Plasmodium berghei* merozoites, and *Neospora caninum* tachyzoites. Interactions were detected as in panel (A), and membranes were reprobed with an anti-*L. infantum* cysteine synthase immune serum for loading control of *L. major* and *L. tarentolae*.

SSC4D Physically Binds to Protozoan Parasites

PRRs are able to recognize not only bacterial but also fungal, viral, or protozoan conserved structural components. In order to test whether the binding properties of SSC4D could be expanded to protozoan targets, protein binding assays were performed with live parasites. We first assessed the binding of SSC4D to bloodstream forms of *T. brucei*, the parasite that causes African trypanosomiasis. Recombinant SSC4D was incubated with 1 × 10^7 parasites, followed by centrifugation and immunoblotting of the cell pellet. As illustrated in Figure 6A, full-length SSC4D and each SSC4D half were capable of physically interacting with the parasite in a Ca^{2+}-dependent manner. To image this interaction by confocal microscopy, a GFP-expressing *T. brucei* Lister 427 strain was incubated with HA-tagged SSC4D, and binding of the protein to *T. brucei* cells was detected using anti-HA mAbs (visualized in red, Figure 6B).

We extended our protein–parasite binding assays to *Leishmania major* and *Leishmania tarentolae* promastigotes, *Plasmodium berghei* merozoites, and *Neospora caninum* tachyzoites. SSC4D and its half-forms bound to all tested parasites, with the exception of SSC4D-d1d2 that did not bind to *P. berghei* merozoites, the stage that infects red blood cells. Noteworthy, in the absence of Ca^{2+}, all SSC4D–parasite interactions were abolished or markedly reduced.

Discussion

In this study, we show for the first time the capacity of SSC4D to physically bind to bacteria and protozoan parasites. SSC4D has been one of the most neglected SRCR proteins, and no functional data were available, but by simple analogy with other family members, we anticipated that this protein could reveal some PRR functions. The identity of bacterial targets of SSC4D does not significantly differ from those of CD5L or SSC5D; however, these proteins do not display identical binding patterns between themselves or even among their own single domains. We have previously shown relevant differences of binding avidities between SSC5D and CD5L toward different types of bacteria (17). We here advance on this conclusion by showing that different parts of SSC4D have preferential binding toward different groups of bacteria.

Contrasting with the strong binding of CD5L, SSC4D, and SSC5D to a variety of bacterial species and strains, the extracellular domain of CD6 displays a significantly lower binding potency. CD6 is a plasma membrane glycoprotein that modulates T-cell activation (23), and it was somewhat unexpected that such a receptor involved in antigen-dependent

signal transduction would be directly involved in the recognition of unprocessed pathogenic determinants (8). Although there was some controversy as to which extent CD6 binding to bacteria would reflect a physiological characteristic of the molecule (50, 51), it seems undisputable that CD6 does protect from bacterial infection-induced septic shock in mouse models possibly via its function as a circulating extracellular form (sCD6), shed from the surface of lymphocytes in pathological conditions (52). Nonetheless, the fact that the levels of bacterial binding of SSC4D, like CD5L and SSC5D, are so much more evident than those of sCD6 clearly suggests that a main function of SSC4D is indeed of pathogen pattern recognition.

SSC4D is expressed by many epithelial cells of several organs and by phagocytic leukocytes, but unlike what has been described for other circulating SRCR proteins, we could not identify any stimulus, cue, or microbial challenge that increased the rate of secretion of the protein. The estimated plasma concentration of SSC4D is in effect very low (1 ng/ml) when compared with those of the other circulating SRCR proteins SSC5D (88 ng/ml), CD5L (4.3 μg/ml), and MAC2BP (7.1 μg/ml) (21, 22), and the abundance of these proteins further increases upon certain inflammatory and infectious challenges or in oncological environments (11, 53, 54). Also, the membrane-bound receptors CD5, CD6, and CD166, expressed by different leukocytes, undergo cleavage of their ecto-domains in particular pathological conditions, resulting in their consequent release into circulation where they display specific immune-related functions (55, 56). And yet, we have not found any similar agonist-dependent behavior for SSC4D, raising the possibility that SSC4D is being continuously secreted at low constant rates either in steady-state or upon external challenges.

Therefore, and despite sharing common functions with other SRCR proteins, namely, as a PRR, SSC4D may be endowed with some distinctive properties. SSC4D behaves differently from CD5L in at least a few aspects, as in contrast with CD5L (16, 49), SSC4D is not involved in the polarization of macrophages upon different inflammatory stimuli. On the other hand, SSC4D can potentiate the phagocytosis of bacteria by macrophages, contrary to human CD5L. Although our results on CD5L concur with those previously reported by Sanjurjo *et al.* (49), there is some controversy regarding the role of CD5L in phagocytosis, which may depend on the experimental setup, the type of particle/microorganism to be internalized, and the molecular and cellular species analyzed. Mouse (m)CD5L was shown to increase the phagocytosis of latex beads by mouse macrophages (57); both mCD5L and human (h) CD5L increase the clearance of debris by mouse macrophages (58); hCD5L increases clearance of apoptotic cells by human monocytes (49); and mCD5L increases phagocytosis by mouse macrophages and

neutrophils of S. aureus (59). However, the presence of hCD5L did not change the phagocytosis of microspheres or *E. coli* or *S. aureus* particles by human peripheral blood cells (49).

We here show that phagocytosis of *E. coli* particles by human monocytes is in fact not influenced by CD5L but is increased in the presence of SSC4D. Given that both *E. coli* particles and SRCR proteins were added to the cells at the same time, it is unlikely that the increase in phagocytosis is due to activation of monocytes induced by SSC4D. It is possible, instead, that the protein intermediates the interaction between monocytes and bacteria. We have screened monocytes with recombinant monovalent SSC4D for the existence of specific receptors and could not detect any interaction by flow cytometry possible due to the low sensitivity of the method. Although with no evidence that SSC4D promotes large-scale bacterial aggregation, an alternative hypothesis is that the coating of bacteria with SSC4D may induce a more efficient recognition of multivalent SSC4D opsonizing the bacteria either by low-affinity SSC4D receptors or eventually by other sensors of microbial structures.

It is known that host defense against protozoan parasites involves different classes of PRR, such as TLRs, C-type lectin receptors, and NOD-like receptors (60–62). Nevertheless, the knowledge on this field lags considerably behind those that focus on the identification of bacterial, viral, and fungal PAMPs. Also, many other components of the innate immune system participate in antiparasitic defenses, including CD36, a scavenger receptor class B that displays multiple functions and a broad range of ligands, including a cytoadherence ligand on *Plasmodium falciparum*-infected erythrocytes (63). However, CD36 belongs to a different family of scavenger receptors characterized by having two transmembrane domains flanking a CD36-type multifunctional domain. SRCR proteins like MARCO and MSR1 have been shown to have a role in defense against protozoan parasites such that, for example, inhibition of MSR1 function reduces *P. berghei* infection and the expression of MARCO in macrophages of CBA/J mice is increased upon *L. major* infection (64, 65). Still, to the best of our knowledge, ours is the first study that describes a physical interaction of an SRCR protein and protozoan targets. Together with its capacity to bind bacteria and to promote macrophage phagocytosis, SSC4D can thus be considered a *bona fide* broad-range PRR, and importantly, this may help to strengthen the concept, so many times overlooked, that the SRCR cluster is a legitimate member of the wider collective family of pathogen PRRs.

Funding

This work was funded by National Funds through FCT–Fundação para a Ciência e a Tecnologia, I.P., under the projects SRecognite Infect-ERA/0003/2015 and UIDB/04293/2020. Individual funding to JT was provided by FCT through CEECIND/02362/2017. MC, RS, and MS were recipients of studentships from FCT, respectively, SFRH/BD/116791/2016, SFRH/BD/110691/2015, and SFRH/BD/13485/2017.

Acknowledgments

This paper is dedicated to our colleague and friend Rui Appelberg (1960-2020). The authors acknowledge the support of the i3S Scientific Platform BioSciences Screening, member of the national infrastructure PPBI–Portuguese Platform of Bioimaging (PPBI-POCI-01-0145-FEDER-022122) and PT-OPENSCREEN. Tissue sections were kindly provided by Amaro Frutuoso, Department of Complementary Means of Diagnosis and Therapy, Service of Pathology, Hospital Pedro Hispano, Matosinhos.

References

1. Beutler B, Jiang Z, Georgel P, Crozat K, Croker B, Rutschmann S, et al. Genetic Analysis of Host Resistance: Toll-Like Receptor Signaling and Immunity at Large. Annu Rev Immunol (2006) 24:353–89. doi: 10.1146/annurev.immunol.24.021605.090552

2. Hoving JC, Wilson GJ, Brown GD. Signalling C-Type Lectin Receptors, Microbial Recognition and Immunity. Cell Microbiol (2014) 16:185–94. doi: 10.1111/cmi.12249

3. Rehwinkel J, Gack MU. RIG-I-Like Receptors: Their Regulation and Roles in RNA Sensing. Nat Rev Immunol (2020) 20:537–51. doi: 10.1038/s41577-020-0288-3

4. Franchi L, Warner N, Viani K, Nunez G. Function of Nod-Like Receptors in Microbial Recognition and Host Defense. Immunol Rev (2009) 227:106–28. doi: 10.1111/j.1600-065X.2008.00734.x

5. Hampton RY, Golenbock DT, Penman M, Krieger M, Raetz CR. Recognition and Plasma Clearance of Endotoxin by Scavenger Receptors. Nature (1991) 352:342–4. doi: 10.1038/352342a0

6. Elomaa O, Kangas M, Sahlberg C, Tuukkanen J, Sormunen R, Liakka A, et al. Cloning of a Novel Bacteria-Binding Receptor Structurally Related to Scavenger Receptors and Expressed in a Subset of Macrophages. Cell (1995) 80:603–9. doi: 10.1016/0092-8674(95)90514-6

7. Fabriek BO, van Bruggen R, Deng DM, Ligtenberg AJ, Nazmi K, Schornagel K, et al. The Macrophage Scavenger Receptor CD163 Functions as an Innate Immune Sensor for Bacteria. Blood (2009) 113:887–92. doi: 10.1182/blood-2008-07-167064

8. Sarrias MR, Farnós M, Mota R, Sánchez-Barbero F, Ibáñez A, Gimferrer I, et al. CD6 Binds to Pathogen-Associated Molecular Patterns and Protects From LPS-Induced Septic Shock. Proc Natl Acad Sci USA (2007) 104:11724–9. doi: 10.1073/pnas.0702815104

9. Vera J, Fenutría R, Cañadas O, Figueras M, Mota R, Sarrias MR, et al. The CD5 Ectodomain Interacts With Conserved Fungal Cell Wall Components and Protects From Zymosan-Induced Septic Shock-Like Syndrome. Proc Natl Acad Sci USA (2009) 106:1506–11. doi: 10.1073/pnas.0805846106

10. Ullrich A, Sures I, D'Egidio M, Jallal B, Powell TJ, Herbst R, et al. The Secreted Tumor-Associated Antigen 90K Is a Potent Immune Stimulator. J Biol Chem (1994) 269:18401–7. doi: 10.1016/S0021-9258(17)32322-0

11. Luo M, Zhang Q, Hu Y, Sun C, Sheng Y, Deng C. LGALS3BP: A Potential Plasma Biomarker Associated With Diagnosis and Prognosis in Patients With Sepsis. Infect Drug Resist (2021) 14:2863–71. doi: 10.2147/IDR.S316402

12. Gebe JA, Kiener PA, Ring HZ, Li X, Francke U, Aruffo A. Molecular Cloning, Mapping to Human Chromosome 1 Q21-Q23, and Cell Binding Characteristics of Spalpha, a New Member of the Scavenger Receptor Cysteine-Rich (SRCR) Family of Proteins. J Biol Chem (1997) 272:6151–8. doi: 10.1074/jbc.272.10.6151

13. Miyazaki T, Hirokami Y, Matsuhashi N, Takatsuka H, Naito M. Increased Susceptibility of Thymocytes to Apoptosis in Mice Lacking AIM, a Novel Murine Macrophage-Derived Soluble Factor Belonging to the Scavenger Receptor Cysteine-Rich Domain Superfamily. J Exp Med (1999) 189:413–22. doi: 10.1084/jem.189.2.413

14. Gonçalves CM, Castro MA, Henriques T, Oliveira MI, Pinheiro HC, Oliveira C, et al. Molecular Cloning and Analysis of SSc5D, a New Member of the Scavenger Receptor Cysteine-Rich Superfamily. Mol Immunol (2009) 46:2585–96. doi: 10.1016/j.molimm.2009.05.006

15. Mollenhauer J, Wiemann S, Scheurlen W, Korn B, Hayashi Y, Wilgenbus KK, et al. DMBT1, a New Member of the SRCR Superfamily, on Chromosome 10q25.3-26.1 Is Deleted in Malignant Brain Tumours. Nat Genet (1997) 17:32–9. doi: 10.1038/ng0997-32

16. Sarrias MR, Roselló S, Sánchez-Barbero F, Sierra JM, Vila J, Yélamos J, et al. A Role for Human Sp Alpha as a Pattern Recognition Receptor. J Biol Chem (2005) 280:35391–8. doi: 10.1074/jbc.M505042200

17. Bessa Pereira C, Bockova M, Santos RF, Santos AM, de Araujo MM, Oliveira L, et al. The Scavenger Receptor SSc5D Physically Interacts With Bacteria Through the SRCR-Containing N-Terminal Domain. Front Immunol (2016) 7:416. doi: 10.3389/fimmu.2016.00416

18. Bikker FJ, Ligtenberg AJ, Nazmi K, Veerman EC, van't Hof W, Bolscher JG, et al. Identification of the Bacteria-Binding Peptide Domain on Salivary Agglutinin (Gp-340/DMBT1), a Member of the Scavenger Receptor Cysteine-Rich Superfamily. J Biol Chem (2002) 277:32109–15. doi: 10.1074/jbc.M203788200

19. Sanjurjo L, Aran G, Roher N, Valledor AF, Sarrias MR. AIM/CD5L: A Key Protein in the Control of Immune Homeostasis and Inflammatory Disease. J Leukoc Biol (2015) 98:173–84. doi: 10.1189/jlb.3RU0215-074R

20. Padilla O, Pujana MA, López-de la Iglesia A, Gimferrer I, Arman M, Vilà JM, et al. Cloning of S4D-SRCRB, a New Soluble Member of the Group B Scavenger Receptor

Cysteine-Rich Family (SRCR-SF) Mapping to Human Chromosome 7q11.23. Immunogenetics (2002) 54:621–34. doi: 10.1007/s00251-002-0507-z

21. Desiere F, Deutsch EW, King NL, Nesvizhskii AI, Mallick P, Eng J, et al. The PeptideAtlas Project. Nucleic Acids Res (2006) 34:D655–8. doi: 10.1093/nar/gkj040

22. Farrah T, Deutsch EW, Omenn GS, Campbell DS, Sun Z, Bletz JA, et al. A High-Confidence Human Plasma Proteome Reference Set With Estimated Concentrations in PeptideAtlas. Mol Cell Proteomics (2011) 10:M110 006353. doi: 10.1074/mcp.M110.006353

23. Oliveira MI, Gonçalves CM, Pinto M, Fabre S, Santos AM, Lee SF, et al. CD6 Attenuates Early and Late Signaling Events, Setting Thresholds for T-Cell Activation. Eur J Immunol (2012) 42:195–205. doi: 10.1002/eji.201040528

24. Aden DP, Fogel A, Plotkin S, Damjanov I, Knowles BB. Controlled Synthesis of HBsAg in a Differentiated Human Liver Carcinoma-Derived Cell Line. Nature (1979) 282:615–6. doi: 10.1038/282615a0

25. Andersson LC, Nilsson K, Gahmberg CG. K562–a Human Erythroleukemic Cell Line. Int J Cancer (1979) 23:143–7. doi: 10.1002/ijc.2910230202

26. Fogh J, Fogh JM, Orfeo T. One Hundred and Twenty-Seven Cultured Human Tumor Cell Lines Producing Tumors in Nude Mice. J Natl Cancer Inst (1977) 59:221–6. doi: 10.1093/jnci/59.1.221

27. Weiss A, Wiskocil RL, Stobo JD. The Role of T3 Surface Molecules in the Activation of Human T Cells: A Two-Stimulus Requirement for IL 2 Production Reflects Events Occurring at a Pre-Translational Level. J Immunol (1984) 133:123–8.

28. Kohler PO, Bridson WE. Isolation of Hormone-Producing Clonal Lines of Human Choriocarcinoma. J Clin Endocrinol Metab (1971) 32:683–7. doi: 10.1210/jcem-32-5-683

29. DuBridge RB, Tang P, Hsia HC, Leong PM, Miller JH, Calos MP. Analysis of Mutation in Human Cells by Using an Epstein-Barr Virus Shuttle System. Mol Cell Biol (1987) 7:379–87. doi: 10.1128/mcb.7.1.379-387.1987

30. Nayak SK, O'Toole C, Price ZH. A Cell Line From an Anaplastic Transitional Cell Carcinoma of Human Urinary Bladder. Br J Cancer (1977) 35:142–51. doi: 10.1038/bjc.1977.21

31. Epstein MA, Achong BG, Barr YM, Zajac B, Henle G, Henle W. Morphological and Virological Investigations on Cultured Burkitt Tumor Lymphoblasts (Strain Raji). J Natl Cancer Inst (1966) 37:547–59. doi: 10.1093/jnci/37.4.547

32. Gallagher R, Collins S, Trujillo J, McCredie K, Ahearn M, Tsai S, et al. Characterization of the Continuous, Differentiating Myeloid Cell Line (HL-60) From a Patient With Acute Promyelocytic Leukemia. Blood (1979) 54:713–33. doi: 10.1182/blood.V54.3.713.713

33. Tsuchiya S, Yamabe M, Yamaguchi Y, Kobayashi Y, Konno T, Tada K. Establishment and Characterization of a Human Acute Monocytic Leukemia Cell Line (THP-1). Int J Cancer (1980) 26:171–6. doi: 10.1002/ijc.2910260208

34. Scherer WF, Syverton JT, Gey GO. Studies on the Propagation In Vitro of Poliomyelitis Viruses. IV. Viral Multiplication in a Stable Strain of Human Malignant Epithelial Cells (Strain HeLa) Derived From an Epidermoid Carcinoma of the Cervix. J Exp Med (1953) 97:695–710. doi: 10.1084/jem.97.5.695

35. Resende M, Cardoso MS, Frois-Martins R, Borges M, Jordan MB, Castro AG, et al. TNF-Mediated Compensatory Immunity to Mycobacterium Avium in the Absence of Macrophage Activation by IFN-Gamma. J Immunol (2019) 203:2451–8. doi: 10.4049/jimmunol.1801594

36. Correia A, Ferreirinha P, Botelho S, Belinha A, Leitao C, Caramalho I, et al. Predominant Role of Interferon-Gamma in the Host Protective Effect of CD8(+) T Cells Against Neospora Caninum Infection. Sci Rep (2015) 5:14913. doi: 10.1038/srep14913

37. Costa DM, Sa M, Teixeira AR, Loureiro I, Thouvenot C, Golba S, et al. TRSP Is Dispensable for the Plasmodium Pre-Erythrocytic Phase. Sci Rep (2018) 8:15101. doi: 10.1038/s41598-018-33398-8

38. Loureiro I, Faria J, Clayton C, Macedo-Ribeiro S, Santarem N, Roy N, et al. Ribose 5-Phosphate Isomerase B Knockdown Compromises Trypanosoma Brucei Bloodstream Form Infectivity. PloS Negl Trop Dis (2015) 9:e3430. doi: 10.1371/journal.pntd.0003430

39. Faria J, Loureiro I, Santarem N, Cecilio P, Macedo-Ribeiro S, Tavares J, et al. Disclosing the Essentiality of Ribose-5-Phosphate Isomerase B in Trypanosomatids. Sci Rep (2016) 6:26937. doi: 10.1038/srep26937

40. Madeira F, Park YM, Lee J, Buso N, Gur T, Madhusoodanan N, et al. The EMBL-EBI Search and Sequence Analysis Tools APIs in 2019. Nucleic Acids Res (2019) 47:W636–41. doi: 10.1093/nar/gkz268

41. Steentoft C, Vakhrushev SY, Joshi HJ, Kong Y, Vester-Christensen MB, Schjoldager KT, et al. Precision Mapping of the Human O-GalNAc Glycoproteome Through SimpleCell Technology. EMBO J (2013) 32:1478–88. doi: 10.1038/emboj.2013.79

42. Carmo AM, Sreenu VB. A Systematic and Thorough Search for Domains of the Scavenger Receptor Cysteine-Rich Group B Family in the Human Genome. In: Mahdavi

MA, editor. Bioinformatics - Trends and Methodologies. Rijeka, Croatia: InTech (2011). p. 195–210.

43. Gupta R, Brunak S. Prediction of Glycosylation Across the Human Proteome and the Correlation to Protein Function. Pac Symp Biocomput (2002) 7:310–22.

44. Gerhard DS, Wagner L, Feingold EA, Shenmen CM, Grouse LH, Schuler G, et al. The Status, Quality, and Expansion of the NIH Full-Length cDNA Project: The Mammalian Gene Collection (MGC). Genome Res (2004) 14:2121–7. doi: 10.1101/gr.2596504

45. Mollenhauer J, Herbertz S, Helmke B, Kollender G, Krebs I, Madsen J, et al. Deleted in Malignant Brain Tumors 1 Is a Versatile Mucin-Like Molecule Likely to Play a Differential Role in Digestive Tract Cancer. Cancer Res (2001) 61:8880–6.

46. Castro MA, Oliveira MI, Nunes RJ, Fabre S, Barbosa R, Peixoto A, et al. Extracellular Isoforms of CD6 Generated by Alternative Splicing Regulate Targeting of CD6 to the Immunological Synapse. J Immunol (2007) 178:4351–61. doi: 10.4049/jimmunol.178.7.4351

47. Uhlen M, Zhang C, Lee S, Sjostedt E, Fagerberg L, Bidkhori G, et al. A Pathology Atlas of the Human Cancer Transcriptome. Science (2017) 357:eaan2507. doi: 10.1126/science.aan2507

48. Simons ER. Measurement of Phagocytosis and of the Phagosomal Environment in Polymorphonuclear Phagocytes by Flow Cytometry. Curr Protoc Cytom (2010) Chapter 9:Unit9 31. doi: 10.1002/0471142956.cy0931s51

49. Sanjurjo L, Aran G, Tellez E, Amezaga N, Armengol C, Lopez D, et al. CD5L Promotes M2 Macrophage Polarization Through Autophagy-Mediated Upregulation of ID3. Front Immunol (2018) 9:480. doi: 10.3389/fimmu.2018.00480

50. Oliveira L, Carmo AM. Response: Commentary: The Scavenger Receptor SSc5D Physically Interacts With Bacteria Through the SRCR-Containing N-Terminal Domain. Front Immunol (2017) 8:1004. doi: 10.3389/fimmu.2017.01004

51. Lozano F, Martinez-Florensa M. Commentary: The Scavenger Receptor SSc5D Physically Interacts With Bacteria Through the SRCR-Containing N-Terminal Domain. Front Immunol (2017) 8:366. doi: 10.3389/fimmu.2017.00366

52. Martínez-Florensa M, Consuegra-Fernández M, Aranda F, Armiger-Borràs N, Di Scala M, Carrasco E, et al. Protective Effects of Human and Mouse Soluble Scavenger-Like CD6 Lymphocyte Receptor in a Lethal Model of Polymicrobial Sepsis. Antimicrob Agents Chemother (2017) 61:e01391–16. doi: 10.1128/AAC.01391-16

53. Aran G, Sanjurjo L, Barcena C, Simon-Coma M, Tellez E, Vazquez-Vitali M, et al. CD5L Is Upregulated in Hepatocellular Carcinoma and Promotes Liver Cancer Cell Proliferation and Antiapoptotic Responses by Binding to HSPA5 (GRP78). FASEB J (2018) 32:3878–91. doi: 10.1096/fj.201700941RR

54. Balakrishnan L, Bhattacharjee M, Ahmad S, Nirujogi RS, Renuse S, Subbannayya Y, et al. Differential Proteomic Analysis of Synovial Fluid From Rheumatoid Arthritis and Osteoarthritis Patients. Clin Proteomics (2014) 11:1. doi: 10.1186/1559-0275-11-1

55. Moller HJ, Peterslund NA, Graversen JH, Moestrup SK. Identification of the Hemoglobin Scavenger Receptor/CD163 as a Natural Soluble Protein in Plasma. Blood (2002) 99:378–80. doi: 10.1182/blood.V99.1.378

56. Ramos-Casals M, Font J, García-Carrasco M, Calvo J, Places L, Padilla O, et al. High Circulating Levels of Soluble Scavenger Receptors (sCD5 and sCD6) in Patients With Primary Sjögren's Syndrome. Rheumatology (Oxford) (2001) 40:1056–9. doi: 10.1093/rheumatology/40.9.1056

57. Haruta I, Kato Y, Hashimoto E, Minjares C, Kennedy S, Uto H, et al. Association of AIM, a Novel Apoptosis Inhibitory Factor, With Hepatitis via Supporting Macrophage Survival and Enhancing Phagocytotic Function of Macrophages. J Biol Chem (2001) 276:22910–4. doi: 10.1074/jbc.M100324200

58. Arai S, Kitada K, Yamazaki T, Takai R, Zhang X, Tsugawa Y, et al. Apoptosis Inhibitor of Macrophage Protein Enhances Intraluminal Debris Clearance and Ameliorates Acute Kidney Injury in Mice. Nat Med (2016) 22:183–93. doi: 10.1038/nm.4012

59. Gao X, Yan X, Zhang Q, Yin Y, Cao J. CD5L Contributes to the Pathogenesis of Methicillin-Resistant Staphylococcus Aureus-Induced Pneumonia. Int Immunopharmacol (2019) 72:40–7. doi: 10.1016/j.intimp.2019.03.057

60. Ghosh D, Stumhofer JS. Do You See What I See: Recognition of Protozoan Parasites by Toll-Like Receptors. Curr Immunol Rev (2013) 9:129–40. doi: 10.2174/15733955096661312032259 29

61. Vazquez-Mendoza A, Carrero JC, Rodriguez-Sosa M. Parasitic Infections: A Role for C-Type Lectins Receptors. BioMed Res Int (2013) 2013:456352. doi: 10.1155/2013/456352

62. Gurung P, Kanneganti TD. Immune Responses Against Protozoan Parasites: A Focus on the Emerging Role of Nod-Like Receptors. Cell Mol Life Sci (2016) 73:3035–51. doi: 10.1007/s00018-016-2212-3

63. Barnwell JW, Asch AS, Nachman RL, Yamaya M, Aikawa M, Ingravallo P. A Human 88-kD Membrane Glycoprotein (CD36) Functions In Vitro as a Receptor for a Cytoadherence

Ligand on Plasmodium Falciparum-Infected Erythrocytes. J Clin Invest (1989) 84:765–72. doi: 10.1172/JCI114234

64. Rodrigues CD, Hannus M, Prudencio M, Martin C, Goncalves LA, Portugal S, et al. Host Scavenger Receptor SR-BI Plays a Dual Role in the Establishment of Malaria Parasite Liver Infection. Cell Host Microbe (2008) 4:271–82. doi: 10.1016/j.chom.2008.07.012

65. Gomes IN, Palma LC, Campos GO, Lima JG, TF DEA, JP DEM, et al. The Scavenger Receptor MARCO Is Involved in Leishmania Major Infection by CBA/J Macrophages. Parasite Immunol (2009) 31:188–98. doi: 10.1111/j.1365-3024.2009.01093.x

Supplementary materials and methods

mRNA analysis of SSC4D in human cell lines, and expression of SSC4D-cytrine fusion protein in Caco-2 cells

Total RNA of different cell lines was isolated using the TripleXtractor directRNA kit (Grisp). Using 5 μg of RNA per sample, cDNA was synthesized using Superscript III reverse transcriptase (Invitrogen). The cDNA obtained was used to analyze the SSC4D expression by PCR with GoTaq DNA Polymerase (Promega). Primer sequences were the following: 5'-GGCGTCCACAATTGCTTTCA-3' and 5'-ACGGATCTGTCTGCCAAG-3'.

SSC4D cDNA was amplified by PCR from Hep G2 cells using the same primers, cloned into the lentiviral expression vector pHR-mCitrine using *Mlu*I and *Bam*HI restriction sites and transduced into Caco-2 cells.

Measurement of SSC4D accumulation in Caco-2 cells

SSC4D-expressing Caco-2 cells were plated at a density of 2 x 10^4 cells/well in a 96-well plate (CellCarrier Ultra). Cell seeding was optimized to achieve a confluency of 70% allowing optimal cell segmentation. Cells were maintained in imaging media and incubated for 3 days for optimal attachment. Culture media was then removed without disturbing the monolayer and replaced by fresh media containing Hoechst, for 45 min at 37 ºC.

For the 0 h time-point, cells were washed with sterile PBS and new medium was added, followed by image acquisition using the IN Cell Analyzer. A 20 x objective was used and 9 fields of view were collected in each well. Then, the plate was spun and different stimuli, IL-1β, IL-4, IL-6, IL-17, TNF-α, IFN-γ, LPS, and LTA, at different concentrations were added to the cells together with 10 μg/ml of Brefeldin A, an inhibitor of protein transport from the ER to the Golgi complex, and thus of protein secretion.

Image acquisition was done at 6 h post-stimuli, similar to the 0 h time-point. To quantify SSC4D intracellular accumulation in the Caco-2-SSC4D cells, first the nuclei of these cells were identified from the Hoechst channel, using a machine-learning-based (bio)image analysis tool – ilastik (65). The resulting pixel probability maps were used for further image analysis and quantification of the mCitrine intensity values per cell using another cell image analysis software – CellProfilerTM (66). Briefly, the image analysis workflow consisted in (i) correction for uneven illumination/lighting/shading on the mCitrine channel, (ii) segmentation of the nuclei from the probability maps, (iii) expansion of the nuclei by 10 pixels to create a bigger mask that covers the majority of the cell cytoplasm,

(iv) then the nucleus mask has been subtracted from the previous expanded mask and then (v) the mean pixel intensity per cell on the mCitrine channel has been quantified.

The mCitrine intensity for each cell was obtained and the average of for each field of view was then calculated. The intensity value of each field of view was normalized to the intensity value of the negative control (WT Caco-2 cells) followed by a normalization to the corresponding baseline condition (0 h).

Measurement of SSC4D secretion upon cytokine stimuli

Caco-2-SSC4D cells were plated at a density of 2 X 105 cells/well in a 12-well plate and incubated for 3 days for an optimum cell attachment. The culture medium was removed and new medium containing cytokines IL-1β, IL-4, IL-6, IL-17, TNF-α or IFN-γ in different concentrations (1, 10, and 100 ng/ml), or endotoxins LPS and LTA (at 10, 100, and 1000 ng/ml) was added to the cells. After the indicated times of incubation, supernatants were collected and then resuspended in Laemmli's sample buffer for SDS-PAGE and western blotting. The presence of SSC4D in the culture supernatants was detected using mouse anti-HA antibody followed by anti-mouse HRP conjugated antibody, and ECL detection.

Supplementary figures

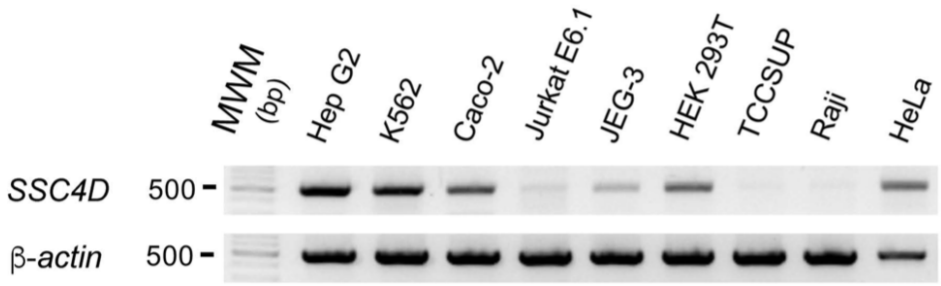

Supplemental Figure 1. SSC4D expression in human cell lines. Representative agarose gel images showing *SSC4D* mRNA expression in different human cell lines, measured by RT-PCR. *β-actin* mRNA is indicated as loading control. MWM, molecular weight markers.

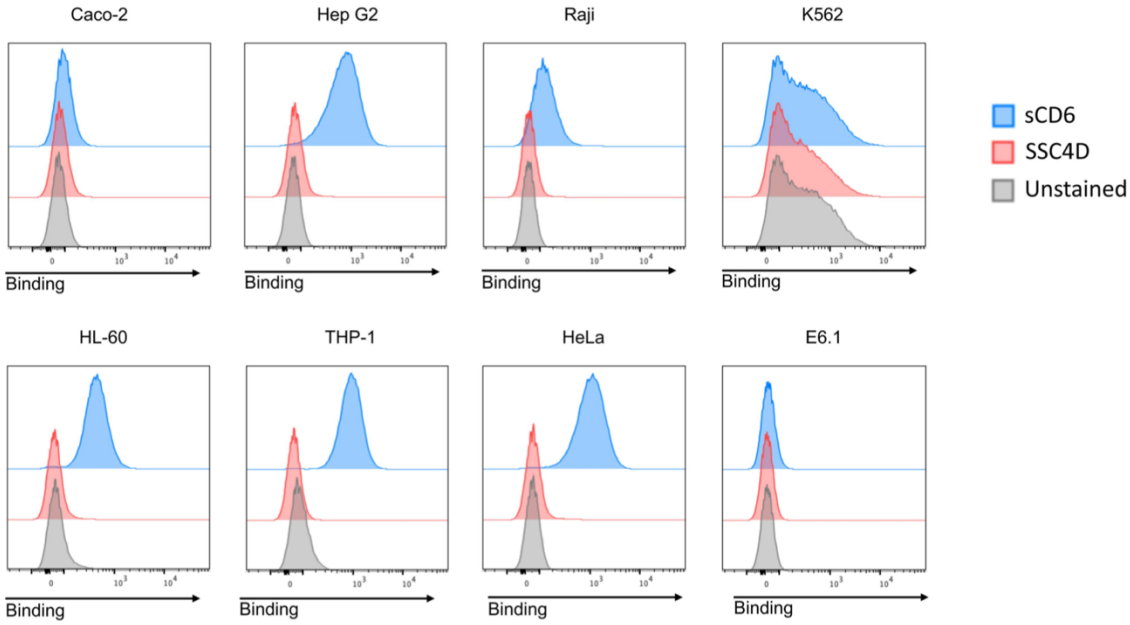

Supplemental Figure 2. No evidence for a cellular ligand for SSC4D. Caco-2, Hep G2, Raji, K562, HL-60, THP-1, HeLa and E6.1 cell suspensions were incubated with 3 μg of SSC4D or sCD6 or left untreated. Cell-bound proteins were detected with anti-HIS antibody followed with 647-conjugated anti-mouse antibody and analyzed by flow cytometry. Gray histograms represent control cells, not stained with SRCR protein but incubated with secondary antibody, red histograms represent cells labeled with SSC4D and blue histograms cells labeled with sCD6.

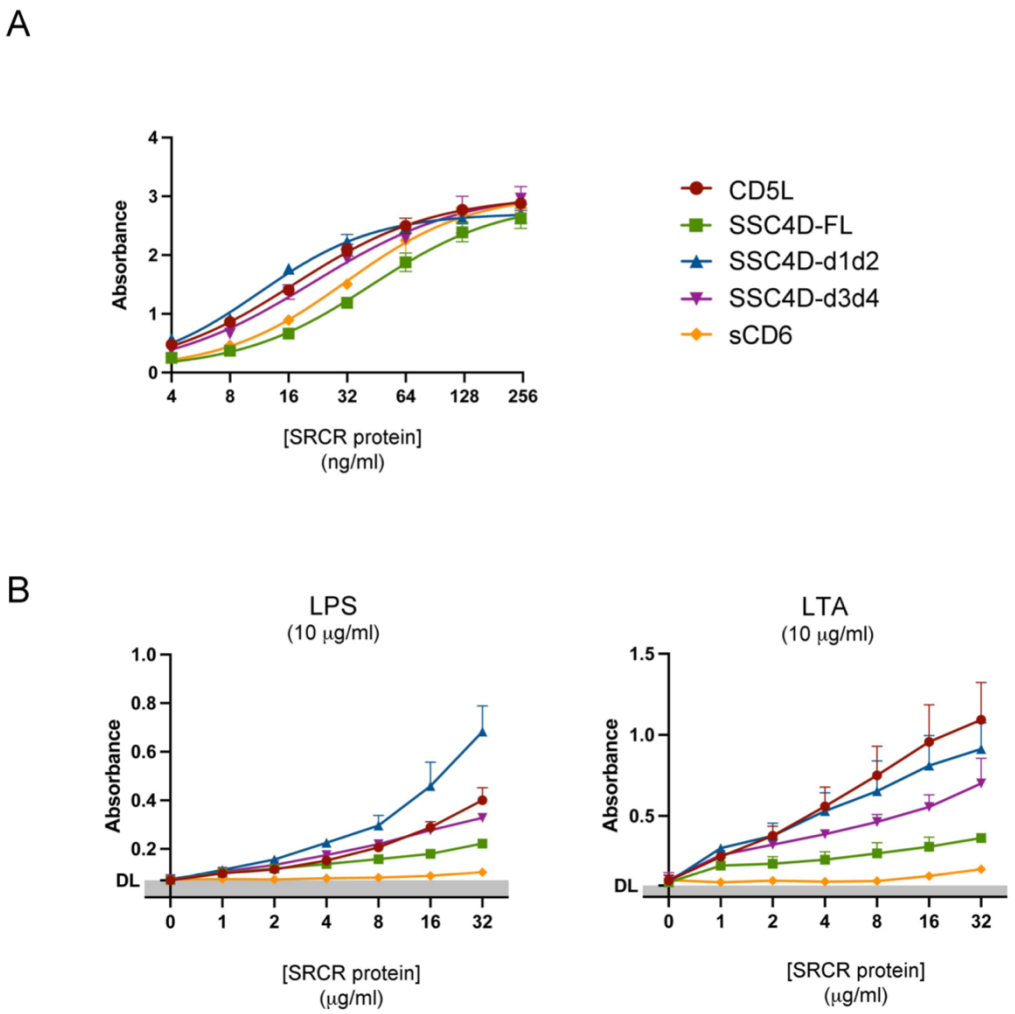

Supplemental Figure 3. Standard curve for detection of human SRCR proteins to LPS and LTA. (A) Serial dilutions of recombinant proteins SSC4D-FL, SSC4D-d1d2, SSC4D-d3d4, CD5L, and sCD6 were performed and proteins were directly coated in a 96-well plate. Plate-bound proteins were detected by anti-HIS antibody followed by HRP-conjugated antibody. Each point represents the mean ± SD of two independent experiments performed in duplicate. (B) 10 mg/ml of purified LPS or LTA were immobilized in a 96-well plate and incubated with different concentrations of recombinant SSC4D-FL, SSC4D-d1d2, SSC4D-d3d4, CD5L, or sCD6. Bound SRCR proteins were detected using anti-HIS antibody followed by HRP-conjugated antibody. Each point represents the mean ± SD of two experiments performed in duplicate.

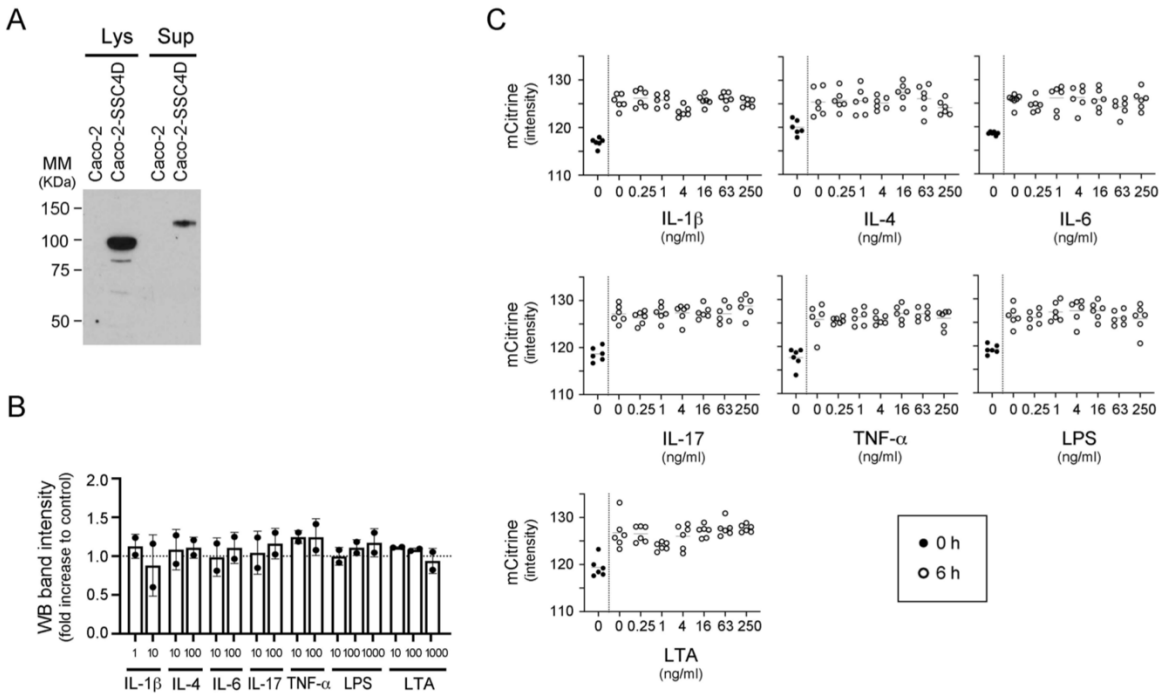

Supplemental Figure 4. SSC4D is secreted at constant rates, independently of external stimuli or cues. (A) Western blot of SSC4D fused to mCitrine and HA tag. The expressed protein displays a molecular mass of ~100 KDa when collected from cell lysates, compatible with the sum of the mass of SSC4D with those of mCitrine and HA, and of ~125 KDa as a secreted protein, also compatible with post-translational modifications observed earlier for recombinant SSC4D. (B) SSC4D secretion by Caco-2-SSC4D cells incubated for 24 h in the presence or absence of different stimuli (IL-1β, IL-4, IL-6, IL-17, TNF-α, LPS, and LTA) at different concentrations. The presence of SSC4D in the supernatants was analyzed by WB. Band densities were quantified and the values were normalized to the control (without stimulation). Graph shows the mean ± SD of two independent experiments. (C) Intracellular accumulation of SSC4D by Caco-2-SSC4D cells incubated for 6 h in the presence or absence of different stimuli (IL-1β, IL-4, IL-6, IL-17, TNF-α, LPS, and LTA) at different concentrations. Brefeldin A was used to block protein secretion, allowing for the determination of accumulation of intracellular SSC4D. Levels of intracellular SSC4D-mCitrine were analyzed using IN Cell. mCitrine intensity was measured before the addition of stimuli (0 h) and 6 h after the incubation with the different cytokines or endotoxins. In each time-point, 6 fields of view were analyzed for each well. Graphs shows one representative experiment of four with matching results, where mCitrine intensity values for each of the 6 fields of view were measured.

Chapter III

A protective role for CD5L in parasite infections involves the regulation of inflammatory responses

Manuscript in preparation

A protective role for CD5L in parasite infections involves the regulation of inflammatory responses

Marcos S. Cardoso[1,2,3], Liliana Oliveira[1,2], Rita F. Santos[1,2,3], Begoña Pérez-Cabezas[1,2], Joana Tavares[1,2], Alexandre M. Carmo[1,2]

[1]Instituto de Investigação e Inovação em Saúde, Universidade do Porto, Porto, Portugal

[2]IBMC–Instituto de Biologia Molecular e Celular, Porto, Portugal

[3]Programa Doutoral em Biologia Molecular e Celular (MCbiology), Instituto de Ciências Biomédicas Abel Salazar, Universidade do Porto, Porto, Portugal

[4]Departamento de Biologia, Universidade de Aveiro, Aveiro, Portugal

Abstract

CD5 antigen-like (CD5L) is a well-characterized pattern recognition receptor (PRR) of bacteria and fungi; however, the role of CD5L in inflammation remains controversial, having been previously reported to act both as pro-inflammatory as well as an anti-inflammatory mediator. Using conventional protein-microbial cell binding assays, we show for the first time that CD5L can establish direct physical interactions with different protozoan parasites, among which *Trypanosoma brucei*, *Plasmodium berghei* and *Leishmania* infantum, agents of the African trypanosomiasis, malaria, and visceral leishmaniasis, respectively. The function of CD5L in the context of immune responses against parasites was then evaluated using *Cd5l*$^{-/-}$ mice, developed by CRISPR/Cas9 gene targeting, analyzing the contribution of CD5L in eliminating the invasive pathogens and at the same time regulate the inflammatory response. Interestingly, whereas the absence of CD5L did not impact on *P. berghei* or *L. infantum* infections, the protein seems crucial in the protection against *T. brucei*. We observed an increased mortality of CD5L-knockout (KO) mice upon *T. brucei* infection compared with wild-type (WT) C57BL/6 mice, but without differences in the parasite burden. Twenty-eight days upon infection, there was an exacerbated inflammatory response in *T. brucei*-infected CD5L-KO mice, characterized by an increase in the frequency of T_H1 $CD4^+$ T cells and increased secretion of pro-inflammatory cytokines, supporting the hypothesis that CD5L is an important anti-inflammatory mediator, and that its absence leads to imbalanced immune responses and pathology.

Key words: scavenger receptor cysteine-rich; pattern recognition receptors; CD5L; parasites; inflammatory response

Introduction

Pattern recognition receptors (PRRs) constitute an important arm of the innate immune system that helps building a swift response to efficiently recognize and neutralize invasive pathogens. Different germline-encoded families of PRRs have unique capabilities to sense and bind distinct conserved pathogen-associated molecular patterns (PAMPs) present on microbes, and directly neutralize them (1). Pathogen recognition by cell-associated or soluble PRRs also triggers a broad and quick inflammatory response, and it additionally signals the information and instructs lymphocytes to induce the appropriate and specific adaptive immune response (2).

Among the diversity of immune-related classes of proteins described to target pathogens, the function of scavenger receptor cysteine-rich (SRCR) proteins as PRRs has been attracting increased attention. As a result of this recent interest, different SRCR molecules have been identified as PRRs for both Gram-negative and Gram-positive bacteria. However, the role of SRCR proteins as neutralizing factors for other pathogen types such as viruses and parasites remains poorly explored (3). Recently, we found that SSC4D, a secreted protein containing four SRCR domains, can recognize protozoan parasites such as *Leishmania* spp, *Trypanosoma brucei*, *Plasmodium berghei*, and *Neospora caninum* (4). Additionally, Leppert *et al.* have shown that macrophage scavenger receptor type A (SR-A) is also involved in T. brucei recognition and phagocytosis (5).

In addition to the PRR function, some scavenger receptors are also involved in the modulation of immune responses, as is the case of the T cell surface antigen CD5 that besides recognizing helminths and fungal cell wall components can also refrain T cell activation (6-8). Also, CD5 antigen-like (CD5L), firstly identified as secreted protein α (Spα) and also known as apoptosis inhibitor molecule (AIM) due to its anti-apoptotic functions (9, 10), is a well-established PRR for bacteria and fungi and, additionally, can promote macrophage polarization towards a pro-healing M2 phenotype (11). Although several studies described an anti-inflammatory role for CD5L (11, 12), others have categorized CD5L as a pro-inflammatory molecule (13, 14). In fact, in sharp contrast with the classical PRRs such as toll-like receptors (TLRs) or nucleotide oligomerization domain (NOD)-like receptors (NLRs), whose main function is to sense invasive pathogens, SRCRs act as pathogen sensors but also as regulators of the inflammatory response (3, 15). Thus, we hypothesized that CD5L is capable to sense microbes and instruct the immune system to an appropriate defensive response and at the same time act as a mediator that orchestrates the inflammatory response.

In this work, we demonstrate for the first time the ability of CD5L to physically interact with different protozoan parasites. We also addressed the involvement of CD5L in models of infection by *Trypanosoma brucei, Plasmodium berghei,* and *Leishmania infantum* but, interestingly, the expression of circulating CD5L in WT C57BL/6 mice was significantly increased only upon T. brucei infection, strongly suggesting a relevant role in trypanosomatid infections. To further detail the contribution of CD5L in the context of parasitic infections, CD5L-KO mice were challenged with the three different species of parasites previously identified. Our results highlighted the potential role of CD5L as a mediator of inflammatory processes in trypanosomatid infections.

Materials and Methods

Recombinant SRCR proteins

Recombinant human CD5L and the extracellular domain of human CD6 were produced in human embryonic kidney 293T cells and supplied in lyophilized form by INVIGATE GmbH. The proteins were translated from cDNA templates already described (16, 17) and modified to obtain a chimeric protein containing a signal peptide, the specific CD5L (Ser20 to Gly347) or CD6 (Asp25 to Glu398) sequences, HA and BirA recognition sequences, and 8-12·His tag sequences.

Mice, parasites, mosquitoes, and infection

CD5L-deficient C57BL/6J mice were generated as described elsewhere (18). All mice were kept in our animal facilities in HEPA filter-bearing cages under 12-h light/dark cycles and fed autoclaved chow and water *ad libitum*. Experimental mice were age- and sex-matched and used at 6- to 8-week-old.

Parasites were prepared as previously described: *Neospora caninum* tachyzoites (Nc-1, ATCC 50843) (19), *Plasmodium berghei* ANKA strain blood merozoites (clone 676cl1) (20), *Trypanosoma brucei brucei* GVR35 (21), *Trypanosoma brucei brucei* Lister 427 bloodstream forms (22), *Leishmania major* strain LV39 and *Leishmania tarentolae* strain Parrot-TarII promastigotes (23).

To produce *Plasmodium* sporozoites, mosquitoes were allowed to feed on infected NMRI mice. *Anopheles stephensi* (Sda500 strain) young female mosquitoes were reared at the Center for Production and Infection of Anopheles (CEPIA) at Institut Pasteur, Paris. Fed mosquitoes were kept in a humidified incubator at 21 ± 0.5 ºC and were further allowed to feed on non-infected NMRI mice, one week after the infectious feeding. Maintenance and rearing of mosquitoes were performed as described before (24, 25).

Mice were infected intraperitoneally with 5 x 10^4 of pleiomorphic *T. brucei brucei* GVR35, or intradermally with 2 x 10^4 of *Plasmodium berghei* sporozoites, or intravenously with 1 x 10^8 of *Leishmania infantum*. All animal experiments were performed in accordance with the recommendations of the European Convention for the Protection of Vertebrate Animals Used for Experimental and Other Scientific Purposes (ETS 123) and 86/609/EEC Directive and Portuguese rules (DL 129/92). All procedures involving mice were approved by the competent national authority Direcção Geral de Alimentação e Veterinária (DGAV) and by the i3S Animal Ethical Committee.

Quantification of soluble factors by ELISA

Blood from WT and CD5L-KO mice were collected from the tail vein at different time points post-infection starting at day 0 into non-heparinized capillaries. Blood was immediately transferred to an Eppendorf, followed by centrifugation to separate serum from the blood clot. Circulating CD5L was quantified in serum by enzyme-linked immunosorbent assay (ELISA) according to the manufacturer's instructions (Sino Biological). Serum IFN-γ, IL-17, and TNF-α levels were measured during *T. brucei* infection by commercial ELISA Max Deluxe kits (BioLegend). All the ELISA plates absorbance was read at 450 nm using Synergy 2 (BioTek). All samples were assayed in duplicate.

Flow cytometry

In the *T. brucei* infection model, splenocytes were collected at day 28 post-infection and 10^6 cells were incubated with FcR blocking (Miltenyi Biotec) for 10 min at 4 ºC followed by staining with distinct antibody panels including the following surface antibodies: CD45 PerCP/Cy5.5 (13/2.3), CD3 APC/Cy7 (17A2), CD19 APC (6D5), CD4 FITC (RM4-5), CD8 PE (53-6.7), CD11b PE/Cy7 (M1/70), CD11c Pacific Blue (N418), F4/80 APC/Cy7 (BM8), Ly6G APC (1A8), Ly6C FITC (HK1.4), CD25 PE (PC61). Intranuclear staining with FOXP3 Alexa Fluor 647 (150D), T-bet Brilliant Violet 421 (4B10), TCRβ (H57-597), RORγ T eFluor 710 (B2D) was performed using a cell fixation and permeabilization kit from eBiosciences. All the above-mentioned antibodies are from BioLegend, except TCRβ and RORγ T, which were obtained from BD Biosciences. Data were acquired in a FACSCanto II flow cytometer (BD Biosciences). Post-acquisition analysis was performed using FlowJo software v10 (Tree Star).

CD5L–Parasite Binding Assays

Binding of SRCR proteins to microbial cells was performed as described previously (16) using 2 μg of recombinant CD5L protein interacting with 1×10^7 live parasites in binding medium (TBS with 1% BSA, with or without 5 mM Ca^{2+}) for 1 h in an orbital shaker at 4 °C. Microbe-bound proteins were detected using mouse anti-Tetra HIS mAb (Qiagen) followed by incubation of anti-mouse HRP-conjugated antibody (BioLegend) for 1 h at RT. Immunoblots were developed using ECL. Sample loading was evaluated with a rabbit anti-*Leishmania infantum* cysteine synthase (at 1:2,000 dilution) for *Leishmania* parasites and a rabbit anti-*T. brucei* aldolase (1:5,000) for *T. brucei*.

Mice bioluminescence imaging

Mice infections with luciferase-expressing *T. brucei* GVR35 bloodstream forms, *P. berghei* sporozoites, and *L. infantum* axenic amastigotes were monitored by bioluminescence imaging using the IVIS Lumina LT system (Perkin Elmer). Ventral fur was shaved prior to image acquisition. Infected mice were anaesthetized with 2.5% isoflurane (O_2 flow of 1 L/min) and injected subcutaneously with D-luciferin potassium salt (2.4 mg, Perkin Elmer) 5 min before image acquisition. The detection of bioluminescent signals by the system resulted in the generation of signal maps automatically superimposed to the grey-scale photograph of the mice. The quantifications were performed using the Living Image software (Perkin Elmer) and the regions of interest (ROI) were manually defined. The total flux (photons/second) and average radiance (photons/second/cm2/steradian) within these ROIs were automatically calculated.

Ex vivo quantifications of the bioluminescence signal in specific organs was performed in the T*. brucei* infection model at day 28 post-infection. Mice were injected subcutaneously with D-luciferin potassium salt and then euthanized for brain, kidney, spleen, lung, and liver collection. Parasite loads were assessed by bioluminescence imaging and quantification using the IVIS Lumina LT system as described above.

Parasitemia

The percentage of infected red blood cells in mice infected with *P. berghei* was quantified by Giemsa-stained thin blood smear starting from the third day after sporozoite inoculation. At least 40 microscopic fields (~ 20,000 red blood cells; detection limit 0.005%) were analyzed.

Results

CD5L physically binds to different protozoan parasites

SRCR proteins can identify a large spectrum of pathogens, including not only bacteria but also viruses and fungi. The broad binding capacities of SRCRs have been recently extended to parasites, with the description that both CD5 and CD6 bind helminths, and that SSC4D can bind protozoan parasites (4, 6). We, therefore, explored whether the SSC4D-related SRCR protein CD5L could also physically interact with different groups of protozoan parasites, including Apicomplexa parasites such as *P. berghei* and *N. caninum* and Trypanosomatida such as *T. brucei* and *Leishmania* spp. In trypanosomatids, we

studied the physical interaction of CD5L with bloodstream forms of *T. brucei*, the parasite that causes African trypanosomiasis, and with promastigotes of *L. major* and *L. infantum*, that in humans cause cutaneous and visceral leishmaniasis, respectively, and with the non-pathogenic *L. tarentolae*.

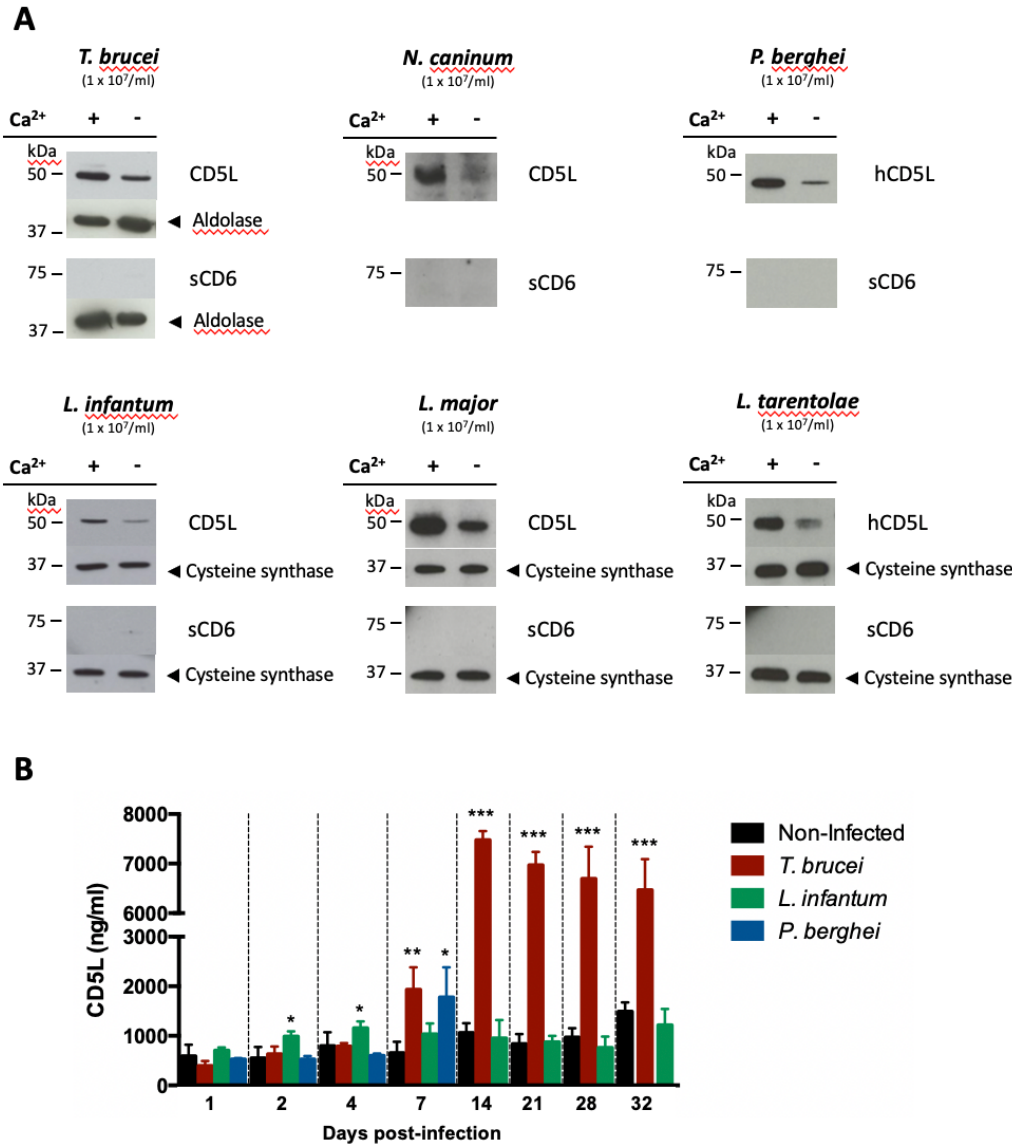

Figure 1 - Physical and functional interactions between CD5L and protozoan parasites. Two μg of recombinant CD5L or sCD6 were incubated with suspensions of 1 × 10^7 live *Trypanosoma brucei brucei* bloodstream forms, *Leishmania infantum*, *Leishmania major*, and *Leishmania tarentolae* promastigotes, *Plasmodium berghei* merozoites, and *Neospora caninum* tachyzoites, in the presence or absence of 5 mM Ca^{2+}. Parasite-bound proteins were detected by immunoblotting using anti-HIS mAb. Membranes were re-probed with an anti-aldolase, or anti-*L. infantum* cysteine synthase immune sera, as loading controls of *T. brucei*, or of *L. infantum, L. major,* and *L. tarentolae*, respectively. Results shown are of one of three independent experiments. (B) Blood was collected from C57BL/6 mice via tail vein and the circulating levels of CD5L were measured by ELISA, at different time-points after infection with *T. brucei* (red bars), *L. infantum* (green bars), or *P. berghei* (blue bars), or from uninfected mice (black bars).

The rodent malaria *P. berghei* merozoites and the *N. caninum* tachyzoites are among the studied apicomplexan parasites. Physical interactions were evaluated by incubating recombinant CD5L and sCD6 with suspensions of live parasites at 4 ºC followed by centrifugation and immunoblotting of the cell pellets. As seen in Fig. 1A, CD5L was found to associate with all the tested parasites in a Ca^{2+}-dependent manner, confirming that CD5L is also capable of physically interacting with protozoan parasites. In contrast, we did not find sCD6 in the parasite pellet, which suggests that CD6 is not capable to bind parasites, or that this capacity is weaker than that of CD5L and SSC4D.

Parasite infections lead to an increase in circulating CD5L

To determine whether the levels of circulating CD5L change upon infection with protozoan parasites, we measured its concentration in the sera of C57BL/6 mice before and after infection with either the (A) pleomorphic *T. b. brucei* GVR35, (B) *P. berghei* sporozoites delivered through skin inoculation or (C) *L. infantum* axenic amastigotes. All the parasite lines used in this study express a luciferase reporter. These three parasites represent three different infection models with distinguished intracellular and extracellular infection strategies, in which (A) *T. brucei* is a circulating extracellular parasite; (B) *P. berghei* is mostly intracellular but alternates with extracellular invasive stages; (C) *L. infantum* is an intracellular parasite. Importantly, as illustrated in Fig. 1A, CD5L is capable of physically interacting with these 3 different parasites.

African trypanosomiasis caused by *T. brucei* has two distinct stages. The first is due to the parasite replication in the blood and lymph, while the second stage begins once the parasite penetrates the blood-brain barrier and accesses the central nervous system. The pleomorphic *T. b. brucei* GVR35 strain is a current murine model of chronic stage II trypanosomiasis (26). In the rodent malaria model, mice were infected through the skin with sporozoites, the parasite stage transmitted by infected mosquitoes. Sporozoites actively migrate in the skin and invade dermal blood vessels, finding their way to the liver. Here, inside a hepatocyte, a single parasite will transform into thousands of red blood cell-infective forms, which will then initiate the symptomatic phase of infection. This pre-clinical phase in the liver lasts around two days in rodents (27). *Leishmania infantum* is responsible for visceral leishmaniasis as parasites infect internal organs including the spleen, liver, and bone marrow (28). Mice were infected by injection through the tail vein of *L. infantum* axenic amastigotes, which are highly infectious to mice (24).

Although no major differences were observed in the circulating levels of CD5L upon infection with *L. infantum*, a slight increase, nevertheless statistically significant, was

observed at days 2 and 4 post-infection (Fig. 1B). This CD5L augment at the very early stages of infection could be due to parasite establishment in target organs which could trigger the production of CD5L by immune cells. Similarly, CD5L levels upon *P. berghei* infection with sporozoites are not considerably altered compared with the uninfected control, except for day 7 post-infection when parasites have undergone several repetitive cycles of invasion and multiplication inside red blood cells (Fig. 1B). By sharp contrast, levels of CD5L were considerably increased upon infection with *T. b. brucei* (Fig. 1B). Although the circulating levels of CD5L were statistically increased already at day 7 post-infection, 3-fold higher than the uninfected control, the increase in CD5L levels reaches up to 7-8-fold when compared with uninfected controls, from day 14 post-infection onwards.

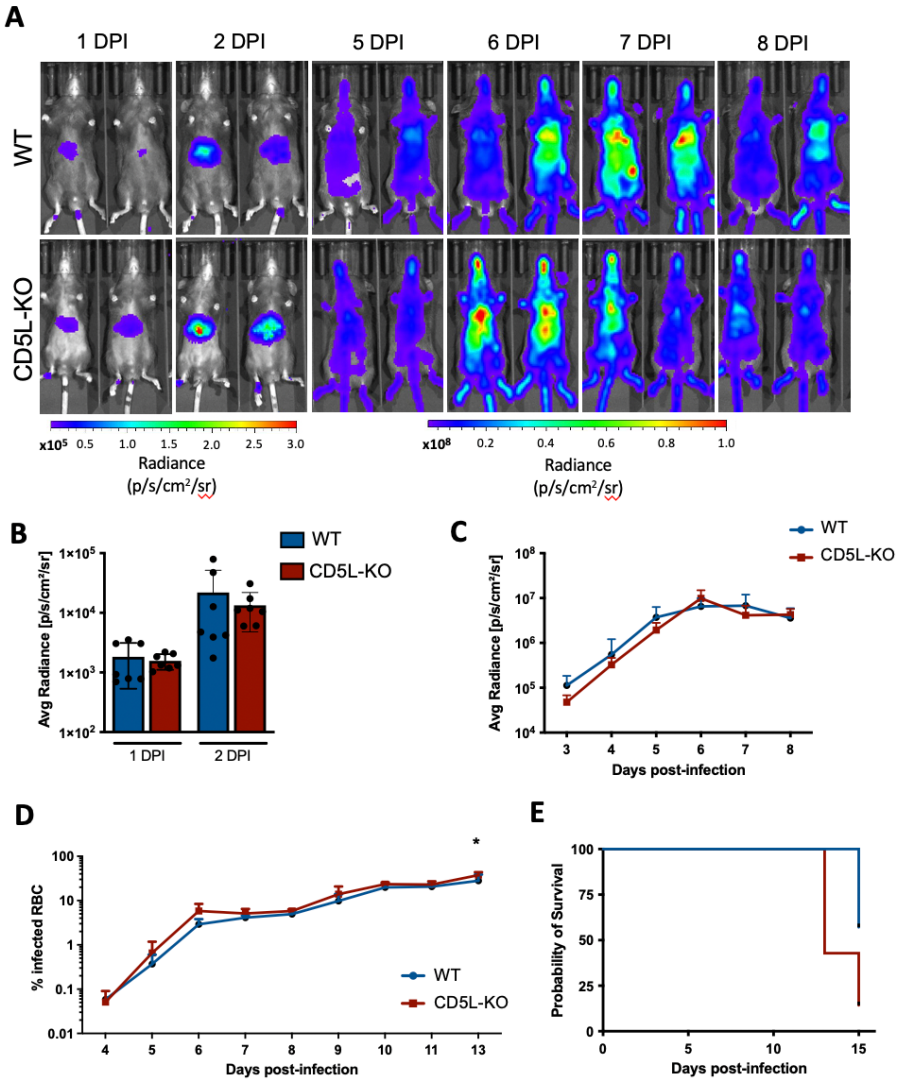

Figure 2 - *Plasmodium berghei* infection progression in WT C57BL/6 and in CD5L-KO mice. (A) WT and CD5L-KO mice were infected intradermally with 2 x 10^4 luciferase-expressing *P. berghei* sporozoites. Whole-mouse bioluminescence imaging was performed using an IVIS Lumina LT. The figure shows representative images on days 1, 2, 5, 6, 7 and 8 after infection, from one of two independent experiments. (Continues on the next page)

Figure 2 (Continuation) - (B) Bioluminescence average radiance (photons per seconds per square centimeter per steradian) quantification during liver stage. Graph shows the mean ± SD of two independent experiments (n= 7). (C) Bioluminescence average radiance (p/sec/cm^2/sr) of whole mouse body was quantified in WT and CD5L-KO mice during the blood stage. Graph shows the mean ± SD of two independent experiments (n= 7). (D) Parasitemia was determined daily by microscopic analysis of Hemacolor-stained blood smears. Graph shows the mean ± SD of two independent experiments (n= 7). *, $p < 0.05$ (two-way ANOVA). (E) Percentage of survival of WT and CD5L-KO mice upon *P. berghei* infection. Graph is from two independent experiments (n= 7).

CD5L does not impact on infection by P. berghei or L. infantum

To determine whether CD5L was required for effective protection against *P. berghei* or *L. infantum* infections, we used a mouse line in which the *Cd5l* gene has been genetically ablated (18). Both WT and CD5L-KO mice were infected by the microinjection of 2 x 10^4 of luciferase-expressing *P. berghei* sporozoites in the skin. Whole-body bioluminescence imaging was used to quantify the liver load in the first two days of infection. No differences in the parasite burden between WT and CD5L-KO mice were observed (Fig. 2A, B). Similarly, in the following days, from days 3 to 8 when parasites actively multiply in the blood, no differences were observed in the whole-body bioluminescence (Fig. 2C), in the percentage of infected red blood cells (Fig. 2D), nor in mouse survival (Fig. 2E). These findings suggest that the lack of CD5L does not impact on P. berghei ANKA strain infection in the susceptible C57BL/6 background. This model induces a neurological disease called experimental cerebral malaria that mirrors many of the pathological features observed in severe cerebral malaria, the most serious complication of the disease caused by P. falciparum, the most dangerous of the human parasites.

WT and CD5L-KO mice were also infected intravenously with luciferase-expressing *L. infantum* axenic amastigotes. Whole-mouse *in vivo* imaging shows parasite establishment in target organs, including the liver and bone marrow; however, no differences in bioluminescence were observed between WT and CD5L-KO mice (Fig. 3A, B). Importantly, the *in vivo* bioluminescent signal decreases over time in both WT and CD5L-KO mice. The parasite burdens in the liver, spleen, and bone marrow were quantified at 41 days post-infection, using the standard limiting dilution assay. No differences were observed between groups (Fig. 3C), which is in accordance with the data obtained using bioluminescence imaging, despite the lower sensitivity of the method (24). Overall, these results suggest that the lack of CD5L does not impact on the recognition, migration, nor on the control of *P. berghei* or *L. infantum* infections in the mouse.

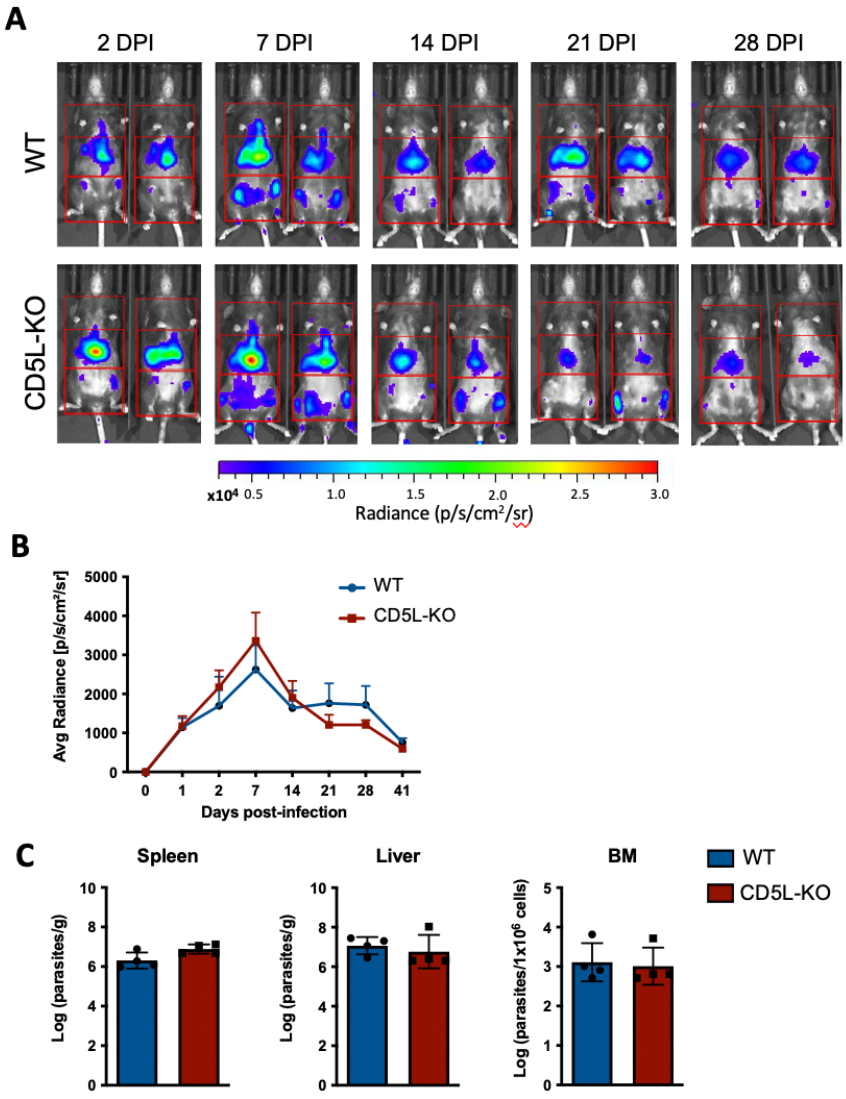

Figure 3 - *Leishmania infantum* infection progression in WT C57BL/6 and in CD5L-KO mice. (A) WT and CD5L-KO mice were infected intravenously with luciferase-expressing *L. infantum* axenic amastigotes. Whole-mouse bioluminescence imaging was performed using an IVIS Lumina LT. The figure shows representative images of WT and CD5L-KO mice in one experiment at days 2, 7, 14, 21, and 28 post-infection. (B) Bioluminescence average radiance (p/sec/cm^2/sr) was quantified in the whole body. Graph shows the mean ± SD (n = 4). (C) Parasite burden in the spleen, liver and bone marrow (BM) from infected WT and CD5L-KO mice was determined by limiting dilution at day 41 post-infection. Graph shows the mean ± SD (n = 4).

CD5L-KO mice are more susceptible to T. brucei infection

To assess the role of CD5L in African trypanosomiasis, WT and CD5L-KO mice were infected intraperitoneally with 5 x 10^4 of luciferase-expressing *T. b. brucei* GVR35 strain. As previously mentioned, this experimental model is characterized by parasite development in cyclic waves that lead to chronic disease and central nervous system infection. At each time point, mice were imaged using bioluminescence imaging, and blood

samples were also collected to quantify the parasitemia levels. Overall, no major differences were observed neither in the bioluminescence signal, parasite distribution nor in parasitemia (Fig. 4A-C). These results suggest that the role of CD5L as PRR does not impact substantially in the control of the infection, even though a slight increase in parasitemia was observed in each of the successive waves of infection, which could be due to the absence of this PRR.

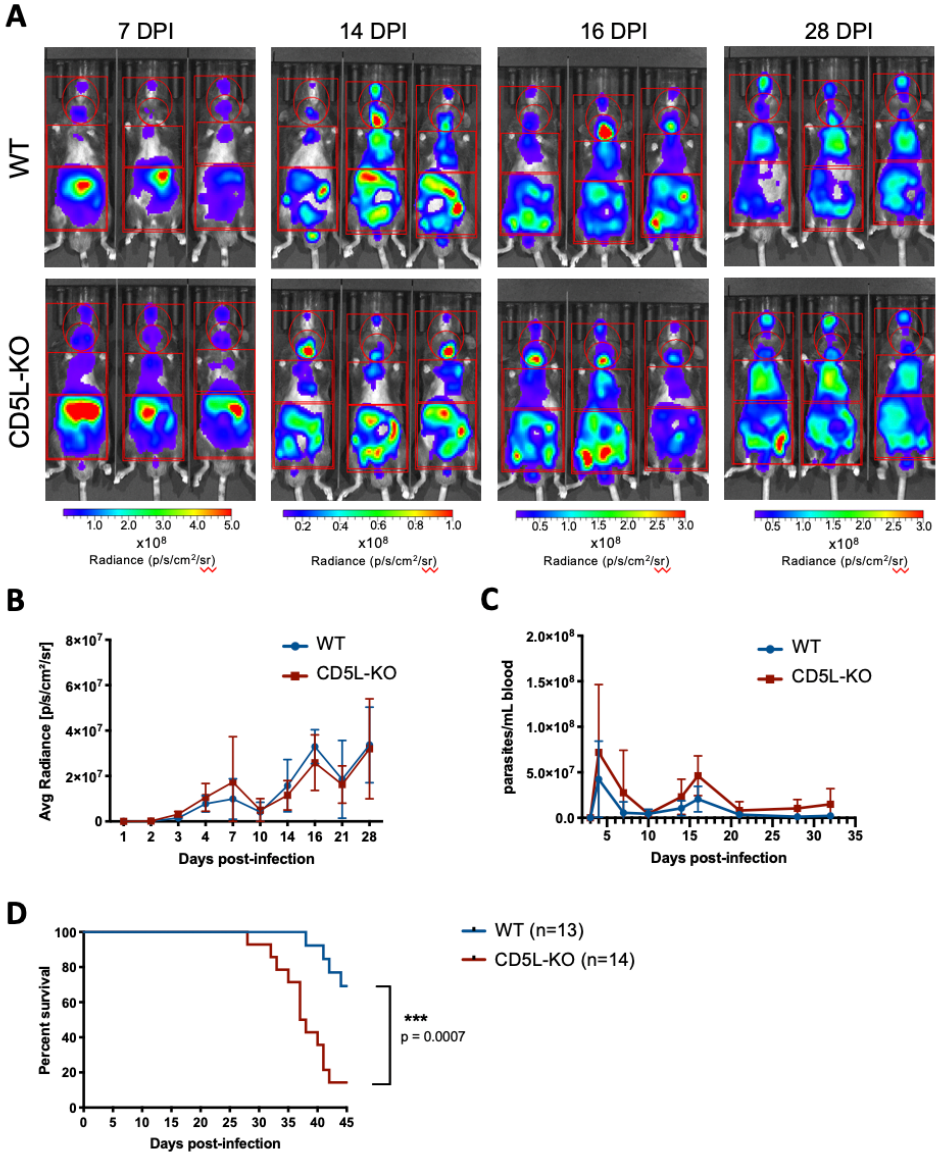

Figure 4 - CD5L-KO mice are more susceptible than WT mice to *T. b brucei* GVR35 infection. (A) WT and CD5L-KO mice were infected intraperitoneally with 5 x 10^4 luciferase-expressing *T. brucei* GVR35 strain. Whole-body bioluminescence imaging of WT and CD5L-KO mice was performed at 1-, 2-, 3-, 4-, 7-, 10-, 14-, 16-, 21-, and 28-days post-infection (DPI) using an IVIS Lumina LT. In the figure, we only show representative images of days 7, 14, 16, and 28 post-infection, from one of four independent experiments. (B) Bioluminescence average radiance (p/sec/cm^2/sr) of whole mouse body was quantified from WT and CD5L-KO mice. Graph shows the mean ± SD of four independent experiments (WT, n = 13; CD5L-KO, n=14). (Continues on the next page)

Figure 4 (Continuation) - (C) Parasitemia was determined using a Neubauer hemocytometer. Graph shows the mean ± SD of three independent experiments (WT, n = 9; CD5L-KO, n=10). (D) Percentage of survival of WT and CD5L-KO mice upon *T. brucei* infection. Graph is representative of four independent experiments. Kaplan–Meier survival curves were generated to compare mortality between the two groups and significance was determined by log-rank (Mantel-Cox) test. ***, $p < 0.005$.

Noticeably, CD5L-KO mice showed faster mortality rates the WT, even though no significant differences were observed in the parasite burden between both groups (Fig. 4D). Over 85% of the CD5L-KO animals died in the first 45 days of infection, compared with only 30.7% of WT mice.

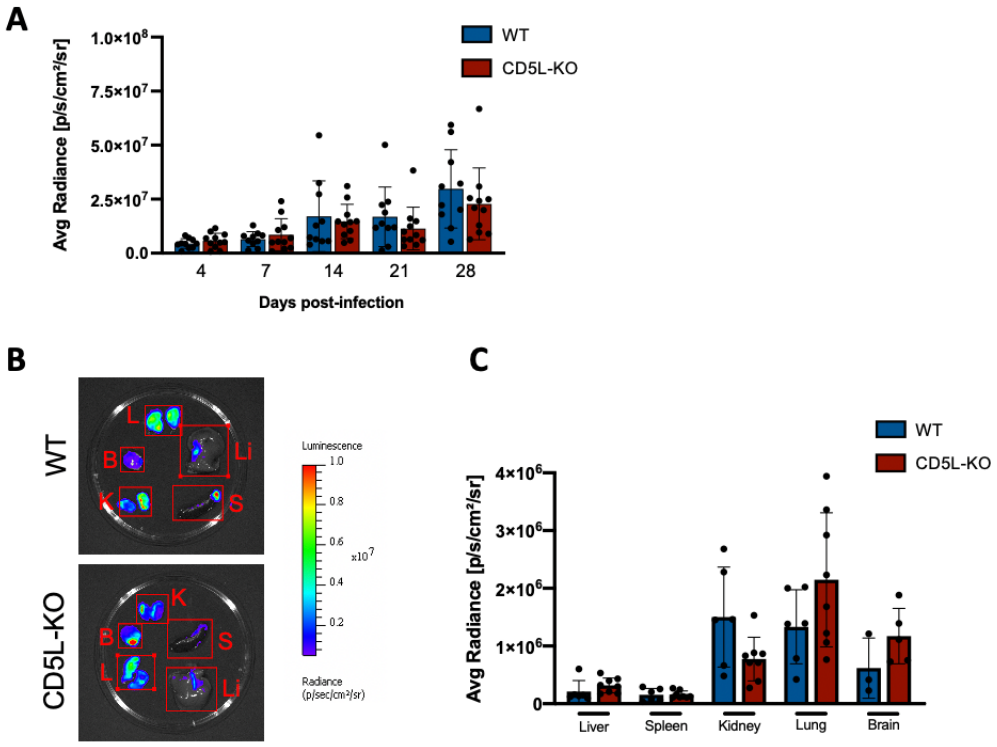

Figure 5 - Impact of the abrogation of CD5L in *T. brucei* infection. (A) Quantification of bioluminescence signal using a Regions of Interest (ROI) in the brain of WT and CD5L-KO mice infected with *T. brucei* GVR35 strain. Graph shows the mean ± SD of four independent experiments. (B) IVIS representative images of *ex vivo* liver (Li), spleen (S), kidney (K), lung (L), and brain (B) from WT and CD5L-KO mice at day 28-post-infection by *T. brucei*. (C) Average radiance of *ex vivo* imaged organs. Graph shows the mean ± SD of two independent experiments.

CD5L controls inflammation during T. brucei infection

The above-described results pointed to the hypothesis that high concentrations of circulating CD5L might have a protective role against the progression of the pathology induced by *T. brucei* infection. On the other hand, CD5L seems to have no effective role, or

only a minor impact, on the clearance of *T. brucei*. It is nevertheless possible that CD5L may be involved in the modulation of the inflammatory response, which could have an impact on disease progression. To assess this premise, we conducted different experiments at day 28 post-infection.

Whole-body bioluminescence imaging shows no obvious differences neither in parasite load nor in parasite distribution. We used rectangular regions of interest (ROIs) to determine the total bioluminescence signal emitted by *T. brucei* in the brains of WT and CD5L-KO mice during the course of infection. Although ROI analysis is not the most accurate method to measure parasite burden in a specific organ, we did not find statistical differences between WT and CD5L-KO mice (Fig 5A). Given that circulating parasites can influence the *in vivo* organ bioluminescence analysis, WT and CD5L-KO animals were euthanized at day 28 post-infection, selected organs were collected, and bioluminescence imaging of *ex vivo* lungs, liver, spleen, brain, and kidney was performed. Despite the differences being not significant, CD5L-KO lungs and brain displayed slightly increased radiance values, compared with the corresponding organs from WT mice, but lower values in the kidney (Fig. 5B, C). This mild increase in parasite burden in the lungs and particularly in the brain during the chronic stage of the disease could lead to a dysregulated inflammatory response (locally and systemically) that might result in increased immune cell infiltration, excessive production of inflammatory mediators like cytokines, and subsequent tissue damage that can lead to organ failure and death.

We thus assessed whether the absence of CD5L could impact on the inflammatory response resulting from the *T. brucei* infection. WT and CD5L-KO mice infected with *T. brucei* GVR35 were euthanized at day 28 post-infection and immune cell populations from spleen were analyzed by multi-color flow cytometry. Although no differences between the two animal groups were observed in total splenocyte counts, a significantly increased accumulation (percentage and numbers) of macrophages, inflammatory monocytes, and $CD4^+$ T_H1 cells were found in the spleen from CD5L-KO when compared with WT mice (Fig. 6A). In addition, we also observed a significant decrease in B cell numbers in the spleen of CD5L-KO mice. Other populations of lymphoid and myeloid cells were also analyzed, showing no significant differences.

Considering that the number of T_H1 cells and macrophages in the spleen were augmented, different cytokines were measured by ELISA at 14- and 28-days post-infection. We observed a statistical increase of IFN-γ in the early time-point and an increase of TNF-α in both time-points. No differences in IL-17 were observed (Fig. 6B). In addition, the frequencies of T_H1 and Treg cells differ substantially between WT and CD5L-KO mice. Whereas CD5L-KO mice display a significant augment in the percentage of T_H1 cells, by

contrast WT mice show a relative increase in the Treg population in infected animals (Fig. 6C). Consequently, the T_H1/Treg ratio is dramatically increased in CD5L-KO mice, showing a clear imbalanced response. Consequently, it is possible that in the absence of CD5L there is an increased susceptibility without differences in parasite burden followed by an amplification of a type 1 immune response. These results corroborate our hypothesis that CD5L might be an important anti-inflammatory mediator, and thus they strongly suggest that the absence of CD5L leads to a marked and predominant T_H1 response with very few suppressor T cells which could impact negatively in moderating the immune response.

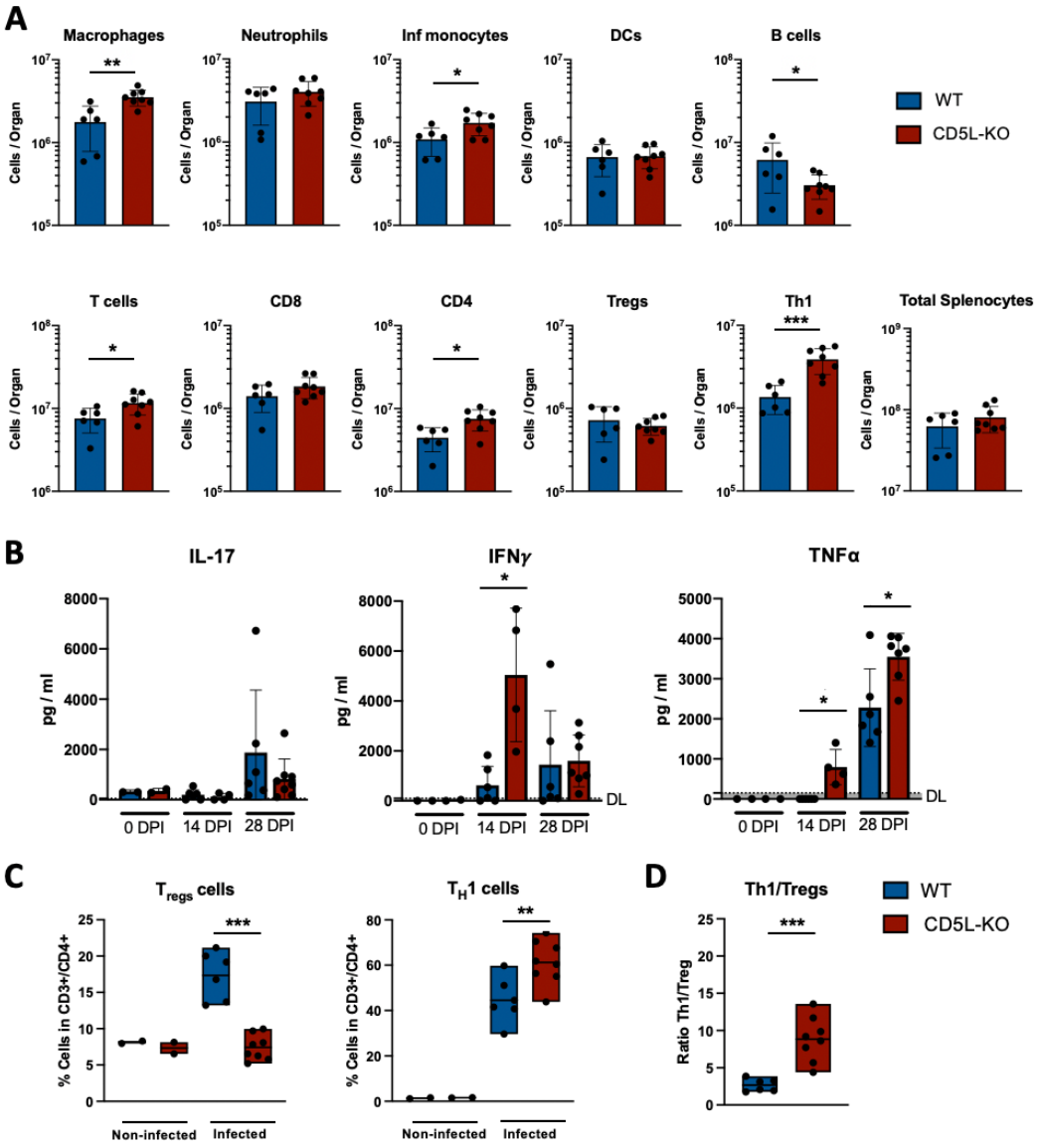

Figure 6 - Absolute numbers and frequency of spleen lymphoid cell populations in WT and CD5L-KO upon *T. brucei* infection. (A) Flow cytometry analysis of immune cell populations from spleens of WT and CD5L-KO mice at day 28 post-infection. Graphs show the mean ± SD of two independent experiments (n = 6). *, $p < 0.05$; **, $p < 0.01$; ***, $p < 0.005$ (unpaired Student's t test with Welch's correction). (Continues on the next page)

Figure 6 (Continuation) - (B) IL-17, IFN-γ, and TNF-α quantification in sera from WT and CD5L-KO mice at 0 (non-infected), 14-, and 28-days post-infection. Graphs show the mean ± SD. *, $p < 0.05$; **, $p < 0.01$; ***, $p < 0.005$ (two-way ANOVA). (C) Percentage of WT and CD5L-KO splenocytes that express FoxP3/CD25$^+$ (T_{regs}) and T-bet/CD25$^+$ (T_H1) from non-infected or *T. brucei* infected mice at 28 days post-infection. Graphs show the mean ± SD. **, $p < 0.01$; ***, $p < 0.005$ (unpaired Student's t test with Welch's correction). (D) Ratio of Treg/TH1 splenocytes from WT and CD5L-KO mice infected with *T. brucei* at 28 days post-infection. ***, $p < 0.005$ (unpaired Student's t test with Welch's correction). DCs: Dendritic cells; Tregs: T regulatory; T_H1: T helper 1 cells.

Discussion

The role of CD5L as PRR for bacteria has been extensively characterized; however, the putative role of CD5L as an immune sensor for parasites remained unexplored until now (29, 30). Recently, we have described that the CD5L-related SRCR protein SSC4D can bind to protozoan parasites (296). Given that SSC4D is also a secreted molecule and shares at the amino acid level a high homology with CD5L, we conjectured that CD5L might also act as PRR for protozoan parasites. The present report shows for the first time that CD5L is indeed capable of physically interacting with protozoan parasites (Fig.1A).

Although it is popularly recognized that pathogen recognition by the innate system involves different classes of PRRs such as toll-like receptors, C-type lectin receptors and NOD-like receptors, only recently there has been support for the concept that SRCR proteins constitute a legitimate branch of the PRR family. Deleted in malignant brain tumors 1 (DMBT1) was the first group B SRCR molecule identified as a PRR (31). Subsequent reports have shown that human and mouse CD5L also have the capacity to bind helminths, fungi, Gram-positive and Gram-negative bacteria (29, 30). The extracellular domains of the T cell receptors CD5 and CD6 can also recognize fungal and helminths parasitic cell wall components (6, 7). In addition, CD6 recognizes Gram-negative and Gram-positive bacteria; nevertheless, these interactions between CD6 and bacteria remain controversial (16, 32). Likewise, the macrophage scavenger receptor CD163 was also identified as a PRR for Gram-positive and Gram-negative bacteria (33). More recently, the soluble SRCR proteins SSC4D and SSC5D were both reported to bind Gram-positive and Gram-negative bacteria, while SSC4D was also reported to bind protozoan parasites (4, 16). The great majority of group B SRCR members have thus been shown to act as immune sensors to different types of pathogens, whereas SCART1 and M160 (CD163 antigen-like 1) remain as the only SRCR members without an unequivocal role in pathogen recognition. Nevertheless, the full binding spectrum of these proteins remains to be established (34). Overall, these pieces of

evidence highlight the relevance of the group B SRCR-SF in host immune surveillance, and strongly suggest that SRCR proteins are *bona fide* PRRs.

At steady-state, CD5L is constitutively secreted mainly by macrophages and monocytes; however, the expression of CD5L can be upregulated by macrophages/monocytes but also by other immune cell types upon an inflammatory stimulus (9). Based on this premise, we analyzed the expression of circulating CD5L upon infection of C57BL/6 mice with luciferase-expressing *T. brucei*, *P. berghei*, or *L. infantum*. These three parasites represent three different infection models, in which, *T. brucei* is a circulating extracellular parasite that leads to systemic infection and chronic disease, *P. berghei* is mostly intracellular but alternates with extracellular invasive stages that cause systemic infection and acute disease (ANKA strain), and *L. infantum* is an intracellular parasite that targets the liver, spleen, and bone marrow and leads to asymptomatic disease in mice. WT mice challenged with *T. brucei* produced significantly more CD5L when compared with non-infected mice (Fig.1B). In contrast, infections with *P. berghei* or *L. infantum* do not impact significantly the circulating levels of CD5L (Fig. 1B). These results can be explained considering the different mechanisms of parasite infections, or by different immune responses to the parasite.

First, we hypothesized that intracellular pathogens may escape circulating immune surveillance mechanisms and thus do not impact on the upregulation of CD5L. In the absence of symptomatology, as occurs in the *L. infantum* infection model, no significant differences in the expression of CD5L were observed. *L. infantum* parasites can subvert the activation of macrophages into a dormancy state, by decreasing the expression of PRRs, cytokine production, and thus we hypothesized that CD5L production/secretion could also be impaired in infected macrophages (35, 36).

We also hypothesized that other mechanisms might be involved. Our results showed that in both *T. brucei* and *P. berghei* experimental models, CD5L expression is increased at day seven post-infection. Curiously, in the *Corynebacterium parvum*-induced granuloma model, CD5L production peaks at day 10 after injection and is coincident with the peak in IL-12 production and with the recruitment of Thy1.2 cells to the liver (37). Additionally, Sanjurjo *et al.* showed that IL-10 polarized monocytes express significantly more CD5L than unstimulated cells (11). Taken together, these studies might indicate a correlation between the activation of the adaptive immune response and CD5L upregulation. Regarding the *P. berghei* infection model, we only observed a statistical difference in the last time-point analyzed. This infection model reflects the complexity of natural infections as it is initiated with sporozoites, the parasite stage transmitted by mosquitos, delivered through the skin.

Thus, the infection is divided into two well-compartmentalized stages in which the initial stage is asymptomatic, with parasites multiplying in the liver, followed by a systemic phase characterized by repetitive cycles of parasites multiplication inside red blood cells that cause the typical symptoms of malaria by triggering a massive immune response, clogging capillaries, and lysing red blood cell (38). However, the experimental *P. berghei* infection used in this work may have some limitations to study the mechanism behind the CD5L upregulation as it is an acute model of experimental cerebral malaria. Indeed, the early and fulminant cerebral pathology tends to limit the time window available as C57BL/6 mice survive for up to 10 days (39). Infections with other *P. berghei* strains that do not cause early fulminant pathology, such as NK65, are needed to fully investigate the role of CD5L in malaria.

The results regarding *T. brucei* infection showed a significant and dramatic augment in the expression of CD5L upon 7 days of infection, which may suggest an important role for CD5L in African trypanosomiasis. Curiously, in both *T. brucei* and *P. berghei* experimental models, the CD5L expression is increased at day seven post-infection which may indicate a correlation between the adaptative immune response activation and CD5L upregulation (Fig. 1C).

It is known that *T. brucei*-derived components sVSG and CpG DNA are recognized by the scavenger receptor (SR)-A and toll-like receptor 9 (TLR9). Mice deficient of this TLR display increased numbers of parasites following clearance of the first peak of parasitemia; however, no differences in survival were observed (5, 40, 41). Since we found that CD5L can bind to *T. brucei* parasites and the expression of CD5L is upregulated upon infection, we hypothesized a putative role for CD5L in *T. brucei* host resistance similar to TLR9. Nevertheless, we found no differences neither in parasitemia nor in the total parasite burden when we compared WT with CD5L-KO mice (Fig. 4A-C). Curiously, despite there being no significant differences in parasitemia, it is possible to observe a slight increase in parasite number in all peaks of parasitemia (Fig. 4C). From our point of view, these results suggest that CD5L is not required to control *T. brucei* infection, even though we do not exclude the possible contribution of CD5L in host resistance against *T. brucei* infection.

Although no differences in parasite numbers were observed throughout the experiments, the CD5L deficient mice showed enhanced susceptibility to *T. brucei* infection (Fig 4D). This striking result led us to hypothesize that the key role of CD5L in *T. brucei* infection was anti-inflammatory rather than anti-microbial. The role of CD5L in the modulation of the inflammatory response has been controversial, whereby some studies show divergent roles (anti-inflammatory *vs.* pro-inflammatory); however, there is a

consensus about the multifunctionality and importance of CD5L in the inflammatory response.

Overall, we observed by flow cytometry an accumulation of myeloid (macrophages and inflammatory monocytes) and lymphoid ($CD4^+$ T_H1 cells) cells in the spleens of CD5L-KO mice at day 28 post-infection (Fig. 6A). This accumulation suggests a marked and predominant T_H1 response, which is further amplified by the increased production of IFN-γ and TNF-α, which is observed 14- and 28-days post-infection in CD5L-KO mice (Fig. 6B). Importantly, we do not observe differences in total splenocyte numbers between WT and CD5L-KO mice. Although the polarization of T_H1 type immunity is associated with protection against *T. brucei* infection, it is also described that it can be detrimental to the host and may influence the host in terms of immunopathology (41-44). Thus, we hypothesized that there might be a correlation between the accumulation of T_H1 cells, immunopathology, and the increased susceptibility of the CD5L-KO mice to *T. brucei* infection. Additionally, Sanjurjo and collaborators have shown that CD5L drives macrophages towards an M2 phenotype using *in vitro* experiments (11). This observation can be a possible explanation for the increased levels of T_H1 cells that we detected in CD5L-KO mice. The deficiency of CD5L might block the polarization of macrophages towards an M2 phenotype, retaining a predominant T_H1 response, which leads to the production of T_H1-signature cytokines and consequently to an increased T_H1 differentiation, thus maintaining a pro-inflammatory environment that can be detrimental in CD5L-KO mice. The increased ratio of T_H1/Treg that is observed in CD5L-KO mice can indirectly support this hypothesis (Fig. 6C). Since M2 macrophages are an important source of IL-10, which is a key cytokine for Treg differentiation, the absence of CD5L may block the polarization to the M2 pro-healing phenotype and consequently downregulate the production of IL-10 and upregulate the production of IL-12, promoting a positive feedback loop that amplifies the T_H1 cell response.

Additionally, IFN-γ and TNF-α also play dual roles in *T. brucei* infection. On one hand, they are linked to host resistance; however, on the other hand they are associated with disease severity. It has been proposed that *T. brucei* parasites penetrate the blood-brain barrier (BBB) in an IFN-γ and TNF-α dependent manner, whereby TNF-α can induce the expression of adhesion molecules (such as ICAM-1 and VCAM-1) in brain endothelial cells, and early IFN-γ production can promote the penetration of T cells and parasites into the brain (45, 46). Moreover, higher levels of TNF-α are correlated with the severity of neuropathological symptoms in the human sleeping sickness (47). Although no significant differences were observed between WT and CD5L-KO mice in the *ex vivo* brain bioluminescence analysis, it is possible to observe an increase in the CD5L-KO brain bioluminescence at day 28 post-infection (Fig. 5B-C). Moreover, we do not know whether

this difference in the bioluminescent signal could reflect a significant or biological difference in parasite burden that impacts on the increased susceptibility observed in CD5L-KO mice. Overall, all these observations may suggest that the early and massive IFN-γ and TNF-α production observed in CD5L-KO mice might be associated with the invasion of parasitic cells into the brain in early time-points, followed by early neuropathological symptoms that could lead to increased susceptibility.

It is also plausible that the susceptibility mechanism in CD5L-KO mice occurs due to the increased numbers of macrophages, inflammatory monocytes, and T_H1 cells observed in CD5L-KO mice, followed by the dramatic enhancement of IFN-γ and TNF-α production. Through these observations, we hypothesized that the abrogation of CD5L could lead to the amplification of a type 1 immune response loop and the maintenance of a chronic pro-inflammatory environment, followed by the increase of an autoreactive inflammatory immune response that could impact dramatically on the survival of *T. brucei* infected mice.

Collectively, our results attribute to CD5L a role as a PRR for parasitic cell wall components. In addition, our data strongly suggest that CD5L can modulate the immune response by promoting the shift between a pro-inflammatory to an anti-inflammatory environment.

References

1. Janeway CA. Approaching the asymptote? Evolution and revolution in immunology. Cold Spring Harb Symp Quant Biol. 1989;54 Pt 1:1-13. doi: 10.1101/sqb.1989.054.01.003. PubMed PMID: 2700931.

2. Iwasaki A, Medzhitov R. Control of adaptive immunity by the innate immune system. Nat Immunol. 2015;16(4):343-53. doi: 10.1038/ni.3123. PubMed PMID: 25789684; PubMed Central PMCID: PMC4507498.

3. Martínez VG, Moestrup SK, Holmskov U, Mollenhauer J, Lozano F. The conserved scavenger receptor cysteine-rich superfamily in therapy and diagnosis. Pharmacol Rev. 2011;63(4):967-1000. Epub 20110831. doi: 10.1124/pr.111.004523. PubMed PMID: 21880988.

4. Cardoso MS, Santos RF, Almeida S, Sá M, Pérez-Cabezas B, Oliveira L, et al. Physical Interactions With Bacteria and Protozoan Parasites Establish the Scavenger Receptor SSC4D as a Broad-Spectrum Pattern Recognition Receptor. Front Immunol. 2021;12:760770. Epub 20211224. doi: 10.3389/fimmu.2021.760770. PubMed PMID: 35003072; PubMed Central PMCID: PMC8739261.

5. Leppert BJ, Mansfield JM, Paulnock DM. The soluble variant surface glycoprotein of African trypanosomes is recognized by a macrophage scavenger receptor and induces I kappa B alpha degradation independently of TRAF6-mediated TLR signaling. J Immunol. 2007;179(1):548-56. doi: 10.4049/jimmunol.179.1.548. PubMed PMID: 17579076.

6. Mourglia-Ettlin G, Miles S, Velasco-De-Andrés M, Armiger-Borràs N, Cucher M, Dematteis S, et al. The ectodomains of the lymphocyte scavenger receptors CD5 and CD6 interact with tegumental antigens from Echinococcus granulosus sensu lato and protect mice against secondary cystic echinococcosis. PLoS Negl Trop Dis. 2018;12(11):e0006891. Epub 20181130. doi: 10.1371/journal.pntd.0006891. PubMed PMID: 30500820; PubMed Central PMCID: PMC6267981.

7. Vera J, Fenutría R, Cañadas O, Figueras M, Mota R, Sarrias MR, et al. The CD5 ectodomain interacts with conserved fungal cell wall components and protects from zymosan-induced septic shock-like syndrome. Proc Natl Acad Sci U S A. 2009;106(5):1506-11. Epub 20090113. doi: 10.1073/pnas.0805846106. PubMed PMID: 19141631; PubMed Central PMCID: PMC2635803.

8. Biancone L, Bowen MA, Lim A, Aruffo A, Andres G, Stamenkovic I. Identification of a novel inducible cell-surface ligand of CD5 on activated lymphocytes. J Exp Med. 1996;184(3):811-9. doi: 10.1084/jem.184.3.811. PubMed PMID: 9064341; PubMed Central PMCID: PMC2192762.

9. Miyazaki T, Hirokami Y, Matsuhashi N, Takatsuka H, Naito M. Increased susceptibility of thymocytes to apoptosis in mice lacking AIM, a novel murine macrophage-derived soluble factor belonging to the scavenger receptor cysteine-rich domain superfamily. J Exp Med. 1999;189(2):413-22. doi: 10.1084/jem.189.2.413. PubMed PMID: 9892623; PubMed Central PMCID: PMC2192994.

10. Gebe JA, Kiener PA, Ring HZ, Li X, Francke U, Aruffo A. Molecular cloning, mapping to human chromosome 1 q21-q23, and cell binding characteristics of Spalpha, a new member of the scavenger receptor cysteine-rich (SRCR) family of proteins. J Biol Chem. 1997;272(10):6151-8. doi: 10.1074/jbc.272.10.6151. PubMed PMID: 9045627.

11. Sanjurjo L, Aran G, Téllez É, Amézaga N, Armengol C, López D, et al. CD5L Promotes M2 Macrophage Polarization through Autophagy-Mediated Upregulation of ID3. Front Immunol. 2018;9:480. Epub 20180312. doi: 10.3389/fimmu.2018.00480. PubMed PMID: 29593730; PubMed Central PMCID: PMC5858086.

12. Wang C, Yosef N, Gaublomme J, Wu C, Lee Y, Clish CB, et al. CD5L/AIM Regulates Lipid Biosynthesis and Restrains Th17 Cell Pathogenicity. Cell. 2015;163(6):1413-27. Epub 20151119. doi: 10.1016/j.cell.2015.10.068. PubMed PMID: 26607793; PubMed Central PMCID: PMC4671820.

13. Gao X, Yan X, Zhang Q, Yin Y, Cao J. CD5L contributes to the pathogenesis of methicillin-resistant Staphylococcus aureus-induced pneumonia. Int Immunopharmacol. 2019;72:40-7. Epub 20190405. doi: 10.1016/j.intimp.2019.03.057. PubMed PMID: 30959370.

14. Hasegawa H, Mizoguchi I, Orii N, Inoue S, Katahira Y, Yoneto T, et al. IL-23p19 and CD5 antigen-like form a possible novel heterodimeric cytokine and contribute to experimental autoimmune encephalomyelitis development. Sci Rep. 2021;11(1):5266. Epub 20210304. doi: 10.1038/s41598-021-84624-9. PubMed PMID: 33664371; PubMed Central PMCID: PMC7933155.

15. Li D, Wu M. Pattern recognition receptors in health and diseases. Signal Transduct Target Ther. 2021;6(1):291. Epub 20210804. doi: 10.1038/s41392-021-00687-0. PubMed PMID: 34344870; PubMed Central PMCID: PMC8333067.

16. Bessa Pereira C, Bocková M, Santos RF, Santos AM, Martins de Araújo M, Oliveira L, et al. The Scavenger Receptor SSc5D Physically Interacts with Bacteria through the SRCR-Containing N-Terminal Domain. Front Immunol. 2016;7:416. Epub 20161013. doi: 10.3389/fimmu.2016.00416. PubMed PMID: 27790215; PubMed Central PMCID: PMC5061727.

17. Farrah T, Deutsch EW, Omenn GS, Campbell DS, Sun Z, Bletz JA, et al. A high-confidence human plasma proteome reference set with estimated concentrations in PeptideAtlas. Mol Cell Proteomics. 2011;10(9):M110.006353. Epub 20110601. doi:

10.1074/mcp.M110.006353. PubMed PMID: 21632744; PubMed Central PMCID: PMC3186192.

18. Oliveira L, Gomes A, Santos R, Cardoso M, Nóvoa A, Luche H, et al. CD5L constraints acute and systemic inflammation and can be a novel potent therapeutic agent against sepsis. BioRxiv. 2022. doi: 10.1101/2022.03.08.483540.

19. Correia A, Ferreirinha P, Botelho S, Belinha A, Leitão C, Caramalho Í, et al. Predominant role of interferon-γ in the host protective effect of CD8(+) T cells against Neospora caninum infection. Sci Rep. 2015;5:14913. Epub 20151009. doi: 10.1038/srep14913. PubMed PMID: 26449650; PubMed Central PMCID: PMC4598874.

20. Costa DM, Sá M, Teixeira AR, Loureiro I, Thouvenot C, Golba S, et al. TRSP is dispensable for the Plasmodium pre-erythrocytic phase. Sci Rep. 2018;8(1):15101. Epub 20181010. doi: 10.1038/s41598-018-33398-8. PubMed PMID: 30305687; PubMed Central PMCID: PMC6180128.

21. McLatchie AP, Burrell-Saward H, Myburgh E, Lewis MD, Ward TH, Mottram JC, et al. Highly sensitive in vivo imaging of Trypanosoma brucei expressing "red-shifted" luciferase. PLoS Negl Trop Dis. 2013;7(11):e2571. Epub 20131121. doi: 10.1371/journal.pntd.0002571. PubMed PMID: 24278497; PubMed Central PMCID: PMC3836995.

22. Loureiro I, Faria J, Clayton C, Macedo-Ribeiro S, Santarém N, Roy N, et al. Ribose 5-phosphate isomerase B knockdown compromises Trypanosoma brucei bloodstream form infectivity. PLoS Negl Trop Dis. 2015;9(1):e3430. Epub 20150108. doi: 10.1371/journal.pntd.0003430. PubMed PMID: 25568941; PubMed Central PMCID: PMC4287489.

23. Faria J, Loureiro I, Santarém N, Cecílio P, Macedo-Ribeiro S, Tavares J, et al. Disclosing the essentiality of ribose-5-phosphate isomerase B in Trypanosomatids. Sci Rep. 2016;6:26937. Epub 20160527. doi: 10.1038/srep26937. PubMed PMID: 27230471; PubMed Central PMCID: PMC4882579.

24. Mendes Costa D, Cecílio P, Santarém N, Cordeiro-da-Silva A, Tavares J. Murine infection with bioluminescent Leishmania infantum axenic amastigotes applied to drug discovery. Sci Rep. 2019;9(1):18989. Epub 20191212. doi: 10.1038/s41598-019-55474-3. PubMed PMID: 31831809; PubMed Central PMCID: PMC6908656.

25. Tavares J, Costa DM, Teixeira AR, Cordeiro-da-Silva A, Amino R. In vivo imaging of pathogen homing to the host tissues. Methods. 2017;127:37-44. Epub 20170515. doi: 10.1016/j.ymeth.2017.05.008. PubMed PMID: 28522323.

26. Jennings FW, Rodgers J, Bradley B, Gettinby G, Kennedy PG, Murray M. Human African trypanosomiasis: potential therapeutic benefits of an alternative suramin and

melarsoprol regimen. Parasitol Int. 2002;51(4):381-8. doi: 10.1016/s1383-5769(02)00044-2. PubMed PMID: 12421636.

27. Ménard R, Tavares J, Cockburn I, Markus M, Zavala F, Amino R. Looking under the skin: the first steps in malarial infection and immunity. Nat Rev Microbiol. 2013;11(10):701-12. doi: 10.1038/nrmicro3111. PubMed PMID: 24037451.

28. Burza S, Croft SL, Boelaert M. Leishmaniasis. Lancet. 2018;392(10151):951-70. Epub 20180817. doi: 10.1016/S0140-6736(18)31204-2. PubMed PMID: 30126638.

29. Sarrias MR, Roselló S, Sánchez-Barbero F, Sierra JM, Vila J, Yélamos J, et al. A role for human Sp alpha as a pattern recognition receptor. J Biol Chem. 2005;280(42):35391-8. Epub 20050719. doi: 10.1074/jbc.M505042200. PubMed PMID: 16030018.

30. Martinez VG, Escoda-Ferran C, Tadeu Simões I, Arai S, Orta Mascaró M, Carreras E, et al. The macrophage soluble receptor AIM/Api6/CD5L displays a broad pathogen recognition spectrum and is involved in early response to microbial aggression. Cell Mol Immunol. 2014;11(4):343-54. Epub 20140303. doi: 10.1038/cmi.2014.12. PubMed PMID: 24583716; PubMed Central PMCID: PMC4085514.

31. Bikker FJ, Ligtenberg AJ, Nazmi K, Veerman EC, van't Hof W, Bolscher JG, et al. Identification of the bacteria-binding peptide domain on salivary agglutinin (gp-340/DMBT1), a member of the scavenger receptor cysteine-rich superfamily. J Biol Chem. 2002;277(35):32109-15. Epub 20020605. doi: 10.1074/jbc.M203788200. PubMed PMID: 12050164.

32. Sarrias MR, Farnós M, Mota R, Sánchez-Barbero F, Ibáñez A, Gimferrer I, et al. CD6 binds to pathogen-associated molecular patterns and protects from LPS-induced septic shock. Proc Natl Acad Sci U S A. 2007;104(28):11724-9. Epub 20070629. doi: 10.1073/pnas.0702815104. PubMed PMID: 17601777; PubMed Central PMCID: PMC1913855.

33. Fabriek BO, van Bruggen R, Deng DM, Ligtenberg AJ, Nazmi K, Schornagel K, et al. The macrophage scavenger receptor CD163 functions as an innate immune sensor for bacteria. Blood. 2009;113(4):887-92. Epub 20081010. doi: 10.1182/blood-2008-07-167064. PubMed PMID: 18849484.

34. Fink DR, Holm D, Schlosser A, Nielsen O, Latta M, Lozano F, et al. Elevated numbers of SCART1+ gammadelta T cells in skin inflammation and inflammatory bowel disease. Mol Immunol. 2010;47(9):1710-8. Epub 20100408. doi: 10.1016/j.molimm.2010.03.002. PubMed PMID: 20381152.

35. Kaye P, Scott P. Leishmaniasis: complexity at the host-pathogen interface. Nat Rev Microbiol. 2011;9(8):604-15. Epub 20110711. doi: 10.1038/nrmicro2608. PubMed PMID: 21747391.

36. Olivier M, Gregory DJ, Forget G. Subversion mechanisms by which Leishmania parasites can escape the host immune response: a signaling point of view. Clin Microbiol Rev. 2005;18(2):293-305. doi: 10.1128/CMR.18.2.293-305.2005. PubMed PMID: 15831826; PubMed Central PMCID: PMC1082797.

37. Kuwata K, Watanabe H, Jiang SY, Yamamoto T, Tomiyama-Miyaji C, Abo T, et al. AIM inhibits apoptosis of T cells and NKT cells in Corynebacterium-induced granuloma formation in mice. Am J Pathol. 2003;162(3):837-47. doi: 10.1016/S0002-9440(10)63880-1. PubMed PMID: 12598318; PubMed Central PMCID: PMC1868086.

38. Cowman AF, Healer J, Marapana D, Marsh K. Malaria: Biology and Disease. Cell. 2016;167(3):610-24. doi: 10.1016/j.cell.2016.07.055. PubMed PMID: 27768886.

39. Swanson PA, Hart GT, Russo MV, Nayak D, Yazew T, Peña M, et al. CD8+ T Cells Induce Fatal Brainstem Pathology during Cerebral Malaria via Luminal Antigen-Specific Engagement of Brain Vasculature. PLoS Pathog. 2016;12(12):e1006022. Epub 20161201. doi: 10.1371/journal.ppat.1006022. PubMed PMID: 27907215; PubMed Central PMCID: PMC5131904.

40. Magez S, Stijlemans B, Baral T, De Baetselier P. VSG-GPI anchors of African trypanosomes: their role in macrophage activation and induction of infection-associated immunopathology. Microbes Infect. 2002;4(9):999-1006. doi: 10.1016/s1286-4579(02)01617-9. PubMed PMID: 12106794.

41. Drennan MB, Stijlemans B, Van den Abbeele J, Quesniaux VJ, Barkhuizen M, Brombacher F, et al. The induction of a type 1 immune response following a Trypanosoma brucei infection is MyD88 dependent. J Immunol. 2005;175(4):2501-9. doi: 10.4049/jimmunol.175.4.2501. PubMed PMID: 16081822.

42. Hertz CJ, Filutowicz H, Mansfield JM. Resistance to the African trypanosomes is IFN-gamma dependent. J Immunol. 1998;161(12):6775-83. PubMed PMID: 9862708.

43. Stijlemans B, Guilliams M, Raes G, Beschin A, Magez S, De Baetselier P. African trypanosomosis: from immune escape and immunopathology to immune intervention. Vet Parasitol. 2007;148(1):3-13. Epub 20070607. doi: 10.1016/j.vetpar.2007.05.005. PubMed PMID: 17560035.

44. Stijlemans B, Caljon G, Van Den Abbeele J, Van Ginderachter JA, Magez S, De Trez C. Immune Evasion Strategies of Trypanosoma brucei within the Mammalian Host: Progression to Pathogenicity. Front Immunol. 2016;7:233. Epub 20160624. doi: 10.3389/fimmu.2016.00233. PubMed PMID: 27446070; PubMed Central PMCID: PMC4919330.

45. Amin DN, Vodnala SK, Masocha W, Sun B, Kristensson K, Rottenberg ME. Distinct Toll-like receptor signals regulate cerebral parasite load and interferon α/β and tumor necrosis factor α-dependent T-cell infiltration in the brains of Trypanosoma brucei-infected

mice. J Infect Dis. 2012;205(2):320-32. Epub 20111123. doi: 10.1093/infdis/jir734. PubMed PMID: 22116836; PubMed Central PMCID: PMC3244369.

46. Zeni P, Doepker E, Schulze-Topphoff U, Schulze Topphoff U, Huewel S, Tenenbaum T, et al. MMPs contribute to TNF-alpha-induced alteration of the blood-cerebrospinal fluid barrier in vitro. Am J Physiol Cell Physiol. 2007;293(3):C855-64. Epub 20070516. doi: 10.1152/ajpcell.00470.2006. PubMed PMID: 17507431.

47. Okomo-Assoumou MC, Daulouede S, Lemesre JL, N'Zila-Mouanda A, Vincendeau P. Correlation of high serum levels of tumor necrosis factor-alpha with disease severity in human African trypanosomiasis. Am J Trop Med Hyg. 1995;53(5):539-43. doi: 10.4269/ajtmh.1995.53.539. PubMed PMID: 7485714.

Chapter IV

General Discussion

The capacity to recognize invasive pathogens defines one of the most critical events in our body. In this thesis we have identified a new PRR member – SSC4D, which can recognize protozoan parasites, Gram-negative, and Gram-positive bacteria. We also focus on CD5L, a well-established PRR for bacteria and fungi. Interestingly, *E. coli* bioparticle phagocytosis by macrophages is augmented in the presence of SSC4D, in contrast with what is witnessed for CD5L that does not impact on phagocytosis.

CD5L is a very complex molecule with different functions in our system, namely in the modulation of the immune response, and we have additionally found a novel type of interactions between CD5L and parasites that advances our current knowledge on the CD5L spectrum of pathogen recognition. We found that expressing levels of circulating CD5L are dramatically augmented upon infection with *Trypanosoma brucei* parasites but not with *Leishmania infantum* or *Plasmodium berghei*. Moreover, CD5L-KO mice are much more susceptible to *T. brucei* infection when compared with WT mice. Curiously, we do not observe differences in the number of parasites within the tissues nor in the number of circulating parasites in CD5L-KO mice. Rather, we observed a dysregulated immune response which is correlated with an increase of macrophages, inflammatory monocytes, and $CD4^+$ T_H1 cells. Moreover, the inflammatory response in the CD5L-KO mice is further amplified with a significant increase of IFN-γ and TNF-α.

In this section, I discuss the major findings obtained in this thesis and integrate them with several key studies that have contributed to our current understanding of the processes underlying pathogen recognition and inflammatory responses.

Pathogen recognition – the unifying function for the SRCR proteins?

Since the elegant and fascinating theory of PRRs proposed by Charles Janeway, followed by the pioneering discovery of the first toll-like receptor by Jules Hoffmann, a myriad of molecules with the capacity to sense pathogenic microorganisms and to instruct the innate and adaptive immune system to respond to the invader pathogen have been identified (2, 60). In this particular matter, we and others have been characterizing SRCR-SF group B proteins as PRRs. The SRCR-SF group B is comprised by a heterogeneous group of proteins that share high levels of structure similarities, highlighted by the presence of genetically conserved SRCR domains. Although there are extraordinary sequence similarities between all individual type B SRCR domains and a nearly perfect conservation of key residues, namely eight regularly spaced cysteine residues that establish intra-domain disulfide bonds in very defined combinations, and also sequences that are 100% conserved

in all known domains, especially in the β1 and β2 strands and in the boundaries between the α1 helix and the β4 strand, the SRCR-SF is characterized by a vast functional diversity **(Results Chapter II, Figure 1A)**. In fact, no unifying function has been described for the superfamily (99).

The multifunctionality among SRCR domain-containing proteins can be in part explained by the numerical variations of SRCR domain tandem repeats, by the presence of non-SRCR domains, namely CUB and ZP domains in some SRCR proteins, and by different protein expression patterns. These features impact significantly by generating multiple SRCR proteins with exclusive functions, which include: modulators of inflammation, iron homeostasis, T cell activation, cell apoptosis, among others (105, 297, 298). Nonetheless, the great majority of the group B SRCR members have been shown to act as immune sensors of different pathogens (99). Upon the recent identification of SSC4D as a PRR, six out of eight group B SRCR proteins were pinpointed with the ability to recognize and bind to microbial structures. SCART1and M160 are the only SRCR group B member without the described ability to bind pathogens; however, the full binding spectrum of SCART1 and M160 remain incomplete (299). Overall, these data highlight two key conclusions. First, they strongly suggest that the ability to bind to pathogens might be the unifying function for this superfamily of proteins. Secondly, these data strengthen the concept that SRCR-SF is a legitimate member of the broader family of PRRs.

SRCR proteins vs. classic PRRs molecules

Regarding their role as PRRs, group B SRCR-SF and classical PRRs families are functionally distinct. One of the major features of classic PRRs, such as TLRs, NLRs, and RLRs, is that each family displays high specificity to a certain antigen. These features are in deep contrast to what is known for the SRCR-SF. For instance, CD5L can bind to protozoan parasites, fungi, Gram-negative, and Gram-positive bacteria (121). Recently, we showed that SSC4D physically interacts with protozoan parasites, Gram-negative, and Gram-positive bacteria **(Results Chapter II, Figure 4A, 6A and B; Results Chapter III, Figure 1A)**. The extracellular domains of the T cell antigens CD5 and CD6 can recognize fungal and helminths parasitic cell wall components (300). In addition, CD6 is reported to Gram-negative and Gram-positive bacteria, although these interactions remain controversial (118, 297). Recently our lab has shown that SSC5D can bind to both Gram-negative and Gram-positive bacteria (118). DMBT1 bind to viruses, including HIV-1 and influenza A virus, and to Gram-negative and Gram-positive bacteria (115, 119, 301). Overall, these observations strongly suggest that each group B SRCR member recognizes

a broad range of microbial pathogens. We hypothesized that these promiscuous interactions between group B SCRC proteins and pathogens can be a potential immunological advantage. Most of these receptors are present in epithelial cells or in circulation, which means they patrol the main body entries, scavenging for putative invasive pathogens. Thus, upon microbial invasion, these promiscuous PRRs will recognize a myriad of pathogens, triggering a faster, even though unspecific, immune response.

According to Medzhitov, the immune response pathway comprises four distinct functional categories: inducers, sensors, effectors, and mediators (59). Briefly, inducers (such as LPS) are signals that activate specific immune sensors (such as TLR4) that stimulate and induce an inflammatory response by effector cells (such as macrophages), producing immune mediators (such as TNF-α) that orchestrate all the inflammatory response. Thus, classical PRRs act exclusively as immune sensors of a specific antigen during the inflammatory response (59, 67). In contrast, recent observations have been addressing the role of some group B SRCR domain-containing proteins as mediators of inflammation. The better studied SRCR protein as mediator of inflammatory responses is CD5L. It is known that CD5L induces the polarization of macrophages into a pro-healing M2 phenotype (143). Additionally, *in vitro* experiments showed that CD5L inhibited monocyte TNFα and IL-1β production while enhancing IL-10 secretion upon stimulation with LPS (113, 121, 143). Bárcena *et al.* tested the therapeutic potential of CD5L administration in an *in vivo* model of hepatic fibrosis. The results suggested that CD5L impacts directly on the hepatic stellate cells by inducing SMAD7 expression while repressing TGF expression, leading to the reduction of collagen deposition. Additionally, they also found a reduction in cell infiltration and a phenotypic shift between high inflammatory monocytes to resident monocytes (302).

We here took advantage of a mouse model where the *cd5l* gene was abrogated, to study the role of this protein in different experimental infectious diseases. Surprisingly, we did not find major differences in parasitic burdens between WT and CD5L-KO mice, even though the latter were much more susceptible to *T. brucei* infection. Instead, we found a dysregulated inflammatory response, which supports the concept that CD5L is a crucial player in the inflammatory response **(Results Chapter III, Figure 4A-C)**. In agreement, different studies using CD5L-KO mice have defined CD5L as a key player in inflammation. Hasegawa *et al.* demonstrated that CD5L binds to the p19 subunit of IL-23 and activates the signal transduction and activator of transcription (STAT) 5, enhancing the generation of GM-CSF-producing $CD4^+$ T cells. Consistent with these observations, the CD5L-deficient mice presented significantly alleviated EAE with reduced frequency of GM-CSF-producing $CD4^+$ T cells in the CNS (151). Wang *et al.* have shown that CD5L mediates the

pathogenicity of T_H17 cells by regulating the T_H17-cell lipidome. Loss of CD5L converts non-pathogenic T_H17 cells into disease-inducing T_H17 cells which leads to more severe clinical EAE (103).

Binding affinities: SRCR protein-microbe interactions

Recent observations from our lab have suggested that SSC5D and CD5L can bind with superior affinity to pathogenic strains of *E. coli* than to a non-pathogenic strain of *E. coli*. These results indicate that SRCR proteins may have discriminatory properties to different pathogenic antigens (118). Although the focus of this thesis is on the characterization of novel interactions between SRCR proteins and microbes, the results obtained may corroborate and give new insights to the hypothesis that SRCR proteins bind preferentially to highly pathogenic microbes. Here, we also show different intensities of binding even when we incubate the same concentration of an SRCR protein with the same amount of different microbes. To validate our results, we used a panel of well-established interactions between CD5L and three different *E. coli* strains (118). While *E. coli* BL21(DE3) is a well-characterized non-pathogenic bacterium strain commonly used in academic laboratories, *E. coli* RS218 is a virulent pathogenic strain associated with neonatal meningitis. *E. coli* IHE3034 is a pathogenic strain that also belongs to the same serotype (O18:K1:H7) and is also associated with neonatal meningitis. In addition, we also tested the binding affinity of CD5L to the uropathogenic *E. coli* CFT073 strain, which is a clinical isolate associated with ascending urinary infections. The binding of CD5L to *E. coli* RS218 and CFT073 strains gave the strongest intensity of binding, whereas the binding of CD5L to *E. coli* IHE3034 and BL21(DE3) were lower but gave similar intensities between both strains **(Results Chapter II, Figure 4A)**. These results are consistent with previously SPR experiments where CD5L-*E. coli* RS218 interactions gave the highest sensor responses, while no differences between CD5L-*E. coli* IHE3034 and *E. coli* BL21(DE3) interactions were observed (118).

Regarding SSC4D, it is possible to observe a different binding pattern when compared with CD5L, suggesting that SRCR proteins may have very defined discriminatory properties on different extracellular components of microbes. Indeed, our ELISA results show that recognition of LPS and LTA by SSC4D or CD5L was different, possibly reflecting a differential sensing of Gram-positive *vs.* Gram-negative bacteria **(Results Chapter II, Figure 4C)**. Likewise, the two recombinant hemi-SSC4D forms, SRCR-d1d2 and SRCR-d3d4, display distinct preferences of binding. SSC4D-d1d2 seems to have a higher affinity to Gram-negative bacteria. In contrast, the binding affinity of SSC4D-d3d4 to Gram-positive and Gram-negative bacteria is more homogeneous; nonetheless, the results may suggest

that SSC4D-d3d4 binds better to Gram-positive bacteria than does SSC4D-d1d2 **(Results Chapter II, Figure 4B)**. We thus measured by ELISA the affinity of each one-half of the SSC4D molecule to each typical endotoxin of Gram-negative and Gram-positive. In general, the results corroborate the WB observations since the SSC4D-d1d2 binding affinity to LPS is higher than SSC4D-d3d4. The binding curves of each half of the SSC4D protein to LTA were indistinguishable between the two subunits **(Results Chapter II, Figure 4C)**. Although the analysis of band intensity may suggest that SSC4D-d3d4 binds better to Gram-positive bacteria than does SSC4D-d1d2, the ELISA measurements show that SRCR-d1d2 and SRCR-d3d4 bind equally to LTA. This inconsistency may be explained by the fact that we used whole-live bacteria in the classic interactions, and SRCR-proteins may recognize other structures present in the surface of a bacteria. Indeed, it is known that CD5L can bind to LPS, LTA, and peptidoglycan (PGN) (121). Moreover, by comparing the intensity of bands, the results suggest that the binding capacity of CD5L to bacteria is superior when compared with SSC4D. In contrast, the affinity of SSC4D to parasites seems to be higher than CD5L **(Results Chapter II, Figure 6A and C; Chapter III, Figure 1A)**. Importantly, all the interactions between SRCR-proteins and parasites were performed simultaneously.

Overall, these data support the hypothesis that SRCR molecules have differential binding avidities to different antigens. These discriminatory properties of SRCR proteins are not exclusive for the distinction between microbes species but also include the ability to distinguish distinct levels of pathogenicity. In addition, the results with the two recombinant hemi-SSC4D forms suggest that an SRCR protein has multiple putative binding motifs that may be responsible for the binding of different antigens. This hypothesis is supported by the evidence that DMBT1 has a binding motif on the SRCR domains that are essential for the bacterial binding, which differs from the binding region responsible for the recognition of influenza A virus and *Helicobacter pylori* (303).

CD5L: Anti-microbial, Anti-inflammatory or Pro-inflammatory protein?

Over the last decade, many different observations have uncovered distinct roles for CD5L, ranging from the well-established function as an anti-apoptotic protein to a PRR molecule, autophagy, regulation of lipid metabolism or iron homeostasis, and cell polarization, among others. This CD5L multifunctionality impacts directly on the modulation of several key immunological events, namely on infection, metabolic disorders, cancer, autoimmune disease, and consequently during either an acute or chronic inflammatory process (304). However, different studies on CD5L have shown divergent or even contradictory results of its involvement, mostly related to its function as an anti-microbial protein or either by promoting or attenuating the inflammatory response.

The ability to recognize microbes is one of the most well-characterized functions attributed to the CD5L protein. In addition, it is also established that CD5L promotes bacterial aggregation (121). Therefore, since CD5L is mainly produced by phagocytic cells and binds to microbes, promoting bacterial aggregation, it was expected that CD5L would also enhance phagocytosis and contribute to pathogen clearance. Here we observed that *ex vivo* human monocytes incubated with *E. coli* pHrodo BioParticles in the presence of CD5L do not induce a significant increase in the phagocytic capacity **(Results Chapter II, Figure 5A)**. This observation is consistent with a recent report showing that CD5L-polarized monocytes do not alter their phagocytic capacity to microspheres, *E. coli*, or *S. aureus* (143). Moreover, Kimura *et al.* showed that CD5L suppresses the phagocytosis of apoptotic neutrophils by bone marrow-derived macrophages or murine cell line RAW 265.7 (202). In addition, we did not observe significant differences in the whole-body bioluminescence imaging analysis nor in circulating parasite numbers in CD5L-KO mice infected either by *T. brucei*, *P. berghei* or *L. infantum* **(Results Chapter III, Figure 2A-D; Figure 3A-C; Figure 4A-C)**. These observations are in deep contrast with *T. brucei* infected TLR9-KO mice that have a marked increase in parasitic burden, which clearly suggest a role in sensing *T. brucei* derived structures and promoting anti-microbicidal activities (228). Although different studies have suggested that CD5L does not impact on phagocytosis, there is some controversy regarding this matter. During acute kidney injury (AKI), CD5L-KO mice exhibited abrogated debris clearance that consequently led to persistent renal inflammation. Curiously, immunofluorescence staining in AKI-induced WT mice demonstrated that CD5L accumulates on necrotic cell debris within the kidney proximal tubules (133). Furthermore, in a mouse model of *Corynebacterium parvum*-induced granuloma, the CD5L-deficient mice presented less phagocyted bacilli by macrophages (305). In addition to these *in vivo* observations, CD5L also has demonstrated the *in vitro* capacity to enhance phagocytosis of latex beads, cellular debris, and apoptotic cells (133, 142, 143). Overall, these data pointed to the fact that under few circumstances CD5L might act as an inducer of phagocytosis.

This controversy regarding the role of CD5L in phagocytosis may depend on the experimental setup, the type of particle/microorganism to be internalized, and the molecular and cellular species analyzed. Nevertheless, based on our results we anticipate that the anti-microbial proprieties are not the leading function of CD5L. This hypothesis is reinforced by different observations that showed that CD5L mostly enhances phagocytosis of cellular debris and apoptotic cells rather than live bacteria (133, 143).

Although the role of CD5L during the inflammatory response is indisputable, whether CD5L promotes the enhancement of a pro-inflammatory response or promotes the maintenance of an anti-inflammatory environment remains unclear.

Several studies have revealed that CD5L expression is up-regulated under inflammatory conditions, namely upon oropharyngeal administration of LPS, heat-killed *Corynebacterium parvum* injection, *Listeria monocytogenes* infection, endotoxin-induced fulminant hepatitis, in atherosclerotic lesions, and in the adipose tissue of obese mice (135, 189, 202, 305, 306). Based on this premise we analyzed the expression of circulating CD5L upon infection with *T. brucei*, *P. berghei*, or *L. infantum*. These three species of parasites represent three different infection models, in which, *T. brucei* is a circulating extracellular parasite that leads to systemic infection and chronic disease, *P. berghei* is mostly intracellular but alternates with extracellular invasive stages that cause systemic infection and acute disease, and *L. infantum* is an intracellular parasite that targets the liver, spleen, and bone marrow and leads to asymptomatic disease. We observed that C57BL6 WT mice challenged with *T. brucei* produced significantly more CD5L when compared with the non-infected mice. In contrast, infections with *P. berghei* or *L. infantum* do not impact significantly on the expression of CD5L **(Results Chapter III, Figure 1B)**. The exact mechanism that leads to CD5L upregulation is still not fully understood. Arai *et al.* have shown that oxLDL uptake by macrophages impacts directly on CD5L overexpression; however, other observations may suggest additional mechanisms involved in the upregulation of CD5L (189). Our results showed that in both *T. brucei* and *P. berghei* experimental models, the CD5L expression is increased at day seven post-infection. Curiously, in the *Corynebacterium parvum*-induced granuloma model, the CD5L production peak occurs at day 10 after injection and is coincident with the IL-12 production peak and with the recruitment of Thy1.2 cells to the liver (305). Additionally, Sanjurjo *et al.* showed that IL-10 polarized monocytes express significantly more CD5L than unstimulated, or IFN-γ/LPS or IL-4 polarized monocytes (143). Taken together, these studies might indicate a correlation between the activation of the adaptive immune response and the upregulation of CD5L. Interestingly, we did not observe differences in the circulating levels of CD5L upon *Leishmania infantum* infection, which could be explained by the well-known ability of *L. infantum* parasites to subvert the activation of macrophages into a dormancy state, by decreasing the expression of PRRs, cytokine production. Thus, we hypothesize that CD5L production/secretion could also be impaired in infected macrophages (251, 257).

The dramatic increase of CD5L expression upon *T. brucei* infection led us to consider a putative role for CD5L in Trypanosomatid infections. Nevertheless, we found no differences neither in parasitemia nor in the whole-body bioluminescence signal analysis

when we compared *T. brucei* infected-WT with infected CD5L-KO mice **(Results Chapter III, Figure 4A-C)**. Strikingly, CD5L-KO mice show greatly enhanced susceptibility to *T. brucei* infection **(Results Chapter III, Figure 4D).** These findings highlight a scenario whereby a CD5L function as inflammatory mediator may be implied. In order to dissect the CD5L mechanism underlying *T. brucei* infection susceptibility, we conducted several analyses at day 28 post-infection. Although tissue *ex vivo* bioluminescence analysis revealed no statistical differences between WT and CD5L-KO tissues, it is possible to observe slight differences, including an increase in the bioluminescence of CD5L-KO brains **(Results Chapter III, Figure 5B-C)**. We do not know whether this trend in the brain bioluminescent signal could reflect a biological difference in *T. brucei* numbers that further impacts on the increase of mouse susceptibility.

In addition, flow cytometry analysis of *T. brucei* infected CD5L-KO splenocytes revealed a decrease of B cells ($CD19^+$ cells) **(Results Chapter III, Figure 6A)**. In both WT and CD5L-KO mice the numbers and percentage of B cells are drastically reduced (WT: ~25%; CD5L-KO: ~10%) when compared with non-infected WT animals (~50% of B cells). It is known that *T. brucei* infection induces a non-specific polyclonal B-cell activation that leads to B-cell clonal exhaustion, destruction of the splenic B cell compartment, and the impairment of B-cell lymphopoiesis. Nevertheless, the reduction of the B cell population is even more considerable in the CD5L-KO mouse. It is hard, in the light of our current knowledge, to interpret this result since no direct link between CD5L and B cells has never made. Although CD5L is a well-established survival factor for macrophages, thymocytes, and NKT cells, whether CD5L also impacts on B cell survival remains unknown (105, 305).

Furthermore, flow cytometry analysis of *T. brucei* infected CD5L-KO splenocytes presented an increase of macrophages ($F4/80^+$ cells), inflammatory monocytes ($F4/80^-$ $Ly6C^{+++}$ cells), and $CD4^+$ T_H1 cells ($CD3^+CD4^+Tbet^+$) **(Results Chapter III, Figure 6A)**. In addition, we also observed a significant augment of IFN-γ at day 14 post-infection, and TNF-α at days 14 and 28 post-infection **(Results Chapter III, Figure 6B)**. The increased cell infiltration in the CD5L-KO mice, underlined by the statistical augment of $CD4^+$ T_H1 cells that likely leads to the observed increase of IFN-γ and TNF-α that will further activate macrophages and monocytes, creates a positive feedback loop that amplifies T_H1 cell responses. According to Sanjurjo *et al.*, CD5L drives macrophages to a pro-healing M2 phenotype, and thus we hypothesized that the increased levels of circulating CD5L in *T. brucei* infected-WT mice drive macrophages polarization to an M2 phenotype, which could impact decisively on the reduction of recruitment of high inflammatory monocytes, but also on the reduction of pro-inflammatory cytokines, while at the same time enhances regulatory mechanisms that contribute to balanced immune responses. On another hand, CD5L

abrogation could sustain a dominant immune type 1 response, whereby T_H1 cells undergo massive clonal expansion producing large amounts of IFN-γ that drive macrophages into an M1 phenotype and consequently leads to the production of ROS and other toxic components that impact dramatically on the increase of tissue damage and may lead to the increased susceptibility observed in CD5L-KO mice.

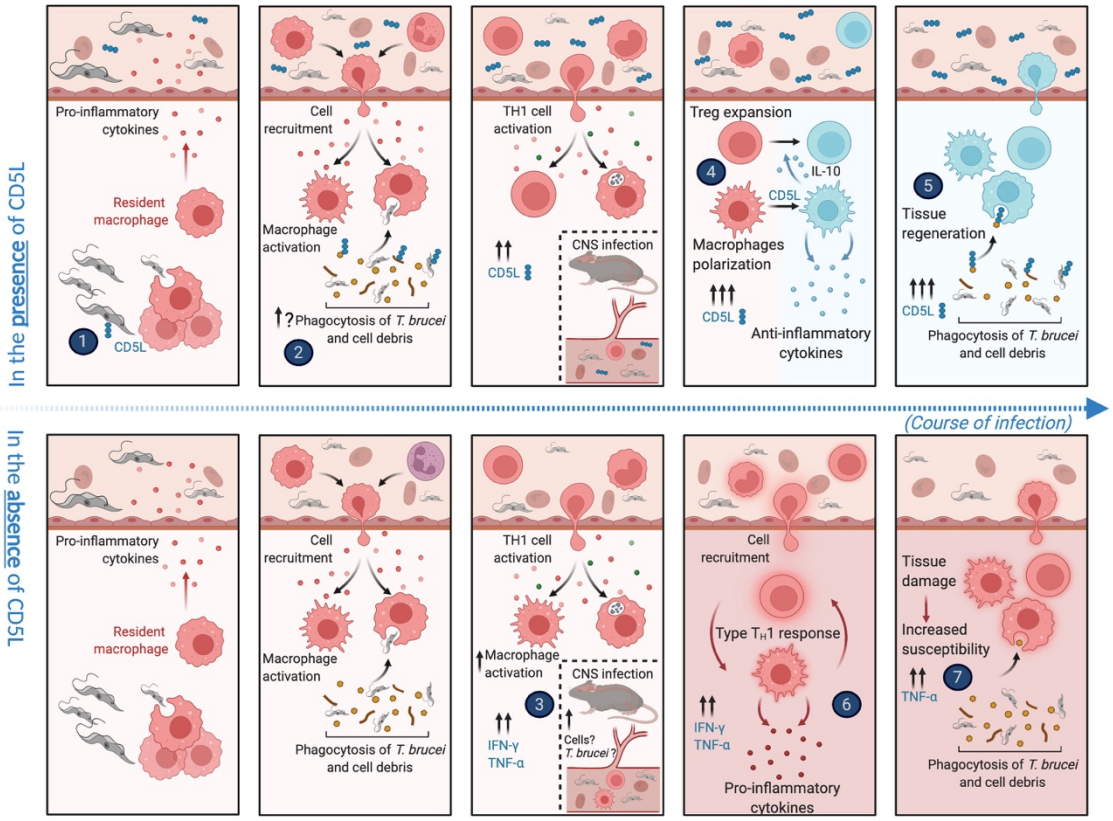

Figure 1 - Role of CD5L in trypanosomatid infections. Our results demonstrated that CD5L can recognize and bind to Trypanosoma brucei (1). To dissect the role of CD5L in trypanosomatid infections, C57BL/6 WT and CD5L-KO mice were infected intraperitoneally with 5 x 10^4 of luciferase-expressing *T. b. brucei* GVR35 strain. Importantly, no differences in the whole-body bioluminescent analysis nor in parasitemia were found between WT and CD5L-KO mice. Although no significant differences were found in the number of parasites, we observed a small reduction in circulating parasites in both parasitemia peaks. Thus, we speculate based on different observations that CD5L may contribute to the enhancement of *T. brucei* and cell debris clearance (2). Central nervous system (CNS) invasion by *T. brucei* is usually associated with a poor prognostic. It is described that IFN-γ and TNF-α can increase the expression of adhesion brain endothelial cells and thus promote the infiltration of T cells and *T. brucei* into the brain parenchyma. Although no statistical differences were observed in the brain bioluminescent signal quantification, we observed an increase of IFN-γ and TNF-α 14 days post-infection. Although more data is needed, we do not exclude the possibility that increased susceptibility observed in CD5L-KO mice might be due to early *T. brucei* invasion into the brain (3). We observed a decreased proportion of T_H1 cells and an increase of Treg cells among the CD4+ T cell population in WT mice. (Continues on the next page)

Figure 1 (Continuation) - Based on recent findings that showed that CD5L promotes the polarization from M1 to M2 phenotype, we hypothesized that in WT mice, high levels of circulating CD5L promote the switch between a pro-inflammatory profile to an anti-inflammatory profile that leads to the secretion of different anti-inflammatory cytokines, including IL-10 that will further promote the expansion of Treg cells (4). Overall, we believe these findings and assumptions may contribute to the promotion of tissue regeneration (5). In deep contrast, flow cytometry analysis revealed an increase of macrophages, inflammatory monocytes, and T_H1 in CD5L-KO mice. In addition, we also observed a significant augment of IFN-γ at day 14 post-infection, and TNF-α at days 14 and 28 post-infection. These results indicate an exacerbated pro-inflammatory response highlighted by the amplification of the T_H1 immune response (6). We hypothesized that this leads to increased tissue damage and consequently increased susceptibility (7).

Final remarks and future directions

Altogether, the recent findings on the SRCR protein interactions provide a considerable part of our current understanding of SRCR-SF functionalities. Nevertheless, the full spectrum of binding of a significant number of SRCR proteins remains unclear. Additionally, it is also evident that many other questions remain unanswered. Many SRCR protein ligands persist unidentified, the mechanism following microbe opsonization remains uncertain for many SRCR proteins, and whether SRCR proteins interact with other PRRs providing a stronger and efficient activation of the innate immune response is still undisclosed. Although we might have uncovered some important observations regarding the ability of some SRCR members to discriminate between different species, strains, or even between different levels of pathogenicity, we still know very little about this mechanism. Further binding assays involving a more refined array of pathogenic and non-pathogenic microbes, using high-throughput screening technologies, are required to address the avidity and specificity of SRCR proteins toward microbes.

Additionally, since the SRCR are extracellular proteins, expressed at the surface of immune cells or secreted and therefore in circulation, we hypothesized that they have exceptional features to fast intercept, recognize, and induce a proper immune response that ultimately leads to the elimination of the invasive pathogen. Moreover, some SRCRs have been described with the capacity to modulate the inflammatory response. Thus, we hypothesized a putative therapeutic potential for some SRCR proteins. Indeed, some SRCR proteins have been explored in therapy, even though the mechanisms underlying their functions are still far to be completely understood.

In this thesis, we have focused our attention on the characterization of biological and functional roles of the circulating human proteins SSC4D, one of the least scrutinized members of the SRCR-SF. Working with SSC4D was challenging since the availability of commercial tools to study this scavenger protein is very limited. Thus, the production of

other resources, including SSC4D-KO mice and recombinant mouse SSC4D proteins, are crucial for the understanding and further characterization of SSC4D.

In addition, we also provided new insights into the multifunctionality of CD5L. It is indisputable that CD5L is a key inflammatory mediator; nevertheless, the biological complexity of CD5L makes interpretation of some data very challenging. We found that in the absence of CD5L, there is a clear and predominant pro-inflammatory response that we link directly to the enhanced susceptibility observed in CD5L-KO mice. Although we speculate that CD5L-KO animals presented high tissue damage resulting from the persistent and dominant pro-inflammatory response, no data were shown in this particular matter. Histopathology evaluation from different infected tissues (lung, brain, liver, and spleen), together with the analysis of biochemical circulating parameters, must be performed to test our hypotheses. Finally, it would be of great value to test whether the injection of recombinant CD5L protein improved the survival of *T. brucei* infected mice.

In conclusion, our studies added new evidence to the puzzling role of CD5L during the inflammatory response. Additionally, our data widens the avenues that lead to the full characterization of SRCR proteins as PRRs.

Chapter V

References

1. Metchnikoff E. Untersuchungen ueber die mesodermalen Phagocyten einiger Wirbeltiere. Biologisches Centralblatt; 1883. p. 560-5.

2. Janeway CA. Approaching the asymptote? Evolution and revolution in immunology. Cold Spring Harb Symp Quant Biol. 1989;54 Pt 1:1-13. doi: 10.1101/sqb.1989.054.01.003. PubMed PMID: 2700931.

3. Barker JR, Koestler BJ, Carpenter VK, Burdette DL, Waters CM, Vance RE, et al. STING-dependent recognition of cyclic di-AMP mediates type I interferon responses during Chlamydia trachomatis infection. mBio. 2013;4(3):e00018-13. Epub 20130430. doi: 10.1128/mBio.00018-13. PubMed PMID: 23631912; PubMed Central PMCID: PMC3663186.

4. Jensen S, Thomsen AR. Sensing of RNA viruses: a review of innate immune receptors involved in recognizing RNA virus invasion. J Virol. 2012;86(6):2900-10. Epub 20120118. doi: 10.1128/JVI.05738-11. PubMed PMID: 22258243; PubMed Central PMCID: PMC3302314.

5. Patin EC, Thompson A, Orr SJ. Pattern recognition receptors in fungal immunity. Semin Cell Dev Biol. 2019;89:24-33. Epub 20180309. doi: 10.1016/j.semcdb.2018.03.003. PubMed PMID: 29522806; PubMed Central PMCID: PMC6461132.

6. Ghosh D, Stumhofer JS. Do you see what I see: Recognition of protozoan parasites by Toll-like receptors. Curr Immunol Rev. 2013;9(3):129-40. doi: 10.2174/15733955096661312032259 29. PubMed PMID: 25383072; PubMed Central PMCID: PMC4223800.

7. Iwasaki A, Medzhitov R. Control of adaptive immunity by the innate immune system. Nat Immunol. 2015;16(4):343-53. doi: 10.1038/ni.3123. PubMed PMID: 25789684; PubMed Central PMCID: PMC4507498.

8. Medzhitov R, Janeway CA. Innate immunity: impact on the adaptive immune response. Curr Opin Immunol. 1997;9(1):4-9. doi: 10.1016/s0952-7915(97)80152-5. PubMed PMID: 9039775.

9. Buchmann K. Evolution of Innate Immunity: Clues from Invertebrates via Fish to Mammals. Front Immunol. 2014;5:459. Epub 20140923. doi: 10.3389/fimmu.2014.00459. PubMed PMID: 25295041; PubMed Central PMCID: PMC4172062.

10. Schatz DG, Ji Y. Recombination centres and the orchestration of V(D)J recombination. Nat Rev Immunol. 2011;11(4):251-63. Epub 20110311. doi: 10.1038/nri2941. PubMed PMID: 21394103.

11. Adams NM, Grassmann S, Sun JC. Clonal expansion of innate and adaptive lymphocytes. Nat Rev Immunol. 2020;20(11):694-707. Epub 20200518. doi: 10.1038/s41577-020-0307-4. PubMed PMID: 32424244.

12. Chaplin DD. Overview of the immune response. J Allergy Clin Immunol. 2010;125(2 Suppl 2):S3-23. doi: 10.1016/j.jaci.2009.12.980. PubMed PMID: 20176265; PubMed Central PMCID: PMC2923430.

13. Bonilla FA, Oettgen HC. Adaptive immunity. J Allergy Clin Immunol. 2010;125(2 Suppl 2):S33-40. Epub 20100112. doi: 10.1016/j.jaci.2009.09.017. PubMed PMID: 20061006.

14. Cooper MD, Alder MN. The evolution of adaptive immune systems. Cell. 2006;124(4):815-22. doi: 10.1016/j.cell.2006.02.001. PubMed PMID: 16497590.

15. Hsieh CS, Macatonia SE, Tripp CS, Wolf SF, O'Garra A, Murphy KM. Development of TH1 CD4+ T cells through IL-12 produced by Listeria-induced macrophages. Science. 1993;260(5107):547-9. doi: 10.1126/science.8097338. PubMed PMID: 8097338.

16. Kaufmann SH. Immunity to intracellular bacteria. Annu Rev Immunol. 1993;11:129-63. doi: 10.1146/annurev.iy.11.040193.001021. PubMed PMID: 8476559.

17. Thieu VT, Yu Q, Chang HC, Yeh N, Nguyen ET, Sehra S, et al. Signal transducer and activator of transcription 4 is required for the transcription factor T-bet to promote T helper 1 cell-fate determination. Immunity. 2008;29(5):679-90. doi: 10.1016/j.immuni.2008.08.017. PubMed PMID: 18993086; PubMed Central PMCID: PMC2768040.

18. Skapenko A, Leipe J, Lipsky PE, Schulze-Koops H. The role of the T cell in autoimmune inflammation. Arthritis Res Ther. 2005;7 Suppl 2:S4-14. Epub 20050316. doi: 10.1186/ar1703. PubMed PMID: 15833146; PubMed Central PMCID: PMC2833981.

19. Prajeeth CK, Dittrich-Breiholz O, Talbot SR, Robert PA, Huehn J, Stangel M. IFN-γ Producing Th1 Cells Induce Different Transcriptional Profiles in Microglia and Astrocytes. Front Cell Neurosci. 2018;12:352. Epub 20181010. doi: 10.3389/fncel.2018.00352. PubMed PMID: 30364000; PubMed Central PMCID: PMC6191492.

20. Tisch R, McDevitt H. Insulin-dependent diabetes mellitus. Cell. 1996;85(3):291-7. doi: 10.1016/s0092-8674(00)81106-x. PubMed PMID: 8616883.

21. Walker JA, McKenzie ANJ. T. Nat Rev Immunol. 2018;18(2):121-33. Epub 20171030. doi: 10.1038/nri.2017.118. PubMed PMID: 29082915.

22. MacDonald AS, Maizels RM. Alarming dendritic cells for Th2 induction. J Exp Med. 2008;205(1):13-7. Epub 20080114. doi: 10.1084/jem.20072665. PubMed PMID: 18195077; PubMed Central PMCID: PMC2234366.

23. Zhu J, Paul WE. CD4 T cells: fates, functions, and faults. Blood. 2008;112(5):1557-69. doi: 10.1182/blood-2008-05-078154. PubMed PMID: 18725574; PubMed Central PMCID: PMC2518872.

24. Kopf M, Le Gros G, Bachmann M, Lamers MC, Bluethmann H, Köhler G. Disruption of the murine IL-4 gene blocks Th2 cytokine responses. Nature. 1993;362(6417):245-8. doi: 10.1038/362245a0. PubMed PMID: 8384701.

25. Weaver CT, Harrington LE, Mangan PR, Gavrieli M, Murphy KM. Th17: an effector CD4 T cell lineage with regulatory T cell ties. Immunity. 2006;24(6):677-88. doi: 10.1016/j.immuni.2006.06.002. PubMed PMID: 16782025.

26. Yao Z, Fanslow WC, Seldin MF, Rousseau AM, Painter SL, Comeau MR, et al. Herpesvirus Saimiri encodes a new cytokine, IL-17, which binds to a novel cytokine receptor. Immunity. 1995;3(6):811-21. doi: 10.1016/1074-7613(95)90070-5. PubMed PMID: 8777726.

27. Kanellopoulou C, Muljo SA. Fine-Tuning Th17 Cells: To Be or Not To Be Pathogenic? Immunity. 2016;44(6):1241-3. doi: 10.1016/j.immuni.2016.06.003. PubMed PMID: 27332724.

28. Lee Y, Awasthi A, Yosef N, Quintana FJ, Xiao S, Peters A, et al. Induction and molecular signature of pathogenic TH17 cells. Nat Immunol. 2012;13(10):991-9. Epub 20120909. doi: 10.1038/ni.2416. PubMed PMID: 22961052; PubMed Central PMCID: PMC3459594.

29. Wu X, Tian J, Wang S. Insight Into Non-Pathogenic Th17 Cells in Autoimmune Diseases. Front Immunol. 2018;9:1112. Epub 20180528. doi: 10.3389/fimmu.2018.01112. PubMed PMID: 29892286; PubMed Central PMCID: PMC5985293.

30. Vignali DA, Collison LW, Workman CJ. How regulatory T cells work. Nat Rev Immunol. 2008;8(7):523-32. doi: 10.1038/nri2343. PubMed PMID: 18566595; PubMed Central PMCID: PMC2665249.

31. Hori S, Nomura T, Sakaguchi S. Control of regulatory T cell development by the transcription factor Foxp3. Science. 2003;299(5609):1057-61. Epub 20030109. doi: 10.1126/science.1079490. PubMed PMID: 12522256.

32. Fontenot JD, Gavin MA, Rudensky AY. Foxp3 programs the development and function of CD4+CD25+ regulatory T cells. Nat Immunol. 2003;4(4):330-6. Epub 20030303. doi: 10.1038/ni904. PubMed PMID: 12612578.

33. Brunkow ME, Jeffery EW, Hjerrild KA, Paeper B, Clark LB, Yasayko SA, et al. Disruption of a new forkhead/winged-helix protein, scurfin, results in the fatal lymphoproliferative disorder of the scurfy mouse. Nat Genet. 2001;27(1):68-73. doi: 10.1038/83784. PubMed PMID: 11138001.

34. Schmitt EG, Williams CB. Generation and function of induced regulatory T cells. Front Immunol. 2013;4:152. Epub 20130619. doi: 10.3389/fimmu.2013.00152. PubMed PMID: 23801990; PubMed Central PMCID: PMC3685796.

35. Moore KW, de Waal Malefyt R, Coffman RL, O'Garra A. Interleukin-10 and the interleukin-10 receptor. Annu Rev Immunol. 2001;19:683-765. doi: 10.1146/annurev.immunol.19.1.683. PubMed PMID: 11244051.

36. Maloy KJ, Powrie F. Regulatory T cells in the control of immune pathology. Nat Immunol. 2001;2(9):816-22. doi: 10.1038/ni0901-816. PubMed PMID: 11526392.

37. Li C, Corraliza I, Langhorne J. A defect in interleukin-10 leads to enhanced malarial disease in Plasmodium chabaudi chabaudi infection in mice. Infect Immun. 1999;67(9):4435-42. doi: 10.1128/IAI.67.9.4435-4442.1999. PubMed PMID: 10456884; PubMed Central PMCID: PMC96762.

38. Veldhoen M, Uyttenhove C, van Snick J, Helmby H, Westendorf A, Buer J, et al. Transforming growth factor-beta 'reprograms' the differentiation of T helper 2 cells and promotes an interleukin 9-producing subset. Nat Immunol. 2008;9(12):1341-6. Epub 20081019. doi: 10.1038/ni.1659. PubMed PMID: 18931678.

39. Takami M, Love RB, Iwashima M. TGF-β converts apoptotic stimuli into the signal for Th9 differentiation. J Immunol. 2012;188(9):4369-75. Epub 20120328. doi: 10.4049/jimmunol.1102698. PubMed PMID: 22461692; PubMed Central PMCID: PMC3331903.

40. Ma CS, Tangye SG, Deenick EK. Human Th9 cells: inflammatory cytokines modulate IL-9 production through the induction of IL-21. Immunol Cell Biol. 2010;88(6):621-3. Epub 20100608. doi: 10.1038/icb.2010.73. PubMed PMID: 20531361.

41. Ramming A, Druzd D, Leipe J, Schulze-Koops H, Skapenko A. Maturation-related histone modifications in the PU.1 promoter regulate Th9-cell development. Blood. 2012;119(20):4665-74. Epub 20120323. doi: 10.1182/blood-2011-11-392589. PubMed PMID: 22446486.

42. Staudt V, Bothur E, Klein M, Lingnau K, Reuter S, Grebe N, et al. Interferon-regulatory factor 4 is essential for the developmental program of T helper 9 cells. Immunity. 2010;33(2):192-202. Epub 20100730. doi: 10.1016/j.immuni.2010.07.014. PubMed PMID: 20674401.

43. Schwartz DM, Farley TK, Richoz N, Yao C, Shih HY, Petermann F, et al. Retinoic Acid Receptor Alpha Represses a Th9 Transcriptional and Epigenomic Program to Reduce Allergic Pathology. Immunity. 2019;50(1):106-20.e10. doi: 10.1016/j.immuni.2018.12.014. PubMed PMID: 30650370; PubMed Central PMCID: PMC6338086.

44. Kim IK, Koh CH, Jeon I, Shin KS, Kang TS, Bae EA, et al. GM-CSF Promotes Antitumor Immunity by Inducing Th9 Cell Responses. Cancer Immunol Res. 2019;7(3):498-509. Epub 20190206. doi: 10.1158/2326-6066.CIR-18-0518. PubMed PMID: 30728152.

45. Chen J, Guan L, Tang L, Liu S, Zhou Y, Chen C, et al. T Helper 9 Cells: A New Player in Immune-Related Diseases. DNA Cell Biol. 2019;38(10):1040-7. Epub 20190816. doi: 10.1089/dna.2019.4729. PubMed PMID: 31414895; PubMed Central PMCID: PMC6791470.

46. Eyerich S, Eyerich K, Pennino D, Carbone T, Nasorri F, Pallotta S, et al. Th22 cells represent a distinct human T cell subset involved in epidermal immunity and remodeling. J Clin Invest. 2009;119(12):3573-85. Epub 20091116. doi: 10.1172/JCI40202. PubMed PMID: 19920355; PubMed Central PMCID: PMC2786807.

47. Plank MW, Kaiko GE, Maltby S, Weaver J, Tay HL, Shen W, et al. Th22 Cells Form a Distinct Th Lineage from Th17 Cells In Vitro with Unique Transcriptional Properties and Tbet-Dependent Th1 Plasticity. J Immunol. 2017;198(5):2182-90. Epub 20170118. doi: 10.4049/jimmunol.1601480. PubMed PMID: 28100680; PubMed Central PMCID: PMC5367520.

48. Trifari S, Kaplan CD, Tran EH, Crellin NK, Spits H. Identification of a human helper T cell population that has abundant production of interleukin 22 and is distinct from T(H)-17, T(H)1 and T(H)2 cells. Nat Immunol. 2009;10(8):864-71. Epub 20090705. doi: 10.1038/ni.1770. PubMed PMID: 19578368.

49. Vinuesa CG, Linterman MA, Yu D, MacLennan IC. Follicular Helper T Cells. Annu Rev Immunol. 2016;34:335-68. Epub 20160222. doi: 10.1146/annurev-immunol-041015-055605. PubMed PMID: 26907215.

50. Yu D, Vinuesa CG. The elusive identity of T follicular helper cells. Trends Immunol. 2010;31(10):377-83. Epub 20100831. doi: 10.1016/j.it.2010.07.001. PubMed PMID: 20810318.

51. Nurieva RI, Chung Y, Martinez GJ, Yang XO, Tanaka S, Matskevitch TD, et al. Bcl6 mediates the development of T follicular helper cells. Science. 2009;325(5943):1001-5. Epub 20090723. doi: 10.1126/science.1176676. PubMed PMID: 19628815; PubMed Central PMCID: PMC2857334.

52. Nurieva RI, Chung Y, Hwang D, Yang XO, Kang HS, Ma L, et al. Generation of T follicular helper cells is mediated by interleukin-21 but independent of T helper 1, 2, or 17 cell lineages. Immunity. 2008;29(1):138-49. Epub 20080703. doi: 10.1016/j.immuni.2008.05.009. PubMed PMID: 18599325; PubMed Central PMCID: PMC2556461.

53. Murphy TL, Grajales-Reyes GE, Wu X, Tussiwand R, Briseño CG, Iwata A, et al. Transcriptional Control of Dendritic Cell Development. Annu Rev Immunol. 2016;34:93-119. Epub 20151223. doi: 10.1146/annurev-immunol-032713-120204. PubMed PMID: 26735697; PubMed Central PMCID: PMC5135011.

54. Tussiwand R, Everts B, Grajales-Reyes GE, Kretzer NM, Iwata A, Bagaitkar J, et al. Klf4 expression in conventional dendritic cells is required for T helper 2 cell responses. Immunity. 2015;42(5):916-28. doi: 10.1016/j.immuni.2015.04.017. PubMed PMID: 25992862; PubMed Central PMCID: PMC4447135.

55. Kamphorst AO, Guermonprez P, Dudziak D, Nussenzweig MC. Route of antigen uptake differentially impacts presentation by dendritic cells and activated monocytes. J Immunol. 2010;185(6):3426-35. Epub 20100820. doi: 10.4049/jimmunol.1001205. PubMed PMID: 20729332; PubMed Central PMCID: PMC3013633.

56. Janeway CA, Medzhitov R. Innate immune recognition. Annu Rev Immunol. 2002;20:197-216. Epub 20011004. doi: 10.1146/annurev.immunol.20.083001.084359. PubMed PMID: 11861602.

57. Takeuchi O, Akira S. Pattern recognition receptors and inflammation. Cell. 2010;140(6):805-20. doi: 10.1016/j.cell.2010.01.022. PubMed PMID: 20303872.

58. Li D, Wu M. Pattern recognition receptors in health and diseases. Signal Transduct Target Ther. 2021;6(1):291. Epub 20210804. doi: 10.1038/s41392-021-00687-0. PubMed PMID: 34344870; PubMed Central PMCID: PMC8333067.

59. Medzhitov R. Recognition of microorganisms and activation of the immune response. Nature. 2007;449(7164):819-26. doi: 10.1038/nature06246. PubMed PMID: 17943118.

60. Lemaitre B, Nicolas E, Michaut L, Reichhart JM, Hoffmann JA. The dorsoventral regulatory gene cassette spätzle/Toll/cactus controls the potent antifungal response in Drosophila adults. Cell. 1996;86(6):973-83. doi: 10.1016/s0092-8674(00)80172-5. PubMed PMID: 8808632.

61. Medzhitov R, Preston-Hurlburt P, Janeway CA. A human homologue of the Drosophila Toll protein signals activation of adaptive immunity. Nature. 1997;388(6640):394-7. doi: 10.1038/41131. PubMed PMID: 9237759.

62. Bell JK, Mullen GE, Leifer CA, Mazzoni A, Davies DR, Segal DM. Leucine-rich repeats and pathogen recognition in Toll-like receptors. Trends Immunol. 2003;24(10):528-33. doi: 10.1016/s1471-4906(03)00242-4. PubMed PMID: 14552836.

63. O'Neill LA, Greene C. Signal transduction pathways activated by the IL-1 receptor family: ancient signaling machinery in mammals, insects, and plants. J Leukoc Biol. 1998;63(6):650-7. PubMed PMID: 9620655.

64. Rock FL, Hardiman G, Timans JC, Kastelein RA, Bazan JF. A family of human receptors structurally related to Drosophila Toll. Proc Natl Acad Sci U S A. 1998;95(2):588-

93. doi: 10.1073/pnas.95.2.588. PubMed PMID: 9435236; PubMed Central PMCID: PMC18464.

65. Fitzgerald KA, Kagan JC. Toll-like Receptors and the Control of Immunity. Cell. 2020;180(6):1044-66. Epub 20200311. doi: 10.1016/j.cell.2020.02.041. PubMed PMID: 32164908.

66. Akira S, Takeda K, Kaisho T. Toll-like receptors: critical proteins linking innate and acquired immunity. Nat Immunol. 2001;2(8):675-80. doi: 10.1038/90609. PubMed PMID: 11477402.

67. Medzhitov R. Toll-like receptors and innate immunity. Nat Rev Immunol. 2001;1(2):135-45. doi: 10.1038/35100529. PubMed PMID: 11905821.

68. Akira S, Uematsu S, Takeuchi O. Pathogen recognition and innate immunity. Cell. 2006;124(4):783-801. doi: 10.1016/j.cell.2006.02.015. PubMed PMID: 16497588.

69. Kawai T, Akira S. Toll-like receptors and their crosstalk with other innate receptors in infection and immunity. Immunity. 2011;34(5):637-50. doi: 10.1016/j.immuni.2011.05.006. PubMed PMID: 21616434.

70. Broz P, Monack DM. Newly described pattern recognition receptors team up against intracellular pathogens. Nat Rev Immunol. 2013;13(8):551-65. Epub 20130712. doi: 10.1038/nri3479. PubMed PMID: 23846113.

71. Akira S, Takeda K. Toll-like receptor signalling. Nat Rev Immunol. 2004;4(7):499-511. doi: 10.1038/nri1391. PubMed PMID: 15229469.

72. Dunne A, O'Neill LA. The interleukin-1 receptor/Toll-like receptor superfamily: signal transduction during inflammation and host defense. Sci STKE. 2003;2003(171):re3. Epub 20030225. doi: 10.1126/stke.2003.171.re3. PubMed PMID: 12606705.

73. Yamamoto M, Sato S, Mori K, Hoshino K, Takeuchi O, Takeda K, et al. Cutting edge: a novel Toll/IL-1 receptor domain-containing adapter that preferentially activates the IFN-beta promoter in the Toll-like receptor signaling. J Immunol. 2002;169(12):6668-72. doi: 10.4049/jimmunol.169.12.6668. PubMed PMID: 12471095.

74. Kawai T, Akira S. TLR signaling. Semin Immunol. 2007;19(1):24-32. Epub 20070201. doi: 10.1016/j.smim.2006.12.004. PubMed PMID: 17275323.

75. Jin MS, Kim SE, Heo JY, Lee ME, Kim HM, Paik SG, et al. Crystal structure of the TLR1-TLR2 heterodimer induced by binding of a tri-acylated lipopeptide. Cell. 2007;130(6):1071-82. doi: 10.1016/j.cell.2007.09.008. PubMed PMID: 17889651.

76. Jin MS, Lee JO. Structures of the toll-like receptor family and its ligand complexes. Immunity. 2008;29(2):182-91. doi: 10.1016/j.immuni.2008.07.007. PubMed PMID: 18701082.

77. Zhong Y, Kinio A, Saleh M. Functions of NOD-Like Receptors in Human Diseases. Front Immunol. 2013;4:333. Epub 20131016. doi: 10.3389/fimmu.2013.00333. PubMed PMID: 24137163; PubMed Central PMCID: PMC3797414.

78. Chen G, Shaw MH, Kim YG, Nuñez G. NOD-like receptors: role in innate immunity and inflammatory disease. Annu Rev Pathol. 2009;4:365-98. doi: 10.1146/annurev.pathol.4.110807.092239. PubMed PMID: 18928408.

79. Ting JP, Lovering RC, Alnemri ES, Bertin J, Boss JM, Davis BK, et al. The NLR gene family: a standard nomenclature. Immunity. 2008;28(3):285-7. doi: 10.1016/j.immuni.2008.02.005. PubMed PMID: 18341998; PubMed Central PMCID: PMC2630772.

80. Inohara N, Ogura Y, Chen FF, Muto A, Nuñez G. Human Nod1 confers responsiveness to bacterial lipopolysaccharides. J Biol Chem. 2001;276(4):2551-4. Epub 20001031. doi: 10.1074/jbc.M009728200. PubMed PMID: 11058605.

81. Chamaillard M, Hashimoto M, Horie Y, Masumoto J, Qiu S, Saab L, et al. An essential role for NOD1 in host recognition of bacterial peptidoglycan containing diaminopimelic acid. Nat Immunol. 2003;4(7):702-7. Epub 20030606. doi: 10.1038/ni945. PubMed PMID: 12796777.

82. Girardin SE, Boneca IG, Viala J, Chamaillard M, Labigne A, Thomas G, et al. Nod2 is a general sensor of peptidoglycan through muramyl dipeptide (MDP) detection. J Biol Chem. 2003;278(11):8869-72. Epub 20030113. doi: 10.1074/jbc.C200651200. PubMed PMID: 12527755.

83. Coulombe F, Divangahi M, Veyrier F, de Léséleuc L, Gleason JL, Yang Y, et al. Increased NOD2-mediated recognition of N-glycolyl muramyl dipeptide. J Exp Med. 2009;206(8):1709-16. Epub 20090706. doi: 10.1084/jem.20081779. PubMed PMID: 19581406; PubMed Central PMCID: PMC2722178.

84. Divangahi M, Mostowy S, Coulombe F, Kozak R, Guillot L, Veyrier F, et al. NOD2-deficient mice have impaired resistance to Mycobacterium tuberculosis infection through defective innate and adaptive immunity. J Immunol. 2008;181(10):7157-65. doi: 10.4049/jimmunol.181.10.7157. PubMed PMID: 18981137.

85. Sabbah A, Chang TH, Harnack R, Frohlich V, Tominaga K, Dube PH, et al. Activation of innate immune antiviral responses by Nod2. Nat Immunol. 2009;10(10):1073-80. Epub 20090823. doi: 10.1038/ni.1782. PubMed PMID: 19701189; PubMed Central PMCID: PMC2752345.

86. Inohara N, Koseki T, Lin J, del Peso L, Lucas PC, Chen FF, et al. An induced proximity model for NF-kappa B activation in the Nod1/RICK and RIP signaling pathways. J Biol Chem. 2000;275(36):27823-31. doi: 10.1074/jbc.M003415200. PubMed PMID: 10880512.

87. Zheng D, Liwinski T, Elinav E. Inflammasome activation and regulation: toward a better understanding of complex mechanisms. Cell Discov. 2020;6(1):36. Epub 20200609. doi: 10.1038/s41421-020-0167-x. PubMed PMID: 34103480.

88. Martinon F, Burns K, Tschopp J. The inflammasome: a molecular platform triggering activation of inflammatory caspases and processing of proIL-beta. Mol Cell. 2002;10(2):417-26. doi: 10.1016/s1097-2765(02)00599-3. PubMed PMID: 12191486.

89. Martinon F, Mayor A, Tschopp J. The inflammasomes: guardians of the body. Annu Rev Immunol. 2009;27:229-65. doi: 10.1146/annurev.immunol.021908.132715. PubMed PMID: 19302040.

90. Dixit E, Kagan JC. Intracellular pathogen detection by RIG-I-like receptors. Adv Immunol. 2013;117:99-125. doi: 10.1016/B978-0-12-410524-9.00004-9. PubMed PMID: 23611287; PubMed Central PMCID: PMC3947775.

91. Yoneyama M, Kikuchi M, Natsukawa T, Shinobu N, Imaizumi T, Miyagishi M, et al. The RNA helicase RIG-I has an essential function in double-stranded RNA-induced innate antiviral responses. Nat Immunol. 2004;5(7):730-7. Epub 20040620. doi: 10.1038/ni1087. PubMed PMID: 15208624.

92. Goubau D, Deddouche S, Reis e Sousa C. Cytosolic sensing of viruses. Immunity. 2013;38(5):855-69. doi: 10.1016/j.immuni.2013.05.007. PubMed PMID: 23706667; PubMed Central PMCID: PMC7111113.

93. Rehwinkel J, Gack MU. RIG-I-like receptors: their regulation and roles in RNA sensing. Nat Rev Immunol. 2020;20(9):537-51. Epub 20200313. doi: 10.1038/s41577-020-0288-3. PubMed PMID: 32203325; PubMed Central PMCID: PMC7094958.

94. Andrejeva J, Childs KS, Young DF, Carlos TS, Stock N, Goodbourn S, et al. The V proteins of paramyxoviruses bind the IFN-inducible RNA helicase, mda-5, and inhibit its activation of the IFN-beta promoter. Proc Natl Acad Sci U S A. 2004;101(49):17264-9. Epub 20041124. doi: 10.1073/pnas.0407639101. PubMed PMID: 15563593; PubMed Central PMCID: PMC535396.

95. Katze MG, He Y, Gale M. Viruses and interferon: a fight for supremacy. Nat Rev Immunol. 2002;2(9):675-87. doi: 10.1038/nri888. PubMed PMID: 12209136.

96. Stok JE, Vega Quiroz ME, van der Veen AG. Self RNA Sensing by RIG-I-like Receptors in Viral Infection and Sterile Inflammation. J Immunol. 2020;205(4):883-91. doi: 10.4049/jimmunol.2000488. PubMed PMID: 32769143.

97. Dhir A, Dhir S, Borowski LS, Jimenez L, Teitell M, Rötig A, et al. Mitochondrial double-stranded RNA triggers antiviral signalling in humans. Nature. 2018;560(7717):238-42. Epub 20180725. doi: 10.1038/s41586-018-0363-0. PubMed PMID: 30046113; PubMed Central PMCID: PMC6570621.

98. Kato H, Fujita T. RIG-I-like receptors and autoimmune diseases. Curr Opin Immunol. 2015;37:40-5. doi: 10.1016/j.coi.2015.10.002. PubMed PMID: 26530735.

99. Martínez VG, Moestrup SK, Holmskov U, Mollenhauer J, Lozano F. The conserved scavenger receptor cysteine-rich superfamily in therapy and diagnosis. Pharmacol Rev. 2011;63(4):967-1000. Epub 20110831. doi: 10.1124/pr.111.004523. PubMed PMID: 21880988.

100. Sarrias MR, Grønlund J, Padilla O, Madsen J, Holmskov U, Lozano F. The Scavenger Receptor Cysteine-Rich (SRCR) domain: an ancient and highly conserved protein module of the innate immune system. Crit Rev Immunol. 2004;24(1):1-37. doi: 10.1615/critrevimmunol.v24.i1.10. PubMed PMID: 14995912.

101. Carmo AM, Sreenu VB. A Systematic and Thorough Search for Domains of the Scavenger Receptor Cysteine-Rich Group-B Family in the Human Genome. In: IntechOpen, editor. Bioinformatics - Trends and Methodologies2011.

102. Resnick D, Chatterton JE, Schwartz K, Slayter H, Krieger M. Structures of class A macrophage scavenger receptors. Electron microscopic study of flexible, multidomain, fibrous proteins and determination of the disulfide bond pattern of the scavenger receptor cysteine-rich domain. J Biol Chem. 1996;271(43):26924-30. doi: 10.1074/jbc.271.43.26924. PubMed PMID: 8900177.

103. Wang C, Yosef N, Gaublomme J, Wu C, Lee Y, Clish CB, et al. CD5L/AIM Regulates Lipid Biosynthesis and Restrains Th17 Cell Pathogenicity. Cell. 2015;163(6):1413-27. Epub 20151119. doi: 10.1016/j.cell.2015.10.068. PubMed PMID: 26607793; PubMed Central PMCID: PMC4671820.

104. Cardenas L, Carrera AC, Yague E, Pulido R, Sánchez-Madrid F, de Landázuri MO. Phosphorylation-dephosphorylation of the CD6 glycoprotein renders two isoforms of 130 and 105 kilodaltons. Effect of serum and protein kinase C activators. J Immunol. 1990;145(5):1450-5. PubMed PMID: 2384666.

105. Miyazaki T, Hirokami Y, Matsuhashi N, Takatsuka H, Naito M. Increased susceptibility of thymocytes to apoptosis in mice lacking AIM, a novel murine macrophage-derived soluble factor belonging to the scavenger receptor cysteine-rich domain superfamily. J Exp Med. 1999;189(2):413-22. doi: 10.1084/jem.189.2.413. PubMed PMID: 9892623; PubMed Central PMCID: PMC2192994.

106. Li XJ, Snyder SH. Molecular cloning of Ebnerin, a von Ebner's gland protein associated with taste buds. J Biol Chem. 1995;270(30):17674-9. doi: 10.1074/jbc.270.30.17674. PubMed PMID: 7629065.

107. Bork P, Sander C. A large domain common to sperm receptors (Zp2 and Zp3) and TGF-beta type III receptor. FEBS Lett. 1992;300(3):237-40. doi: 10.1016/0014-5793(92)80853-9. PubMed PMID: 1313375.

108. Gonçalves CM, Castro MA, Henriques T, Oliveira MI, Pinheiro HC, Oliveira C, et al. Molecular cloning and analysis of SSc5D, a new member of the scavenger receptor cysteine-rich superfamily. Mol Immunol. 2009;46(13):2585-96. Epub 20090616. doi: 10.1016/j.molimm.2009.05.006. PubMed PMID: 19535143.

109. Brown MS, Goldstein JL. Receptor-mediated endocytosis: insights from the lipoprotein receptor system. Proc Natl Acad Sci U S A. 1979;76(7):3330-7. doi: 10.1073/pnas.76.7.3330. PubMed PMID: 226968; PubMed Central PMCID: PMC383819.

110. Brown MS, Goldstein JL, Krieger M, Ho YK, Anderson RG. Reversible accumulation of cholesteryl esters in macrophages incubated with acetylated lipoproteins. J Cell Biol. 1979;82(3):597-613. doi: 10.1083/jcb.82.3.597. PubMed PMID: 229107; PubMed Central PMCID: PMC2110476.

111. Arai S, Miyazaki T. A scavenging system against internal pathogens promoted by the circulating protein apoptosis inhibitor of macrophage (AIM). Semin Immunopathol. 2018;40(6):567-75. Epub 20181011. doi: 10.1007/s00281-018-0717-6. PubMed PMID: 30310974; PubMed Central PMCID: PMC6223838.

112. Areschoug T, Gordon S. Scavenger receptors: role in innate immunity and microbial pathogenesis. Cell Microbiol. 2009;11(8):1160-9. Epub 20090422. doi: 10.1111/j.1462-5822.2009.01326.x. PubMed PMID: 19388903.

113. Martinez VG, Escoda-Ferran C, Tadeu Simões I, Arai S, Orta Mascaró M, Carreras E, et al. The macrophage soluble receptor AIM/Api6/CD5L displays a broad pathogen recognition spectrum and is involved in early response to microbial aggression. Cell Mol Immunol. 2014;11(4):343-54. Epub 20140303. doi: 10.1038/cmi.2014.12. PubMed PMID: 24583716; PubMed Central PMCID: PMC4085514.

114. Miró-Julià C, Roselló S, Martínez VG, Fink DR, Escoda-Ferran C, Padilla O, et al. Molecular and functional characterization of mouse S5D-SRCRB: a new group B member of the scavenger receptor cysteine-rich superfamily. J Immunol. 2011;186(4):2344-54. Epub 20110107. doi: 10.4049/jimmunol.1000840. PubMed PMID: 21217009.

115. Hartshorn KL, Ligtenberg A, White MR, Van Eijk M, Hartshorn M, Pemberton L, et al. Salivary agglutinin and lung scavenger receptor cysteine-rich glycoprotein 340 have broad anti-influenza activities and interactions with surfactant protein D that vary according to donor source and sialylation. Biochem J. 2006;393(Pt 2):545-53. doi: 10.1042/BJ20050695. PubMed PMID: 16190864; PubMed Central PMCID: PMC1360705.

116. Fabriek BO, van Bruggen R, Deng DM, Ligtenberg AJ, Nazmi K, Schornagel K, et al. The macrophage scavenger receptor CD163 functions as an innate immune sensor for bacteria. Blood. 2009;113(4):887-92. Epub 20081010. doi: 10.1182/blood-2008-07-167064. PubMed PMID: 18849484.

117. Peiser L, De Winther MP, Makepeace K, Hollinshead M, Coull P, Plested J, et al. The class A macrophage scavenger receptor is a major pattern recognition receptor for Neisseria meningitidis which is independent of lipopolysaccharide and not required for secretory responses. Infect Immun. 2002;70(10):5346-54. doi: 10.1128/IAI.70.10.5346-5354.2002. PubMed PMID: 12228258; PubMed Central PMCID: PMC128305.

118. Bessa Pereira C, Bocková M, Santos RF, Santos AM, Martins de Araújo M, Oliveira L, et al. The Scavenger Receptor SSc5D Physically Interacts with Bacteria through the SRCR-Containing N-Terminal Domain. Front Immunol. 2016;7:416. Epub 20161013. doi: 10.3389/fimmu.2016.00416. PubMed PMID: 27790215; PubMed Central PMCID: PMC5061727.

119. Bikker FJ, Ligtenberg AJ, Nazmi K, Veerman EC, van't Hof W, Bolscher JG, et al. Identification of the bacteria-binding peptide domain on salivary agglutinin (gp-340/DMBT1), a member of the scavenger receptor cysteine-rich superfamily. J Biol Chem. 2002;277(35):32109-15. Epub 20020605. doi: 10.1074/jbc.M203788200. PubMed PMID: 12050164.

120. Brännström A, Sankala M, Tryggvason K, Pikkarainen T. Arginine residues in domain V have a central role for bacteria-binding activity of macrophage scavenger receptor MARCO. Biochem Biophys Res Commun. 2002;290(5):1462-9. doi: 10.1006/bbrc.2002.6378. PubMed PMID: 11820786.

121. Sarrias MR, Roselló S, Sánchez-Barbero F, Sierra JM, Vila J, Yélamos J, et al. A role for human Sp alpha as a pattern recognition receptor. J Biol Chem. 2005;280(42):35391-8. Epub 20050719. doi: 10.1074/jbc.M505042200. PubMed PMID: 16030018.

122. Krieger M, Abrams JM, Lux A, Steller H. Molecular flypaper, atherosclerosis, and host defense: structure and function of the macrophage scavenger receptor. Cold Spring Harb Symp Quant Biol. 1992;57:605-9. doi: 10.1101/sqb.1992.057.01.066. PubMed PMID: 1339697.

123. Gebe JA, Kiener PA, Ring HZ, Li X, Francke U, Aruffo A. Molecular cloning, mapping to human chromosome 1 q21-q23, and cell binding characteristics of Spalpha, a new member of the scavenger receptor cysteine-rich (SRCR) family of proteins. J Biol Chem. 1997;272(10):6151-8. doi: 10.1074/jbc.272.10.6151. PubMed PMID: 9045627.

124. Sarrias MR, Padilla O, Monreal Y, Carrascal M, Abian J, Vives J, et al. Biochemical characterization of recombinant and circulating human Spalpha. Tissue Antigens. 2004;63(4):335-44. doi: 10.1111/j.0001-2815.2004.00193.x. PubMed PMID: 15009805.

125. Valledor AF, Hsu LC, Ogawa S, Sawka-Verhelle D, Karin M, Glass CK. Activation of liver X receptors and retinoid X receptors prevents bacterial-induced macrophage apoptosis. Proc Natl Acad Sci U S A. 2004;101(51):17813-8. Epub 20041215. doi: 10.1073/pnas.0407749101. PubMed PMID: 15601766; PubMed Central PMCID: PMC539759.

126. Hamada M, Nakamura M, Tran MT, Moriguchi T, Hong C, Ohsumi T, et al. MafB promotes atherosclerosis by inhibiting foam-cell apoptosis. Nat Commun. 2014;5:3147. doi: 10.1038/ncomms4147. PubMed PMID: 24445679.

127. Yamazaki T, Mori M, Arai S, Tateishi R, Abe M, Ban M, et al. Circulating AIM as an indicator of liver damage and hepatocellular carcinoma in humans. PLoS One. 2014;9(10):e109123. Epub 20141010. doi: 10.1371/journal.pone.0109123. PubMed PMID: 25302503; PubMed Central PMCID: PMC4193837.

128. Kai T, Yamazaki T, Arai S, Miyazaki T. Stabilization and augmentation of circulating AIM in mice by synthesized IgM-Fc. PLoS One. 2014;9(5):e97037. Epub 20140507. doi: 10.1371/journal.pone.0097037. PubMed PMID: 24804991; PubMed Central PMCID: PMC4013091.

129. Gebe JA, Llewellyn M, Hoggatt H, Aruffo A. Molecular cloning, genomic organization and cell-binding characteristics of mouse Spalpha. Immunology. 2000;99(1):78-86. doi: 10.1046/j.1365-2567.2000.00903.x. PubMed PMID: 10651944; PubMed Central PMCID: PMC2327131.

130. Hiramoto E, Tsutsumi A, Suzuki R, Matsuoka S, Arai S, Kikkawa M, et al. The IgM pentamer is an asymmetric pentagon with an open groove that binds the AIM protein. Sci Adv. 2018;4(10):eaau1199. Epub 20181010. doi: 10.1126/sciadv.aau1199. PubMed PMID: 30324136; PubMed Central PMCID: PMC6179379.

131. Arai S, Maehara N, Iwamura Y, Honda S, Nakashima K, Kai T, et al. Obesity-associated autoantibody production requires AIM to retain the immunoglobulin M immune complex on follicular dendritic cells. Cell Rep. 2013;3(4):1187-98. Epub 20130404. doi: 10.1016/j.celrep.2013.03.006. PubMed PMID: 23562157.

132. Tissot JD, Sanchez JC, Vuadens F, Scherl A, Schifferli JA, Hochstrasser DF, et al. IgM are associated to Sp alpha (CD5 antigen-like). Electrophoresis. 2002;23(7-8):1203-6. doi: 10.1002/1522-2683(200204)23:7/8<1203::AID-ELPS1203>3.0.CO;2-1. PubMed PMID: 11981870.

133. Arai S, Kitada K, Yamazaki T, Takai R, Zhang X, Tsugawa Y, et al. Apoptosis inhibitor of macrophage protein enhances intraluminal debris clearance and ameliorates acute kidney injury in mice. Nat Med. 2016;22(2):183-93. Epub 20160104. doi: 10.1038/nm.4012. PubMed PMID: 26726878.

134. Koyama N, Yamazaki T, Kanetsuki Y, Hirota J, Asai T, Mitsumoto Y, et al. Activation of apoptosis inhibitor of macrophage is a sensitive diagnostic marker for NASH-associated hepatocellular carcinoma. J Gastroenterol. 2018;53(6):770-9. Epub 20171030. doi: 10.1007/s00535-017-1398-y. PubMed PMID: 29086016.

135. Joseph SB, Bradley MN, Castrillo A, Bruhn KW, Mak PA, Pei L, et al. LXR-dependent gene expression is important for macrophage survival and the innate immune response. Cell. 2004;119(2):299-309. doi: 10.1016/j.cell.2004.09.032. PubMed PMID: 15479645.

136. Zou T, Garifulin O, Berland R, Boyartchuk VL. Listeria monocytogenes infection induces prosurvival metabolic signaling in macrophages. Infect Immun. 2011;79(4):1526-35. Epub 20110124. doi: 10.1128/IAI.01195-10. PubMed PMID: 21263022; PubMed Central PMCID: PMC3067555.

137. Amézaga N, Sanjurjo L, Julve J, Aran G, Pérez-Cabezas B, Bastos-Amador P, et al. Human scavenger protein AIM increases foam cell formation and CD36-mediated oxLDL uptake. J Leukoc Biol. 2014;95(3):509-20. Epub 20131202. doi: 10.1189/jlb.1212660. PubMed PMID: 24295828.

138. Smole U, Kratzer B, Pickl WF. Soluble pattern recognition molecules: Guardians and regulators of homeostasis at airway mucosal surfaces. Eur J Immunol. 2020;50(5):624-42. doi: 10.1002/eji.201847811. PubMed PMID: 32246830; PubMed Central PMCID: PMC7216992.

139. Deban L, Jaillon S, Garlanda C, Bottazzi B, Mantovani A. Pentraxins in innate immunity: lessons from PTX3. Cell Tissue Res. 2011;343(1):237-49. Epub 20100804. doi: 10.1007/s00441-010-1018-0. PubMed PMID: 20683616.

140. Holmskov U, Thiel S, Jensenius JC. Collections and ficolins: humoral lectins of the innate immune defense. Annu Rev Immunol. 2003;21:547-78. Epub 20011219. doi: 10.1146/annurev.immunol.21.120601.140954. PubMed PMID: 12524383.

141. Foo SS, Reading PC, Jaillon S, Mantovani A, Mahalingam S. Pentraxins and Collectins: Friend or Foe during Pathogen Invasion? Trends Microbiol. 2015;23(12):799-811. Epub 20151017. doi: 10.1016/j.tim.2015.09.006. PubMed PMID: 26482345; PubMed Central PMCID: PMC7127210.

142. Haruta I, Kato Y, Hashimoto E, Minjares C, Kennedy S, Uto H, et al. Association of AIM, a novel apoptosis inhibitory factor, with hepatitis via supporting macrophage survival and enhancing phagocytotic function of macrophages. J Biol Chem. 2001;276(25):22910-4. Epub 20010409. doi: 10.1074/jbc.M100324200. PubMed PMID: 11294859.

143. Sanjurjo L, Aran G, Téllez É, Amézaga N, Armengol C, López D, et al. CD5L Promotes M2 Macrophage Polarization through Autophagy-Mediated Upregulation of ID3. Front Immunol. 2018;9:480. Epub 20180312. doi: 10.3389/fimmu.2018.00480. PubMed PMID: 29593730; PubMed Central PMCID: PMC5858086.

144. Gao X, Yan X, Zhang Q, Yin Y, Cao J. CD5L contributes to the pathogenesis of methicillin-resistant Staphylococcus aureus-induced pneumonia. Int Immunopharmacol. 2019;72:40-7. Epub 20190405. doi: 10.1016/j.intimp.2019.03.057. PubMed PMID: 30959370.

145. Romani L. Immunity to fungal infections. Nat Rev Immunol. 2011;11(4):275-88. Epub 20110311. doi: 10.1038/nri2939. PubMed PMID: 21394104.

146. Curtis MM, Way SS. Interleukin-17 in host defence against bacterial, mycobacterial and fungal pathogens. Immunology. 2009;126(2):177-85. doi: 10.1111/j.1365-2567.2008.03017.x. PubMed PMID: 19125888; PubMed Central PMCID: PMC2632692.

147. Khader SA, Gaffen SL, Kolls JK. Th17 cells at the crossroads of innate and adaptive immunity against infectious diseases at the mucosa. Mucosal Immunol. 2009;2(5):403-11. Epub 20090708. doi: 10.1038/mi.2009.100. PubMed PMID: 19587639; PubMed Central PMCID: PMC2811522.

148. Kleinewietfeld M, Hafler DA. The plasticity of human Treg and Th17 cells and its role in autoimmunity. Semin Immunol. 2013;25(4):305-12. Epub 20131105. doi: 10.1016/j.smim.2013.10.009. PubMed PMID: 24211039; PubMed Central PMCID: PMC3905679.

149. Gaublomme JT, Yosef N, Lee Y, Gertner RS, Yang LV, Wu C, et al. Single-Cell Genomics Unveils Critical Regulators of Th17 Cell Pathogenicity. Cell. 2015;163(6):1400-12. Epub 20151119. doi: 10.1016/j.cell.2015.11.009. PubMed PMID: 26607794; PubMed Central PMCID: PMC4671824.

150. Bird L. T cells: Seq-ing out the 'bad' guys. Nat Rev Immunol. 2016;16(1):3. Epub 20151221. doi: 10.1038/nri.2015.15. PubMed PMID: 26688347.

151. Hasegawa H, Mizoguchi I, Orii N, Inoue S, Katahira Y, Yoneto T, et al. IL-23p19 and CD5 antigen-like form a possible novel heterodimeric cytokine and contribute to experimental autoimmune encephalomyelitis development. Sci Rep. 2021;11(1):5266. Epub 20210304. doi: 10.1038/s41598-021-84624-9. PubMed PMID: 33664371; PubMed Central PMCID: PMC7933155.

152. Goerdt S, Orfanos CE. Other functions, other genes: alternative activation of antigen-presenting cells. Immunity. 1999;10(2):137-42. doi: 10.1016/s1074-7613(00)80014-x. PubMed PMID: 10072066.

153. Gordon S. Alternative activation of macrophages. Nat Rev Immunol. 2003;3(1):23-35. doi: 10.1038/nri978. PubMed PMID: 12511873.

154. Dalton DK, Pitts-Meek S, Keshav S, Figari IS, Bradley A, Stewart TA. Multiple defects of immune cell function in mice with disrupted interferon-gamma genes. Science. 1993;259(5102):1739-42. doi: 10.1126/science.8456300. PubMed PMID: 8456300.

155. Mantovani A, Sica A, Sozzani S, Allavena P, Vecchi A, Locati M. The chemokine system in diverse forms of macrophage activation and polarization. Trends Immunol. 2004;25(12):677-86. doi: 10.1016/j.it.2004.09.015. PubMed PMID: 15530839.

156. Mosser DM. The many faces of macrophage activation. J Leukoc Biol. 2003;73(2):209-12. doi: 10.1189/jlb.0602325. PubMed PMID: 12554797.

157. Stein M, Keshav S, Harris N, Gordon S. Interleukin 4 potently enhances murine macrophage mannose receptor activity: a marker of alternative immunologic macrophage activation. J Exp Med. 1992;176(1):287-92. doi: 10.1084/jem.176.1.287. PubMed PMID: 1613462; PubMed Central PMCID: PMC2119288.

158. Murray PJ, Allen JE, Biswas SK, Fisher EA, Gilroy DW, Goerdt S, et al. Macrophage activation and polarization: nomenclature and experimental guidelines. Immunity. 2014;41(1):14-20. doi: 10.1016/j.immuni.2014.06.008. PubMed PMID: 25035950; PubMed Central PMCID: PMC4123412.

159. Jaggi U, Yang M, Matundan HH, Hirose S, Shah PK, Sharifi BG, et al. Increased phagocytosis in the presence of enhanced M2-like macrophage responses correlates with increased primary and latent HSV-1 infection. PLoS Pathog. 2020;16(10):e1008971. Epub

20201008. doi: 10.1371/journal.ppat.1008971. PubMed PMID: 33031415; PubMed Central PMCID: PMC7575112.

160. Kim TH, Yang K, Kim M, Kim HS, Kang JL. Apoptosis inhibitor of macrophage (AIM) contributes to IL-10-induced anti-inflammatory response through inhibition of inflammasome activation. Cell Death Dis. 2021;12(1):19. Epub 20210104. doi: 10.1038/s41419-020-03332-w. PubMed PMID: 33414479; PubMed Central PMCID: PMC7791024.

161. Shintani T, Klionsky DJ. Autophagy in health and disease: a double-edged sword. Science. 2004;306(5698):990-5. doi: 10.1126/science.1099993. PubMed PMID: 15528435; PubMed Central PMCID: PMC1705980.

162. Deretic V. Autophagy in innate and adaptive immunity. Trends Immunol. 2005;26(10):523-8. doi: 10.1016/j.it.2005.08.003. PubMed PMID: 16099218.

163. Deretic V, Saitoh T, Akira S. Autophagy in infection, inflammation and immunity. Nat Rev Immunol. 2013;13(10):722-37. doi: 10.1038/nri3532. PubMed PMID: 24064518; PubMed Central PMCID: PMC5340150.

164. Ogawa M, Yoshimori T, Suzuki T, Sagara H, Mizushima N, Sasakawa C. Escape of intracellular Shigella from autophagy. Science. 2005;307(5710):727-31. Epub 20041202. doi: 10.1126/science.1106036. PubMed PMID: 15576571.

165. Gutierrez MG, Master SS, Singh SB, Taylor GA, Colombo MI, Deretic V. Autophagy is a defense mechanism inhibiting BCG and Mycobacterium tuberculosis survival in infected macrophages. Cell. 2004;119(6):753-66. doi: 10.1016/j.cell.2004.11.038. PubMed PMID: 15607973.

166. White E, Karp C, Strohecker AM, Guo Y, Mathew R. Role of autophagy in suppression of inflammation and cancer. Curr Opin Cell Biol. 2010;22(2):212-7. Epub 20100106. doi: 10.1016/j.ceb.2009.12.008. PubMed PMID: 20056400; PubMed Central PMCID: PMC2857707.

167. Sanjurjo L, Amézaga N, Vilaplana C, Cáceres N, Marzo E, Valeri M, et al. The scavenger protein apoptosis inhibitor of macrophages (AIM) potentiates the antimicrobial response against Mycobacterium tuberculosis by enhancing autophagy. PLoS One. 2013;8(11):e79670. Epub 20131104. doi: 10.1371/journal.pone.0079670. PubMed PMID: 24223991; PubMed Central PMCID: PMC3817138.

168. Sonawane A, Santos JC, Mishra BB, Jena P, Progida C, Sorensen OE, et al. Cathelicidin is involved in the intracellular killing of mycobacteria in macrophages. Cell Microbiol. 2011;13(10):1601-17. Epub 20110811. doi: 10.1111/j.1462-5822.2011.01644.x. PubMed PMID: 21790937.

169. Liu PT, Stenger S, Tang DH, Modlin RL. Cutting edge: vitamin D-mediated human antimicrobial activity against Mycobacterium tuberculosis is dependent on the induction of cathelicidin. J Immunol. 2007;179(4):2060-3. doi: 10.4049/jimmunol.179.4.2060. PubMed PMID: 17675463.

170. Fabri M, Modlin RL. A vitamin for autophagy. Cell Host Microbe. 2009;6(3):201-3. doi: 10.1016/j.chom.2009.08.008. PubMed PMID: 19748462.

171. Sanjurjo L, Amézaga N, Aran G, Naranjo-Gómez M, Arias L, Armengol C, et al. The human CD5L/AIM-CD36 axis: A novel autophagy inducer in macrophages that modulates

inflammatory responses. Autophagy. 2015;11(3):487-502. doi: 10.1080/15548627.2015.1017183. PubMed PMID: 25713983; PubMed Central PMCID: PMC4502645.

172. Saitoh T, Fujita N, Jang MH, Uematsu S, Yang BG, Satoh T, et al. Loss of the autophagy protein Atg16L1 enhances endotoxin-induced IL-1beta production. Nature. 2008;456(7219):264-8. Epub 20081005. doi: 10.1038/nature07383. PubMed PMID: 18849965.

173. Agostini L, Martinon F, Burns K, McDermott MF, Hawkins PN, Tschopp J. NALP3 forms an IL-1beta-processing inflammasome with increased activity in Muckle-Wells autoinflammatory disorder. Immunity. 2004;20(3):319-25. doi: 10.1016/s1074-7613(04)00046-9. PubMed PMID: 15030775.

174. Kanneganti TD, Ozören N, Body-Malapel M, Amer A, Park JH, Franchi L, et al. Bacterial RNA and small antiviral compounds activate caspase-1 through cryopyrin/Nalp3. Nature. 2006;440(7081):233-6. Epub 20060111. doi: 10.1038/nature04517. PubMed PMID: 16407888.

175. Mariathasan S, Newton K, Monack DM, Vucic D, French DM, Lee WP, et al. Differential activation of the inflammasome by caspase-1 adaptors ASC and Ipaf. Nature. 2004;430(6996):213-8. Epub 20040609. doi: 10.1038/nature02664. PubMed PMID: 15190255.

176. Latz E. The inflammasomes: mechanisms of activation and function. Curr Opin Immunol. 2010;22(1):28-33. Epub 20100108. doi: 10.1016/j.coi.2009.12.004. PubMed PMID: 20060699; PubMed Central PMCID: PMC2844336.

177. Gurung P, Li B, Subbarao Malireddi RK, Lamkanfi M, Geiger TL, Kanneganti TD. Chronic TLR Stimulation Controls NLRP3 Inflammasome Activation through IL-10 Mediated Regulation of NLRP3 Expression and Caspase-8 Activation. Sci Rep. 2015;5:14488. Epub 20150928. doi: 10.1038/srep14488. PubMed PMID: 26412089; PubMed Central PMCID: PMC4585974.

178. Ip WKE, Hoshi N, Shouval DS, Snapper S, Medzhitov R. Anti-inflammatory effect of IL-10 mediated by metabolic reprogramming of macrophages. Science. 2017;356(6337):513-9. doi: 10.1126/science.aal3535. PubMed PMID: 28473584; PubMed Central PMCID: PMC6260791.

179. Sorbara MT, Girardin SE. Mitochondrial ROS fuel the inflammasome. Cell Res. 2011;21(4):558-60. Epub 20110201. doi: 10.1038/cr.2011.20. PubMed PMID: 21283134; PubMed Central PMCID: PMC3203657.

180. Gisterå A, Hansson GK. The immunology of atherosclerosis. Nat Rev Nephrol. 2017;13(6):368-80. Epub 20170410. doi: 10.1038/nrneph.2017.51. PubMed PMID: 28392564.

181. Libby P, Buring JE, Badimon L, Hansson GK, Deanfield J, Bittencourt MS, et al. Atherosclerosis. Nat Rev Dis Primers. 2019;5(1):56. Epub 20190816. doi: 10.1038/s41572-019-0106-z. PubMed PMID: 31420554.

182. Ross R. Atherosclerosis--an inflammatory disease. N Engl J Med. 1999;340(2):115-26. doi: 10.1056/NEJM199901143400207. PubMed PMID: 9887164.

183. Goldstein JL, Ho YK, Basu SK, Brown MS. Binding site on macrophages that mediates uptake and degradation of acetylated low density lipoprotein, producing massive cholesterol deposition. Proc Natl Acad Sci U S A. 1979;76(1):333-7. doi: 10.1073/pnas.76.1.333. PubMed PMID: 218198; PubMed Central PMCID: PMC382933.

184. Suzuki H, Kurihara Y, Takeya M, Kamada N, Kataoka M, Jishage K, et al. A role for macrophage scavenger receptors in atherosclerosis and susceptibility to infection. Nature. 1997;386(6622):292-6. doi: 10.1038/386292a0. PubMed PMID: 9069289.

185. Febbraio M, Podrez EA, Smith JD, Hajjar DP, Hazen SL, Hoff HF, et al. Targeted disruption of the class B scavenger receptor CD36 protects against atherosclerotic lesion development in mice. J Clin Invest. 2000;105(8):1049-56. doi: 10.1172/JCI9259. PubMed PMID: 10772649; PubMed Central PMCID: PMC300837.

186. Kunjathoor VV, Febbraio M, Podrez EA, Moore KJ, Andersson L, Koehn S, et al. Scavenger receptors class A-I/II and CD36 are the principal receptors responsible for the uptake of modified low density lipoprotein leading to lipid loading in macrophages. J Biol Chem. 2002;277(51):49982-8. Epub 20021009. doi: 10.1074/jbc.M209649200. PubMed PMID: 12376530.

187. Salvayre R, Auge N, Benoist H, Negre-Salvayre A. Oxidized low-density lipoprotein-induced apoptosis. Biochim Biophys Acta. 2002;1585(2-3):213-21. doi: 10.1016/s1388-1981(02)00343-8. PubMed PMID: 12531556.

188. Guerrini V, Gennaro ML. Foam Cells: One Size Doesn't Fit All. Trends Immunol. 2019;40(12):1163-79. Epub 20191112. doi: 10.1016/j.it.2019.10.002. PubMed PMID: 31732284; PubMed Central PMCID: PMC6925453.

189. Arai S, Shelton JM, Chen M, Bradley MN, Castrillo A, Bookout AL, et al. A role for the apoptosis inhibitory factor AIM/Spalpha/Api6 in atherosclerosis development. Cell Metab. 2005;1(3):201-13. doi: 10.1016/j.cmet.2005.02.002. PubMed PMID: 16054063.

190. Liu J, Thewke DP, Su YR, Linton MF, Fazio S, Sinensky MS. Reduced macrophage apoptosis is associated with accelerated atherosclerosis in low-density lipoprotein receptor-null mice. Arterioscler Thromb Vasc Biol. 2005;25(1):174-9. Epub 20041021. doi: 10.1161/01.ATV.0000148548.47755.22. PubMed PMID: 15499039; PubMed Central PMCID: PMC2649706.

191. van Vlijmen BJ, Gerritsen G, Franken AL, Boesten LS, Kockx MM, Gijbels MJ, et al. Macrophage p53 deficiency leads to enhanced atherosclerosis in APOE*3-Leiden transgenic mice. Circ Res. 2001;88(8):780-6. doi: 10.1161/hh0801.089261. PubMed PMID: 11325869.

192. Lai KN, Tang SC, Schena FP, Novak J, Tomino Y, Fogo AB, et al. IgA nephropathy. Nat Rev Dis Primers. 2016;2:16001. Epub 20160211. doi: 10.1038/nrdp.2016.1. PubMed PMID: 27189177.

193. Robert T, Berthelot L, Cambier A, Rondeau E, Monteiro RC. Molecular Insights into the Pathogenesis of IgA Nephropathy. Trends Mol Med. 2015;21(12):762-75. Epub 20151121. doi: 10.1016/j.molmed.2015.10.003. PubMed PMID: 26614735.

194. Suzuki H, Kiryluk K, Novak J, Moldoveanu Z, Herr AB, Renfrow MB, et al. The pathophysiology of IgA nephropathy. J Am Soc Nephrol. 2011;22(10):1795-803. Epub

20110923. doi: 10.1681/ASN.2011050464. PubMed PMID: 21949093; PubMed Central PMCID: PMC3892742.

195. Lai KN. Pathogenesis of IgA nephropathy. Nat Rev Nephrol. 2012;8(5):275-83. Epub 20120320. doi: 10.1038/nrneph.2012.58. PubMed PMID: 22430056.

196. Takahata A, Arai S, Hiramoto E, Kitada K, Kato R, Makita Y, et al. Crucial Role of AIM/CD5L in the Development of Glomerular Inflammation in IgA Nephropathy. J Am Soc Nephrol. 2020;31(9):2013-24. Epub 20200701. doi: 10.1681/ASN.2019100987. PubMed PMID: 32611589; PubMed Central PMCID: PMC7461693.

197. Dolin HH, Papadimos TJ, Chen X, Pan ZK. Characterization of Pathogenic Sepsis Etiologies and Patient Profiles: A Novel Approach to Triage and Treatment. Microbiol Insights. 2019;12:1178636118825081. Epub 20190127. doi: 10.1177/1178636118825081. PubMed PMID: 30728724; PubMed Central PMCID: PMC6350122.

198. Gao X, Liu Y, Xu F, Lin S, Song Z, Duan J, et al. Assessment of Apoptosis Inhibitor of Macrophage/CD5L as a Biomarker to Predict Mortality in the Critically Ill With Sepsis. Chest. 2019;156(4):696-705. Epub 20190530. doi: 10.1016/j.chest.2019.04.134. PubMed PMID: 31154043.

199. Gao X, Yan X, Yin Y, Lin X, Zhang Q, Xia Y, et al. Therapeutic Targeting of Apoptosis Inhibitor of Macrophage/CD5L in Sepsis. Am J Respir Cell Mol Biol. 2019;60(3):323-34. doi: 10.1165/rcmb.2018-0272OC. PubMed PMID: 30326743.

200. Wang P, Mu X, Zhao H, Li Y, Wang L, Wolfe V, et al. Administration of GDF3 Into Septic Mice Improves Survival. Front Immunol. 2021;12:647070. Epub 20210217. doi: 10.3389/fimmu.2021.647070. PubMed PMID: 33679812; PubMed Central PMCID: PMC7925632.

201. Tomita T, Arai S, Kitada K, Mizuno M, Suzuki Y, Sakata F, et al. Apoptosis inhibitor of macrophage ameliorates fungus-induced peritoneal injury model in mice. Sci Rep. 2017;7(1):6450. Epub 20170725. doi: 10.1038/s41598-017-06824-6. PubMed PMID: 28743989; PubMed Central PMCID: PMC5527077.

202. Kimura H, Suzuki M, Konno S, Shindou H, Shimizu T, Nagase T, et al. Orchestrating Role of Apoptosis Inhibitor of Macrophage in the Resolution of Acute Lung Injury. J Immunol. 2017;199(11):3870-82. Epub 20171025. doi: 10.4049/jimmunol.1601798. PubMed PMID: 29070674.

203. Padilla O, Pujana MA, López-de la Iglesia A, Gimferrer I, Arman M, Vilà JM, et al. Cloning of S4D-SRCRB, a new soluble member of the group B scavenger receptor cysteine-rich family (SRCR-SF) mapping to human chromosome 7q11.23. Immunogenetics. 2002;54(9):621-34. Epub 20021106. doi: 10.1007/s00251-002-0507-z. PubMed PMID: 12466895.

204. Medzhitov R. Origin and physiological roles of inflammation. Nature. 2008;454(7203):428-35. doi: 10.1038/nature07201. PubMed PMID: 18650913.

205. Medzhitov R. Inflammation 2010: new adventures of an old flame. Cell. 2010;140(6):771-6. doi: 10.1016/j.cell.2010.03.006. PubMed PMID: 20303867.

206. Büscher P, Cecchi G, Jamonneau V, Priotto G. Human African trypanosomiasis. Lancet. 2017;390(10110):2397-409. Epub 20170630. doi: 10.1016/S0140-6736(17)31510-6. PubMed PMID: 28673422.

207. Rocha G, Martins A, Gama G, Brandão F, Atouguia J. Possible cases of sexual and congenital transmission of sleeping sickness. Lancet. 2004;363(9404):247. doi: 10.1016/S0140-6736(03)15345-7. PubMed PMID: 14738812.

208. Hira PR, Husein SF. Some transfusion-induced parasitic infections in Zambia. J Hyg Epidemiol Microbiol Immunol. 1979;23(4):436-44. PubMed PMID: 399289.

209. Simarro PP, Cecchi G, Paone M, Franco JR, Diarra A, Ruiz JA, et al. The Atlas of human African trypanosomiasis: a contribution to global mapping of neglected tropical diseases. Int J Health Geogr. 2010;9:57. Epub 20101101. doi: 10.1186/1476-072X-9-57. PubMed PMID: 21040555; PubMed Central PMCID: PMC2988709.

210. Jamonneau V, Truc P, Grébaut P, Herder S, Ravel S, Solano P, et al. Trypanosoma brucei gambiense Group 2: The Unusual Suspect. Trends Parasitol. 2019;35(12):983-95. Epub 20191024. doi: 10.1016/j.pt.2019.09.002. PubMed PMID: 31668893.

211. Kennedy PGE, Rodgers J. Clinical and Neuropathogenetic Aspects of Human African Trypanosomiasis. Front Immunol. 2019;10:39. Epub 20190125. doi: 10.3389/fimmu.2019.00039. PubMed PMID: 30740102; PubMed Central PMCID: PMC6355679.

212. Franco JR, Cecchi G, Priotto G, Paone M, Diarra A, Grout L, et al. Monitoring the elimination of human African trypanosomiasis at continental and country level: Update to 2018. PLoS Negl Trop Dis. 2020;14(5):e0008261. Epub 20200521. doi: 10.1371/journal.pntd.0008261. PubMed PMID: 32437391; PubMed Central PMCID: PMC7241700.

213. Bouyer J, Bouyer F, Donadeu M, Rowan T, Napier G. Community- and farmer-based management of animal African trypanosomosis in cattle. Trends Parasitol. 2013;29(11):519-22. Epub 20130906. doi: 10.1016/j.pt.2013.08.003. PubMed PMID: 24012356.

214. Van den Bossche P, de La Rocque S, Hendrickx G, Bouyer J. A changing environment and the epidemiology of tsetse-transmitted livestock trypanosomiasis. Trends Parasitol. 2010;26(5):236-43. Epub 20100319. doi: 10.1016/j.pt.2010.02.010. PubMed PMID: 20304707.

215. Kristensson K, Masocha W, Bentivoglio M. Mechanisms of CNS invasion and damage by parasites. Handb Clin Neurol. 2013;114:11-22. doi: 10.1016/B978-0-444-53490-3.00002-9. PubMed PMID: 23829898.

216. Grab DJ, Nikolskaia O, Kim YV, Lonsdale-Eccles JD, Ito S, Hara T, et al. African trypanosome interactions with an in vitro model of the human blood-brain barrier. J Parasitol. 2004;90(5):970-9. doi: 10.1645/GE-287R. PubMed PMID: 15562595.

217. Ooi CP, Bastin P. More than meets the eye: understanding Trypanosoma brucei morphology in the tsetse. Front Cell Infect Microbiol. 2013;3:71. Epub 20131113. doi: 10.3389/fcimb.2013.00071. PubMed PMID: 24312899; PubMed Central PMCID: PMC3826061.

218. MacGregor P, Savill NJ, Hall D, Matthews KR. Transmission stages dominate trypanosome within-host dynamics during chronic infections. Cell Host Microbe. 2011;9(4):310-8. doi: 10.1016/j.chom.2011.03.013. PubMed PMID: 21501830; PubMed Central PMCID: PMC3094754.

219. Matthews KR. Developments in the differentiation of Trypanosoma brucei. Parasitol Today. 1999;15(2):76-80. doi: 10.1016/s0169-4758(98)01381-7. PubMed PMID: 10234191.

220. Ferguson MA, Homans SW, Dwek RA, Rademacher TW. Glycosyl-phosphatidylinositol moiety that anchors Trypanosoma brucei variant surface glycoprotein to the membrane. Science. 1988;239(4841 Pt 1):753-9. doi: 10.1126/science.3340856. PubMed PMID: 3340856.

221. Mehlert A, Bond CS, Ferguson MA. The glycoforms of a Trypanosoma brucei variant surface glycoprotein and molecular modeling of a glycosylated surface coat. Glycobiology. 2002;12(10):607-12. doi: 10.1093/glycob/cwf079. PubMed PMID: 12244073.

222. Bartossek T, Jones NG, Schäfer C, Cvitković M, Glogger M, Mott HR, et al. Structural basis for the shielding function of the dynamic trypanosome variant surface glycoprotein coat. Nat Microbiol. 2017;2(11):1523-32. Epub 20170911. doi: 10.1038/s41564-017-0013-6. PubMed PMID: 28894098.

223. Magez S, Schwegmann A, Atkinson R, Claes F, Drennan M, De Baetselier P, et al. The role of B-cells and IgM antibodies in parasitemia, anemia, and VSG switching in Trypanosoma brucei-infected mice. PLoS Pathog. 2008;4(8):e1000122. Epub 20080808. doi: 10.1371/journal.ppat.1000122. PubMed PMID: 18688274; PubMed Central PMCID: PMC2483930.

224. Corsini AC, Clayton C, Askonas BA, Ogilvie BM. Suppressor cells and loss of B-cell potential in mice infected with Trypanosoma brucei. Clin Exp Immunol. 1977;29(1):122-31. PubMed PMID: 302169; PubMed Central PMCID: PMC1541048.

225. Bockstal V, Guirnalda P, Caljon G, Goenka R, Telfer JC, Frenkel D, et al. T. brucei infection reduces B lymphopoiesis in bone marrow and truncates compensatory splenic lymphopoiesis through transitional B-cell apoptosis. PLoS Pathog. 2011;7(6):e1002089. Epub 20110630. doi: 10.1371/journal.ppat.1002089. PubMed PMID: 21738467; PubMed Central PMCID: PMC3128123.

226. Magez S, Stijlemans B, Baral T, De Baetselier P. VSG-GPI anchors of African trypanosomes: their role in macrophage activation and induction of infection-associated immunopathology. Microbes Infect. 2002;4(9):999-1006. doi: 10.1016/s1286-4579(02)01617-9. PubMed PMID: 12106794.

227. Leppert BJ, Mansfield JM, Paulnock DM. The soluble variant surface glycoprotein of African trypanosomes is recognized by a macrophage scavenger receptor and induces I kappa B alpha degradation independently of TRAF6-mediated TLR signaling. J Immunol. 2007;179(1):548-56. doi: 10.4049/jimmunol.179.1.548. PubMed PMID: 17579076.

228. Drennan MB, Stijlemans B, Van den Abbeele J, Quesniaux VJ, Barkhuizen M, Brombacher F, et al. The induction of a type 1 immune response following a Trypanosoma brucei infection is MyD88 dependent. J Immunol. 2005;175(4):2501-9. doi: 10.4049/jimmunol.175.4.2501. PubMed PMID: 16081822.

229. Paulnock DM, Freeman BE, Mansfield JM. Modulation of innate immunity by African trypanosomes. Parasitology. 2010;137(14):2051-63. doi: 10.1017/S0031182010001460. PubMed PMID: 21087532.

230. Mansfield JM, Olivier M. Immune Evasion by Parasites. In: Kaufmann SHE, Rouse BT, Sacks DL, editors. The Immune Response to Infection: ASM Press; 2010. p. 453-69.

231. Amin DN, Vodnala SK, Masocha W, Sun B, Kristensson K, Rottenberg ME. Distinct Toll-like receptor signals regulate cerebral parasite load and interferon α/β and tumor necrosis factor α-dependent T-cell infiltration in the brains of Trypanosoma brucei-infected mice. J Infect Dis. 2012;205(2):320-32. Epub 20111123. doi: 10.1093/infdis/jir734. PubMed PMID: 22116836; PubMed Central PMCID: PMC3244369.

232. Cnops J, De Trez C, Stijlemans B, Keirsse J, Kauffmann F, Barkhuizen M, et al. NK-, NKT- and CD8-Derived IFNγ Drives Myeloid Cell Activation and Erythrophagocytosis, Resulting in Trypanosomosis-Associated Acute Anemia. PLoS Pathog. 2015;11(6):e1004964. Epub 20150612. doi: 10.1371/journal.ppat.1004964. PubMed PMID: 26070118; PubMed Central PMCID: PMC4466398.

233. Hertz CJ, Filutowicz H, Mansfield JM. Resistance to the African trypanosomes is IFN-gamma dependent. J Immunol. 1998;161(12):6775-83. PubMed PMID: 9862708.

234. Namangala B, Noël W, De Baetselier P, Brys L, Beschin A. Relative contribution of interferon-gamma and interleukin-10 to resistance to murine African trypanosomosis. J Infect Dis. 2001;183(12):1794-800. Epub 20010515. doi: 10.1086/320731. PubMed PMID: 11372033.

235. Salmon D, Vanwalleghem G, Morias Y, Denoeud J, Krumbholz C, Lhommé F, et al. Adenylate cyclases of Trypanosoma brucei inhibit the innate immune response of the host. Science. 2012;337(6093):463-6. Epub 20120614. doi: 10.1126/science.1222753. PubMed PMID: 22700656.

236. Stijlemans B, Guilliams M, Raes G, Beschin A, Magez S, De Baetselier P. African trypanosomosis: from immune escape and immunopathology to immune intervention. Vet Parasitol. 2007;148(1):3-13. Epub 20070607. doi: 10.1016/j.vetpar.2007.05.005. PubMed PMID: 17560035.

237. Stijlemans B, Caljon G, Van Den Abbeele J, Van Ginderachter JA, Magez S, De Trez C. Immune Evasion Strategies of Trypanosoma brucei within the Mammalian Host: Progression to Pathogenicity. Front Immunol. 2016;7:233. Epub 20160624. doi: 10.3389/fimmu.2016.00233. PubMed PMID: 27446070; PubMed Central PMCID: PMC4919330.

238. Stijlemans B, Beschin A, Magez S, Van Ginderachter JA, De Baetselier P. Iron Homeostasis and Trypanosoma brucei Associated Immunopathogenicity Development: A Battle/Quest for Iron. Biomed Res Int. 2015;2015:819389. Epub 20150518. doi: 10.1155/2015/819389. PubMed PMID: 26090446; PubMed Central PMCID: PMC4450282.

239. Zeni P, Doepker E, Schulze-Topphoff U, Schulze Topphoff U, Huewel S, Tenenbaum T, et al. MMPs contribute to TNF-alpha-induced alteration of the blood-cerebrospinal fluid barrier in vitro. Am J Physiol Cell Physiol. 2007;293(3):C855-64. Epub 20070516. doi: 10.1152/ajpcell.00470.2006. PubMed PMID: 17507431.

240. Mansfield JM, Paulnock DM. Regulation of innate and acquired immunity in African trypanosomiasis. Parasite Immunol. 2005;27(10-11):361-71. doi: 10.1111/j.1365-3024.2005.00791.x. PubMed PMID: 16179030.

241. Magez S, Radwanska M, Beschin A, Sekikawa K, De Baetselier P. Tumor necrosis factor alpha is a key mediator in the regulation of experimental Trypanosoma brucei infections. Infect Immun. 1999;67(6):3128-32. doi: 10.1128/IAI.67.6.3128-3132.1999. PubMed PMID: 10338530; PubMed Central PMCID: PMC96631.

242. Bosschaerts T, Guilliams M, Stijlemans B, Morias Y, Engel D, Tacke F, et al. Tip-DC development during parasitic infection is regulated by IL-10 and requires CCL2/CCR2, IFN-gamma and MyD88 signaling. PLoS Pathog. 2010;6(8):e1001045. Epub 20100812. doi: 10.1371/journal.ppat.1001045. PubMed PMID: 20714353; PubMed Central PMCID: PMC2920868.

243. Okomo-Assoumou MC, Daulouede S, Lemesre JL, N'Zila-Mouanda A, Vincendeau P. Correlation of high serum levels of tumor necrosis factor-alpha with disease severity in human African trypanosomiasis. Am J Trop Med Hyg. 1995;53(5):539-43. doi: 10.4269/ajtmh.1995.53.539. PubMed PMID: 7485714.

244. Sileghem M, Flynn JN, Logan-Henfrey L, Ellis J. Tumour necrosis factor production by monocytes from cattle infected with Trypanosoma (Duttonella) vivax and Trypanosoma (Nannomonas) congolense: possible association with severity of anaemia associated with the disease. Parasite Immunol. 1994;16(1):51-4. doi: 10.1111/j.1365-3024.1994.tb00304.x. PubMed PMID: 7908735.

245. Hunter CA, Gow JW, Kennedy PG, Jennings FW, Murray M. Immunopathology of experimental African sleeping sickness: detection of cytokine mRNA in the brains of Trypanosoma brucei brucei-infected mice. Infect Immun. 1991;59(12):4636-40. doi: 10.1128/iai.59.12.4636-4640.1991. PubMed PMID: 1718878; PubMed Central PMCID: PMC259089.

246. Guilliams M, Movahedi K, Bosschaerts T, VandenDriessche T, Chuah MK, Hérin M, et al. IL-10 dampens TNF/inducible nitric oxide synthase-producing dendritic cell-mediated pathogenicity during parasitic infection. J Immunol. 2009;182(2):1107-18. doi: 10.4049/jimmunol.182.2.1107. PubMed PMID: 19124754.

247. Kaushik RS, Uzonna JE, Zhang Y, Gordon JR, Tabel H. Innate resistance to experimental African trypanosomiasis: differences in cytokine (TNF-alpha, IL-6, IL-10 and IL-12) production by bone marrow-derived macrophages from resistant and susceptible mice. Cytokine. 2000;12(7):1024-34. doi: 10.1006/cyto.2000.0685. PubMed PMID: 10880248.

248. Guilliams M, Oldenhove G, Noel W, Hérin M, Brys L, Loi P, et al. African trypanosomiasis: naturally occurring regulatory T cells favor trypanotolerance by limiting pathology associated with sustained type 1 inflammation. J Immunol. 2007;179(5):2748-57. doi: 10.4049/jimmunol.179.5.2748. PubMed PMID: 17709488.

249. Bosschaerts T, Guilliams M, Noel W, Hérin M, Burk RF, Hill KE, et al. Alternatively activated myeloid cells limit pathogenicity associated with African trypanosomiasis through the IL-10 inducible gene selenoprotein P. J Immunol. 2008;180(9):6168-75. doi: 10.4049/jimmunol.180.9.6168. PubMed PMID: 18424738.

250. Burza S, Croft SL, Boelaert M. Leishmaniasis. Lancet. 2018;392(10151):951-70. Epub 20180817. doi: 10.1016/S0140-6736(18)31204-2. PubMed PMID: 30126638.

251. Kaye P, Scott P. Leishmaniasis: complexity at the host-pathogen interface. Nat Rev Microbiol. 2011;9(8):604-15. Epub 20110711. doi: 10.1038/nrmicro2608. PubMed PMID: 21747391.

252. Herwaldt BL. Leishmaniasis. Lancet. 1999;354(9185):1191-9. doi: 10.1016/S0140-6736(98)10178-2. PubMed PMID: 10513726.

253. Kupani M, Pandey RK, Mehrotra S. Neutrophils and Visceral Leishmaniasis: Impact on innate immune response and cross-talks with macrophages and dendritic cells. J Cell Physiol. 2021;236(4):2255-67. Epub 20201220. doi: 10.1002/jcp.30029. PubMed PMID: 33345353.

254. Hurrell BP, Regli IB, Tacchini-Cottier F. Different Leishmania Species Drive Distinct Neutrophil Functions. Trends Parasitol. 2016;32(5):392-401. Epub 20160301. doi: 10.1016/j.pt.2016.02.003. PubMed PMID: 26944469.

255. Volpedo G, Pacheco-Fernandez T, Bhattacharya P, Oljuskin T, Dey R, Gannavaram S, et al. Determinants of Innate Immunity in Visceral Leishmaniasis and Their Implication in Vaccine Development. Front Immunol. 2021;12:748325. Epub 20211012. doi: 10.3389/fimmu.2021.748325. PubMed PMID: 34712235; PubMed Central PMCID: PMC8546207.

256. Honoré S, Garin YJ, Sulahian A, Gangneux JP, Derouin F. Influence of the host and parasite strain in a mouse model of visceral Leishmania infantum infection. FEMS Immunol Med Microbiol. 1998;21(3):231-9. doi: 10.1111/j.1574-695X.1998.tb01170.x. PubMed PMID: 9718213.

257. Olivier M, Gregory DJ, Forget G. Subversion mechanisms by which Leishmania parasites can escape the host immune response: a signaling point of view. Clin Microbiol Rev. 2005;18(2):293-305. doi: 10.1128/CMR.18.2.293-305.2005. PubMed PMID: 15831826; PubMed Central PMCID: PMC1082797.

258. Paul J, Karmakar S, De T. TLR-mediated distinct IFN-γ/IL-10 pattern induces protective immunity against murine visceral leishmaniasis. Eur J Immunol. 2012;42(8):2087-99. doi: 10.1002/eji.201242428. PubMed PMID: 22622993.

259. Murray HW. Prevention of relapse after chemotherapy in a chronic intracellular infection: mechanisms in experimental visceral leishmaniasis. J Immunol. 2005;174(8):4916-23. doi: 10.4049/jimmunol.174.8.4916. PubMed PMID: 15814719.

260. McConville MJ, Schnur LF, Jaffe C, Schneider P. Structure of Leishmania lipophosphoglycan: inter- and intra-specific polymorphism in Old World species. Biochem J. 1995;310 (Pt 3):807-18. doi: 10.1042/bj3100807. PubMed PMID: 7575413; PubMed Central PMCID: PMC1135969.

261. Faleiro RJ, Kumar R, Hafner LM, Engwerda CR. Immune regulation during chronic visceral leishmaniasis. PLoS Negl Trop Dis. 2014;8(7):e2914. Epub 20140710. doi: 10.1371/journal.pntd.0002914. PubMed PMID: 25010815; PubMed Central PMCID: PMC4091888.

262. Tuon FF, Amato VS, Bacha HA, Almusawi T, Duarte MI, Amato Neto V. Toll-like receptors and leishmaniasis. Infect Immun. 2008;76(3):866-72. Epub 20071210. doi: 10.1128/IAI.01090-07. PubMed PMID: 18070909; PubMed Central PMCID: PMC2258802.

263. Sacramento LA, da Costa JL, de Lima MH, Sampaio PA, Almeida RP, Cunha FQ, et al. Toll-Like Receptor 2 Is Required for Inflammatory Process Development during. Front Microbiol. 2017;8:262. Epub 20170223. doi: 10.3389/fmicb.2017.00262. PubMed PMID: 28280488; PubMed Central PMCID: PMC5322192.

264. Jafarzadeh A, Nemati M, Sharifi I, Nair A, Shukla D, Chauhan P, et al. Leishmania species-dependent functional duality of toll-like receptor 2. IUBMB Life. 2019;71(11):1685-700. Epub 20190722. doi: 10.1002/iub.2129. PubMed PMID: 31329370.

265. Schleicher U, Liese J, Knippertz I, Kurzmann C, Hesse A, Heit A, et al. NK cell activation in visceral leishmaniasis requires TLR9, myeloid DCs, and IL-12, but is independent of plasmacytoid DCs. J Exp Med. 2007;204(4):893-906. Epub 20070326. doi: 10.1084/jem.20061293. PubMed PMID: 17389237; PubMed Central PMCID: PMC2118560.

266. Sacramento L, Trevelin SC, Nascimento MS, Lima-Jùnior DS, Costa DL, Almeida RP, et al. Toll-like receptor 9 signaling in dendritic cells regulates neutrophil recruitment to inflammatory foci following Leishmania infantum infection. Infect Immun. 2015;83(12):4604-16. Epub 20150914. doi: 10.1128/IAI.00975-15. PubMed PMID: 26371124; PubMed Central PMCID: PMC4645391.

267. Ashley EA, Pyae Phyo A, Woodrow CJ. Malaria. Lancet. 2018;391(10130):1608-21. Epub 20180406. doi: 10.1016/S0140-6736(18)30324-6. PubMed PMID: 29631781.

268. Keeling PJ, Rayner JC. The origins of malaria: there are more things in heaven and earth …. Parasitology. 2015;142 Suppl 1:S16-25. Epub 20140625. doi: 10.1017/S0031182014000766. PubMed PMID: 24963725; PubMed Central PMCID: PMC4413824.

269. Mota MM, Rodriguez A. Migration through host cells: the first steps of Plasmodium sporozoites in the mammalian host. Cell Microbiol. 2004;6(12):1113-8. doi: 10.1111/j.1462-5822.2004.00460.x. PubMed PMID: 15527491.

270. Prudêncio M, Mota MM, Mendes AM. A toolbox to study liver stage malaria. Trends Parasitol. 2011;27(12):565-74. Epub 20111017. doi: 10.1016/j.pt.2011.09.004. PubMed PMID: 22015112.

271. Tavares J, Formaglio P, Thiberge S, Mordelet E, Van Rooijen N, Medvinsky A, et al. Role of host cell traversal by the malaria sporozoite during liver infection. J Exp Med. 2013;210(5):905-15. Epub 20130422. doi: 10.1084/jem.20121130. PubMed PMID: 23610126; PubMed Central PMCID: PMC3646492.

272. de Koning-Ward TF, Dixon MW, Tilley L, Gilson PR. Plasmodium species: master renovators of their host cells. Nat Rev Microbiol. 2016;14(8):494-507. Epub 20160704. doi: 10.1038/nrmicro.2016.79. PubMed PMID: 27374802.

273. De Niz M, Burda PC, Kaiser G, Del Portillo HA, Spielmann T, Frischknecht F, et al. Progress in imaging methods: insights gained into Plasmodium biology. Nat Rev Microbiol. 2017;15(1):37-54. Epub 20161128. doi: 10.1038/nrmicro.2016.158. PubMed PMID: 27890922.

274. Moxon CA, Gibbins MP, McGuinness D, Milner DA, Marti M. New Insights into Malaria Pathogenesis. Annu Rev Pathol. 2020;15:315-43. Epub 20191024. doi: 10.1146/annurev-pathmechdis-012419-032640. PubMed PMID: 31648610.

275. Storm J, Craig AG. Pathogenesis of cerebral malaria--inflammation and cytoadherence. Front Cell Infect Microbiol. 2014;4:100. Epub 20140729. doi: 10.3389/fcimb.2014.00100. PubMed PMID: 25120958; PubMed Central PMCID: PMC4114466.

276. Gallego-Delgado J, Rodriguez A. Rupture and Release: A Role for Soluble Erythrocyte Content in the Pathology of Cerebral Malaria. Trends Parasitol. 2017;33(11):832-5. Epub 20170711. doi: 10.1016/j.pt.2017.06.005. PubMed PMID: 28709836; PubMed Central PMCID: PMC5685654.

277. Hunt NH, Grau GE. Cytokines: accelerators and brakes in the pathogenesis of cerebral malaria. Trends Immunol. 2003;24(9):491-9. doi: 10.1016/s1471-4906(03)00229-1. PubMed PMID: 12967673.

278. Dobbs KR, Crabtree JN, Dent AE. Innate immunity to malaria-The role of monocytes. Immunol Rev. 2020;293(1):8-24. Epub 20191216. doi: 10.1111/imr.12830. PubMed PMID: 31840836; PubMed Central PMCID: PMC6986449.

279. Kalantari P. The Emerging Role of Pattern Recognition Receptors in the Pathogenesis of Malaria. Vaccines (Basel). 2018;6(1). Epub 20180228. doi: 10.3390/vaccines6010013. PubMed PMID: 29495555; PubMed Central PMCID: PMC5874654.

280. Schofield L, Hackett F. Signal transduction in host cells by a glycosylphosphatidylinositol toxin of malaria parasites. J Exp Med. 1993;177(1):145-53. doi: 10.1084/jem.177.1.145. PubMed PMID: 8418196; PubMed Central PMCID: PMC2190877.

281. Gowda DC. TLR-mediated cell signaling by malaria GPIs. Trends Parasitol. 2007;23(12):596-604. Epub 20071105. doi: 10.1016/j.pt.2007.09.003. PubMed PMID: 17980663.

282. Wu X, Gowda NM, Kumar S, Gowda DC. Protein-DNA complex is the exclusive malaria parasite component that activates dendritic cells and triggers innate immune responses. J Immunol. 2010;184(8):4338-48. Epub 20100315. doi: 10.4049/jimmunol.0903824. PubMed PMID: 20231693; PubMed Central PMCID: PMC2851449.

283. Miller JL, Sack BK, Baldwin M, Vaughan AM, Kappe SHI. Interferon-mediated innate immune responses against malaria parasite liver stages. Cell Rep. 2014;7(2):436-47. Epub 20140403. doi: 10.1016/j.celrep.2014.03.018. PubMed PMID: 24703850.

284. Arese P, Schwarzer E. Malarial pigment (haemozoin): a very active 'inert' substance. Ann Trop Med Parasitol. 1997;91(5):501-16. doi: 10.1080/00034989760879. PubMed PMID: 9329987.

285. Erdman LK, Cosio G, Helmers AJ, Gowda DC, Grinstein S, Kain KC. CD36 and TLR interactions in inflammation and phagocytosis: implications for malaria. J Immunol. 2009;183(10):6452-9. Epub 20091028. doi: 10.4049/jimmunol.0901374. PubMed PMID: 19864601; PubMed Central PMCID: PMC2853812.

286. Liehl P, Zuzarte-Luís V, Chan J, Zillinger T, Baptista F, Carapau D, et al. Host-cell sensors for Plasmodium activate innate immunity against liver-stage infection. Nat Med. 2014;20(1):47-53. Epub 20131222. doi: 10.1038/nm.3424. PubMed PMID: 24362933; PubMed Central PMCID: PMC4096771.

287. Hansen DS, Siomos MA, Buckingham L, Scalzo AA, Schofield L. Regulation of murine cerebral malaria pathogenesis by CD1d-restricted NKT cells and the natural killer complex. Immunity. 2003;18(3):391-402. doi: 10.1016/s1074-7613(03)00052-9. PubMed PMID: 12648456.

288. Riley EM. Is T-cell priming required for initiation of pathology in malaria infections? Immunol Today. 1999;20(5):228-33. doi: 10.1016/s0167-5699(99)01456-5. PubMed PMID: 10322302.

289. Artavanis-Tsakonas K, Riley EM. Innate immune response to malaria: rapid induction of IFN-gamma from human NK cells by live Plasmodium falciparum-infected erythrocytes. J Immunol. 2002;169(6):2956-63. doi: 10.4049/jimmunol.169.6.2956. PubMed PMID: 12218109.

290. Amani V, Vigário AM, Belnoue E, Marussig M, Fonseca L, Mazier D, et al. Involvement of IFN-gamma receptor-medicated signaling in pathology and anti-malarial immunity induced by Plasmodium berghei infection. Eur J Immunol. 2000;30(6):1646-55. doi: 10.1002/1521-4141(200006)30:6<1646::AID-IMMU1646>3.0.CO;2-0. PubMed PMID: 10898501.

291. Villegas-Mendez A, Greig R, Shaw TN, de Souza JB, Gwyer Findlay E, Stumhofer JS, et al. IFN-γ-producing CD4+ T cells promote experimental cerebral malaria by modulating CD8+ T cell accumulation within the brain. J Immunol. 2012;189(2):968-79. Epub 20120620. doi: 10.4049/jimmunol.1200688. PubMed PMID: 22723523; PubMed Central PMCID: PMC3393641.

292. Baptista FG, Pamplona A, Pena AC, Mota MM, Pied S, Vigário AM. Accumulation of Plasmodium berghei-infected red blood cells in the brain is crucial for the development of cerebral malaria in mice. Infect Immun. 2010;78(9):4033-9. Epub 20100706. doi: 10.1128/IAI.00079-10. PubMed PMID: 20605973; PubMed Central PMCID: PMC2937458.

293. Pais TF, Penha-Gonçalves C. Brain Endothelium: The "Innate Immunity Response Hypothesis" in Cerebral Malaria Pathogenesis. Front Immunol. 2018;9:3100. Epub 20190129. doi: 10.3389/fimmu.2018.03100. PubMed PMID: 30761156; PubMed Central PMCID: PMC6361776.

294. Coban C, Lee MSJ, Ishii KJ. Tissue-specific immunopathology during malaria infection. Nat Rev Immunol. 2018;18(4):266-78. Epub 20180115. doi: 10.1038/nri.2017.138. PubMed PMID: 29332936; PubMed Central PMCID: PMC7097228.

295. Jambou R, Combes V, Jambou MJ, Weksler BB, Couraud PO, Grau GE. Plasmodium falciparum adhesion on human brain microvascular endothelial cells involves transmigration-like cup formation and induces opening of intercellular junctions. PLoS Pathog. 2010;6(7):e1001021. Epub 20100729. doi: 10.1371/journal.ppat.1001021. PubMed PMID: 20686652; PubMed Central PMCID: PMC2912387.

296. Cardoso MS, Santos RF, Almeida S, Sá M, Pérez-Cabezas B, Oliveira L, et al. Physical Interactions With Bacteria and Protozoan Parasites Establish the Scavenger Receptor SSC4D as a Broad-Spectrum Pattern Recognition Receptor. Front Immunol. 2021;12:760770. Epub 20211224. doi: 10.3389/fimmu.2021.760770. PubMed PMID: 35003072; PubMed Central PMCID: PMC8739261.

297. Sarrias MR, Farnós M, Mota R, Sánchez-Barbero F, Ibáñez A, Gimferrer I, et al. CD6 binds to pathogen-associated molecular patterns and protects from LPS-induced

septic shock. Proc Natl Acad Sci U S A. 2007;104(28):11724-9. Epub 20070629. doi: 10.1073/pnas.0702815104. PubMed PMID: 17601777; PubMed Central PMCID: PMC1913855.

298. Biancone L, Bowen MA, Lim A, Aruffo A, Andres G, Stamenkovic I. Identification of a novel inducible cell-surface ligand of CD5 on activated lymphocytes. J Exp Med. 1996;184(3):811-9. doi: 10.1084/jem.184.3.811. PubMed PMID: 9064341; PubMed Central PMCID: PMC2192762.

299. Fink DR, Holm D, Schlosser A, Nielsen O, Latta M, Lozano F, et al. Elevated numbers of SCART1+ gammadelta T cells in skin inflammation and inflammatory bowel disease. Mol Immunol. 2010;47(9):1710-8. Epub 20100408. doi: 10.1016/j.molimm.2010.03.002. PubMed PMID: 20381152.

300. Mourglia-Ettlin G, Miles S, Velasco-De-Andrés M, Armiger-Borràs N, Cucher M, Dematteis S, et al. The ectodomains of the lymphocyte scavenger receptors CD5 and CD6 interact with tegumental antigens from Echinococcus granulosus sensu lato and protect mice against secondary cystic echinococcosis. PLoS Negl Trop Dis. 2018;12(11):e0006891. Epub 20181130. doi: 10.1371/journal.pntd.0006891. PubMed PMID: 30500820; PubMed Central PMCID: PMC6267981.

301. Wu Z, Golub E, Abrams WR, Malamud D. gp340 (SAG) binds to the V3 sequence of gp120 important for chemokine receptor interaction. AIDS Res Hum Retroviruses. 2004;20(6):600-7. doi: 10.1089/0889222041217400. PubMed PMID: 15242536.

302. Bárcena C, Aran G, Perea L, Sanjurjo L, Téllez É, Oncins A, et al. CD5L is a pleiotropic player in liver fibrosis controlling damage, fibrosis and immune cell content. EBioMedicine. 2019;43:513-24. Epub 20190508. doi: 10.1016/j.ebiom.2019.04.052. PubMed PMID: 31076347; PubMed Central PMCID: PMC6558273.

303. Ligtenberg AJ, Karlsson NG, Veerman EC. Deleted in malignant brain tumors-1 protein (DMBT1): a pattern recognition receptor with multiple binding sites. Int J Mol Sci. 2010;11(12):5212-33. Epub 20101217. doi: 10.3390/ijms1112521. PubMed PMID: 21614203; PubMed Central PMCID: PMC3100851.

304. Sanjurjo L, Aran G, Roher N, Valledor AF, Sarrias MR. AIM/CD5L: a key protein in the control of immune homeostasis and inflammatory disease. J Leukoc Biol. 2015;98(2):173-84. Epub 20150605. doi: 10.1189/jlb.3RU0215-074R. PubMed PMID: 26048980.

305. Kuwata K, Watanabe H, Jiang SY, Yamamoto T, Tomiyama-Miyaji C, Abo T, et al. AIM inhibits apoptosis of T cells and NKT cells in Corynebacterium-induced granuloma formation in mice. Am J Pathol. 2003;162(3):837-47. doi: 10.1016/S0002-9440(10)63880-1. PubMed PMID: 12598318; PubMed Central PMCID: PMC1868086.

306. Kurokawa J, Arai S, Nakashima K, Nagano H, Nishijima A, Miyata K, et al. Macrophage-derived AIM is endocytosed into adipocytes and decreases lipid droplets via inhibition of fatty acid synthase activity. Cell Metab. 2010;11(6):479-92. doi: 10.1016/j.cmet.2010.04.013. PubMed PMID: 20519120.

Chapter VI

Appendix

frontiers in Immunology

ORIGINAL RESEARCH
published: 24 December 2021
doi: 10.3389/fimmu.2021.760770

Physical Interactions With Bacteria and Protozoan Parasites Establish the Scavenger Receptor SSC4D as a Broad-Spectrum Pattern Recognition Receptor

Marcos S. Cardoso[1,2,3], *Rita F. Santos*[1,2,3], *Sarah Almeida*[1,2,4], *Mónica Sá*[1,2,5], *Begoña Pérez-Cabezas*[1,2], *Liliana Oliveira*[1,2], *Joana Tavares*[1,2] *and Alexandre M. Carmo*[1,2*]

[1] Instituto de Investigação e Inovação em Saúde, Universidade do Porto, Porto, Portugal, [2] IBMC–Instituto de Biologia Molecular e Celular, Porto, Portugal, [3] Programa Doutoral em Biologia Molecular e Celular (MCbiology), Instituto de Ciências Biomédicas Abel Salazar, Universidade do Porto, Porto, Portugal, [4] Departamento de Biologia, Universidade de Aveiro, Aveiro, Portugal, [5] Doutoramento em Ciências Farmacêuticas (especialidade Microbiologia), Faculdade de Farmácia, Universidade do Porto, Porto, Portugal

OPEN ACCESS

Edited by:
Chaofeng Han,
Second Military Medical University, China

Reviewed by:
Satoko Arai,
The University of Tokyo, Japan
Luisa Martinez-Pomares,
University of Nottingham, United Kingdom

***Correspondence:**
Alexandre M. Carmo
acarmo@ibmc.up.pt

Specialty section:
This article was submitted to Molecular Innate Immunity, a section of the journal Frontiers in Immunology

Received: 18 August 2021
Accepted: 29 November 2021
Published: 24 December 2021

Citation:
Cardoso MS, Santos RF, Almeida S, Sá M, Pérez-Cabezas B, Oliveira L, Tavares J and Carmo AM (2021) Physical Interactions With Bacteria and Protozoan Parasites Establish the Scavenger Receptor SSC4D as a Broad-Spectrum Pattern Recognition Receptor. Front. Immunol. 12:760770. doi: 10.3389/fimmu.2021.760770

Since the pioneering discoveries, by the Nobel laureates Jules Hoffmann and Bruce Beutler, that Toll and Toll-like receptors can sense pathogenic microorganisms and initiate, in vertebrates and invertebrates, innate immune responses against microbial infections, many other families of pattern recognition receptors (PRRs) have been described. One of such receptor clusters is composed by, if not all, at least several members of the scavenger receptor cysteine-rich (SRCR) superfamily. Many SRCR proteins are plasma membrane receptors of immune cells; however, a small subset consists of secreted receptors that are therefore in circulation. We here describe the first characterization of biological and functional roles of the circulating human protein SSC4D, one of the least scrutinized members of the family. Within leukocyte populations, SSC4D was found to be expressed by monocytes/macrophages, neutrophils, and B cells, but its production was particularly evident in epithelial cells of several organs and tissues, namely, in the kidney, thyroid, lung, placenta, intestinal tract, and liver. Similar to other SRCR proteins, SSC4D shows the capacity of physically binding to different species of bacteria, and this opsonization can increase the phagocytic capacity of monocytes. Importantly, we have uncovered the capacity of SSC4D of binding to several protozoan parasites, a singular feature seldom described for PRRs in general and here demonstrated for the first time for an SRCR family member. Overall, our study is pioneer in assigning a PRR role to SSC4D.

Keywords: scavenger receptor cysteine-rich, pattern recognition receptors, bacteria, parasites, circulating receptors

INTRODUCTION

The initial sensing of an invasive pathogen is one of the most critical events during an infection and is mediated by germline-encoded pattern recognition receptors (PRRs), which identify and bind conserved pathogen-associated molecular patterns (PAMPs) of microbes. Many different families of PRRs displaying either target-specific or broad recognition of different types of microbes have been described. Membrane-bound Toll-like receptors (TLRs) or C-type lectin receptors bind or sense microbe-exposed PAMPs and initiate signaling cascades to trigger innate immune cell activation, whereas intracellular pathogens or their by-products are recognized by intracellular PRRs such as cytoplasmic NOD-like receptors or by RIG-I-like receptors and endosomal TLRs that identify microbial genetic material (1–4).

Recent work has revealed that pattern recognition is a common feature of many scavenger receptor cysteine-rich (SRCR) proteins. The macrophage scavenger receptor type I (MSR1) and MARCO plasma membrane trimeric proteins have long been known to bind bacteria or bacterial endotoxins and to promote microbial phagocytosis (5, 6), but only more recently it was described that the cell surface receptors CD6 and CD163 of T cells and macrophages, respectively, can recognize Gram-positive and Gram-negative bacteria (7, 8). By contrast, CD5 has not been shown to bind bacteria, but its extracellular domain interacts with fungal cell wall components (9).

A small subset of SRCR consists of secreted receptors that are therefore in circulation and as such they have exceptional features to intercept, recognize, and neutralize invasive microbes and thus to contain infections. Galectin-3-binding protein (MAC2BP, LGALS3BP) is a small mosaic protein that contains, besides an SRCR domain, a BTB dimerization domain and a BACK domain (10). Although historically viewed as a malignant tumor-associated antigen, this protein has recently been identified as a possible biomarker for human sepsis (11). Better known for their infection-related immune functions, the circulating proteins CD5 antigen-like (CD5L), also known as apoptosis inhibitor expressed by macrophages (AIM) or secreted protein α (Spα) (12, 13), soluble scavenger protein with 5 SRCR domains (SSC5D) (14), and deleted in malignant brain tumors 1 (DMBT1) (15), containing respectively three, five, and 14 SRCR domains, display characteristic PRR features including a strong avidity to bind Gram-positive and Gram-negative bacteria (16–18).

Compared with the wealth of information gathered on the various roles of, for example, CD5L, spreading across a multitude of functions in numerous biological systems and phenomena (19), the attention on the very similar SSC4D protein has been almost inexistent. SSC4D is a 575-amino acid (aa)-long protein containing an N-terminal signal peptide, no transmembrane-encoding sequence, and four SRCR domains, all indicating that SSC4D is the last member of the subgroup of circulating SRCR proteins (20). In fact, SSC4D can be found in human blood plasma, albeit at a very low concentration (1 ng/ml) (21, 22). Although no extensive protein characterization, tissue distribution, or functional studies have been performed, northern blotting analyses imply that SSC4D is well expressed in the human kidney and placenta and moderately expressed in the liver, small intestine, spleen, and thymus (20).

Here, we describe the first comprehensive data on the roles and distribution of the SSC4D glycoprotein in a mammalian organism and how the evidence obtained clearly indicates that SSC4D functionally belongs to the PRR arm within the SRCR family.

MATERIALS AND METHODS

Recombinant Scavenger Receptor Cysteine-Rich Proteins

Recombinant soluble proteins were produced in human embryonic kidney 293T cells and supplied in lyophilized form by INVIGATE GmbH. Specifically, recombinant forms of human CD5L and of the extracellular domain of human CD6 were produced from templates already described (17, 23) and modified to obtain chimeric proteins containing a signal peptide, the specific CD5L (Ser^{20} to Gly^{347}) or CD6 (Asp^{25} to Glu^{398}) sequences, HA and BirA recognition sequences, and 8—12-His tag sequences. Recombinant human SSC4D (UniProtKB accession no. Q8WTU2) was produced in a similar manner to include the specific protein sequence spanning domains 1–4 (Leu^{48}-Ser^{575}) of SSC4D. Recombinant human SSC4D-d1d2 (spanning SRCR domains 1 and 2) and SSC4D-d3d4 (domains 3 and 4) were produced to result in the SSC4D sequences Leu^{48}-Gly^{318} and Ser^{324}-Ser^{575} being fused to 8·His tag sequences.

For the expression in Caco-2 cells of full-length SSC4D fused to citrine and containing an HA tag, cDNA was amplified by PCR from Hep G2 cells using forward (5′-TAGACGCGTATGCA CAAGGAAGCAGAGA-3′) and reverse (5′-CTAGGATCCC GAGCGTAGTCTGGGACGTCGTATGGGTATGAAGGCT GGCACAGGACACT-3′) primers. The resulting PCR product was cloned into the lentiviral expression vector pHR-mCitrine, using *Mlu*I and *Bam*HI restriction sites, to be under the control of the spleen focus-forming virus (SFFV) promoter and transduced into Caco-2 cells.

Analysis of SSC4D Protein Expression

Cell lysates were prepared using radioimmunoprecipitation assay (RIPA) lysis buffer containing a mixture of protease and phosphatase inhibitors (Sigma-Aldrich). Protein concentration was measured by Bradford assay (Bio-Rad), and 60 μg of each sample were denatured in Laemmli's sample buffer at 95°C for 10 min. Cell lysates and supernatants were separated by sodium dodecyl sulfate polyacrylamide gel electrophoresis (SDS-PAGE) and transferred to nitrocellulose membranes using Trans-Blot Turbo Transfer System (Bio-Rad). Membranes were blocked with 5% non-fat dried milk in Tris-buffered saline, 0.1% Tween 20 (TBS-T) for 1 h and probed with rabbit anti-SSC4D polyclonal antibody (raised against polypeptides corresponding to sequences R346-C364 and E470-R485 of mouse SSC4D; BIOTEM), followed by a goat anti-rabbit horseradish peroxidase (HRP) secondary antibody

(Sigma-Aldrich). Immunoblots were developed using enhanced chemiluminescence (ECL) detection reagent (GE Healthcare Life Sciences), and luminescence signals were detected using the Fujifilm FPM-100A film processor (Fujifilm).

To determine the molecular mass of the recombinant proteins, 5 μg of recombinant SSC4D, SSC4D-d1d2, and SSC4D-d3d4 were run on SDS-PAGE, and proteins were detected by Coomassie blue staining; also, 0.5 μg of each recombinant protein were detected by western blotting.

Cells and Cell Lines

Human peripheral blood mononuclear cells (PBMCs) were obtained from buffy coats of healthy adult volunteers at Banco de Sangue, Hospital São João, Porto, and were separated by Lymphoprep density gradient (STEMCELL Technologies). $CD14^+$ monocytes were then isolated by positive magnetic cell sorting using CD14 microbeads (Miltenyi Biotec).

Differentiation of *ex vivo* monocytes into macrophages was achieved using 30 ng/ml of macrophage colony-stimulating factor (M-CSF) for 6 days in culture. Macrophages were then polarized toward an M1-like phenotype with 100 ng/ml lipopolysaccharide (LPS; *Escherichia coli* O111:B4; Sigma) and 25 ng/ml interferon (IFN)-γ (PeproTech), an M2a-like phenotype using 20 ng/ml interleukin (IL)-4 (PeproTech), or an M2c-like phenotype using 25 ng/ml IL-10 (PeproTech), all for 24 h. Polarization of undifferentiated monocytes was done similarly but for 72 h. Cell surface labeling using CD80 APC (2D10), CD206 PE (15.2), and CD163 BV421 (6H1/61) mAbs (all from BioLegend) confirmed the polarization of monocytes and macrophages into the correct subtype. Treatments with CD5L (1 μg/ml) or SSC4D (1 μg/ml) were assayed to check whether either of these stimuli would polarize cells toward any given subtype. Data were acquired in FACSCanto II (BD Biosciences). Post-acquisition analysis was performed using FlowJo software v10 (Tree Star).

Cell lines used in this study were Hep G2 (24), K562 (25), Caco-2 (26), E6.1 (27), JEG-3 (28), HEK 293T (29), TCCSUP (30), Raji (31), HL-60 (32), THP-1 (33), and HeLa (34). All lines were maintained at 37°C in a 5% CO_2 humidified incubator in RPMI 1640 supplemented with 10% fetal calf serum (FCS), 1 mM sodium pyruvate, 2 mM L-glutamine, 50 U/ml penicillin G, and 50 μg/ml streptomycin, except HEK 293T, HeLa, Hep G2, and Caco-2 that were grown in Dulbecco's modified Eagle's medium (DMEM)/high-glucose medium containing 10% FCS, 1 mM sodium pyruvate, 4 mM L-glutamine, 50 U/ml penicillin, and 50 μg/ml streptomycin.

Flow Cytometry and Cell Sorting

Blood from buffy coats was added to red blood cell (RBC) lysis buffer (BioLegend), and after washing, 1×10^6 leukocytes were incubated with FcR blocking (Miltenyi Biotec) for 10 min at 4°C. Cells were stained with mAbs CD14 Pacific Blue (63D3), CD177 APC/Cy7 (MEM-166), CD19 PE/Cy7 (HIB19), CD4 Alexa Fluor 488 (OKT4), and CD8 APC (HIT8a) (all from BioLegend), fixed, and permeabilized with the eBioscience fixation/permeabilization kit (Thermo Fisher Scientific).

Intracellular staining was performed with rabbit anti-SSC4D polyclonal antibody, followed by anti-rabbit PE labeling (Life Technologies). Data were acquired in the FACSCanto II and post-acquisition analysis performed using FlowJo v10.

For cell sorting, blood from buffy coats was added to RBC lysis buffer, and 1×10^7 leukocytes were stained with mAbs CD14 APC (63D3), CD177 APC/Cy7 (MEM-166), CD19 PE/Cy7 (HIB19), and CD3 PerCP/Cy5 (OKT3). The labeled cells were sorted with FACSAria (BD Biosciences).

Immunostaining

SSC4D protein expression was detected in sections of human tissues kindly provided by the Unidade Local de Saúde de Matosinhos–Hospital Pedro Hispano. All ethical and legal issues were secured, along with the guarantee of confidentiality/no disclosure or violation of personal information or other data of the patients.

Four-micrometer sections of paraffin-embedded human blocks were deparaffinized and hydrated. Antigen retrieval was performed in 10 mM sodium citrate buffer for 30 min in a 96°C water bath.

Immunohistochemistry (IHC) was performed using UltraVision Quanto Detection System HRP DAB (Thermo Scientific). Endogenous peroxidase activity and nonspecific background staining were blocked using Hydrogen Peroxidase Block and Ultra V Block reagents, respectively. Tissues were immunostained with mouse anti-human SSC4D mAb 46-M or with a negative control normal mouse IgG sc-2025 (Santa Cruz Biotechnology) at 4°C overnight (ON), incubated with the primary antibody amplifier for 10 min followed by incubation with HRP Polymer Quanto and developed with 3, 3'-diaminobenzidine (DAB). The slides were counterstained with hematoxylin and visualized under light microscopy.

Colon, stomach, and liver sections were analyzed by immunofluorescence (IF). Non-specific staining was blocked with PBS containing 1% bovine serum albumin (BSA) for 1 h at room temperature (RT). Slides were then immunostained at 4°C ON with rabbit anti-SSC4D polyclonal followed by incubation with goat anti-rabbit Alexa Fluor 488-conjugated antibody (Life Technologies) for 1 h at RT. Nuclei were stained with "4′,6-diamidino-2-phenylindole (DAPI)" (Invitrogen), and cell preparations were mounted with Vectashield mounting media (Vector Laboratories). The slides were analyzed using confocal microcopy (Leica TCS SP5).

Fluorescence-activated cell sorting (FACS)-separated blood cells were adhered to poly-L-lysine (Sigma-Aldrich)-treated coverslips followed by blocking of non-specific staining with PBS containing 1% BSA for 1 h at RT. SSC4D was then detected with rabbit anti-SSC4D antibody ON at 4°C followed by incubation with goat anti-rabbit Alexa Fluor 488- conjugated antibody for 1 h at RT. Nuclei were stained with DAPI, and cell preparations were mounted with Vectashield. The slides were analyzed using confocal microcopy.

Bacteria and Parasites

E. coli strains [BL21(DE3), IHE3034, RS218, and CFT073] were kindly provided by Claire Poyart (Institut Cochin, Paris), *Listeria*

monocytogenes strain EGD-e and *Salmonella enterica* serovar typhimurium were provided by Didier Cabanes (i3S, Porto), and *Streptococcus agalactiae* [group B streptococcus (GBS)] strain BM110 was provided by Patrick Trieu-Cuot (Institut Pasteur, Paris). *Klebsiella pneumoniae*, *Enterococcus faecalis*, and *Pseudomonas aeruginosa* were also used in this study. Bacteria were grown to mid-logarithmic phase (OD_{600} of 0.45) in brain heart infusion medium at 37°C. *Mycobacterium avium* strain 2447 was prepared as described previously (35).

Parasites were prepared as previously described: *Neospora caninum* tachyzoites (Nc-1, ATCC 50843) (36), *Plasmodium berghei* ANKA strain blood merozoites (clone 676cl1) (37), *Trypanosoma brucei brucei* Lister 427 bloodstream forms (38), *Leishmania major* strain LV39, and *Leishmania tarentolae* strain Parrot-TarII promastigotes (39). A green fluorescent protein (GFP)-expressing *T. brucei brucei* Lister 427 line was engineered by cloning an enhanced *gfp* into a modified pHD1034 vector where the puromycin resistance cassette was replaced by the hygromycin resistance from the pHD1145 vector. Transfected parasites were selected with 5 μg/ml hygromycin (38).

Scavenger Receptor Cysteine-Rich Protein–Microbial Cell Binding Assays

Binding of SRCR proteins to microbial cells was performed as described previously (17) using 2 μg of each protein interacting with 1×10^8 live bacteria or 1×10^7 live parasites in binding medium (TBS with 1% BSA, 5 mM Ca^{2+}) for 1 h in an orbital shaker at 4°C. Microbe-bound proteins were detected using mouse anti-Tetra HIS mAb (Qiagen) followed by incubation of anti-mouse HRP-conjugated antibody (BioLegend) for 1 h at RT. Immunoblots were developed using ECL. Sample loading was evaluated with a rabbit anti-*Leishmania infantum* cysteine synthase (at 1:2,000 dilution) for *Leishmania* parasites and a rabbit anti-*T. brucei* aldolase (1:5,000) for *T. brucei*.

For the visualization of SSC4D binding to *T. brucei* bloodstream forms by IF, a GFP-expressing *T. brucei* Lister 427 line was incubated with 2 μg of HA-tagged SSC4D-FL in the binding medium. The cell pellet was transferred onto poly-L-lysine-treated coverslips and fixed with PFA 4% for 15 min at RT, and the presence of SSC4D was detected using anti-HA mAb 16B12 (BioLegend) followed by incubation with anti-mouse Alexa Fluor 568-conjugated antibody (Invitrogen). Nuclei were stained with DAPI, and the preparations were mounted with Vectashield. The slides were analyzed using confocal microcopy.

Scavenger Receptor Cysteine-Rich Protein–Endotoxin Binding Assays

High-binding 96-well microtiter plates were coated ON with 10 μg/ml of purified LPS (*E. coli* O111:B4; Sigma) or 10 μg/ml lipoteichoic acid (LTA; Staphylococcus aureus; Sigma) in PBS at 4°C. The plates were blocked with PBS, 1% BSA, for 1 h at RT. Serial 2-fold dilutions of HIS-tagged SRCR proteins were added to the plates and incubated for 2 h at RT. Bound proteins were detected using mouse anti-HIS mAb for 1 h at RT, followed by goat anti-mouse HRP-conjugated antibody for 1 h at RT. Reactions were developed using SIGMAFAST o-Phenylenediamine dihydrochloride (OPD) for 30 min at RT and stopped with 1 M H_2SO_4. Absorbance was read at 490 nm using Synergy 2 (BioTek).

To calculate the calibration of the LPS- and LTA-binding assays, samples of serially diluted HIS-tagged SRCR proteins were directly coated on 96-well microtiter plates ON in PBS at 4°C. Plates were blocked with blocking solution for 1 h at RT, followed by detection of bound protein, as described above.

In between each step, plates were washed four times with PBS, 0.1% Tween-20.

Scavenger Receptor Cysteine-Rich Protein–Eukaryotic Cell Binding Assays

To detect binding of SSC4D to putative ligands in eukaryotic plasma membranes, 2×10^5 primary monocytes or Caco-2, Hep G2, Raji, K562, HL-60, THP-1, HeLa, or E6.1 cells were incubated with 3 μg of recombinant soluble extracellular CD6 (sCD6) or SSC4D-FL, or left untreated, in binding medium for 1 h at 4°C. Cells were then washed twice and incubated with fixable viability dye (Invitrogen) to exclude dead cells. The presence of SRCR proteins was detected with anti-HIS primary antibody followed by incubation with anti-mouse Alexa Fluor 647-conjugated antibody (Invitrogen) at 4°C. Data were acquired in FACSCanto II, and post-acquisition analysis was performed using FlowJo v10.

Phagocytosis Assays

Monocytes were plated at a density of 2×10^5 cells/well using imaging media (RPMI without phenol red, 10% FBS, 50 U/ml penicillin, and 50 μg/ml streptomycin) in 96-well plates (CellCarrier Ultra, PerkinElmer). After ON incubation, imaging media were removed without disturbing the monolayer and replaced with new media containing Hoechst for 45 min at 37°C. Then, 40 μg/ml of Invitrogen™ pHrodo™ Red *E. coli* BioParticles™ (Fisher Scientific) were added to the cells alone or with 5 μg/ml of recombinant SSC4D or CD5L. Immediately after, the 96-well plates were inserted in the IN Cell Analyzer (GE Healthcare Life Sciences), previously heated for 37°C, and nine images per well were collected 45 and 120 min after the addition of the BioParticles. Images were analyzed using FIJI software, and the percentage of cells containing *E. coli* BioParticles was determined.

SSC4D Secretion Upon Infection of Caco-2 Cells

Caco-2 cells expressing an SSC4D-citrine-HA fusion protein were plated at a density of 3.5×10^5 cells/well in 12-well plates. After cell attachment, cultures were infected for 1 h with live *E. coli* RS218 or *L. monocytogenes* EGD-e with a multiplicity of infection (MOI) of 1:50 or left uninfected. Cells were then washed with PBS and supplied with new media containing 20 μg/ml gentamicin. Supernatants were collected 2, 8, and 24 h after infection and resuspended in Laemmli's sample buffer for SDS-PAGE and western blotting. SSC4D from supernatants was detected using mouse anti-HA mAb followed by anti-mouse HRP-conjugated antibody and ECL detection.

RESULTS

Human SSC4D Protein Structure and Expression

SSC4D belongs to the group B of SRCR domain-containing proteins characterized by having an extraordinary sequence similarity between all individual domains and a nearly perfect conservation of key residues, namely, eight regularly spaced cysteine residues that establish intra-domain disulfide bonds in very defined combinations, also sequences that are 100% conserved in all known domains, especially in the β1 and β2 strands and in the boundaries between the α1 helix and the β4 strand (14) (**Figure 1A**). One other characteristic feature of this family of extracellular proteins consists of its extended level of glycosylation, as assessed by the high number of putative *O*-GalNAc glycosylation sites, characteristic of mucins. In particular, the four SRCR domains of SSC4D are interspaced with sequences rich in *O*-linked sugars, as predicted by NetOGlyc 4.0 (41) (**Figure 1B**). However, a certain separation can be established between the SRCR group B members that are secreted from those that are membrane bound, such as CD5, CD6, CD163, and CD163 antigen-like 1 (M160), in that in this latter set, *N*-linked glycosylation seems to be more prevalent, despite that the whole level of sequence similarity between the different proteins would not predict that sort of cleavage (14, 42). In fact, neither SSC4D nor CD5L, which are here investigated, contain any *N*-linked sugars as predicted by NetNGlyc 1.0 (43), contrasting with the extracellular domain of CD6 that contains seven such modifications.

We assessed the expression of SSC4D in lysates of several human cell lines and detected by western blotting the expression of the SSC4D protein in Hep G2, Caco-2, K562, and HeLa cells, and the molecular mass of intracellular SSC4D was calculated to be 70.8 kDa (**Figure 1C**). Few smaller bands of lower intensity could be observed in the blots, and these could hypothetically represent alternative splicing-dependent isoforms. Indeed, a common property of most SRCR members is the generation of alternative splicing-dependent isoforms, many of them resulting in the absence of individual or multiple SRCR domains, as described for DMTB1, CD6, CD163, and M160 (44–46). Padilla et al. (20) had in fact detected by northern blotting different transcripts that could account for alternative SSC4D isoforms, and one *SSC4D* mRNA isoform described in a transcriptome-wide study does miss the sequences encoding domains 3 and 4 (44). However, it is unlikely that the smaller bands in the gel correspond to this isoform because the detecting antibody was raised against sequences within domains 3 and 4 of the protein; rather, they either are unspecific blot bands or may represent degradation products.

Nevertheless, for the purpose of this study, we generated and expressed recombinant human full-length SSC4D and two recombinant hemi-SSC4D forms, each corresponding to one-half of the molecule and consisting of either the SRCR domains 1 and 2 (SSC4D-d1d2) or 3 and 4 (SSC4D-d3d4) (**Figure 1B**). The recombinant proteins were run on SDS and stained with Coomassie blue (**Figure 1D**) and detected by western blotting using an anti-SSC4D-d3d4 polyclonal antibody (**Figure 1E**). The molecular mass of the mature full-length extracellular protein was measured at 90.6 kDa, suggesting that the secreted protein undergoes posttranslational modifications, possibly *O*-linked glycosylation.

SSC4D Expression in Human Epithelia and Leukocytes

Based on the reported tissue distribution of the mRNA coding for human SSC4D (20), we screened by PCR different human cell lines for the presence of *SSC4D* mRNA. We found that *SSC4D* is mostly expressed in cell lines with epithelial morphology like Hep G2 (hepatocellular carcinoma), Caco-2 (colorectal adenocarcinoma), JEG-3 (placental choriocarcinoma), HEK 293T (adenovirus 5 DNA-transfected embryonic adrenal precursor cells), and HeLa (cervical adenocarcinoma), but not in TCCSUP (urinary bladder carcinoma) (**Supplementary Figure S1**). Also, *SSC4D* mRNA was detected in hematopoietic-derived cells such as K562 (myelogenous leukemia) and very faintly in E6.1 (acute T-cell leukemia), but not in Raji (Burkitt's lymphoma).

We then assessed the expression of the protein in human organs. Relevant expression was observed in the gastrointestinal tract, with SSC4D being detected in intestinal crypts, namely, in mucous goblet cells in the colon, while in the stomach, staining was visualized in the simple columnar epithelium of the gastric mucosa and showing a broad distribution in gastric glands, compatible with SSC4D being expressed by surface mucous cells, mucous neck cells, and chief cells (**Figure 2A**). SSC4D was also expressed in the parenchyma of hepatic lobules in hepatocytes.

Regarding the genitourinary tract, strong SSC4D expression was detected in the epithelial cells of the tubules (**Figure 2B**). SSC4D was also found in follicular and parafollicular cells of the thyroid and in pneumocytes of the alveolar ducts. Interestingly, strong and specific expression of SSC4D was found in chorionic villi in placenta, mostly in the outer layer corresponding to the syncytiotrophoblasts.

We additionally assessed the expression of SSC4D in leukocyte subpopulations by flow cytometry and IF of FACS-sorted cells and detected the presence of intracellular SSC4D in monocytes, neutrophils, and B cells, but not in $CD4^+$ or $CD8^+$ T lymphocytes (**Figure 3**). Being a secreted protein, we questioned whether SSC4D could bind and exert any effect in target cells. For that purpose, we tested the binding of recombinant SSC4D to a panel of cell lines; however, none of the cells used were bound by SSC4D, whereas recombinant soluble extracellular CD6 (sCD6), used as a positive control, displayed the characteristic pattern of binding to cells that express its ligand, CD166 (47) (**Supplementary Figure S2**). This raises the possibility that SSC4D does not have a binding receptor at the surface of human cells or that a hypothetical receptor is not widespread.

SSC4D Physically Binds to Gram-Positive and Gram-Negative Bacteria

The SSC4D-related proteins CD5L and SSC5D are able to identify a large spectrum of bacterial species and strains

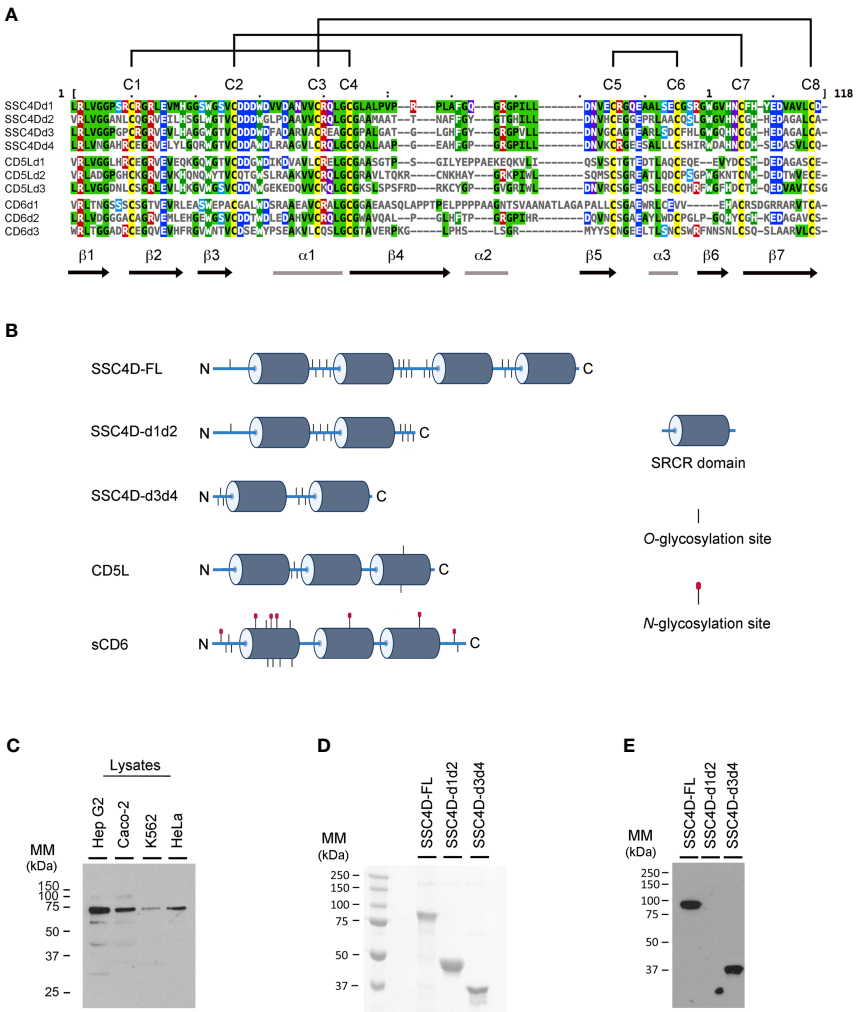

FIGURE 1 | Amino acid sequence and structure of group B scavenger receptor cysteine-rich (SRCR) domains of SSC4D, CD5L, and CD6. **(A)** SRCR domains are typically ~100–110 amino acids in length compacted into a heart-shaped fold, where a six/seven-stranded β sheet cradles a core α1-helix. Each line represents one SRCR domain of the indicated protein. Amino acid sequences were aligned using Clustal Omega and MView (40). Amino acid side chain color codes for conserved residues: Green/black, aliphatic; Green/white, aromatic; Blue, anionic; Red, cationic; Cyan, polar; Magenta, amide; Yellow, sulfur-containing. Intrachain disulfide bonds established between conserved cysteine residues are shown on the top by connecting lines. **(B)** Schematic representation of the protein structures of SSC4D-FL, SSC4D-d1d2, SSC4D-d3d4, CD5L, and extracellular domain of CD6 (sCD6). SRCR domains are represented as dark cylinders. Putative *O*-linked glycosylation sites are represented as short vertical lines and *N*-linked glycosylation sites as lines topped with red circles. N and C termini of the proteins are indicated by "N" and "C," respectively. Design was created using BioRender.com. **(C)** SSC4D protein expression detected by western blotting from cell lysates of Hep G2, Caco-2, K562, and HeLa cells. The molecular mass of intracellular SSC4D was calculated as 70.8 kDa. **(D)** Recombinant SSC4D, SSC4D-d1d2, and SSC4D-d3d4 were run on sodium dodecyl sulfate polyacrylamide gel electrophoresis (SDS-PAGE), and gels were stained with Coomassie blue. The size of recombinant extracellular full-length SSC4D was measured as 90.6 kDa, SSC4D-d1d2 as 45 kDa, and SSC4D-d3d4 as 36 kDa. **(E)** Recombinant SSC4D, SSC4D-d1d2, and SSC4D-d3d4 were run on SDS-PAGE, transferred to nitrocellulose membranes, and detected by immunoblotting. SSC4D and SSC4D-d3d4 were confirmed at the correct sizes, while SSC4D-d1d2 is not detected given that the polyclonal antibodies recognize sequences within domains 3 and 4.

(16, 17); moreover, the ectodomain of CD6 was reported to bind and induce the aggregation of bacteria through the recognition of the bacterial endotoxins LTA and LPS (8). We investigated whether SSC4D could also detect different bacterial species and how the strength of interactions would compare with those of other SRCR family members.

Recombinant SSC4D, CD5L, and sCD6 were incubated with samples of live *E. coli* strains BL21(DE3), IHE3034, and RS218, with *L. monocytogenes* EGD-e, and with GBS BM110, followed by centrifugation and immunoblotting of the pelleted bacteria. As anticipated, we observed a strong interaction between CD5L and all tested bacteria, particularly in the presence of calcium given that many SRCR protein-mediated interactions are Ca^{2+}-dependent (**Figure 4A**). By contrast, the interactions between sCD6 and the different bacteria were not visually detectable. Importantly, SSC4D clearly bound all bacteria tested, demonstrating its ability to physically interact with conserved structures present at the surface of these microorganisms.

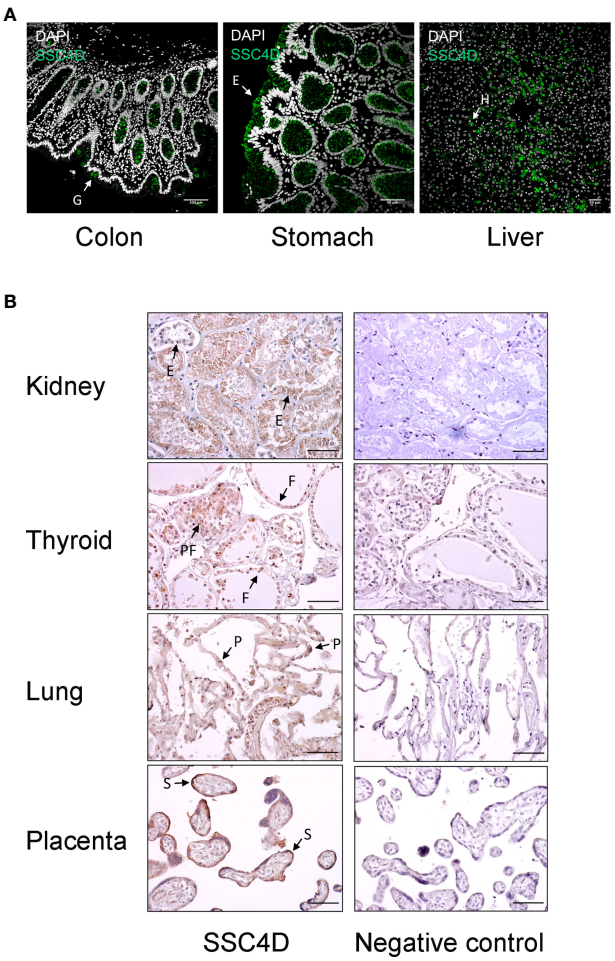

FIGURE 2 | SSC4D distribution in human organs. **(A)** Detection of SSC4D by immunofluorescence (IF) in sections of the colon, stomach, and liver from normal human subjects. SSC4D labeling in mucous goblet cells (G) in the colon, simple columnar epithelium cells (E) in the stomach, and hepatocytes (H) in hepatic lobules is shown by arrows. Cell nuclei were stained with 4′,6-diamidino-2-phenylindole (DAPI; white). No unspecific staining was seen following incubation with secondary antibody alone, confirming specificity of the primary antibody. Scale bar, 50 μm. **(B)** Immunohistochemical analysis of SSC4D expression in sections of the kidney, thyroid, lung, and placenta. On the left column, SSC4D labeling was visualized by horseradish peroxidase (HRP) and substrate chromogen 3, 3'-diaminobenzidine (DAB). Positive staining of tubular epithelial cells (E) in the kidney, follicular (F) and parafollicular cells (PF) in the thyroid, pneumocytes (P) of the alveolar ducts, and of syncytiotrophoblasts (S) in the placenta is indicated by arrows. On the right column, images of sections labeled with unspecific mouse IgG mAb (negative control, sc-2025). Scale bar, 50 μm. Immunohistochemistry (IHC) and IF experiments were performed multiple times using samples from at least three different individuals.

Consequently, we included in our bacteria binding assays the two recombinant hemi-SSC4D forms, SRCR-d1d2 and SRCR-d3d4. Performing the assays using the same bacterial samples, we observed in several cases that the two halves of the molecule had differential binding profiles, such that SSC4D-d3d4 bound well to *Listeria* and GBS, whereas binding of SSC4D-d1d2 to these bacteria was much less evident (**Figure 4A**, lower panels). Conversely, although not as clear as the above, it seemed that the *E. coli* strains, with the exception of *E. coli* CFT073, were better recognized by SSC4D-d1d2.

We hypothesized that each half of SSC4D might bind preferentially to different groups of bacteria and therefore increased the sampling of our assays by adding supplementary bacterial species. In each assay, recombinant SSC4D-d1d2 or SSC4D-d3d4 was incubated with live Gram-negative *S. enterica*, *K. pneumoniae*, and *P. aeruginosa* and with Gram-positive *E. faecalis* or *M. avium* (**Figure 4B**). Although there was not an absolute compartmentalization in the recognition profiles, in general, it appears that SSC4D-d1d2 displays a preference for binding Gram-negative bacteria. Although the converse correlation cannot be fully established for SSC4D-d3d4, as this half of the molecule is more homogeneous in the identification of both bacterial groups, it appears that SSC4D-d3d4 binds better to Gram-positive bacteria than does SSC4D-d1d2 (**Figure 4B**).

We thus evaluated whether each typical endotoxin of Gram-negative and Gram-positive bacteria would be a preferential target of one-half of the SSC4D molecule over the other using an ELISA to measure the affinity of each protein to LPS and LTA. We first assessed the sensitivity of the detecting antibody to plate-bound purified SRCR proteins (**Supplementary Figure S3A**), following which we measured the binding of serially diluted HIS-tagged SRCR

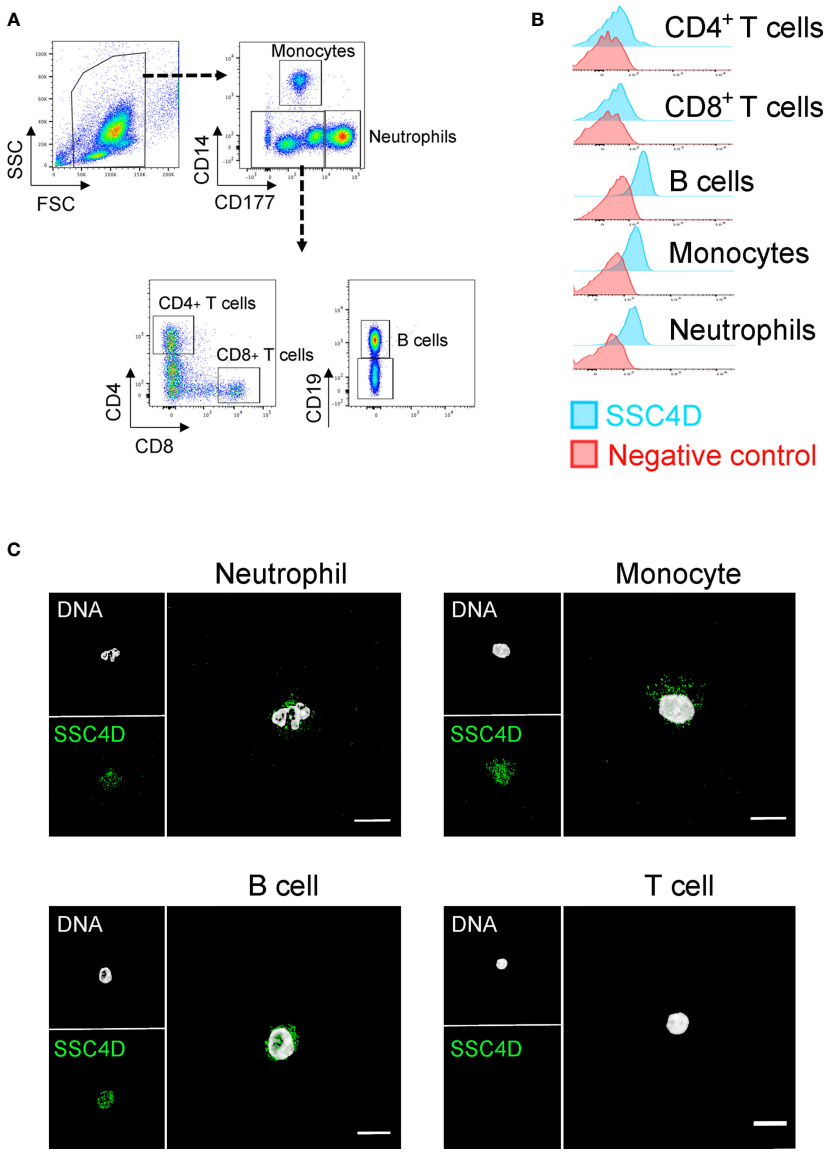

FIGURE 3 | SSC4D expression in human leukocytes. **(A)** Flow cytometry gating strategy for the identification of monocytes, neutrophils, B cells, and CD4$^+$ and CD8$^+$ T cells from human blood. **(B)** Intracellular labeling of SSC4D in different human cell populations, visualized by flow cytometry. In the control samples, the anti-SSC4D antibody was omitted. Representative results shown are from one of four independent experiments. **(C)** Representative single-cell images of FACS-sorted leukocytes, immunostained for SSC4D (green) and visualized by immunofluorescence (IF). White indicates DAPI staining. Representative results shown are from one of three independent experiments using different donors.

proteins to microtiter plates coated with 10 µg/ml of purified LTA or LPS (**Supplementary Figure S3B**). The conversion of the obtained values to binding detection units showed that both SSC4D hemi-forms bound to LPS and LTA in a dose-dependent manner, but whereas in fact LPS was superiorly targeted by SSC4D-d1d2 than by SSC4D-d3d4 at higher protein concentrations, the plots for binding to LTA were indistinguishable between the two subunits (**Figure 4C**).

Comparing the binding forces to LPS and LTA between CD5L, SSC4D, and sCD6, again binding of the proteins to the endotoxins is differentiated: SSC4D binds to LPS with higher avidity than CD5L, whereas binding to LTA is not significantly different between these two proteins (**Figure 4D**). In accordance with the previous experiments and our earlier work (17), binding of sCD6 to either live or fixed bacteria, or to bacterial endotoxins, although detectable, is inferior when compared with the microbe-binding capacity of the natural circulating SRCR proteins.

SSC4D Promotes Phagocytosis but Does Not Induce Macrophage Polarization

Because SSC4D is produced by phagocytes and binds to bacteria, we questioned whether this circulating molecule could have a

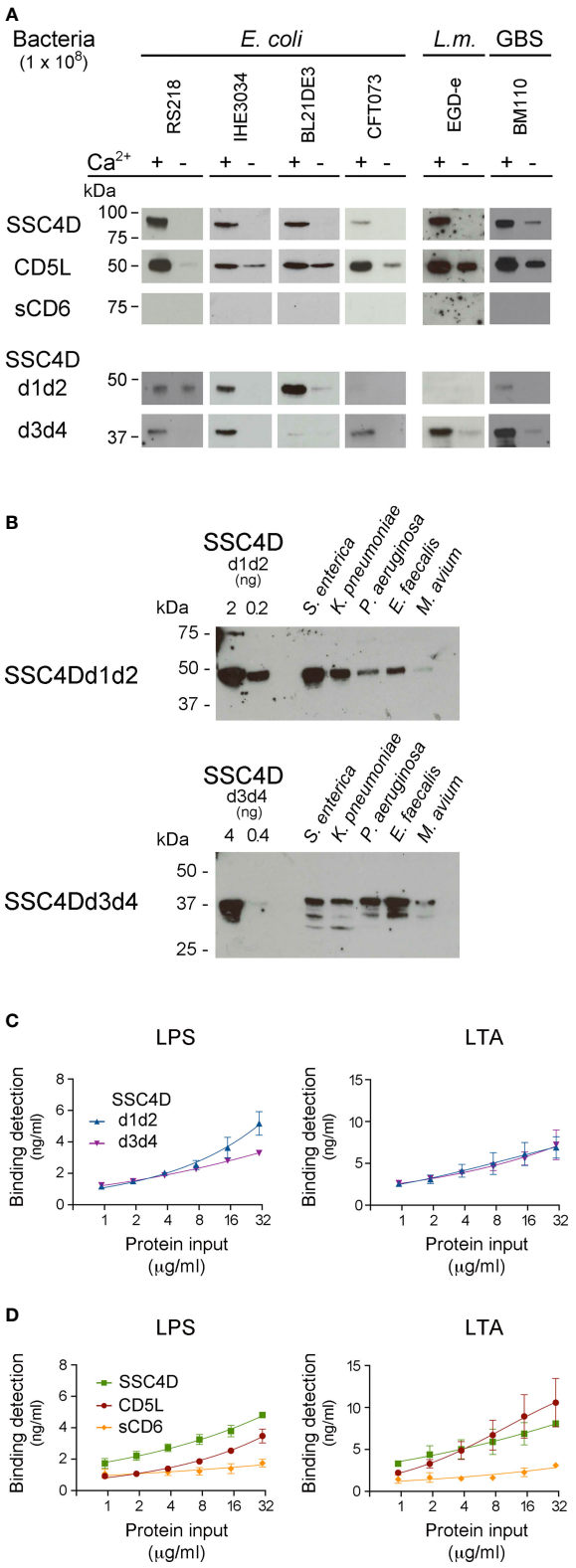

FIGURE 4 | Continued

FIGURE 4 | SSC4D physically binds to bacteria and bacterial endotoxins. **(A)** Two micrograms of each recombinant protein SSC4D, CD5L, sCD6, SSC4D-d1d2, and SSC4D-d3d4 were incubated with suspensions of 1×10^8 CFU of live *Escherichia coli* strains BL21(DE3), RS218, IHE3034, or CFT073, *Listeria monocytogenes* strain EGD-e, or GBS strain BM110 in the presence or absence of Ca^{2+}. Cell-bound proteins were detected by immunoblotting using anti-HIS mAb. Blots are representative of at least three independent experiments. **(B)** Recombinant SSC4D-d1d2 and SSC4D-d3d4 (2 μg each sample) were incubated with suspensions of 1×10^8 CFU of live *Salmonella enterica*, *Klebsiella pneumoniae*, *Enterococcus faecalis*, *Pseudomonas aeruginosa*, or *Mycobacterium avium* in the presence of Ca^{2+}. Bacteria-bound proteins were detected by immunoblotting using an anti-HIS mAb. The sensitivity of detection of this mAb for each of the recombinant hemi-forms of SSC4D can be evaluated by the detection, shown on the left side of the membranes, of 2 and 0.2 ng of purified SSC4D-d1d2 (upper blot) or 4 and 0.4 ng of purified SSC4D-d3d4 (lower blot). **(C)** Binding of SSC4D-d1d2 and SSC4D-d3d4 to plate-bound lipopolysaccharide (LPS) and lipoteichoic acid (LTA). Proteins were added at the indicated concentrations, and signals were detected by anti-HIS mAb followed by horseradish peroxidase (HRP)-conjugated antibody and o-Phenylenediamine dihydrochloride (OPD) substrate. Absorbance was read at 490 nm. Binding values shown were interpolated from standard curves of detection of plate-bound SSC4D-d1d2 and SSC4D-d3d4, shown in **Supplementary Figure S3**. Graphs show the mean ± SD of two independent experiments performed in duplicate. **(D)** Binding of SSC4D, CD5L, and sCD6 to plate-bound purified LPS and LTA. Detection and measurement of binding were as in panel **(C)**.

direct impact on pathogen clearance. To measure protein-mediated phagocytosis, monocytes were incubated with pHrodo™ Red *E. coli* BioParticles™ in the presence of CD5L or SSC4D or in the absence of the recombinant proteins. These BioParticles become fluorescent in acidic pH, only identifying those bacteria that are inside phagosomes (48). Monocyte phagocytosis of the *E. coli* particles increased over time but was not different whether CD5L was present or not (**Figures 5A, B**). By contrast, the presence of SSC4D induced a significant increase in the phagocytic capacity. To test whether SSC4D could mediate the internalization of the bacteria through an interaction to a putative cellular receptor in the phagocyte, we checked for a direct interaction between recombinant SSC4D and monocytes. However, as can be seen in **Figure 5C**, no such interaction is obvious, whereas sCD6, used as a binding control, is able to interact slightly with monocytes, given that these cells express low levels of CD166. An alternative explanation is that the increase in phagocytosis could be due to increased activation of monocytes induced by SSC4D. Although conceivable, this possibility is unlikely, given that SSC4D was added to the cells at the same time as the *E. coli* particles and the duration of the experiment was perhaps too short to allow for a vigorous monocyte activation-mediated phagocytosis.

Also displaying opposite effects from CD5L, SSC4D did not induce the polarization of macrophages toward an M2 phenotype (**Figure 5D**). Differentiation of *ex vivo* monocytes with CD5L for 3 days had an equivalent result as utilizing IL-4 in the development of an M2a-like phenotype, as previously reported (49). However, in no other differentiation and polarization protocol did SSC4D, nor CD5L, induce monocyte/macrophage polarization, including no effect on an M1-type phenotype.

SSC4D is normally detected in cell culture media at very low levels, so we questioned whether SSC4D secretion could escalate due to any type of immune response and what would be the external cues that could stimulate this secretion. Caco-2 cells that were engineered to produce a chimeric protein consisting of SSC4D fused to mCitrine and an HA-tag sequence (**Supplementary Figure S4A**) were incubated with live *E. coli* RS218 or *L. monocytogenes* EGD-e at a 1:50 MOI or left uninfected. Culture supernatants were collected at different time points, and the presence of SSC4D was assessed by western blotting. As seen in **Figure 5E**, secreted SSC4D was detected at 24 h post infection, but there were no differences between infected (with *E. coli* or *L. monocytogenes*) and non-infected cultures. It is possible that in this specific case, the detection of SSC4D in the media could result from cell death instead of induced, or passive, secretion; nonetheless, in all other tested conditions using different immune-inflammatory mediators or bacterial endotoxins to stimulate SSC4D secretion, there was no single specific stimulus that would further augment the rate of secretion (**Supplementary Figures S4B, C**). Instead, SSC4D was being continuously released into the medium at moderate levels, independently of any tested external cues.

SSC4D Physically Binds to Protozoan Parasites

PRRs are able to recognize not only bacterial but also fungal, viral, or protozoan conserved structural components. In order to test whether the binding properties of SSC4D could be expanded to protozoan targets, protein binding assays were performed with live parasites. We first assessed the binding of SSC4D to bloodstream forms of *T. brucei*, the parasite that causes African trypanosomiasis. Recombinant SSC4D was incubated with 1×10^7 parasites, followed by centrifugation and immunoblotting of the cell pellet. As illustrated in **Figure 6A**, full-length SSC4D and each SSC4D half were capable of physically interacting with the parasite in a Ca^{2+}-dependent manner. To image this interaction by confocal microscopy, a GFP-expressing *T. brucei* Lister 427 strain was incubated with HA-tagged SSC4D, and binding of the protein to *T. brucei* cells was detected using anti-HA mAbs (visualized in red, **Figure 6B**).

We extended our protein–parasite binding assays to *Leishmania major* and *Leishmania tarentolae* promastigotes, *Plasmodium berghei* merozoites, and *Neospora caninum* tachyzoites. SSC4D and its half-forms bound to all tested parasites, with the exception of SSC4D-d1d2 that did not bind to *P. berghei* merozoites, the stage that infects red blood cells. Noteworthy, in the absence of Ca^{2+}, all SSC4D–parasite interactions were abolished or markedly reduced.

DISCUSSION

In this study, we show for the first time the capacity of SSC4D to physically bind to bacteria and protozoan parasites. SSC4D has been one of the most neglected SRCR proteins, and no functional data were available, but by simple analogy with other family members, we anticipated that this protein could reveal some PRR

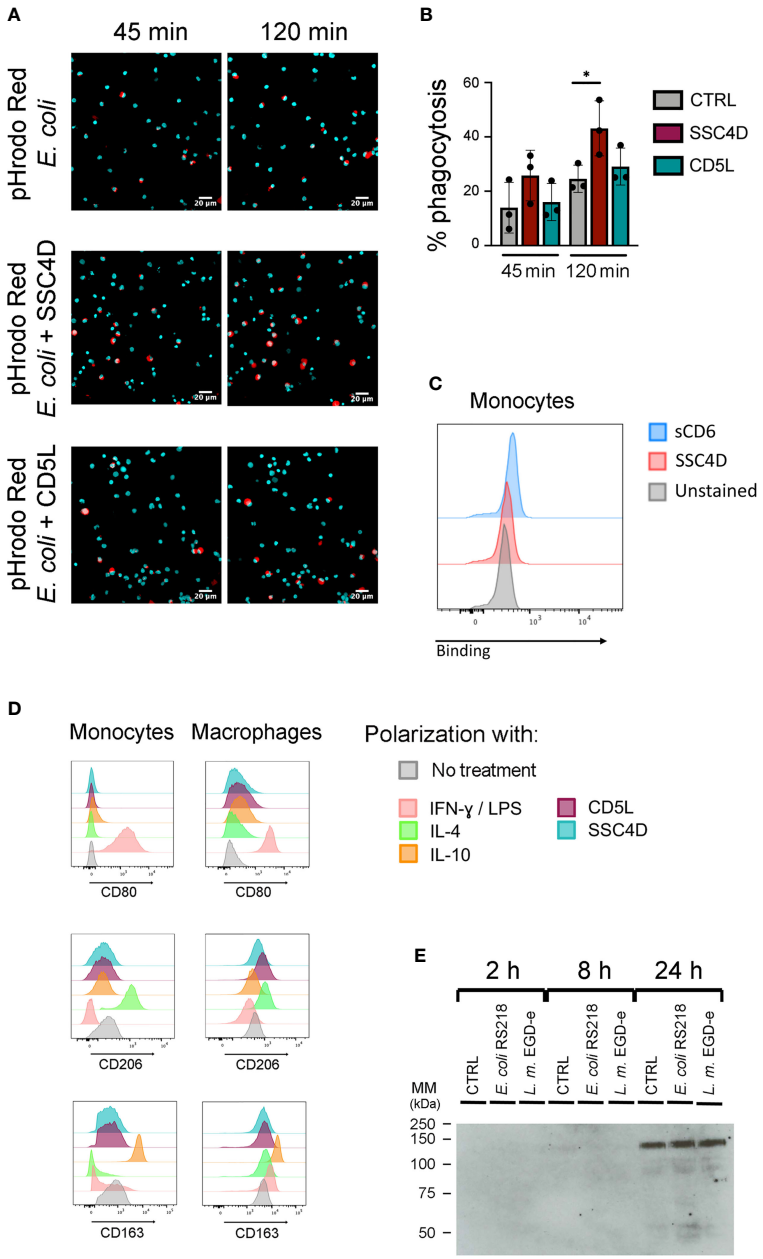

FIGURE 5 | SSC4D promotes phagocytosis without binding to a ligand on human monocytes and does not induce macrophage polarization. **(A)** *Escherichia coli* pHrodo BioParticles (40 μg/ml) were added to isolated human monocytes, together with 5 μg/ml of SSC4D (middle panels) or CD5L (bottom panels), or no protein (top panels). Images were acquired for each well at 45 and 120 min after the addition of *E. coli* BioParticles using an IN Cell Analyzer, followed by analysis using FIJI software. Blue indicates DAPI staining, and red indicates phagocytosed *E. coli* BioParticles. **(B)** The percentage of monocytes containing *E. coli* BioParticles was quantified. Graph shows the mean ± SD of three independent experiments performed in duplicate. Statistical analysis was performed using Student's t test. *$p < 0.05$. **(C)** *Ex vivo* monocytes were incubated with 3 μg of SSC4D or sCD6 or left unstained. Cell-bound proteins were detected with anti-HIS antibody followed with Alexa Fluor 647-conjugated anti-mouse antibody and analyzed by flow cytometry. Gray histograms represent control cells, not stained with scavenger receptor cysteine-rich (SRCR) protein but incubated with secondary antibody, red histograms represent labeling with SSC4D, and blue histograms represent labeling with sCD6. **(D)** Flow cytometry analysis of *ex vivo* monocytes (left column) and macrophage colony-stimulating factor (M-CSF)-differentiated macrophages (right column). Monocytes received for 72 h the appropriate stimuli to polarize toward M1 [interferon (IFN)-γ/lipopolysaccharide (LPS)], M2a [interleukin (IL)-4], or M2C (IL-10) subtypes. Macrophages received the same treatment, but for 24 h. CD80, CD206, and CD163 labeling confirms the polarization of monocytes and macrophages into the correct subtype. Stimulations with SSC4D or CD5L had no effect on cell polarization except for a slight effect of CD5L in polarizing macrophages into an M2a-like phenotype. Representative histograms are from one of three independent experiments. **(E)** SSC4D secretion upon culture infection with live bacteria. Caco-2 cells were engineered to express SSC4D fused to citrine and were cultured for 3 days at 3×10^5 cells/well in a 12-well plate. Live *E. coli* RS218 or *L. monocytogenes* EGD-e were added at 1:50 multiplicity of infection (MOI). Supernatants were collected at the indicated time points, and the presence of HA-tagged SSC4D-citrine was detected by western blotting. The blot shown is representative of two independent experiments.

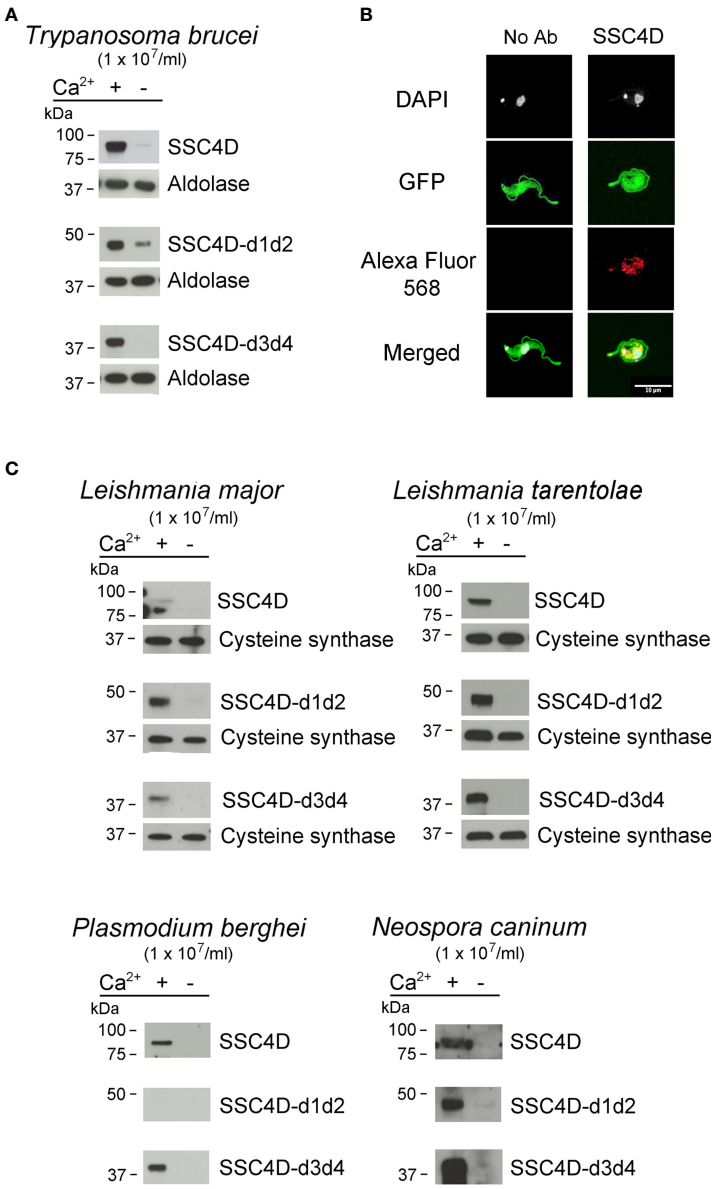

FIGURE 6 | SSC4D binds to protozoan parasites. **(A)** Two micrograms of recombinant SSC4D, or of the hemi-forms SSC4D-d1d2 and SSC4Dd3d4, were incubated with suspensions of 1 × 10^7 live *Trypanosoma brucei brucei* bloodstream forms in the presence or absence of Ca^{2+}. Parasite-bound proteins were detected by immunoblotting using anti-HIS mAb. Membranes were reprobed with an anti-aldolase immune serum for loading control. Results shown are of one of three independent experiments. **(B)** Representative images of SSC4D interacting with green fluorescent protein (GFP)-expressing *T. brucei*. In both panels, GFP^+ parasites (green) were allowed to interact with SSC4D (red), being the primary antibody omitted in the left panel, as control. DAPI (white) indicates DNA staining. The results shown are representative of four independent experiments. **(C)** Two micrograms of recombinant SSC4D, SSC4D-d1d2, and SSC4D-d3d4 were incubated with suspensions of 1 × 10^7 live *Leishmania major* and *Leishmania tarentolae* promastigotes, *Plasmodium berghei* merozoites, and *Neospora caninum* tachyzoites. Interactions were detected as in panel **(A)**, and membranes were reprobed with an anti-*L. infantum* cysteine synthase immune serum for loading control of *L. major* and *L. tarentolae*.

functions. The identity of bacterial targets of SSC4D does not significantly differ from those of CD5L or SSC5D; however, these proteins do not display identical binding patterns between themselves or even among their own single domains. We have previously shown relevant differences of binding avidities between SSC5D and CD5L toward different types of bacteria (17). We here advance on this conclusion by showing that different parts of SSC4D have preferential binding toward different groups of bacteria.

Contrasting with the strong binding of CD5L, SSC4D, and SSC5D to a variety of bacterial species and strains, the extracellular domain of CD6 displays a significantly lower

binding potency. CD6 is a plasma membrane glycoprotein that modulates T-cell activation (23), and it was somewhat unexpected that such a receptor involved in antigen-dependent signal transduction would be directly involved in the recognition of unprocessed pathogenic determinants (8). Although there was some controversy as to which extent CD6 binding to bacteria would reflect a physiological characteristic of the molecule (50, 51), it seems undisputable that CD6 does protect from bacterial infection-induced septic shock in mouse models possibly *via* its function as a circulating extracellular form (sCD6), shed from the surface of lymphocytes in pathological conditions (52). Nonetheless, the fact that the levels of bacterial binding of SSC4D, like CD5L and SSC5D, are so much more evident than those of sCD6 clearly suggests that a main function of SSC4D is indeed of pathogen pattern recognition.

SSC4D is expressed by many epithelial cells of several organs and by phagocytic leukocytes, but unlike what has been described for other circulating SRCR proteins, we could not identify any stimulus, cue, or microbial challenge that increased the rate of secretion of the protein. The estimated plasma concentration of SSC4D is in effect very low (1 ng/ml) when compared with those of the other circulating SRCR proteins SSC5D (88 ng/ml), CD5L (4.3 μg/ml), and MAC2BP (7.1 μg/ml) (21, 22), and the abundance of these proteins further increases upon certain inflammatory and infectious challenges or in oncological environments (11, 53, 54). Also, the membrane-bound receptors CD5, CD6, and CD166, expressed by different leukocytes, undergo cleavage of their ecto-domains in particular pathological conditions, resulting in their consequent release into circulation where they display specific immune-related functions (55, 56). And yet, we have not found any similar agonist-dependent behavior for SSC4D, raising the possibility that SSC4D is being continuously secreted at low constant rates either in steady-state or upon external challenges.

Therefore, and despite sharing common functions with other SRCR proteins, namely, as a PRR, SSC4D may be endowed with some distinctive properties. SSC4D behaves differently from CD5L in at least a few aspects, as in contrast with CD5L (16, 49), SSC4D is not involved in the polarization of macrophages upon different inflammatory stimuli. On the other hand, SSC4D can potentiate the phagocytosis of bacteria by macrophages, contrary to human CD5L. Although our results on CD5L concur with those previously reported by Sanjurjo et al. (49), there is some controversy regarding the role of CD5L in phagocytosis, which may depend on the experimental setup, the type of particle/microorganism to be internalized, and the molecular and cellular species analyzed. Mouse (m)CD5L was shown to increase the phagocytosis of latex beads by mouse macrophages (57); both mCD5L and human (h) CD5L increase the clearance of debris by mouse macrophages (58); hCD5L increases clearance of apoptotic cells by human monocytes (49); and mCD5L increases phagocytosis by mouse macrophages and neutrophils of *S. aureus* (59). However, the presence of hCD5L did not change the phagocytosis of microspheres or *E. coli* or *S. aureus* particles by human peripheral blood cells (49).

We here show that phagocytosis of *E. coli* particles by human monocytes is in fact not influenced by CD5L but is increased in the presence of SSC4D. Given that both *E. coli* particles and SRCR proteins were added to the cells at the same time, it is unlikely that the increase in phagocytosis is due to activation of monocytes induced by SSC4D. It is possible, instead, that the protein intermediates the interaction between monocytes and bacteria. We have screened monocytes with recombinant monovalent SSC4D for the existence of specific receptors and could not detect any interaction by flow cytometry possible due to the low sensitivity of the method. Although with no evidence that SSC4D promotes large-scale bacterial aggregation, an alternative hypothesis is that the coating of bacteria with SSC4D may induce a more efficient recognition of multivalent SSC4D opsonizing the bacteria either by low-affinity SSC4D receptors or eventually by other sensors of microbial structures.

It is known that host defense against protozoan parasites involves different classes of PRR, such as TLRs, C-type lectin receptors, and NOD-like receptors (60–62). Nevertheless, the knowledge on this field lags considerably behind those that focus on the identification of bacterial, viral, and fungal PAMPs. Also, many other components of the innate immune system participate in antiparasitic defenses, including CD36, a scavenger receptor class B that displays multiple functions and a broad range of ligands, including a cytoadherence ligand on *Plasmodium falciparum*-infected erythrocytes (63). However, CD36 belongs to a different family of scavenger receptors characterized by having two transmembrane domains flanking a CD36-type multifunctional domain. SRCR proteins like MARCO and MSR1 have been shown to have a role in defense against protozoan parasites such that, for example, inhibition of MSR1 function reduces *P. berghei* infection and the expression of MARCO in macrophages of CBA/J mice is increased upon *L. major* infection (64, 65). Still, to the best of our knowledge, ours is the first study that describes a physical interaction of an SRCR protein and protozoan targets. Together with its capacity to bind bacteria and to promote macrophage phagocytosis, SSC4D can thus be considered a *bona fide* broad-range PRR, and importantly, this may help to strengthen the concept, so many times overlooked, that the SRCR cluster is a legitimate member of the wider collective family of pathogen PRRs.

DATA AVAILABILITY STATEMENT

The original contributions presented in the study are included in the article/**Supplementary Material**. Further inquiries can be directed to the corresponding author.

AUTHOR CONTRIBUTIONS

MC designed and performed the experiments and wrote the paper. RS performed IHC and flow cytometry. SA performed IHC and produced Caco-2-SSC4D cells. MS developed GFP+

parasites. BP-C performed protein–parasite assays. LO designed protein expression vectors, produced proteins, and handled bacterial experiments. JT designed all experiments handling parasites. AC planned and designed the study and wrote the paper. All authors contributed to the article and approved the submitted version.

FUNDING

This work was funded by National Funds through FCT–Fundação para a Ciência e a Tecnologia, I.P., under the projects SRecognite Infect-ERA/0003/2015 and UIDB/04293/2020. Individual funding to JT was provided by FCT through CEECIND/02362/2017. MC, RS, and MS were recipients of studentships from FCT, respectively, SFRH/BD/116791/2016, SFRH/BD/110691/2015, and SFRH/BD/133485/2017.

ACKNOWLEDGMENTS

This paper is dedicated to our colleague and friend Rui Appelberg (1960-2020). The authors acknowledge the support of the i3S Scientific Platform BioSciences Screening, member of the national infrastructure PPBI–Portuguese Platform of Bioimaging (PPBI-POCI-01-0145-FEDER-022122) and PT-OPENSCREEN. Tissue sections were kindly provided by Amaro Frutuoso, Department of Complementary Means of Diagnosis and Therapy, Service of Pathology, Hospital Pedro Hispano, Matosinhos.

SUPPLEMENTARY MATERIAL

The Supplementary Material for this article can be found online at: https://www.frontiersin.org/articles/10.3389/fimmu.2021.760770/full#supplementary-material

REFERENCES

1. Beutler B, Jiang Z, Georgel P, Crozat K, Croker B, Rutschmann S, et al. Genetic Analysis of Host Resistance: Toll-Like Receptor Signaling and Immunity at Large. *Annu Rev Immunol* (2006) 24:353–89. doi: 10.1146/annurev.immunol.24.021605.090552
2. Hoving JC, Wilson GJ, Brown GD. Signalling C-Type Lectin Receptors, Microbial Recognition and Immunity. *Cell Microbiol* (2014) 16:185–94. doi: 10.1111/cmi.12249
3. Rehwinkel J, Gack MU. RIG-I-Like Receptors: Their Regulation and Roles in RNA Sensing. *Nat Rev Immunol* (2020) 20:537–51. doi: 10.1038/s41577-020-0288-3
4. Franchi L, Warner N, Viani K, Nunez G. Function of Nod-Like Receptors in Microbial Recognition and Host Defense. *Immunol Rev* (2009) 227:106–28. doi: 10.1111/j.1600-065X.2008.00734.x
5. Hampton RY, Golenbock DT, Penman M, Krieger M, Raetz CR. Recognition and Plasma Clearance of Endotoxin by Scavenger Receptors. *Nature* (1991) 352:342–4. doi: 10.1038/352342a0
6. Elomaa O, Kangas M, Sahlberg C, Tuukkanen J, Sormunen R, Liakka A, et al. Cloning of a Novel Bacteria-Binding Receptor Structurally Related to Scavenger Receptors and Expressed in a Subset of Macrophages. *Cell* (1995) 80:603–9. doi: 10.1016/0092-8674(95)90514-6
7. Fabriek BO, van Bruggen R, Deng DM, Ligtenberg AJ, Nazmi K, Schornagel K, et al. The Macrophage Scavenger Receptor CD163 Functions as an Innate Immune Sensor for Bacteria. *Blood* (2009) 113:887–92. doi: 10.1182/blood-2008-07-167064
8. Sarrias MR, Farnós M, Mota R, Sánchez-Barbero F, Ibáñez A, Gimferrer I, et al. CD6 Binds to Pathogen-Associated Molecular Patterns and Protects From LPS-Induced Septic Shock. *Proc Natl Acad Sci USA* (2007) 104:11724–9. doi: 10.1073/pnas.0702815104
9. Vera J, Fenutría R, Cañadas O, Figueras M, Mota R, Sarrias MR, et al. The CD5 Ectodomain Interacts With Conserved Fungal Cell Wall Components and Protects From Zymosan-Induced Septic Shock-Like Syndrome. *Proc Natl Acad Sci USA* (2009) 106:1506–11. doi: 10.1073/pnas.0805846106
10. Ullrich A, Sures I, D'Egidio M, Jallal B, Powell TJ, Herbst R, et al. The Secreted Tumor-Associated Antigen 90K Is a Potent Immune Stimulator. *J Biol Chem* (1994) 269:18401–7. doi: 10.1016/S0021-9258(17)32322-0
11. Luo M, Zhang Q, Hu Y, Sun C, Sheng Y, Deng C. LGALS3BP: A Potential Plasma Biomarker Associated With Diagnosis and Prognosis in Patients With Sepsis. *Infect Drug Resist* (2021) 14:2863–71. doi: 10.2147/IDR.S316402
12. Gebe JA, Kiener PA, Ring HZ, Li X, Francke U, Aruffo A. Molecular Cloning, Mapping to Human Chromosome 1 Q21-Q23, and Cell Binding Characteristics of Spalpha, a New Member of the Scavenger Receptor Cysteine-Rich (SRCR) Family of Proteins. *J Biol Chem* (1997) 272:6151–8. doi: 10.1074/jbc.272.10.6151
13. Miyazaki T, Hirokami Y, Matsuhashi N, Takatsuka H, Naito M. Increased Susceptibility of Thymocytes to Apoptosis in Mice Lacking AIM, a Novel Murine Macrophage-Derived Soluble Factor Belonging to the Scavenger Receptor Cysteine-Rich Domain Superfamily. *J Exp Med* (1999) 189:413–22. doi: 10.1084/jem.189.2.413
14. Gonçalves CM, Castro MA, Henriques T, Oliveira MI, Pinheiro HC, Oliveira C, et al. Molecular Cloning and Analysis of SSc5D, a New Member of the Scavenger Receptor Cysteine-Rich Superfamily. *Mol Immunol* (2009) 46:2585–96. doi: 10.1016/j.molimm.2009.05.006
15. Mollenhauer J, Wiemann S, Scheurlen W, Korn B, Hayashi Y, Wilgenbus KK, et al. DMBT1, a New Member of the SRCR Superfamily, on Chromosome 10q25.3-26.1 Is Deleted in Malignant Brain Tumours. *Nat Genet* (1997) 17:32–9. doi: 10.1038/ng0997-32
16. Sarrias MR, Roselló S, Sánchez-Barbero F, Sierra JM, Vila J, Yélamos J, et al. A Role for Human Sp Alpha as a Pattern Recognition Receptor. *J Biol Chem* (2005) 280:35391–8. doi: 10.1074/jbc.M505042200
17. Bessa Pereira C, Bockova M, Santos RF, Santos AM, de Araujo MM, Oliveira L, et al. The Scavenger Receptor SSc5D Physically Interacts With Bacteria Through the SRCR-Containing N-Terminal Domain. *Front Immunol* (2016) 7:416. doi: 10.3389/fimmu.2016.00416
18. Bikker FJ, Ligtenberg AJ, Nazmi K, Veerman EC, van't Hof W, Bolscher JG, et al. Identification of the Bacteria-Binding Peptide Domain on Salivary Agglutinin (Gp-340/DMBT1), a Member of the Scavenger Receptor Cysteine-Rich Superfamily. *J Biol Chem* (2002) 277:32109–15. doi: 10.1074/jbc.M203788200
19. Sanjurjo L, Aran G, Roher N, Valledor AF, Sarrias MR. AIM/CD5L: A Key Protein in the Control of Immune Homeostasis and Inflammatory Disease. *J Leukoc Biol* (2015) 98:173–84. doi: 10.1189/jlb.3RU0215-074R
20. Padilla O, Pujana MA, López-de la Iglesia A, Gimferrer I, Arman M, Vilà JM, et al. Cloning of S4D-SRCRB, a New Soluble Member of the Group B Scavenger Receptor Cysteine-Rich Family (SRCR-SF) Mapping to Human Chromosome 7q11.23. *Immunogenetics* (2002) 54:621–34. doi: 10.1007/s00251-002-0507-z
21. Desiere F, Deutsch EW, King NL, Nesvizhskii AI, Mallick P, Eng J, et al. The PeptideAtlas Project. *Nucleic Acids Res* (2006) 34:D655–8. doi: 10.1093/nar/gkj040
22. Farrah T, Deutsch EW, Omenn GS, Campbell DS, Sun Z, Bletz JA, et al. A High-Confidence Human Plasma Proteome Reference Set With Estimated Concentrations in PeptideAtlas. *Mol Cell Proteomics* (2011) 10:M110 006353. doi: 10.1074/mcp.M110.006353
23. Oliveira MI, Gonçalves CM, Pinto M, Fabre S, Santos AM, Lee SF, et al. CD6 Attenuates Early and Late Signaling Events, Setting Thresholds for T-Cell Activation. *Eur J Immunol* (2012) 42:195–205. doi: 10.1002/eji.201040528
24. Aden DP, Fogel A, Plotkin S, Damjanov I, Knowles BB. Controlled Synthesis of HBsAg in a Differentiated Human Liver Carcinoma-Derived Cell Line. *Nature* (1979) 282:615–6. doi: 10.1038/282615a0

25. Andersson LC, Nilsson K, Gahmberg CG. K562–a Human Erythroleukemic Cell Line. *Int J Cancer* (1979) 23:143–7. doi: 10.1002/ijc.2910230202
26. Fogh J, Fogh JM, Orfeo T. One Hundred and Twenty-Seven Cultured Human Tumor Cell Lines Producing Tumors in Nude Mice. *J Natl Cancer Inst* (1977) 59:221–6. doi: 10.1093/jnci/59.1.221
27. Weiss A, Wiskocil RL, Stobo JD. The Role of T3 Surface Molecules in the Activation of Human T Cells: A Two-Stimulus Requirement for IL 2 Production Reflects Events Occurring at a Pre-Translational Level. *J Immunol* (1984) 133:123–8.
28. Kohler PO, Bridson WE. Isolation of Hormone-Producing Clonal Lines of Human Choriocarcinoma. *J Clin Endocrinol Metab* (1971) 32:683–7. doi: 10.1210/jcem-32-5-683
29. DuBridge RB, Tang P, Hsia HC, Leong PM, Miller JH, Calos MP. Analysis of Mutation in Human Cells by Using an Epstein-Barr Virus Shuttle System. *Mol Cell Biol* (1987) 7:379–87. doi: 10.1128/mcb.7.1.379-387.1987
30. Nayak SK, O'Toole C, Price ZH. A Cell Line From an Anaplastic Transitional Cell Carcinoma of Human Urinary Bladder. *Br J Cancer* (1977) 35:142–51. doi: 10.1038/bjc.1977.21
31. Epstein MA, Achong BG, Barr YM, Zajac B, Henle G, Henle W. Morphological and Virological Investigations on Cultured Burkitt Tumor Lymphoblasts (Strain Raji). *J Natl Cancer Inst* (1966) 37:547–59. doi: 10.1093/jnci/37.4.547
32. Gallagher R, Collins S, Trujillo J, McCredie K, Ahearn M, Tsai S, et al. Characterization of the Continuous, Differentiating Myeloid Cell Line (HL-60) From a Patient With Acute Promyelocytic Leukemia. *Blood* (1979) 54:713–33. doi: 10.1182/blood.V54.3.713.713
33. Tsuchiya S, Yamabe M, Yamaguchi Y, Kobayashi Y, Konno T, Tada K. Establishment and Characterization of a Human Acute Monocytic Leukemia Cell Line (THP-1). *Int J Cancer* (1980) 26:171–6. doi: 10.1002/ijc.2910260208
34. Scherer WF, Syverton JT, Gey GO. Studies on the Propagation *In Vitro* of Poliomyelitis Viruses. IV. Viral Multiplication in a Stable Strain of Human Malignant Epithelial Cells (Strain HeLa) Derived From an Epidermoid Carcinoma of the Cervix. *J Exp Med* (1953) 97:695–710. doi: 10.1084/jem.97.5.695
35. Resende M, Cardoso MS, Frois-Martins R, Borges M, Jordan MB, Castro AG, et al. TNF-Mediated Compensatory Immunity to Mycobacterium Avium in the Absence of Macrophage Activation by IFN-Gamma. *J Immunol* (2019) 203:2451–8. doi: 10.4049/jimmunol.1801594
36. Correia A, Ferreirinha P, Botelho S, Belinha A, Leitao C, Caramalho I, et al. Predominant Role of Interferon-Gamma in the Host Protective Effect of CD8 (+) T Cells Against Neospora Caninum Infection. *Sci Rep* (2015) 5:14913. doi: 10.1038/srep14913
37. Costa DM, Sa M, Teixeira AR, Loureiro I, Thouvenot C, Golba S, et al. TRSP Is Dispensable for the Plasmodium Pre-Erythrocytic Phase. *Sci Rep* (2018) 8:15101. doi: 10.1038/s41598-018-33398-8
38. Loureiro I, Faria J, Clayton C, Macedo-Ribeiro S, Santarem N, Roy N, et al. Ribose 5-Phosphate Isomerase B Knockdown Compromises Trypanosoma Brucei Bloodstream Form Infectivity. *PloS Negl Trop Dis* (2015) 9:e3430. doi: 10.1371/journal.pntd.0003430
39. Faria J, Loureiro I, Santarem N, Cecilio P, Macedo-Ribeiro S, Tavares J, et al. Disclosing the Essentiality of Ribose-5-Phosphate Isomerase B in Trypanosomatids. *Sci Rep* (2016) 6:26937. doi: 10.1038/srep26937
40. Madeira F, Park YM, Lee J, Buso N, Gur T, Madhusoodanan N, et al. The EMBL-EBI Search and Sequence Analysis Tools APIs in 2019. *Nucleic Acids Res* (2019) 47:W636–41. doi: 10.1093/nar/gkz268
41. Steentoft C, Vakhrushev SY, Joshi HJ, Kong Y, Vester-Christensen MB, Schjoldager KT, et al. Precision Mapping of the Human O-GalNAc Glycoproteome Through SimpleCell Technology. *EMBO J* (2013) 32:1478–88. doi: 10.1038/emboj.2013.79
42. Carmo AM, Sreenu VB. A Systematic and Thorough Search for Domains of the Scavenger Receptor Cysteine-Rich Group B Family in the Human Genome. In: MA Mahdavi, editor. *Bioinformatics - Trends and Methodologies*. Rijeka, Croatia: InTech (2011). p. 195–210.
43. Gupta R, Brunak S. Prediction of Glycosylation Across the Human Proteome and the Correlation to Protein Function. *Pac Symp Biocomput* (2002) 7:310–22.
44. Gerhard DS, Wagner L, Feingold EA, Shenmen CM, Grouse LH, Schuler G, et al. The Status, Quality, and Expansion of the NIH Full-Length cDNA Project: The Mammalian Gene Collection (MGC). *Genome Res* (2004) 14:2121–7. doi: 10.1101/gr.2596504
45. Mollenhauer J, Herbertz S, Helmke B, Kollender G, Krebs I, Madsen J, et al. Deleted in Malignant Brain Tumors 1 Is a Versatile Mucin-Like Molecule Likely to Play a Differential Role in Digestive Tract Cancer. *Cancer Res* (2001) 61:8880–6.
46. Castro MA, Oliveira MI, Nunes RJ, Fabre S, Barbosa R, Peixoto A, et al. Extracellular Isoforms of CD6 Generated by Alternative Splicing Regulate Targeting of CD6 to the Immunological Synapse. *J Immunol* (2007) 178:4351–61. doi: 10.4049/jimmunol.178.7.4351
47. Uhlen M, Zhang C, Lee S, Sjostedt E, Fagerberg L, Bidkhori G, et al. A Pathology Atlas of the Human Cancer Transcriptome. *Science* (2017) 357: eaan2507. doi: 10.1126/science.aan2507
48. Simons ER. Measurement of Phagocytosis and of the Phagosomal Environment in Polymorphonuclear Phagocytes by Flow Cytometry. *Curr Protoc Cytom* (2010) Chapter 9:Unit9 31. doi: 10.1002/0471142956.cy0931s51
49. Sanjurjo L, Aran G, Tellez E, Amezaga N, Armengol C, Lopez D, et al. CD5L Promotes M2 Macrophage Polarization Through Autophagy-Mediated Upregulation of ID3. *Front Immunol* (2018) 9:480. doi: 10.3389/fimmu.2018.00480
50. Oliveira L, Carmo AM. Response: Commentary: The Scavenger Receptor SSc5D Physically Interacts With Bacteria Through the SRCR-Containing N-Terminal Domain. *Front Immunol* (2017) 8:1004. doi: 10.3389/fimmu.2017.01004
51. Lozano F, Martinez-Florensa M. Commentary: The Scavenger Receptor SSc5D Physically Interacts With Bacteria Through the SRCR-Containing N-Terminal Domain. *Front Immunol* (2017) 8:366. doi: 10.3389/fimmu.2017.00366
52. Martínez-Florensa M, Consuegra-Fernández M, Aranda F, Armiger-Borràs N, Di Scala M, Carrasco E, et al. Protective Effects of Human and Mouse Soluble Scavenger-Like CD6 Lymphocyte Receptor in a Lethal Model of Polymicrobial Sepsis. *Antimicrob Agents Chemother* (2017) 61:e01391–16. doi: 10.1128/AAC.01391-16
53. Aran G, Sanjurjo L, Barcena C, Simon-Coma M, Tellez E, Vazquez-Vitali M, et al. CD5L Is Upregulated in Hepatocellular Carcinoma and Promotes Liver Cancer Cell Proliferation and Antiapoptotic Responses by Binding to HSPA5 (GRP78). *FASEB J* (2018) 32:3878–91. doi: 10.1096/fj.201700941RR
54. Balakrishnan L, Bhattacharjee M, Ahmad S, Nirujogi RS, Renuse S, Subbannayya Y, et al. Differential Proteomic Analysis of Synovial Fluid From Rheumatoid Arthritis and Osteoarthritis Patients. *Clin Proteomics* (2014) 11:1. doi: 10.1186/1559-0275-11-1
55. Moller HJ, Peterslund NA, Graversen JH, Moestrup SK. Identification of the Hemoglobin Scavenger Receptor/CD163 as a Natural Soluble Protein in Plasma. *Blood* (2002) 99:378–80. doi: 10.1182/blood.V99.1.378
56. Ramos-Casals M, Font J, García-Carrasco M, Calvo J, Places L, Padilla O, et al. High Circulating Levels of Soluble Scavenger Receptors (sCD5 and sCD6) in Patients With Primary Sjögren's Syndrome. *Rheumatology (Oxford)* (2001) 40:1056–9. doi: 10.1093/rheumatology/40.9.1056
57. Haruta I, Kato Y, Hashimoto E, Minjares C, Kennedy S, Uto H, et al. Association of AIM, a Novel Apoptosis Inhibitory Factor, With Hepatitis *via* Supporting Macrophage Survival and Enhancing Phagocytotic Function of Macrophages. *J Biol Chem* (2001) 276:22910–4. doi: 10.1074/jbc.M100324200
58. Arai S, Kitada K, Yamazaki T, Takai R, Zhang X, Tsugawa Y, et al. Apoptosis Inhibitor of Macrophage Protein Enhances Intraluminal Debris Clearance and Ameliorates Acute Kidney Injury in Mice. *Nat Med* (2016) 22:183–93. doi: 10.1038/nm.4012
59. Gao X, Yan X, Zhang Q, Yin Y, Cao J. CD5L Contributes to the Pathogenesis of Methicillin-Resistant Staphylococcus Aureus-Induced Pneumonia. *Int Immunopharmacol* (2019) 72:40–7. doi: 10.1016/j.intimp.2019.03.057
60. Ghosh D, Stumhofer JS. Do You See What I See: Recognition of Protozoan Parasites by Toll-Like Receptors. *Curr Immunol Rev* (2013) 9:129–40. doi: 10.2174/15733955096661312032259 29
61. Vazquez-Mendoza A, Carrero JC, Rodriguez-Sosa M. Parasitic Infections: A Role for C-Type Lectins Receptors. *BioMed Res Int* (2013) 2013:456352. doi: 10.1155/2013/456352
62. Gurung P, Kanneganti TD. Immune Responses Against Protozoan Parasites: A Focus on the Emerging Role of Nod-Like Receptors. *Cell Mol Life Sci* (2016) 73:3035–51. doi: 10.1007/s00018-016-2212-3
63. Barnwell JW, Asch AS, Nachman RL, Yamaya M, Aikawa M, Ingravallo P. A Human 88-kD Membrane Glycoprotein (CD36) Functions *In Vitro* as a Receptor for a Cytoadherence Ligand on Plasmodium Falciparum-Infected Erythrocytes. *J Clin Invest* (1989) 84:765–72. doi: 10.1172/JCI114234

64. Rodrigues CD, Hannus M, Prudencio M, Martin C, Goncalves LA, Portugal S, et al. Host Scavenger Receptor SR-BI Plays a Dual Role in the Establishment of Malaria Parasite Liver Infection. *Cell Host Microbe* (2008) 4:271–82. doi: 10.1016/j.chom.2008.07.012
65. Gomes IN, Palma LC, Campos GO, Lima JG, TF DEA, JP DEM, et al. The Scavenger Receptor MARCO Is Involved in Leishmania Major Infection by CBA/J Macrophages. *Parasite Immunol* (2009) 31:188–98. doi: 10.1111/j.1365-3024.2009.01093.x

Conflict of Interest: The authors declare that the research was conducted in the absence of any commercial or financial relationships that could be construed as a potential conflict of interest.

Publisher's Note: All claims expressed in this article are solely those of the authors and do not necessarily represent those of their affiliated organizations, or those of the publisher, the editors and the reviewers. Any product that may be evaluated in this article, or claim that may be made by its manufacturer, is not guaranteed or endorsed by the publisher.

SUPPLEMENTARY MATERIAL

METHODS

mRNA analysis of SSC4D in human cell lines, and expression of SSC4D-citrine fusion protein in Caco-2 cells

Total RNA of different cell lines was isolated using the TripleXtractor directRNA kit (Grisp). Using 5 μg of RNA per sample, cDNA was synthesized using Superscript III reverse transcriptase (Invitrogen). The cDNA obtained was used to analyze the SSC4D expression by PCR with GoTaq DNA Polymerase (Promega). Primer sequences were the following: forward, 5'-GGCGTCCACAATTGCTTTCA-3'; and reverse, 5'-ACGGATCTGTCTGCCAAG-3'.

Measurement of SSC4D accumulation in Caco-2 cells

SSC4D-expressing Caco-2 cells were plated at a density of 2 x 10^4 cells/well in a 96-well plate (CellCarrier Ultra). Cell seeding was optimized to achieve a confluency of 70% allowing optimal cell segmentation. Cells were maintained in imaging media and incubated for 3 days for optimal attachment. Culture media was then removed without disturbing the monolayer and replaced by fresh media containing Hoechst, for 45 min at 37 ºC.

For the 0 h time-point, cells were washed with sterile PBS and new medium was added, followed by image acquisition using the IN Cell Analyzer. A 20 x objective was used and 9 fields of view were collected in each well. Then, the plate was spun and different stimuli, IL-1β, IL-4, IL-6, IL-17, TNF-α, IFN-γ, LPS, and LTA, at different concentrations were added to the cells together with 10 μg/ml of Brefeldin A, an inhibitor of protein transport from the ER to the Golgi complex, and thus of protein secretion.

Image acquisition was done at 6 h post-stimuli, similar to the 0 h time-point. To quantify SSC4D intracellular accumulation in the Caco-2-SSC4D cells, first the nuclei of these cells were identified from the Hoechst channel, using a machine-learning-based (bio)image analysis tool – ilastik (66). The resulting pixel probability maps were used for further image analysis and quantification of the mCitrine intensity values per cell using another cell image analysis software – CellProfiler™ (67). Briefly, the image analysis workflow consisted in (i) correction for uneven

illumination/lighting/shading on the mCitrine channel, (ii) segmentation of the nuclei from the probability maps, (iii) expansion of the nuclei by 10 pixels to create a bigger mask that covers the majority of the cell cytoplasm, (iv) then the nucleus mask has been subtracted from the previous expanded mask and then (v) the mean pixel intensity per cell on the mCitrine channel has been quantified.

The mCitrine intensity for each cell was obtained and the average of for each field of view was then calculated. The intensity value of each field of view was normalized to the intensity value of the negative control (WT Caco-2 cells) followed by a normalization to the corresponding baseline condition (0 h).

Measurement of SSC4D secretion upon cytokine stimuli

Caco-2-SSC4D cells were plated at a density of 2 X 10^5 cells/well in a 12-well plate and incubated for 3 days for an optimum cell attachment. The culture medium was removed and new medium containing cytokines IL-1β, IL-4, IL-6, IL-17, TNF-α or IFN-γ in different concentrations (1, 10, and 100 ng/ml), or endotoxins LPS and LTA (at 10, 100, and 1000 ng/ml) was added to the cells. After the indicated times of incubation, supernatants were collected and then resuspended in Laemmli's sample buffer for SDS-PAGE and western blotting. The presence of SSC4D in the culture supernatants was detected using mouse anti-HA antibody followed by anti-mouse HRP conjugated antibody, and ECL detection.

REFERENCES

66. Berg, S., Kutra, D., Kroeger, T., Straehle, C. N., Kausler, B. X., Haubold, C., Schiegg, M., Ales, J., Beier, T., Rudy, M., Eren, K., Cervantes, J. I., Xu, B., Beuttenmueller, F., Wolny, A., Zhang, C., Koethe, U., Hamprecht, F. A., and Kreshuk, A. (2019) ilastik: interactive machine learning for (bio)image analysis. *Nat Methods* **16**, 1226-1232

67. McQuin, C., Goodman, A., Chernyshev, V., Kamentsky, L., Cimini, B. A., Karhohs, K. W., Doan, M., Ding, L., Rafelski, S. M., Thirstrup, D., Wiegraebe, W., Singh, S., Becker, T., Caicedo, J. C., and Carpenter, A. E. (2018) CellProfiler 3.0: Next-generation image processing for biology. *PLoS Biol* **16**, e2005970

Supplementary Figure 1

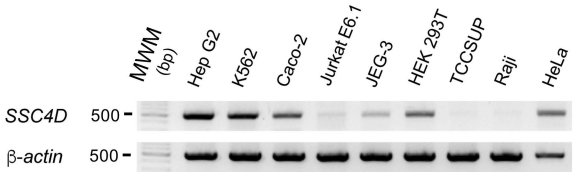

Supplemental Figure 1. *SSC4D* expression in human cell lines. Representative agarose gel images showing *SSC4D* mRNA expression in different human cell lines, measured by RT-PCR. *β-actin* mRNA is shown as loading control. MWM, molecular weight markers.

Supplementary Figure 2

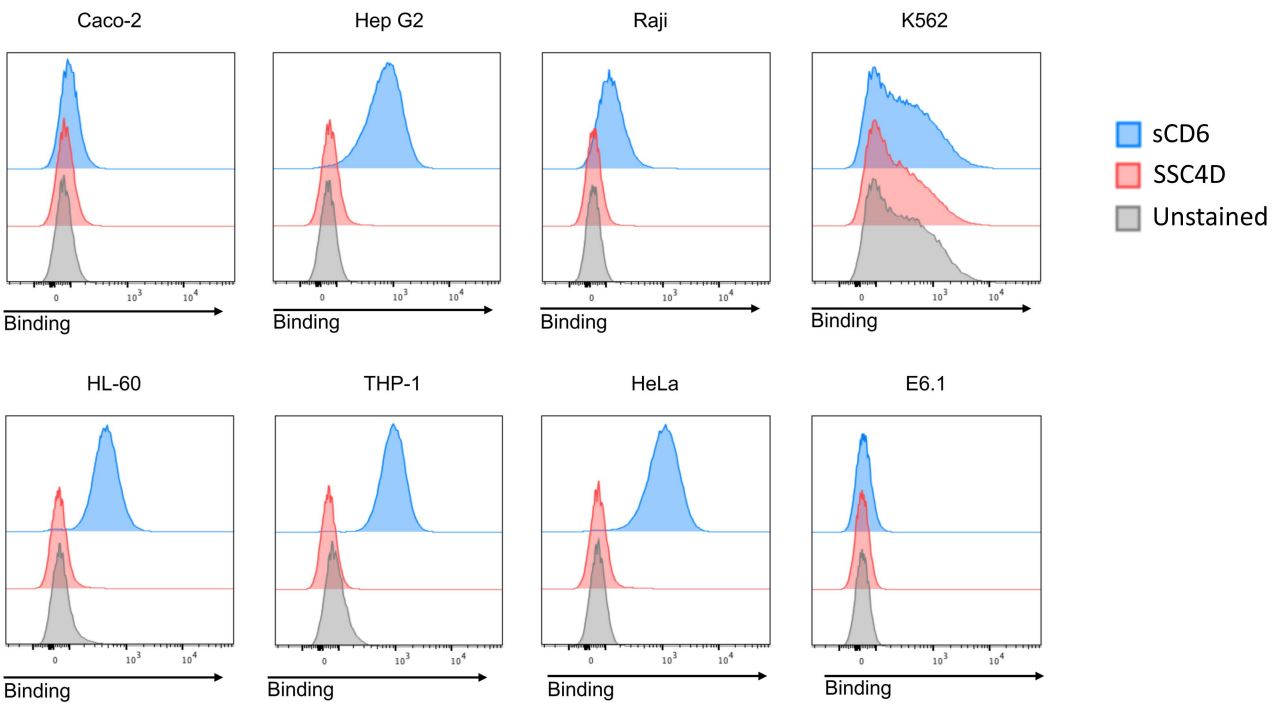

Supplemental Figure 2. No evidence for a cellular ligand for SSC4D. Caco-2, Hep G2, Raji, K562, HL-60, THP-1, HeLa and E6.1 cell suspensions were incubated with 3 μg of SSC4D or sCD6 or left untreated. Cell-bound proteins were detected with anti-HIS antibody followed with 647-conjugated anti-mouse antibody and analyzed by flow cytometry. Gray histograms represent control cells, not stained with SRCR protein but incubated with secondary antibody, red histograms represent cells labeled with SSC4D and blue histograms cells labeled with sCD6.

Supplementary Figure 3

A

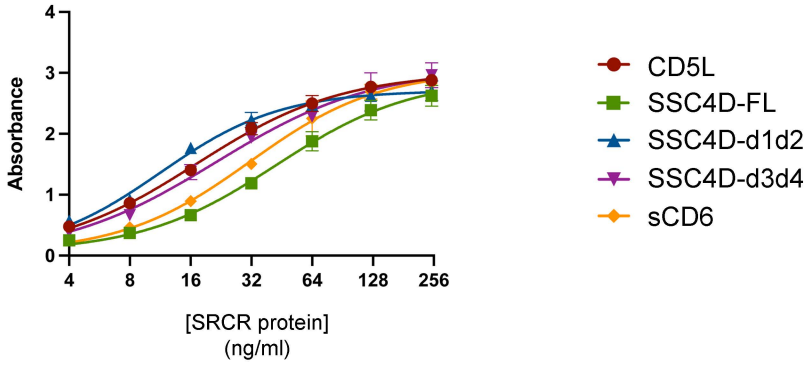

B

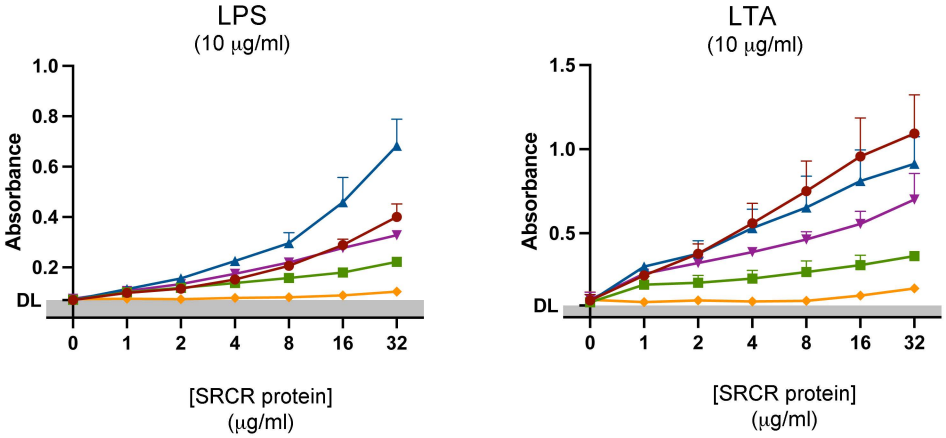

Supplemental Figure 3. Standard curve for detection of human SRCR proteins to LPS and LTA. **(A)** Serial dilutions of recombinant proteins SSC4D-FL, SSC4D-d1d2, SSC4D-d3d4, CD5L, and sCD6 were performed and proteins were directly coated in a 96-well plate. Plate-bound proteins were detected by anti-HIS antibody followed by HRP-conjugated antibody. Each point represents the mean ± SD of two independent experiments performed in duplicate. **(B)** 10 μg/ml of purified LPS or LTA were immobilized in a 96-well plate and incubated with different concentrations of recombinant SSC4D-FL, SSC4D-d1d2, SSC4D-d3d4, CD5L, or sCD6. Bound SRCR proteins were detected using anti-HIS antibody followed by HRP-conjugated antibody. Each point represents the mean ± SD of two experiments performed in duplicate.

Supplementary Figure 4

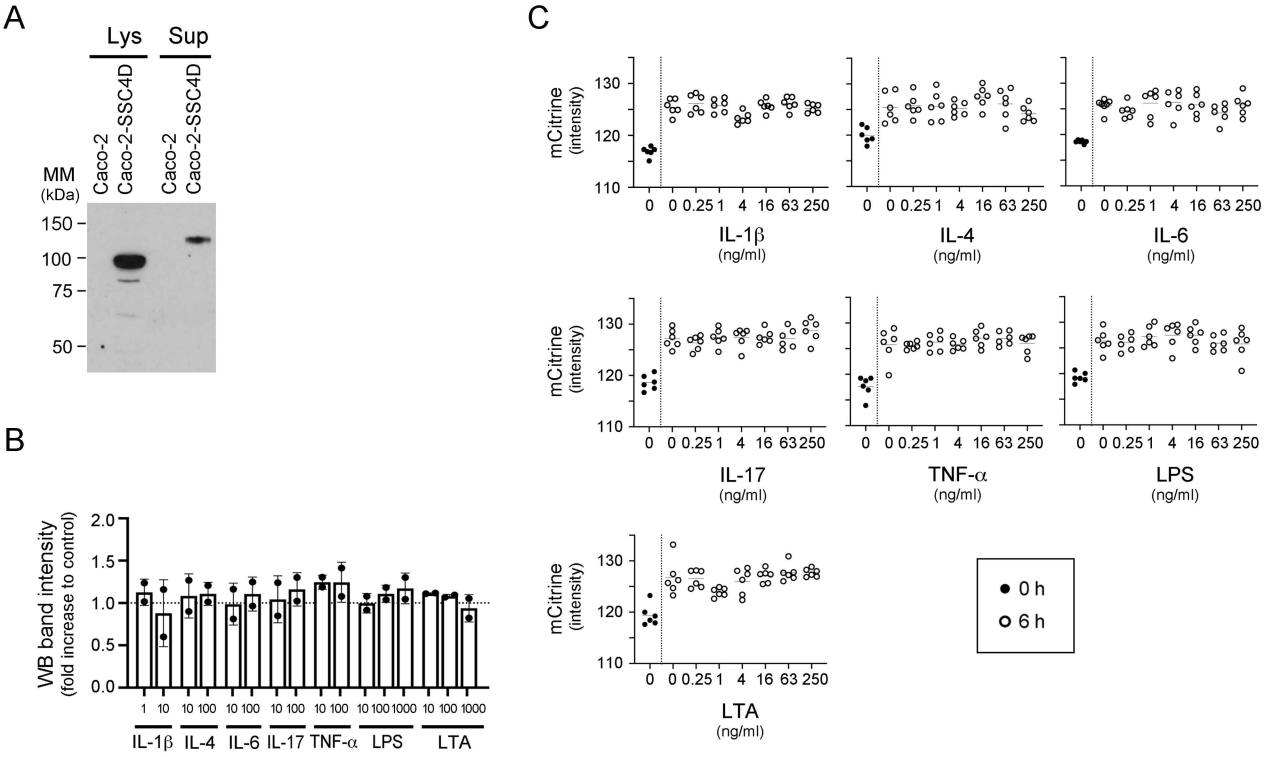

Supplemental Figure 4. SSC4D is secreted at constant rates, independently of external stimuli or cues. (A) Western blot of SSC4D fused to mCitrine and HA tag. The expressed protein displays a molecular mass of ~100 KDa when collected from cell lysates, compatible with the sum of the mass of SSC4D with those of mCitrine and HA, and of ~125 KDa as a secreted protein, also compatible with post-translational modifications observed earlier for recombinant SSC4D. **(B)** SSC4D secretion by Caco-2-SSC4D cells incubated for 24 h in the presence or absence of different stimuli (IL-1β, IL-4, IL-6, IL-17, TNF-α, LPS, and LTA) at different concentrations. The presence of SSC4D in the supernatants was analyzed by WB. Band densities were quantified and the values were normalized to the control (without stimulation). Graph shows the mean ± SD of two independent experiments. **(C)** Intracellular accumulation of SSC4D by Caco-2-SSC4D cells incubated for 6 h in the presence or absence of different stimuli (IL-1β, IL-4, IL-6, IL-17, TNF-α, LPS, and LTA) at different concentrations. Brefeldin A was used to block protein secretion, allowing for the determination of accumulation of intracellular SSC4D. Levels of intracellular SSC4D-mCitrine were analyzed using IN Cell. mCitrine intensity was measured before the addition of stimuli (0 h) and 6 h after the incubation with the different cytokines or endotoxins. In each time-point, 6 fields of view were analyzed for each well. Graphs shows one representative experiment of four with matching results, where mCitrine intensity values for each of the 6 fields of view were measured.